October 2022

CONSTRAINTS OF THE IMAGINATION: HOW PHENOTYPES ARE SHAPED THROUGH GENETICS, THE ENVIRONMENT, AND DEVELOPMENT

Michelle Gilbert
University of Massachusetts Amherst

CONSTRAINTS OF THE IMAGINATION: HOW PHENOTYPES ARE SHAPED THROUGH GENETICS, THE ENVIRONMENT, AND DEVELOPMENT

A Dissertation Presented

By

Michelle C Gilbert

Submitted to the Graduate School of the
University of Massachusetts Amherst in partial fulfillment
of the requirements for the degree of

DOCTOR OF PHILOSOPHY

September 2022

Organismic & Evolutionary Biology

CONSTRAINTS OF THE IMAGINATION: HOW PHENOTYPES ARE SHAPED THROUGH GENETICS, THE ENVIRONMENT, AND DEVELOPMENT

A Dissertation Presented

by

MICHELLE C GILBERT

Approved as to style and content by:

_____
R Craig Albertson, Chair

_____
Cristina Cox Fernandes, Member

_____
Steve McCormick, Member

_____
Jason Kamilar, Member

_____
R Craig Albertson, Graduate Program Director
Organismic & Evolutionary Biology

ACKNOWLEDGEMENTS

In the words of Bernard of Chartres, and later paraphrased by Isaac Newton, *"If I have seen a little further, it is by standing on the shoulders of giants."* This statement, and the sentiment accompanying it, have increasingly touched me throughout my academic career. Each of us are successful due to the work that was established by our predecessors. Throughout my doctoral work, several individuals have come to mind. To this end, I would like to acknowledge François Jacob, who in 1977 published "Evolution and Tinkering", inspiring me on numerous intellectual fronts. Various works by Stephen Jay Gould, especially his and Lewontin's 1979 paper "The Spandrels of San Marco and the Panglossian Paradigm" and a later paper in 1980 "The Evolutionary Biology of Constraint." These two authors, and many others, have helped inspire me on countless levels and have provided me with countless hours of intellectual discussion, debate, and thought.

Much of the work done here was made possible by numerous institutions, many of which are natural history museums. I have been privileged to work with collections made by my predecessors, and hope that my work further contributes to my field and will, one day, aid another young scientist in their studies and discoveries. Andrew Williston and Meaghan Source at the Harvard Museum of Comparative Zoology. Amanda Hay and Kerryn Parkinson at the Australian Museum. Oswaldo Oyakawa and Alessio Davoto at the Museu de Zoologia da Universidade de São Paulo. Lúcia Rapp Py-Daniel at the Instituto Nacional de Pesquisas da Amazônia fish collections. Masanori Nakae at the National Museum of History and Science in Tokyo. Katherine Doyle and Cristina Cox Fernandes at the University of Massachusetts Amherst.

R. Craig Albertson has been a better mentor than I could have hoped for. Not only has Craig given me wise and fruitful guidance over the past five years, but he has also been an incredible supporter and friend. It is because of Craig that I feel that I have finally found a home in the academic world and now can ask questions, and seek answers, in ways that are personally fulfilling. I will always appreciate my friendship with Craig and look forward to working with him in the years to come.

Not only has Craig been an unbelievably good mentor and role model, but he has also strived to create a diverse lab, both in terms of scientific backgrounds, but also in social backgrounds. The Albertson lab has been consistently full of supportive people that have made my time in the lab joyous, productive, and overwhelmingly delightful. The acceptance of me as a member of the lab throughout difficult parts of my life is cherished and is a testament to the socially diverse and academically holistic environment that is the Albertson Lab.

When I first interviewed with Craig, prior to joining the lab, I was clear that I wanted to continue working with undergraduate students and help get students engaged in research. Unsurprisingly, Craig has been immensely supportive and during my time here, I have had the privilege to mentor numerous (16) undergraduates and two Master's students. I would like to acknowledge the hard work of Leah Delorenzo, Catherine Lerose, Maxwell Olsen, Sofia Piggott, Niah Holtz, Jackelyn Raymundo Santizo, Rashad Batley, Ashley Harrop, Leticja Flamaraj, and Margaret Oftring. These students have all contributed in substantial ways to my development as a mentor and researcher. They are beyond capable of doing great things and I'm honored to have been a part of their academic journey.

I have no shortage of friends that have provided me with unwavering support in not only my pursuit of this degree, but also as I have sought to discover myself. In particular, I would like to thank Cindy Moschella, who has guided me and been an ear throughout my most difficult journey to date. Dina Navon, my lab sister, who has been an encouraging, supporting, and loving woman that I am fortunate know. Craig Albertson, Andrew Conith, Emily Tetrault, Elsa Cousins, Josh Moyer, Gina Georgadirellis, Niah Holtz, Harry Mangold, Mary Packard, and many others for their friendship, acceptance and support, guidance, and collaboration.

Kristen Lindsey, my oldest friend, has provided me with a love that I can only hope to have repaid. Your steadfastness, unwavering support, and unquestionable reliability has graced my life in a previously unimaginable way. Without you, I question my ability to have not only completed this dissertation, but also found the strength to persevere in my journey of self-discovery. Kristen, thank you, for all that you do, have done, and will do for me. I hope that I give you the same love and friendship that you have provided me. You will always be my boo and one of my greatest friends. I love you.

Skylar Mannan, perhaps one of the people that I have most closely resonated, my friend and partner whom I share a deep, passionate bond – not only has your strength and love blessed me in ways that I can only hope to I reciprocate, but your joyous personality, companionship, and reliability have helped me through some of the darkest and most difficult challenges of my life. My transition would have not been possible without your support and love, and I question the capacity in which I would currently exist without you. You will always hold a unique place in my heart. You brought me to life. I love you.

ABSTRACT

CONSTRAINTS OF THE IMAGINATION: HOW PHENOTYPES ARE SHAPED THROUGH GENETICS, THE ENVIRONMENT, AND DEVELOPMENT

September 2022

MICHELLE C GILBERT, M.Sc., WESTERN KENTUCKY UNIVERSITY

Ph.D., UNIVERSITY OF MASSACHUSETTS AMHERST

Directed by: Dr. R. Craig Albertson

Phenotypic constraints are ubiquitous throughout nature, being found throughout all stages of life and at multiple different biological levels including cellular, genetic, environmental, behavioral, evolutionary, and developmental. These constraints have shaped, not only the natural world, but the way that we perceive what is possible, or impossible, an observation made clear by François Jacob in his 1977 paper "Evolution and Tinkering". This is reflected in the literature, repeatedly, by the regular occurrence of densely packed visualization of phenotypic space that seemingly always have large areas that go unoccupied. Despite constrained regions of space being observable across countless taxa, identifying the mechanisms of those constraints remains elusive. Given that constraints are widespread and have influenced how evolution may work, my aim was to identify mechanisms of constraint throughout multiple biological levels. Chapter one is divided into two parts, sections A and B, but largely focuses on how constraints are influenced by genetics. For this, we investigated *crocc2*, a protein that encodes for a structural component of the ciliary rootlet which in turn plays a major role as a mechanosensory for nearly all cells. We found dysfunctional *crocc2* resulted in both dysmorphic bone development and a decrease in the plastic response potential of

zebrafish (section A), as well as altered developmental trajectories in juvenile morphology, presumably due to alterations in cellular polarity and inadequate extracellular communication. Importantly, all results from this chapter point toward crocc2 play a canalizing role in the production of phenotypes at multiple life-history stages. Chapter 2 takes a different approach into understanding constrains by looking at broad ecological alterations and how those alterations may alter morphology of resident taxa. Here, we utilized the heavily altered habitat of the Tocantins River in the Amazon and the existing museum collections to evaluate how select representatives of the cichlid community had responded to such change. We found significant changes in contemporary morphology across all included cichlid species compared to their historical counterparts. These data show that alterations to the environment have resulted in changes to the local resident species, and possibly an alteration to their future evolutionary trajectories. Among the species included, one was found to have the most substantial morphological changes, which is what we followed up in the next chapter. Chapter 3 dug into the morphological changes of *Satanoperca*, a Geophagine cichlid with a unique feeding mechanism known as winnowing. Winnowing is a poorly understood mechanical process involving substrate manipulation. Given that anthropogenic alterations to local hydrology oft result in changes to the benthic sediment composition, we wanted to know if differing substrates was enough to induce a plastic response in winnowing fishes, and if so which traits were effected. We found significant differences across our experimental populations in both shape and disparity and present evidence in support of wide-spread integration across craniofacial traits. In addition, these data suggest that the novel anatomical structure, the epibranchial lobe, is more modular than

other craniofacial traits involved in the winnowing process. Chapters 4 and 5 utilize a unique lineage of fishes, the Bramidae, to understand how developmental and evolutionary constraints are broken to produce morphological novelties. We used a combination of DNA sequences from GenBank and numerous museum specimens to illuminate constraints and determine how constraints are broken to produce complex phenotypic novelties. In Chapter 4, we found that the fanfishes had experienced greater rates of morphological evolution than other members of the Bramidae family, resulting in their occupation of an entirely novel region of phenotypic space. In Chapter 5, we elaborated on this by investigating the developmental processes involved in producing an extreme morphological novelty. The data presented in Chapter 5 provide evidence suggesting that the fanfishes have broken various constraints, resulting in prominent anatomical and morphological changes to accommodate their novel phenotype. In all, my dissertation provides examples of how constraints have shaped the variability that we see throughout life and shows examples of how constraints can be identified, what happens when they are broken, and how they work to control the pace and trajectory of evolutionary processes.

TABLE OF CONTENTS

1. CHAPTER 1

Part A: CILIARY ROOTLET COILED-COIL 2 (CROCC2) IS ASSOCIATED WITH EVOLUTIONARY DIVERGENCE AND PLASTICITY OF CICHLID JAW SHAPE

Michelle C. Gilbert[1#], Emily Tetrault[2#], Mary Packard[3], Dina Navon[1,4], R. Craig Albertson[3]*

1 Graduate Program in Organismic and Evolutionary Biology, University of Massachusetts, Amherst MA 01003 USA.

2 Graduate Program in Molecular and Cellular Biology, University of Massachusetts, Amherst MA 01003 USA.

3 Department of Biology, University of Massachusetts, Amherst MA 01003 USA.

4 Current affiliation, Rutgers University, NJ USA.

[#] Contributed equally to this work

* Contact: albertson@bio.umass.edu

PUBLISHED IN: Molecular Biology and Evolution

FULL CITATION: MC Gilbert and E Tetrault, M Packard, D Navon, RC Albertson. 2021. *Ciliary rootlet coiled-coil 2 (crocc2)* is associated with evolutionary divergence and plasticity of cichlid jaw shape. Molecular Biology and Evolution. 38 (8): 3078-3092.

Abstract

Cichlid fishes exhibit rapid, extensive, and replicative adaptive radiation in feeding morphology. Plasticity of the cichlid jaw has also been well documented, and this combination of iterative evolution and developmental plasticity has led to the proposition that the cichlid feeding apparatus represents a morphological "flexible stem". Under this scenario, the fixation of environmentally sensitive genetic variation drives evolutionary divergence along a phenotypic axis established by the initial plastic response. Thus, if plasticity is predictable then so too should be the evolutionary response. We set out to explore these ideas at the molecular level by identifying genes that underlie both the evolution and plasticity of the cichlid jaw. As a first step, we fine-mapped an environment-specific QTL for lower jaw shape in cichlids, and identified a non-synonymous mutation in the *ciliary rootlet coiled-coil 2 (crocc2)*, which encodes a major structural component of the primary cilium. Given that primary cilia play key roles in skeletal mechanosensing, we reasoned that this gene may confer its effects by regulating the sensitivity of bone to respond to mechanical input. Using both cichlids and zebrafish, we confirmed this prediction through a series of experiments targeting multiple levels of biological organization. Taken together, our results implicate *crocc2* as a novel mediator of bone formation, plasticity and evolution.

Introduction

Plasticity is a core concept in the extended evolutionary synthesis

The Modern Synthesis of the 1930s and 1940s united Darwin's theory of natural selection with Mendelian genetics to explain the origin and maintenance of adaptive variation within populations, and has since been the prevailing paradigm in evolutionary biology (Mayr 1993). The Modern Synthesis set out a largely gene-centric view of adaptation wherein new variation arises in a population through genetic mutation, and

natural selection leads to the differential survival of variants. In recent decades, however, it has become apparent that several elements are missing from the Modern Synthesis (Pigliucci 2007), including a consideration for previously unrecognized sources of variation, such as development (Waddington 1959; Jamniczky et al. 2010) and the environment (West-Eberhard 1989; 2003). In other words, the mechanisms for how phenotypic variation arises and is maintained within populations are not yet well understood (Hendrikse et al. 2007). These conceptual omissions have led to the idea that the field is in need of an Extended Evolutionary Synthesis (Mayr 1993; Pigliucci 2009).

Within the context of the Extended Evolutionary Synthesis, phenotypic plasticity has emerged as a core concept as it can have a potent effect on the degree and type of genetic variation that is exposed to natural selection (Mayr 1993; Pigliucci 2005; 2008; Laland et al. 2014). Operationally, plasticity is the capacity of a single genotype to produce two or more phenotypes in response to environmental stimuli (Bradshaw 1965), which may increase fitness in fluctuating environments (West-Eberhard 1989; Schlichting and Pigliucci 1998). Phenotypic plasticity also has the potential to influence several evolutionary phenomena, including the origins of novel traits (Moczek 2008), speciation (Price et al. 2003; West-Eberhard 2005; Pfennig et al. 2010), and adaptive radiations (West-Eberhard 2003; Wund et al. 2008). While plasticity is often considered separate from (or even opposite to) genetics, it is important to note that the two are inextricably linked, and that plasticity manifests due to the sensitivity of (genetically encoded) molecules and/or pathways to environmental input (Pigliucci 2005). In other words, if phenotypic variance is due to the combined effects of genetics, the environment, and their interaction (i.e., $P = G + E + GXE$), then plasticity may be considered the interaction

term (GxE). A genetic basis for plasticity is supported by its heritability (reviewed by, Scheiner 1993), but many questions remain including what are the specific genetic components of plasticity and at what level (e.g., nucleotide, transcript, protein) do they confer environmental sensitivity (Pigliucci 2005; Gibert 2017). This uncertainty about the genetic nature of plasticity has hindered progress into understanding the mechanisms through which plasticity may evolve (Via et al. 1995). Thus, phenotypic plasticity is recognized as an important process in evolution, but we still lack an understanding of many fundamental aspects of its biology (Ehrenreich and Pfennig 2016; Schneider and Meyer 2017).

The cichlid jaw as a flexible stem

Over the past two decades, we and others have worked to reveal the genetic bases for jaw shape differences among cichlid species (e.g., Albertson et al. 2003; 2005; Parnell et al. 2012; Hu and Albertson, 2014; Powder et al. 2014; Irisarri et al. 2018). In addition, plasticity is well documented for the cichlid jaw. Specifically, when reared in the lab on diets that imposed distinct functional demands on the feeding apparatus, cichlids will develop distinct oral jaw morphologies (Bouton et al. 2002; Stauffer et al. 2004). Notably, variation in cichlid feeding morphology induced by alternate feeding regimes can be strikingly similar to patterns of natural craniofacial variation among species (Parsons et al. 2014). Repeated lacustrine cichlid radiations are defined by a conserved primary axis of craniofacial variation that involves differences in head depth and jaw length/rotation, traits that are intimately associated with adaptations to alternate benthic and pelagic trophic habitats (Cooper et al. 2010), and it is this pattern of variation that is typically observed in studies of developmental plasticity of the cichlid jaw (Bouton et al.

2002; Stauffer et al. 2004; Parsons et al. 2014). Moreover, similar patterns of craniofacial plasticity have been observed in several other fish lineages when fed alternate benthic/pelagic diets (Parsons and Robinson 2006; 2007; Wund et al. 2008), which suggests a common mechanism may be at work.

The combination of morphological diversity and developmental plasticity has led to the assertion that the cichlid jaw represents a morphological "flexible stem" (West-Eberhard 2003). The flexible stem hypothesis of adaptive radiation postulates that patterns of developmental plasticity in an ancestral population will generate independently derived radiations along similar eco-morphological axes (West-Eberhard 1989; 2003). In other words, the nature of developmental plasticity in an ancestral population can influence the direction of adaptive radiations by determining what genetic variation is exposed to selection through its phenotypic expression. Under this hypothesis, repeated evolution along a conserved benthic-pelagic eco-morphological axis in cichlids is the result of sorting, and ultimately fixing, genetic variation that is exposed to selection via plasticity. If true, we would expect that the same loci that underlie evolutionary divergence in cichlid jaw shape will also regulate plasticity of the structure (Gibert 2017). Here we test this prediction.

Results and Discussion

Genetic variation in crocc2 is associated with functionally salient aspects of cichlid jaw shape

We generated a hybrid mapping pedigree by crossing two cichlid species that differ in jaw shape as well as their ability to remodel their jaws under different environmental conditions (Parsons et al. 2014; Navon et al. 2020). The first species, *Labeotropheus fuelleborni* (LF hereafter), is an obligate algal scrapper, with a robust

craniofacial skeleton and limited plasticity. The second, *Tropheops sp. "*red cheek" (TRC), is a more generalized benthic forager, with smaller jaws and greater plasticity. With this genetic cross, we mapped variation in feeding architecture under distinct, ecologically relevant feeding regimes, whereby families were split and progeny were made to feed with either "biting" or "sucking" modes of feeding, mimicking a major ecological axis of divergence (see, Parsons et al. 2016 for details). Results from this study demonstrated that the craniofacial G-P map is strongly influenced by the environment, as most quantitative trait loci (QTL) were specific to one environment (Parsons et al. 2016; Zogbaum et al. 2020).

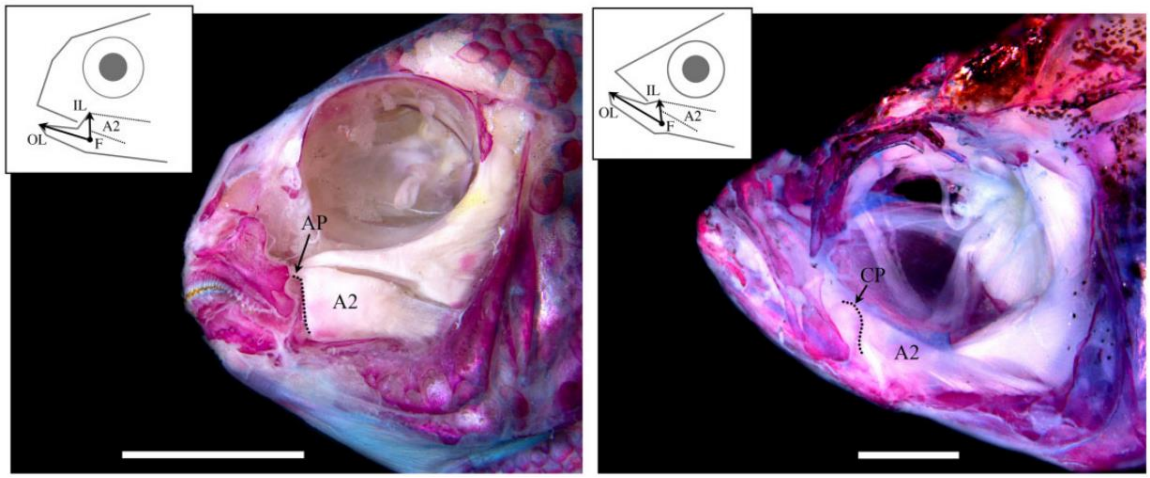

Figure 1.1. Functional anatomy of the cichlid and zebrafish head. A dissected and alizarin red stained head of a representative cichlid, *Tropheops* sp. "red cheek", is depicted at left, and a zebrafish is shown at right. Craniofacial bones are red, and muscles are white. The lever mechanism that defines the mechanical advantage of jaw closing is illustrated for each species, whereby the jaw joint acts as the fulcrum (F), jaw length is the out-lever (OL), and a dorsally projecting bony process, on which the second subunit of the adductor mandibulae (A2) inserts, acts as the in-lever (IL). In cichlids, the in-lever is the ascending arm of the articular (AP), whereas in zebrafish it is the coronoid process (CP). Thus, in each species, this functional system is comprised of nonhomologous bony processes. Scale bar equals 1 cm in the cichlid image (left), and 1mm in the zebrafish image (right).

Among the environmentally sensitive loci was a QTL for the mechanical advantage of jaw closing, which is defined as the height of the ascending arm of the articular bone (e.g., articular process, AP), relative to overall jaw length (fig. 1). In cichlids, this bony process is where a major muscle involved in jaw closing inserts (the

second subunit of the adductor mandibulae, A2), establishing this structure as the in-lever for this functional system. A longer AP relative to jaw length, predicts greater mechanical advantage and a stronger bite. Lower jaw mechanical advantage tracks closely with feeding ecology in a range of vertebrate taxa (Westneat 2004; Manabu 2010; Roberts et al. 2011; Dumont et al. 2012; Casanovas-Vilar and van Dam 2013; Arbour et al. 2014), and is thought to drive evolutionary diversification (Dumont et al. 2014); however, its genetic basis is largely unknown (but see, Albertson et al. 2005; Powder et al. 2014).

In this genetic cross, relative AP height mapped to LG21 in the benthic/biting environment (but not the pelagic/suction feeding environment) (Parsons et al. 2016; fig. 2A). Fine mapping across the physical scaffold associated with the QTL interval showed that the peak genotype-phenotype association occurred at a SNP (i.e., G/A) within the gene *ciliary rootlet coiled-coil* 2 (*crocc2*) (fig. 2B-D). A genome scan for divergent loci between natural populations of the parental species used in this cross demonstrated that these species possess alternate *crocc2* alleles (i.e., F_{ST}=0.95; fig. 2D; full dataset published in Albertson et al 2014). Notably, the SNP that underlies divergence within our mapping pedigree and between natural populations corresponds to a non-synonymous change within *crocc2* (fig. 2B). This gene encodes an important structural component of the primary cilia, the ciliary rootlet. The alanine residue at position 963 appears to be conserved across African cichlids, but is a valine in LF, the obligate benthic forager with a long AP and low magnitudes of plasticity (fig. 2B). In addition, the A963V change is predicted to alter protein function based on a PolyPhen-2 (Adzhubei et al. 2010) protein prediction algorithm score of 0.904 (scores approaching 1.0 are considered functionally

relevant), making this gene a robust candidate for regulating bone shape differences in cichlids.

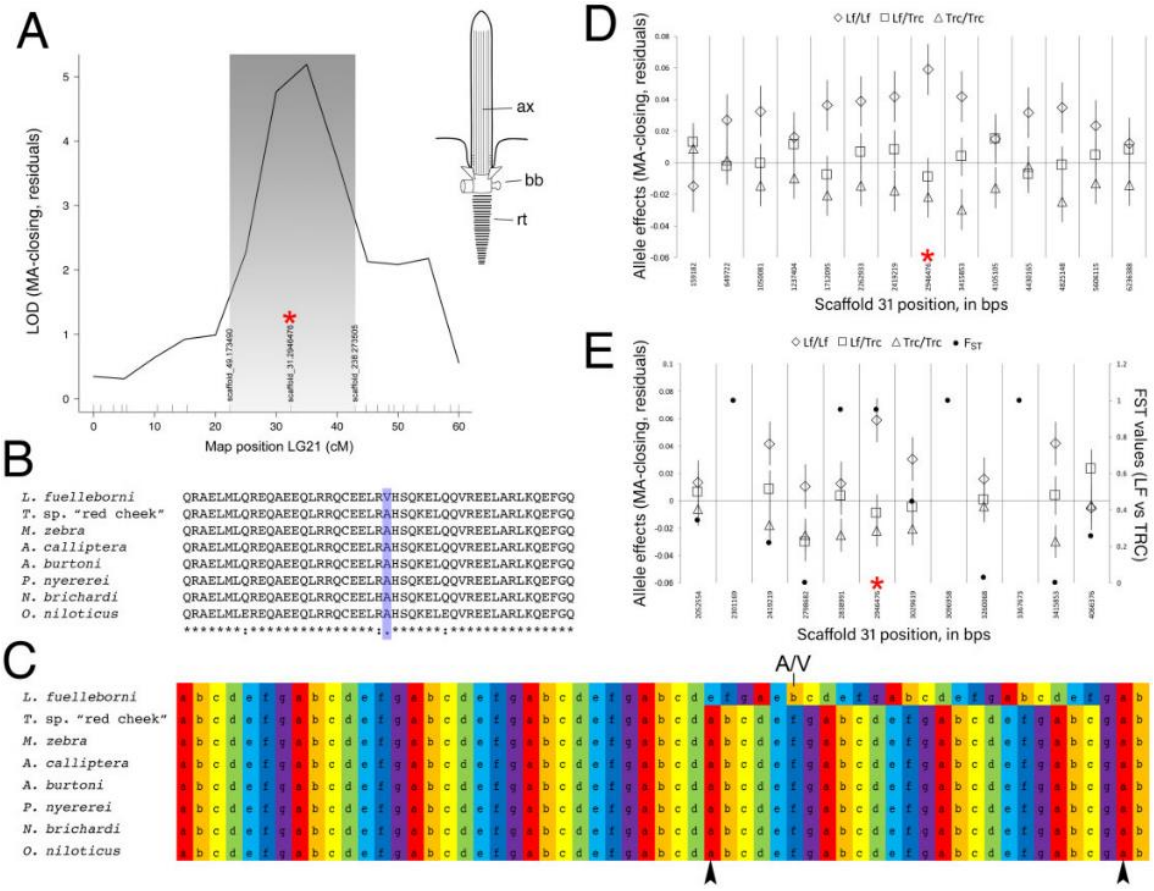

Figure 1.2. Mapping of lower jaw mechanical advantage in cichlids. The QTL for relative height of the articular process (i.e., mechanical advantage of jaw closing, "MA-closing") maps to LG21 and peaks over a marker on physical scaffold number 31 (A). A schematic of a primary cilium is shown in (A)as well, where "ax" is the axoneme, "bb" is the basal body, and "rt" illustrates the striated rootlet. The SNP at the QTL peak (red asterisk) encodes a nonsynonymous (A/V) polymorphism within Crocc2, where the A allele is conserved across African cichlids (B), and is associated with two predicted interruptions (arrowheads, C) in the heptad repeat (i.e., denoted, and color-coded, a–g). The V allele in LF is predicted to result in contiguous heptad repeats in this region of the protein (C). With additional markers every ~0.5 Mb, we queried the phenotype–genotype relationship along scaffold 31 and show that the peak association remains at ~2.9 Mb (red asterisk, D). We sought to refine the interval even further using markers every ~100-200 kb, between ~2–4Mb on scaffold 31, and find that the peak association holds at the crocc2 SNP (red asterisk, D). Further, this marker is nearly alternatively fixed between -wild populations of LF and TRC (e.g., FST¼ 9.5).

Crocc2 encodes a large protein composed almost entirely of coiled-coil domains (Yang et al. 2002). This structural motif forms alpha-helices through hydrophobic interactions, wherein the polypeptide chain coils in order to bury hydrophobic residues

and expose polar side chains (reviewed by Woolfson 2005). The pairing of coiled-coil proteins occurs through heptad repeats, usually denoted as *abcdefg*, where *a* and *d* represent the hydrophobic residues (fig. 2E; fig. S1C). Interactions between opposing *a* and *d* residues represent the main "hydrophobic seam" in dimer formation (Woolfson 2005). In addition, residues that flank the hydrophobic seam in the alpha-helix, *e* and *g*, contribute to the specificity and stability between helices via ionic interactions (e.g., salt bridges). Coiled-coils are dynamic and flexible structural motifs, which participate in myriad biological functions.

In the cilium, Crocc2 monomers homodimerize to form filamentous rootlets, which originate from the basal body and extend proximally toward the cell nucleus (fig. 2A, inset). Rootlets are thought to provide structural support for the cilia by integrating the cilium with actin filaments (Yang et al. 2005). Cells lacking rootlets are structurally unstable and degenerate over time (Yang et al. 2005; Mohan et al. 2013). Notably, the A963V change in African cichlids is predicted to affect this structural motif. Specifically, this change occurs in a stretch of residues where the heptad repeat is interrupted twice in African cichlids with the A allele (black arrowheads, fig. 2E). The V allele in LF is predicted to re-establish the heptad repeat across this region (fig. 2E). Consistent with this, the stability of the dimerization between helices is predicted to be higher in the V allele (Tm = 95ºC), compared to the A allele (Tm = 85ºC) (bCIPA, Mason et al. 2006). Notably, dimerization between the two different alleles is predicted to be the least stable (Tm = 80ºC), which suggests that hybrids could be at a disadvantage if dimerization of this protein serves a core function. Collectively, these data suggest that this

polymorphism may affect protein structure and cilia integrity/stability, with the V allele acting to increase stability.

When extending the Crocc2 sequence comparison across additional fish species several notable patterns emerged (fig. S1). First, we found that all perciform species examined (n=15) possessed either an A or V at this position, and further that all ray-finned fished possessed a non-polar, hydrophobic amino acid (fig. S1B). In addition, the A/V polymorphism noted in non-cichlid perciforms was associated with the same G/A nucleotide polymorphism. Thus, all species within this order seem to have one of two nucleotides at this position, leading to either an A or V, and correspondingly a stretch of Crocc2 characterized by interrupted or contiguous heptad repeats, respectively (fig. S1C). The functional significance of this pattern with respect to bone/jaw shape remains unclear. On one hand, this region of the protein is characterized by increased variation in the continuity of the coiled-coil motif (relative to flanking regions), and so it may represent an area more permissive of variation, and therefore a target of selection. On the other hand, no obvious pattern emerges in terms jaw morphology when comparing species with continuous (e.g., LF, orangethroat darter, Antarctic dragonfish) versus interrupted (e.g., TRC, damselfishes, threespine stickleback) heptad repeats across this region. It is worth noting, however, that Crocc2 is a relatively large protein (>1600aa in cichlids), and so it may be that the consequences of variation in amino acid sequence on bone biology has less to do with any one region of the protein, and more to do with the number and/or integrity of coiled-coil motifs across the entire protein, especially when making broad taxonomic comparisons. This could represent a fruitful line of future inquiry. Within African rift lake cichlids, however, where amino acid sequence homology

is high (>95%), this particular mutation, and its predicted structural consequences, are more likely to have a direct effect on jaw shape.

Rates of bone matrix deposition are canalized in the African cichlid species with the divergent crocc2 allele

In the context of plasticity, a mutation that influences the integrity of a structural protein could provide a mechanism through which genetic assimilation occurs. We know from previous work that the cichlid species with the divergent *crocc2* allele, LF, exhibits reduced craniofacial plasticity, relative to TRC, in response to alternate feeding regimes (Parsons et al. 2016; Navon et al. 2020). To determine the degree to which this finding holds specifically within the AP, we subjected LF and TRC to alternate feeding regimes, and then assessed rates of bone matrix deposition in the AP using two different fluorochromes injected at the beginning and end of the experiment (described in Navon et al. 2020). We expected the generalized forager, TRC, to deposit more bone on the AP in the benthic/biting, compared to the pelagic/suction feeding, environment. Furthermore, we expected the obligate benthic foraging species, LF, to deposit relatively high rates of bone matrix deposition in both environments, consistent with the assimilation of a "biting" bone geometry. Our results support these predictions (fig. 3). We found a significant species-by-treatment effect in terms of matrix deposition ($F=4.108$, $p=0.0137$), with pair-wise differences noted for TRC (TukeyHSD, $p=0.0770$) but not LF (TukeyHSD, $p=0.9345$) reared in different environments. These results show that bone formation is canalized in LF, resulting in consistently high-levels of bone matrix deposition on the AP, and greater mechanical advantage of jaw closing.

Taken together, our results in cichlids suggest roles for *crocc2* in regulating species-specific bone geometry and plasticity, and that both phenotypes are related to differential mechanosensing. To test this hypothesis, we utilized the zebrafish system.

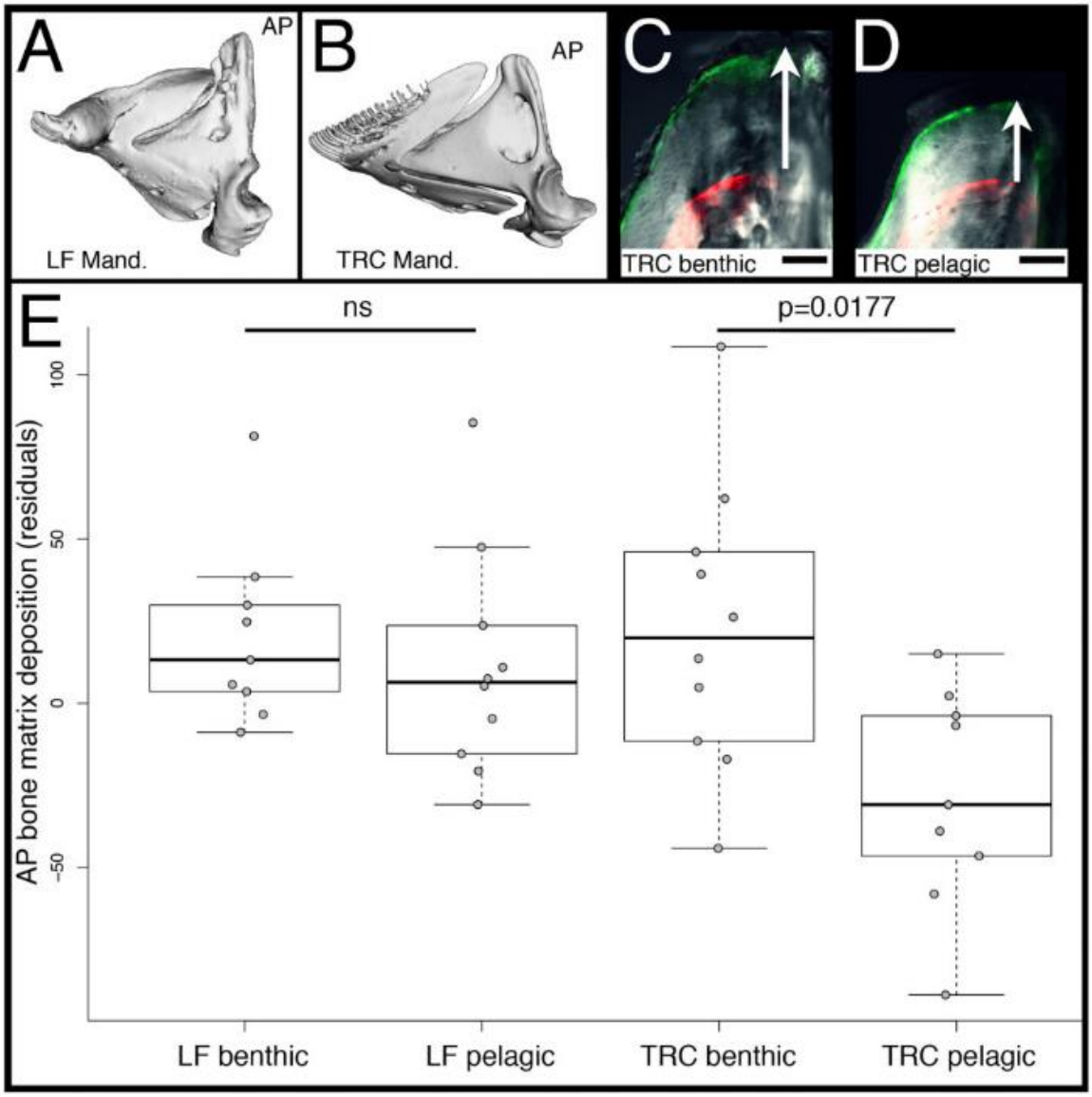

Figure 1.3. Rates of bone matrix deposition in cichlids. Mandibles of LF (A) and TRC (B) are shown, and the ascending arm of the articular bone (AP) is labeled. The tip of the AP in TRC reared in either a benthic/biting (C) and pelagic/sucking (D) environment is shown. Panels (C and D) are overlays of bright field, GFP, and RFP illumination. The RFP filter shows where alizarin red was incorporated into the bone. GFP is the calcein green label 5 weeks later. The distance between labels (white arrows) represents the amount of matrix deposited during that time. Scale bars equal 50 mm. Quantification of the rates of bone matrix deposition are shown in (E). Significance was determined via an ANOVA followed by a Tukey's multiple comparison test.

Crocc2 ***is required for the maintenance of primary cilia***

Bone is a dynamic tissue that can sense and respond to its mechanical environment, and the primary cilia on bone cells are thought to play critical roles in mediating this process (Xio et al. 2006; Papachroni et al. 2009; Nguyen and Jacobs 2013). Mice lacking functional cilia in bone precursor cells exhibit normal larval skeletal patterning, but impaired growth (Qiu et al. 2012), as well as a reduced ability to form bone in response to mechanical loading (Temiyasathit et al. 2012). Unlike the axoneme and basil body, roles for the ciliary rootlet in bone biology are unknown. The limited data on this structure suggests that rootlets are important for maintaining ciliary integrity over time (Yang et al. 2005). Consistently, we find that zebrafish *crocc2* mutants possess primary cilia as larvae (e.g., 4 day), but exhibit a dramatic reduction in cilia number, compared to wild-type siblings, as adults (e.g., >12 mos.) (fig. 4). Based on these data as well as known roles for the primary cilia and bone mechanosensing, we predict that *crocc2* mutants will exhibit bone phenotypes that include (1) dysmorphic skeletal architecture in areas of high mechanical stress, (2) degenerative bone homeostasis, and (3) a reduced ability to mechanosense.

Jaw defects in crocc2 mutants localize to regions of adaptive morphological variation in cichlid jaws

We found that homozygous recessive *crocc2* mutants are viable through adult stages, enabling the analysis of bone phenotypes throughout life history stages. Consistent with our prediction, patterning of the *crocc2* craniofacial skeleton appears relatively normal, but shape is distinct, especially at adult stages. A geometric morphometric analysis of craniofacial shape revealed key differences in foraging related bones, specifically in regions with direct mechanical input (e.g., attachment points for

tendons and ligaments) (fig. 5). For instance, variation that distinguished mutant and wild-type jaw shapes was largely limited to the size and shape of the coronoid process (CP, fig. 5A-B). In zebrafish, this structure represents the point of insertion for the A2 muscle (fig. 1), and is functionally analogous to the region of the cichlid jaw that maps to the *crocc2* locus. Thus, genetic/genomic mapping in cichlids and mutagenesis in zebrafish implicate *crocc2* in the formation of non-homologous but functionally equivalent structures of the jaw.

Shape defects were also noted in other bony elements. For example, the kinethmoid, which drives zebrafish jaw protrusion through a complex arrangement of ligamentous attachments, exhibits a unique shape in mutants (fig. 5C-D). Regions of this bone most affected in *crocc2* mutants include the rostral- and caudal-most surfaces, which serve as attachment sites for ligaments that connect the kinethmoid to the neurocranium and premaxilla, respectively (Staab and Hernandez, 2010). In all, *crocc2* appears to be required to maintain bone integrity in zebrafish, especially in areas subjected to mechanical stress.

Crocc2 *is required for bone homeostasis*

We next examined bone growth and homeostasis in *crocc2* mutants at the transcript-level. Specifically, we performed quantitative RT-PCR on freshly dissected craniofacial bones from mutant and wild-type animals at 2 different stages, young (3-5 mos.) and aging (10-15 mos.) adults. We used a panel of known and presumptive bone markers for this analysis (n=10, table S1). We reasoned that if (1) cilia are required for normal bone growth and homeostasis, and (2) *crocc2* mutants lose cilia over time, then

we should observe a mis-regulation of bone marker genes in older, compared to younger, mutant animals.

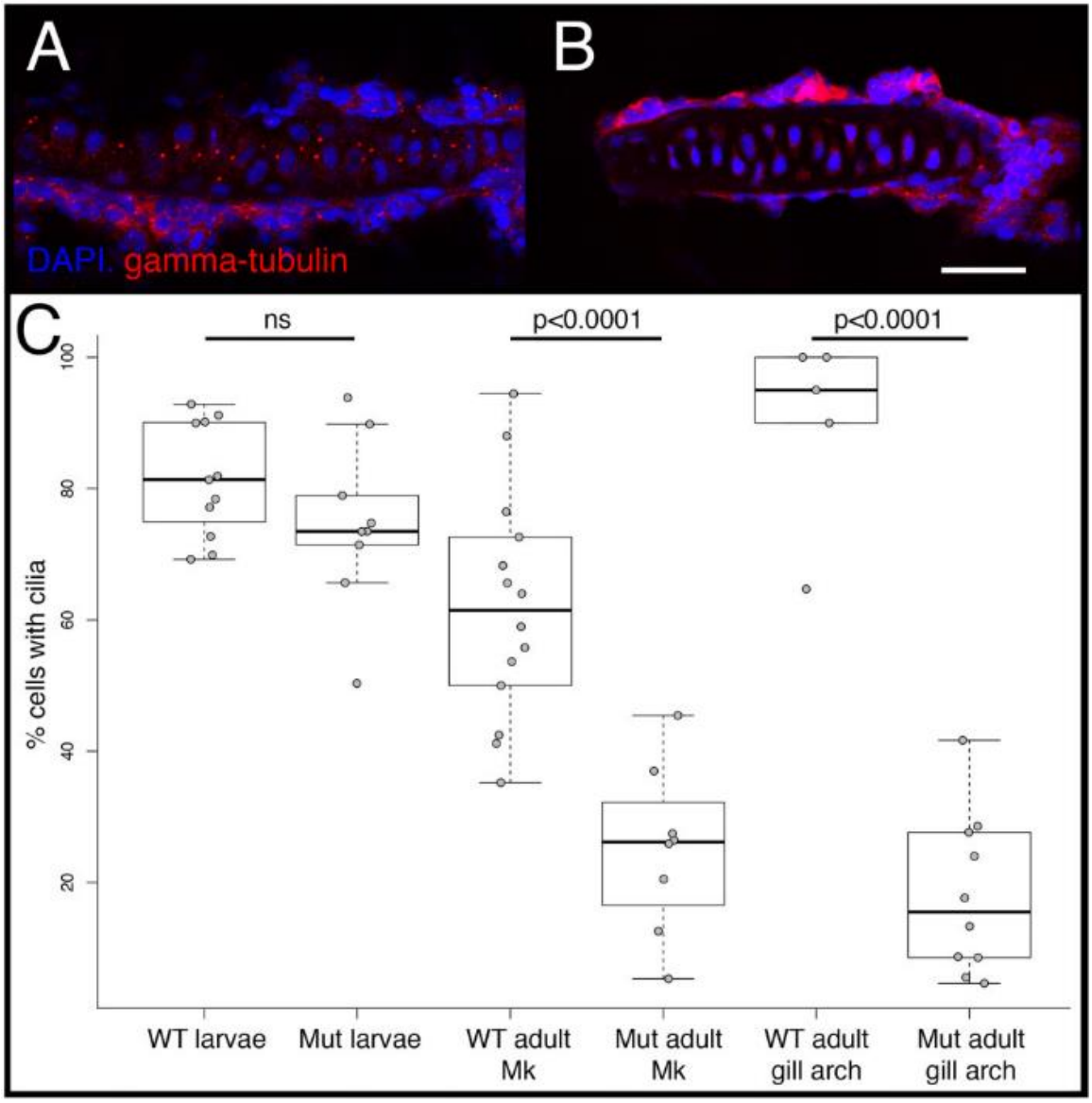

Figure 1.4. Cilia number in WT and mutant zebrafish. Cilia were visualized via immunohistochemistry using either anti-gamma-tubulin (shown), which labels the basal bodies, or anti-alpha acetylated-tubulin (not shown), which labels the axoneme, and imaged via confocal microscopy. Representative images are shown for the gill arch cartilage in WT (A) and full-sibling crooc2 mutants (B). Scale bar equals 20 mm. Quantification of cilia number per cartilage, calculated as the percentage of nondividing cells containing cilia, is shown in (C). Significance was determined via an ANOVA followed by a Tukey's multiple comparison test. In larval (4dpf) fish, each data point represents a count from a different cartilage across n¼3 WT and n¼3 crocc2 mutant animals. In adults (>12 months), data points represent counts from different sections of Meckel's cartilage (i.e., Mk), or from different gill arch cartilages. Sample sizes for adults are also n¼3 for each genotype.

When considering the expression of bone marker genes, we find evidence for mis-regulation (table 1; fig. S2). ANOVA models indicate significant effects of genotype on gene expression for three osteoblast markers (including *col10a1*), and all three Hedgehog (Hh) markers. Hh signaling was assessed given that members of this pathway localize to the primary cilia (Goetz et al. 2009), and that it plays important roles in bone development and homeostasis (reviewed by Long 2011; Alman 2015). Genotype was not significant for osteoclast markers, nor the mature chondroblast marker, *col2a1a.* Age also had a significant effect on the expression levels of 3/4 osteoblast genes, 2/3 Hh markers, as well as the osteoclast marker, *csf1ra*. Genotype-by-age was significant for the osteoblast markers, *runx2b* and *AP*, as well as for the Hh target gene, *ptch2*. The significant GxA effect for *runx2b* appears to be driven by relatively higher expression in young mutant bones and lower expression in old mutant bones (fig. S2). For *AP,* higher expression was documented in older mutant fish, compared to old WT or young mutants, whereas for the Hh markers, *ptch1* and *ptch2*, mutants exhibited relatively lower expression than WT at either stage.

Since bone homeostasis requires the coordinated expression of multiple genes, we next sought to assess the degree to which these genes exhibited coordinated expression in mutant and WT animals. Specifically, we performed partial correlations analyses on expression data within mutant and wild-type animals at both life-history stages, and report correlation coefficients and *p*-values for all pair-wise comparisons with the effect of the other variables removed (table 2). Among young adults, differences between genotypes were modest, with mutants exhibiting 8/45 significant ($p<0.05$) pairwise correlations, compared to 11/45 in similarly aged WT siblings (table 2). Further, of the 11

significant correlations in WTs, only 3 were shared with mutants. This pattern is reflected in a network analyses of expression data, where both WT and mutant animals are characterized by four modules of correlated gene expression; however, the composition of genes within each module is different, as is the overall strength of correlation between gene expression, which is higher in WT bone (i.e., a greater number of lines connecting traits, fig. 6A-B).

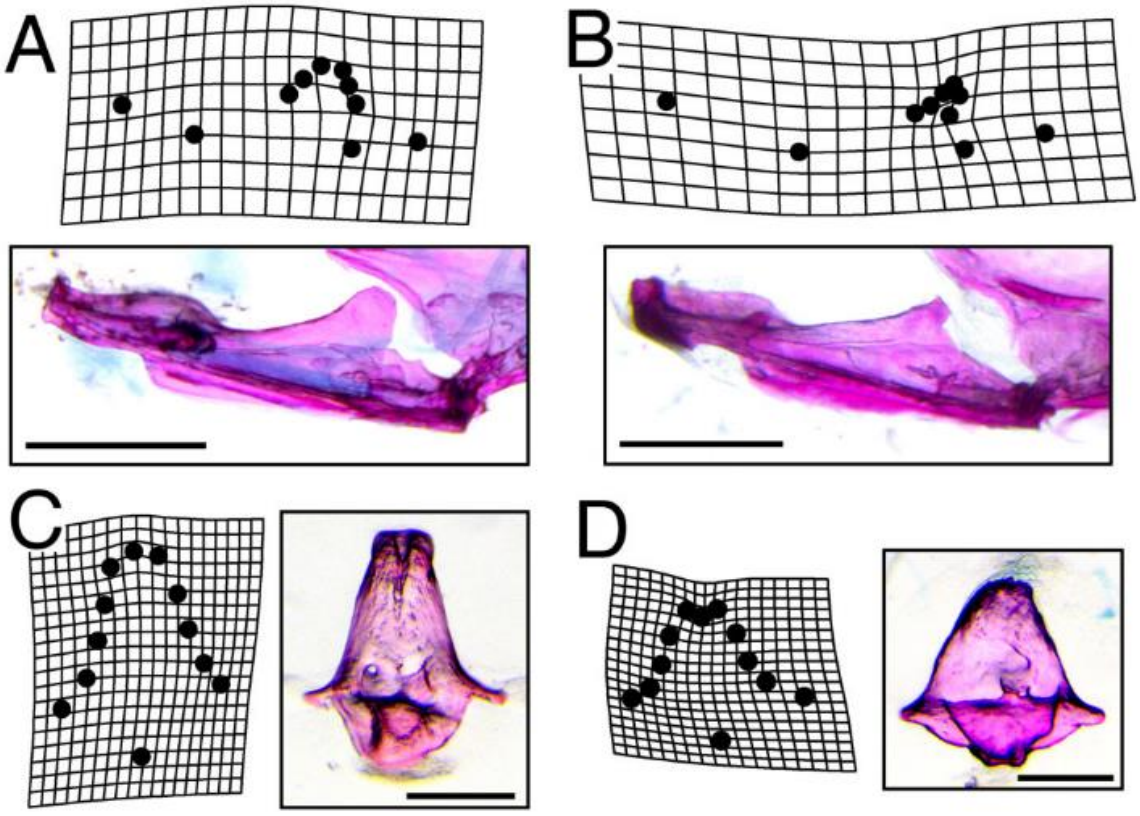

Figure 1.5. Dysmorphic bone geometry in crocc2 mutants. A geometric morphometric shape analysis was performed on various elements of the feeding apparatus in WT and crocc2 mutant fish. Mutants exhibit distinct mandible shapes compared to WT siblings, with the most conspicuous differences occurring in the size and shape of the coronoid process (B vs. A). Scale bars in (A) and (B) equal 1 mm. Shape differences were also noted for the kinethmoid, with mutants exhibiting an overall shortening of the element in the dorsal–ventral dimension (D vs. C). Scale bars in (C) and (D) equal 200 mm. Deformation grids represent commonly seen phenotypes in the mandible and exaggerated mean shapes in the kinethmoid. Procrustes ANOVA with post-hoc pairwise comparisons of group means (procD.lm, advanced.procD.lm), was significant for mandible mean shapes at P¼0.02, and for kinethmoid means at P¼ 0.12.

Differences in correlated gene expression were substantially greater older adults, with mutants exhibiting 17/45 significant pairwise correlations, compared to 31/45

significant correlations in age-matched WT animals (table 2). These data suggest a far more integrated expression network of bone markers in WT versus *crocc2* mutants, an assertion that is supported by the network analyses (fig. 6C-D). Four modules were recovered for older WT animals, but they were characterized by a high degree of correlation both within and between modules. Alternatively, gene expression in older mutants was characterized by two distinct modules, consistent with a dissociated gene network. This idea is supported by the spatial localization of TRAP and AP activities in WT versus *crocc2* mutants. In WT animals the enzymatic signature of bone resorption (i.e., TRAP) and deposition (i.e., AP) was typically co-localized (fig. 6C, inset), as expected based on the literature (e.g., Albertson and Yelick 2007; Cooper et al. 2013), and the interconnected expression of these two factors in the network (e.g., linked by various bone markers, fig. 6C). Alternatively, TRAP and AP activities are conspicuously distinct in *crocc2* mutants (fig. 6D, inset), which is consistent with their dissociated expression in network-space (fig. 6D).

All in all, these genetic data complement the analysis of *crocc2* bone phenotypes (e.g., fig. 5), and suggest that dysmorphic bone shape in *crocc2* mutants is underlain by mis-regulated marker gene expression.

Crocc2 *is required for bone plasticity*

To more explicitly test the hypothesis that *crocc2*-induced bone defects are due to impaired mechanosensing, we subjected fish to alternate feeding regimes intended to impose different functional demands on the craniofacial skeleton (fig. 7), similar to what was performed in cichlids (fig. 3). We then assessed rates of bone matrix deposition in the coronoid process (CP) of animals reared in different environments (fig. 7B-C). Our

expectation was that WT animals would exhibit greater rates of CP bone deposition in the benthic foraging treatment where fish were required to leverage food from the substrate. We predicted further that this plastic response would be limited in c*rocc2* mutants. Our data supported both predictions: Rates of bone matrix deposition were higher in the CP from wild-type fish reared in the benthic versus pelagic treatment, and this response was absent in mutants (fig. 7D). Thus, mutant fish reared in the benthic environment appear to have lost the ability to deposit bone in response to increased mechanical load. More generally, these results are consistent with the hypothesis that dysmorphic bone shape in *crocc2* mutants arises due to impaired mechanosensing.

Table 1.1. Expression differences of bone marker genes.

Osteoblast markers:	*Runx2b*		*Osx*		*AP*	
	F-value	P-value	F-value	P-value	F-value	P-value
Genotype	5.982	0.0163	2.796	0.0982	5.994	0.01621
Age	*31.757*	*1.78E-07*	3.23	0.0759	*11.466*	*0.00104*
GxA	*22.254*	*8.20E-06*	0.908	0.3435	*10.043*	*0.00206*
Osteoclast markers:	*Csf1ra*		*TRAP*			
	F-value	P-value	F-value	P-value		
Genotype	2.824	0.097185	1.567	0.214		
Age	*13.951*	*3.73E-04*	2.589	0.111		
GxA	1.557	0.216196	0.381	0.539		
Chondroblast markers:	*Col10a1**		*Col2a1a*			
	F-value	P-value	F-value	P-value		
Genotype	3.986	0.048744	0.045	0.8317		
Age	*12.967*	*5.06E-04*	4.929	0.0291		
GxA	0.009	0.925719	0.217	0.6424		
Hedgehog markers:	*Ptch1*		*Ptch2*		*Gli*	
	F-value	P-value	F-value	P-value	F-value	P-value
Genotype	6.758	0.0111	*18.683*	*6.39E-05*	5.373	0.0233
Age	6.351	*1.37E-02*	*18.93*	*5.80E-05*	0.845	0.361
GxA	1.09	0.2996	4.324	0.0422	0.04	0.8415

Note i. Expression of genes involved in bone/cartilage development was assessed in WT and mutant animals at two life-history stages, young adult (3–5 months) and old adult (10–15 months). The ANOVA model was (expression ~ genotype X age), and the effects of genotype, age, and their interaction are presented. Marker genes are organized by general function. Col10a1 has an asterisk next to it, because it plays roles in both endochondral and dermal bone formation in fishes. Values with significance after Bonferroni- correction are italicized.

During this analysis we noted variation in CP shape, consistent with the results from the shape analysis described above. We therefore explored CP shape in these

Table 1.2. Covariation in the expression of bone marker genes.

Young WT Bone	*runx2b*	*col10a1*	*AP*	*TRAP*	*osx*	*ptch1*	*col2a1a*	*csf1ra*	*gli1*	*ptch2*
runx2b		0.413	0.637	0.757	*0.022*	0.480	0.080	0.869	0.830	0.343
col10a1	0.200		0.119	0.630	0.114	*0.003*	0.654	0.558	*0.040*	0.124
AP	−0.116	0.370		*0.004*	0.098	0.509	0.200	0.814	0.115	*0.040*
TRAP	0.076	−0.118	*−0.622*		0.356	0.649	0.922	0.426	*0.025*	*0.007*
osx	*0.523*	0.375	−0.391	−0.224		*0.002*	0.293	0.872	0.804	0.123
ptch1	−0.172	*−0.637*	0.161	−0.112	*0.659*		0.866	0.778	*0.005*	0.916
col2a1a	0.411	−0.110	0.308	0.024	−0.254	0.041		*0.009*	0.205	0.596
csf1ra	−0.041	0.143	0.058	0.194	0.040	0.069	*0.585*		0.310	0.395
gli1	0.053	*0.475*	0.374	*0.511*	−0.061	*0.612*	−0.305	0.246		*0.019*
ptch2	0.230	−0.365	*−0.476*	*−0.601*	−0.366	−0.026	−0.130	0.207	*0.531*	

Young Mutant Bone	*runx2b*	*col10a1*	*AP*	*TRAP*	*osx*	*ptch1*	*col2a1a*	*csf1ra*	*gli1*	*ptch2*
runx2b		*0.026*	0.176	*0.000*	0.420	0.169	0.425	0.205	0.754	0.244
col10a1	*−0.474*		0.177	0.664	*0.030*	0.448	*0.052*	0.785	0.734	0.132
AP	0.299	0.299		0.145	0.482	0.913	0.123	0.304	0.161	0.597
TRAP	*0.746*	0.098	−0.322		0.860	0.307	0.822	0.158	0.910	0.727
osx	0.181	*0.462*	−0.158	−0.040		*0.002*	0.083	0.928	*0.000*	0.845
ptch1	0.304	0.171	−0.025	−0.228	*0.622*		0.251	0.060	*0.000*	0.736
col2a1a	0.179	*0.419*	0.339	−0.051	−0.378	−0.256		*0.015*	0.553	0.521
csf1ra	−0.281	0.062	−0.229	0.312	−0.020	0.407	*0.512*		0.452	0.537
gli1	−0.071	−0.077	−0.309	−0.026	*−0.702*	*0.768*	0.134	−0.169		0.657
ptch2	−0.259	−0.332	0.119	0.079	−0.044	0.076	−0.144	0.139	0.100	

Old WT Bone	*runx2b*	*col10a1*	*AP*	*TRAP*	*osx*	*ptch1*	*col2a1a*	*csf1ra*	*gli1*	*ptch2*
runx2b		*0.028*	*0.051*	*0.008*	*0.001*	*0.000*	*0.013*	0.078	0.151	0.063
col10a1	*−0.549*		*0.007*	*0.001*	*0.000*	*0.005*	*0.000*	0.735	*0.000*	0.230
AP	*−0.496*	*−0.641*		0.175	*0.005*	0.229	*0.011*	0.182	*0.003*	0.630
TRAP	*−0.633*	*−0.735*	−0.357		*0.000*	*0.000*	*0.001*	0.195	*0.051*	*0.051*
osx	*0.752*	*0.832*	*0.664*	*0.904*		*0.002*	*0.000*	0.590	*0.004*	0.087
ptch1	*0.771*	*0.663*	0.319	*0.781*	*−0.708*		*0.000*	0.083	*0.049*	*0.037*
col2a1a	*0.606*	*0.867*	*0.618*	*0.768*	*−0.772*	*−0.775*		0.674	*0.005*	0.221
csf1ra	−0.453	0.092	0.351	−0.342	0.146	0.447	0.114		0.131	0.679
gli1	−0.376	*−0.873*	*−0.701*	*−0.496*	*0.681*	*0.499*	*0.664*	0.394		0.433
ptch2	−0.475	−0.318	−0.131	*−0.495*	0.441	*0.525*	0.324	−0.112	−0.211	

Old Mutant Bone	*runx2b*	*col10a1*	*AP*	*TRAP*	*osx*	*ptch1*	*col2a1a*	*csf1ra*	*gli1*	*ptch2*
runx2b		*0.025*	*0.011*	0.664	*0.000*	0.747	*0.000*	0.843	0.211	0.124
col10a1	*−0.699*		*0.000*	0.648	*0.025*	0.400	*0.005*	0.636	0.529	*0.006*
AP	*0.761*	*0.954*		0.498	*0.029*	0.740	*0.004*	0.586	0.298	*0.020*
TRAP	−0.157	−0.165	0.243		0.408	0.225	0.850	0.807	0.117	0.668
osx	*0.926*	*0.698*	*−0.685*	0.295		0.715	*0.000*	0.942	0.207	0.117
ptch1	0.117	0.300	−0.121	−0.422	−0.133		0.470	0.713	0.072	0.379
col2a1a	*0.967*	*0.807*	*−0.822*	0.069	*−0.915*	−0.259		0.674	0.343	*0.022*
csf1ra	−0.072	−0.172	0.197	0.089	0.027	−0.134	0.152		0.127	0.252
gli1	0.433	0.226	−0.366	0.528	−0.437	0.590	−0.336	0.516		0.824
ptch2	0.519	*0.795*	*−0.715*	−0.155	−0.528	−0.312	*−0.709*	0.400	−0.081	

Note ii. Partial correlation coefficients (below diagonal) and P values (above diagonal) are shown for both genotypes at young (3–5 months) and old (10–15 months) stages. Values are italicized if significant at the ~0.05-level.

experimental animals and found that it was distinct between treatments (Treatment: Z=2.470, p=0.003) and genotypes (Genotype: Z=2.197, p=0.005), and that there was a significant interaction effect between these two variables (Genotype-by-Treatment:

Z=2.194, p=0.006). In addition, by quantifying shape using both fluorochrome labels, we were able to track shape over time, and document a significant effect of this variable on CP shape (Time: Z=2.96, p=0.001). Another notable outcome of this analysis was that WT shape, across time and treatments, exhibited relatively less variation compared to that across mutants, which constituted a far greater range of shape space (fig. S3). This qualitative assessment is supported by quantitative tests of morphological disparity, which show that mutants exhibit 2x the disparity as WT animals (0.0238 vs 0.0119, respectively; p=0.065). Increased disparity in mutant CP shape may be related to mis-regulated bone homeostasis (e.g., fig. 6).

Conclusion - Adaptive radiations and the root of flexible stems

Adaptive radiations constitute a major source of biodiversity on this planet and have played a central role in our understanding of evolutionary processes. One attribute of adaptive radiations that has long intrigued and confounded biologists is their repeated, almost stereotypical, nature. For example, stem lineages that recurrently invade a novel environment (e.g., marine to freshwater among threespine stickleback) often diverge along highly predictable eco-morphological axes. While similarities in ecological opportunity may explain some of these patterns, the extent of consistent divergence between replicate adaptive radiations has led to the proposition that other mechanisms may be at work. One notable hypothesis suggests that phenotypic plasticity in the stem lineage has the potential to bias the direction of adaptive radiations. Formalized as the flexible stem hypothesis (West-Eberhard 2003), this theory sets out to provide a mechanistic explanation for the repeated nature of adaptive radiations – e.g., as an ancestral population is exposed to a novel environment, new phenotypic and genetic variants will be exposed to natural selection as individuals within the population mount a

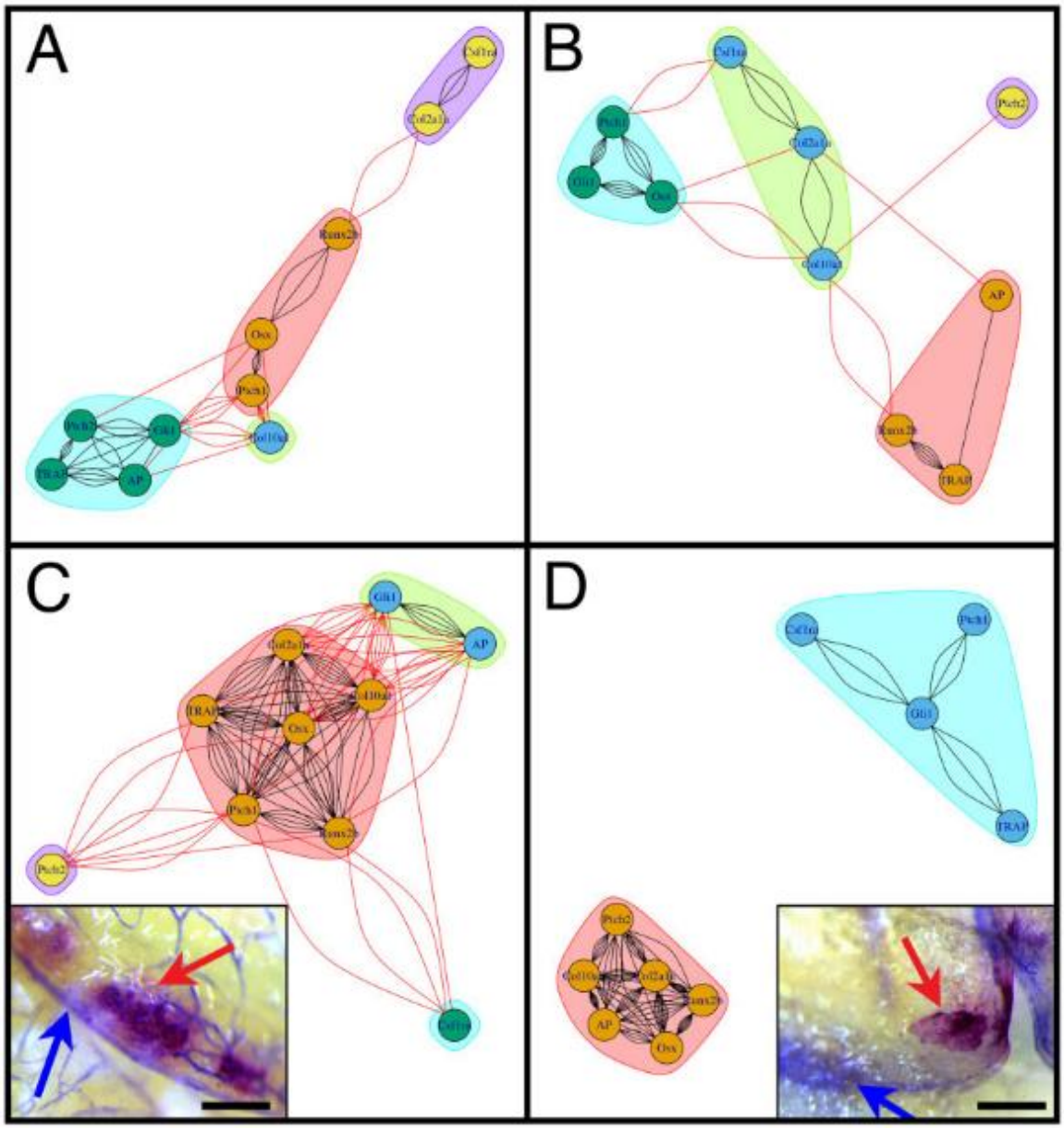

Figure 1.6. Mis-regulation of the bone marker gene expression in crocc2 mutants. Network output of partial correlations (from table 2). Red lines represent correlations between genes in different modules, whereas black lines represent correlations within modules. Colors denote distinct modules in each analysis. Panel (A) illustrates the interaction between bone marker expression in WT animals at the young adult stage (3– 5 months), whereas panel (B) shows data for comparably staged mutants. Note that, although there are a greater number of correlations in WT versus crocc2 mutant animals, both networks are characterized by four interconnected modules. Covariation ofgene expression in old adult (10– 15 months) bone is shown for WT (C) and mutant (D) animals. WT zebrafish show a relatively high number of correlations both within and between modules, consistent with a tightly integrated gene network. Alternatively, mutants show a dissociated pattern characterized by two distinct modules, which is reflected in in vivo patterns of bone cell activity (insets, C and D). In WT bone (i.e., interopercle), TRAP and AP are generally in close approximation, whereas in mutants these factors are often expressed in distinct areas of the bone. Scale bars equal 200 mm.

plastic response. Over time, those cryptic genetic variants that enable animals to more effectively exploit new resources may become fixed (i.e., genetic assimilation, *sensu* Waddington 1953), thereby biasing the direction of evolution along the eco-morphological axis established by the initial plastic response. Thus, if ancestral patterns of plasticity are similar across taxa, then the genetically-fixed evolutionary responses should reflect that similarity. One empirical sign of such flexible stem evolution is predicted to be molecular similarity between morphological plasticity and evolution (Gibert 2017; Navon et al. 2020). Our work seeks to detect such signals.

We first set out to study cryptic genetic variation underlying cichlid jaw shape, with a focus on loci that underlie variation within distinct foraging environments. Fine-mapping implicated the *crocc2* locus, and functional studies in zebrafish support the assertion that this gene is necessary for load-induced bone growth and remodeling. These results are consistent with the broader literature on the primary cilia and bone remodeling (Xiao et al. 2006; Papachroni et al. 2009; Qiu et al. 2012; Temiyasathit et al. 2012; Nguyen et al. 2013). However, whereas the overwhelming majority of studies focus on the basal body, axoneme and other more distal components of primary cilia, ours is unusual in implicating the proximal rootlets in bone biology. Whether the effect is due to ciliary integrity or a more nuanced, and as yet undescribed, role for the rootlets remains to be determined. Regardless of the specific mechanism, we show that the African cichlid species with the divergent *crocc2* allele exhibits an assimilated phenotype - i.e., high levels of bone matrix deposition regardless of mechanical environment. In the context of variation in the coiled-coil motif, this raises the interesting question of whether the number and/or integrity of the motif (i.e., fewer interruptions) might influence

mechanosensing. In zebrafish, the loss (or reduction) of Crocc2 function results in reduced plasticity, supporting critical roles for this molecule in mechanosensing. In LF, loss of plasticity is associated with a putative gain-of-function polymorphism, where Crocc2 is characterized by fewer disruptions in the motif and correspondingly higher homodimerization affinity. Taken together, these insights suggest that the ability of bone cells to mechanosense may actually require a degree of interruption in the Crocc2 coiled-coil motif. In other words, this region of interrupted heptad repeats may serve to "sensitize" Crocc2/rootlets to environmental input. If true, this configuration may be actively selected for in African cichlids, several of which are known to be plastic in head/jaw shape (Parsons et al 2014; Gunter et al 2017; Hu and Albertson, 2017; Navon et al, 2020).

This work constitutes the second in a set of experiments aimed at understanding the molecular basis of plasticity. The other has focused on Hh signaling (Parsons et al. 2016; Hu and Albertson, 2017; Navon et al. 2020), which is notable given the close association between the primary cilium and the Hh signal transduction pathway. Members of the Hh pathway localize to the cilium (Yuan et al. 2015), and cells lacking cilia are unable to transduce a signal in response to the Hh ligand (Haycraft et al. 2005; Berbari et al. 2009). Thus, cilia have been said to constitute the "Hh signal transduction machine" (Goetz et al. 2009). Given the conservation of molecular mechanisms across vertebrates, understanding how, or if, Hh signaling and rootlets interact to effect bone biology in general, and mechanical load-induced plasticity in particular, could be a fruitful line of study. More generally, we suggest that the Hh-cilia signaling mechanism represents a robust molecular candidate for flexible stem evolution of the cichlid jaw.

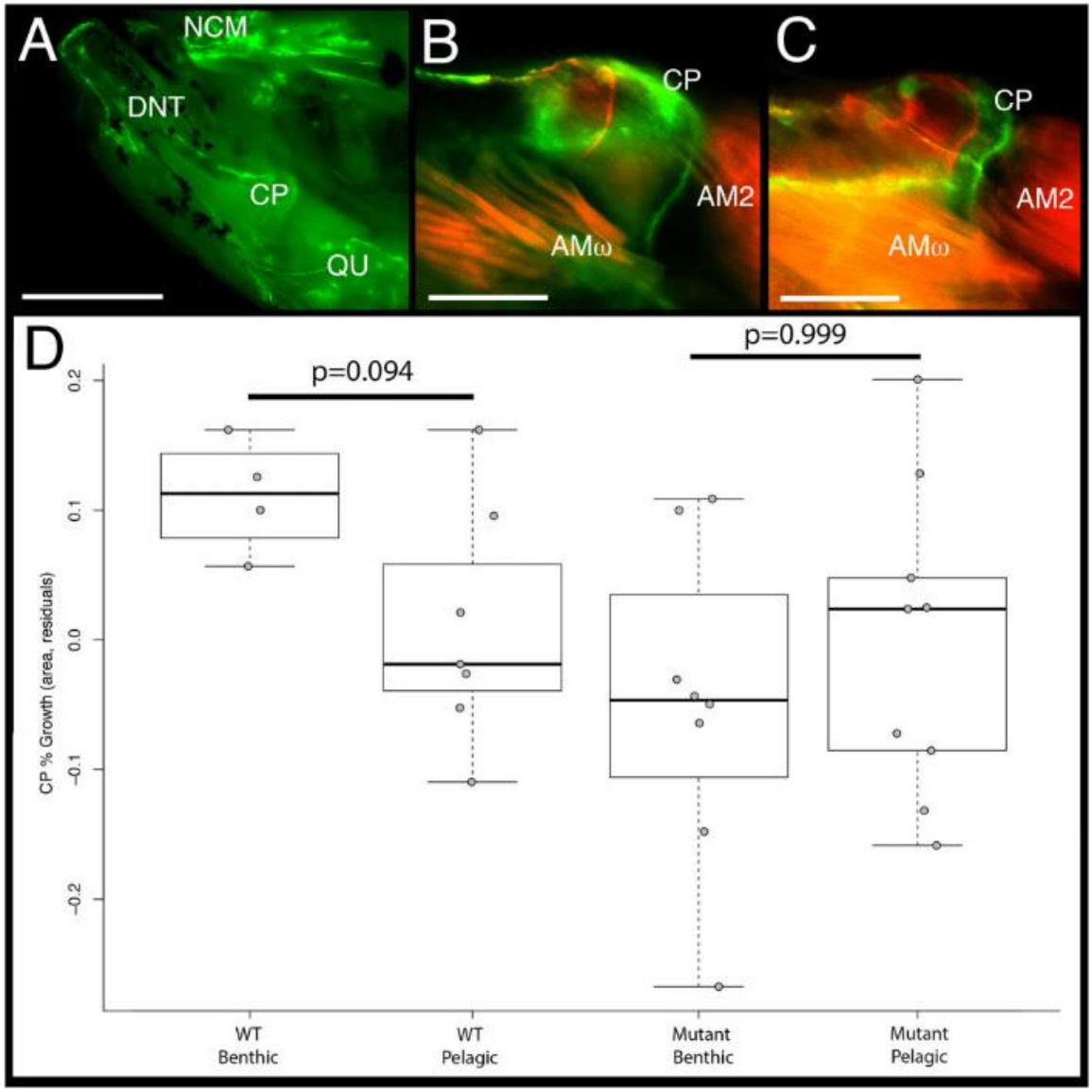

Figure 1.7. Rates of bone matrix deposition do not respond to environmental stimuli in crocc2 mutants. Bone deposition rate was measured as the ratio between the area of the coronoid process (CP) at time 0 (red label) over the area at time 1 (green label) in WT and crocc2 mutant zebrafish reared under alternate foraging regimes. Panel (A) shows the medial view of the oral jaw skeleton, under GFP illumination, depicting the anterior neurocranium (NCM), dentary (DNT), CP, and quadrate (QU). Scale bar for (A) equals 1 mm. Panel (B) depicts a composite image of red and green fluorochromes in the CP of a WT animal, whereas panel (C) shows the CP of a crocc2 mutant. Two subdivisions of the adductor mandibulae can be seen in (B and C)—AM2 and AMx. Scale bars in (B) and (C) equal 200 mm. Panel (D) presents the results of a comparison of bone deposition rates. Pairwise significance was assessed via an ANOVA followed by a Tukey's multiple comparison test.

Methods

Species and husbandry

Both cichlids and zebrafish were used for this project. All cichlids were raised in 10gal glass aquaria on standard flake food until two months of age, before being transferred to 40gal glass aquaria. A single LF female was crossed to a single TRC male, creating a hybrid mapping population that was used for pedigree mapping. These species differ in craniofacial geometry and plasticity (Parsons et al. 2014; Albertson and Pauers 2019; Navon et al. 2020). A full-sibling F_1 family was interbred to produce 25 F_2 families, which were interbred to generate 265 F_3 individuals used in this study. Different F_3 families were split into 2 diet treatments, pelagic or benthic, as described (Parsons et al. 2016). For more detailed methods on these treatments and this cross, see previously published papers by Parsons and colleagues. Briefly, a combination of flake food, algae wafers, and freeze-dried daphnia was ground and either sprinkled directly into the water column (pelagic treatment) or mixed with a ~1-1.5% food-grade agar (Carolina Biological Supply Co., Burlington, NC, USA) solution and spread over lava rocks (benthic treatment). Fish were raised to ~7 months of age on each diet, euthanized with MS-222 according to approved IACUC protocols, fixed in 4% PFA and stored in 75% ethanol. Prior to fixation, flank muscular tissue was taken for DNA extraction. Animals were dissected to reveal functionally salient bones and muscles, and imaged using a digital camera (Olympus E520).

Zebrafish were raised in 2.8-L plastic aquaria on a diet of rotifers from 5- to 12-days post fertilization, and then on a combination of GM-300 (Skretting) and brine shrimp thereafter. For the foraging experiment, zebrafish in the pelagic treatment received GM-300 sprinkled directly into the water column, while benthic fish received

GM-300 mixed with a ~1% food-grade agar solution spread over the rough side of 2-inch ceramic tiles. *Crocc2* mutant alleles were obtained from the Zebrafish International Resource Center (ZIRC). Allele 20707 consists of an ENU induced C>T nonsense mutation mapped to exon 8 that encodes a premature stop codon at amino acid 272. Allele 20708 contains a C>T nonsense mutation in exon 14 that creates a premature stop at amino acid 585. Fish harboring either allele yield comparable bone phenotypes; only 20707 phenotypes are reported here. Both alleles were contributed to ZIRC by the Stemple Lab (Busch-Nentwich et al. 2013) and map positions are based upon Zebrafish genome assembly GRCz11.

Pedigree mapping

QTL mapping methods and results are described elsewhere (Parsons et al. 2016; Zogbaum et al. 2020). Briefly, genomic DNA was extracted from flank muscle tissue using DNeasy blood and tissue kits (Qiagen Inc., CA, USA), digested with the SbfI restriction enzyme, processed into RAD libraries as described (Chutimanitsakun et al. 2011), barcoded and sequenced using an Illumina HiSeq 2000 (Illumina, San Diego, CA) and single-read (1x100 bp) chemistry. Here we focus on a locus for lower jaw mechanical advantage, which mapped to an interval on linkage group (LG) 21, with a peak genotype-phenotype association at a marker on physical scaffold 31 @ 2,946,476Mb (fig. 2A). Since a F_3 hybrid cross allows for a relatively higher number of recombination events and mapping resolution, we used additional, unmapped, RAD-seq SNPs to assess genotypic effects along this scaffold at increasingly fine scales, using makers every ~0.5Mb (fig. 2C) and ~0.1-0.2Mb (fig. 2D). In addition, genetic divergence between wild-caught LF and TRC (imported directly from the lake) was explored, using a

panel of 3087 RAD-seq SNPs, and F_{ST} values following Nei (1987) and calculated in the R package HIERFSTAT. These fishes were genotyped following the same RAD procedures and SNP calling pipeline, and at the same time as the hybrids.

Immunohistochemistry

Immunostaining was performed with mouse anti-acetylated alpha tubulin (1:500; Sigma T6793) or rabbit anti-gamma tubulin (1:500; Sigma T6557). Amplification of T6793 signal was performed using donkey anti-mouse Biotin (1:100) and Alexa 488 Streptavidin Conjugate (1:1000) (Jackson Immunoresearch). Donkey anti-Rabbit Alexa 594 was used to visualize gamma tubulin antibodies. Briefly, animals were anesthetized and sacrificed using MS222 (Western Chemical, Inc.) and fixed for 1.5h in 4% paraformaldehyde, ph 7.4, at room temperature. For young zebrafish, 4dpf larval samples were permeabilized in acetone at -20C for 20 min followed by 1% Triton X-100 in PBS for 1 hour, and blocked in 5% donkey serum (Jackson Immunoresearch) in 0.1% Triton X-100 in PBS. For adult zebrafish, samples were embedded in 1.5% agar/5% sucrose and 20um cryosections were blocked for 1 hour before immunostaining. All Washes were performed in 0.1% PBS-Tween 20, pH 7.4. To prevent photobleaching, all samples were mounted using Vectashield with DAPI (H-1200; Vector Labs).

Geometric morphometrics

Adult zebrafish were cleared and stained using traditional methods (Potthoff 1984; Taylor and Van Dyke 1985). All dissections, and subsequent imagery, was performed using a Leica M165 FC microscope and attached Leica DFC450 camera (Leica Camera AG, Wetzlar, Germany). We imaged the lateral profile of the lower jaw

and dorsal surface (when premaxillae are protruding) of the kinethmoid (Hernandez et al. 2007) for morphological analyses. Geometric morphometric data were collected using Stereomorph (Olsen and Westneat 2015) in R (R Core Team 2018). In total, we summarized the lower jaw using 6 fixed and 4 semi-landmarks (sliding) and the kinethmoid using 4 fixed and 8 semi-landmarks (see Rohlf and Slice 1990; Gunz and Mitteroecker 2013, for more information on fixed/semi-landmarks).

Morphological data were aligned via generalized Procrustes superimposition (Goodall 1991) and then analyzed via ANOVA to test for significance in mean shape among homozygous genotype comparisons for both the lower jaw and kinethmoid. In all analyses, we compared null models (shape ~ size) to full models (shape ~ size + genotype) to control for the effects of size. Tests were conducted utilizing a randomized residual permutation procedure (RRPP) and the data were subjected to 10,000 random permutations (Collyer and Adams 2007, 2018; Collyer et al. 2015). All morphological analyses were performed using Geomorph v3.1 (Adams et al. 2014, 2018).

Quantitative Real-Time PCR (qPCR) and network

We purified RNA from homogenized whole heads of zebrafish excluding eyes and brain, between the ages of 3 months and 15 months, in Trizol (Invitrogen) using the phenol-chloroform method. We standardized resulting cDNA to 70ng/μL using a High-Capacity cDNA Reverse Transcription Kit (Applied Biosystems). To determine relative gene expression levels, we used a 10μL total reaction in triplicate using a QuantStudio3 Real-Time PCR System (Applied Biosystems). Each gene assessed was compared to expression levels of β-actin to determine relative expression levels via the ΔΔCT method (Livak and Schmittgen 2001). n=5 for all genes of each age group/genotype except 10-

15mos. mutant *ptch2* where n=4. We used the ANOVA model for statistical analyses in R.

In order to determine the covariation of gene sets in our qPCR dataset, we constructed gene networks in R. First, we used pairwise partial correlations with the ppcor package using the Pearson method to account for multicollinearity (table 2). We next used the iGraph package to perform and visualize network analyses for each dataset. These analyses weight the relationships between each gene based on the pairwise partial correlation value strengths. Correlations with a p value below 0.15 were included in the construction of the gene networks (fig. 6). The number of lines between each pair of genes indicates the strength of the covariation between them (i.e., 5 lines represents stronger correlation than 2).

Bone deposition analysis

Bone deposition experiments are described in detail elsewhere (Navon et al. 2020). Briefly, fish were anesthetized using MS-222 in cool water during injections and handling. They were injected with alizarin red [50 mg-fluorochrome/kg fish] at the first timepoint and with calcein green [0.5 mg-fluorochrome/kg fish] at the second timepoint, approximately 5 weeks apart. One week after the final fluorochrome injection, fish were euthanized with a lethal dose of MS-222 and stored in 95% ethanol at 4°C. Craniofacial bones and flank scales were dissected from the head and body, cleaned of surrounding soft tissue, flat mounted on glass slides, and imaged with a Zeiss Axioplan2 fluorescent apotome microscope. Bones were imaged in triplicate using a red fluorescent filter, a green fluorescent filter, and a DCIM bright-field view. Cichlid bones were imaged at 10x; zebrafish at 20x. Trunk scales were flat mounted and imaged in the same way. Bone

deposition was quantified by calculating the distance between the red and the green fluorochrome labels in each bone using Photoshop. Bone deposition was standardized for individual growth rate by regressing bone growth on scale growth and taking the residual values for downstream analysis. A series of ANOVAs using treatment and species (cichlids) or genotype (zebrafish) were performed in R (R Core Team 2018). Tukey's post-hoc analyses (i.e., TukeyHSD) were performed to identify significant pairwise differences.

Acknowledgements

The authors would like to acknowledge many individuals who provided support for this project, including C. Barba, B. Chhouk, and J. Courtney for fish husbandry, as well as L. Suttenfield, M. Chen, C. Lerose, A. MacManus, and L. Delorenzo for assistance during the initial characterization of the *crocc2* mutant. While their work didn't contribute data to this manuscript, the efforts of this excellent team of undergraduate researchers established an important foundation upon which this project arose. Finally, we thank members of the Albertson lab as well as the Friday fish and friends journal club for critical evaluation and input of these data. This research was supported by grants from the NSF (IOS-1558003) and NIH/NIDCR (R01 DE026446-01) to R.C.A..

Data Availability

The data underlying this article is available via Dryad Digital Repository.

References

Adams D, Collyer ML, Kaliontzopoulou A. 2018. Geomorph: Software for geometric morphometric analysis.

Adams DC, Collyer ML, Otarola-Castillo E. 2014. R: package, geomorph: Software for geometric morphometric analysishttp//cranr Proj.

Adzhubei I, Jordan DM, Sunyaev SR. 2013. Predicting functional effect of human missense mutations using PolyPhen-2. *Curr Protoc Hum Genet.* Chapter 7: Unit7.20.

Albertson RC, Streelman JT, Kocher TD. 2003. Directional selection has shaped the oral jaws of Lake Malawi cichlid fishes. *Proc Natl Acad Sci USA* 100(9):5252-7.

Albertson RC, Streelman JT, Kocher TD, Yelick PC. 2005. Integration and evolution of the cichlid mandible: the molecular basis of alternate feeding strategies. *Proc Natl Acad Sci USA* 102(45):16287-92.

Albertson RC, Yelick PC. 2007. *Fgf8* haploinsufficiency results in distinct craniofacial defects in adult zebrafish. *Dev Biol*. 306(2):505-15.

Albertson RC, Pauers MJ. 2019. Morphological disparity in ecologically diverse versus constrained lineages of Lake Malawi rock-dwelling cichlids. *Hydrobiologia* 832:153-174.

Alman BA. 2015. The role of hedgehog signalling in skeletal health and disease. *Nat Rev Rheumatol*. 11(9):552-60.

Arbour JH, López-Fernández H. 2014. Adaptive landscape and functional diversity of Neotropical cichlids: implications for the ecology and evolution of Cichlinae (Cichlidae; Cichliformes). *J Evol Biol.* 27(11):2431-42.

Berbari NF, O'Connor AK, Haycraft CJ, Yoder BK. 2009. The Primary Cilium as a Complex Signaling Center. *Curr Biol.* 19(13):R526-R535.

Bouton N, Witte F, Van Alphen JJM. 2002. Experimental evidence for adaptive phenotypic plasticity in a rock-dwelling cichlid fish from Lake Victoria. *Biol J Linn Soc.* 77(2):185-192.

Bradshaw AD. 1965. Evolutionary significance of phenotypic plasticity in plants. *Adv Gene.* 13:115-55.

Busch-Nentwich E, Kettleborough R, Dooley CM, Scahill C, Sealy I, White R, Herd C, Mehroke S, Wali N, Carruthers S, et al. 2013. Sanger Institute Zebrafish Mutation Project mutant data submission. ZFIN Direct Data Submission. (http://zfin.org).

Casanovas-Vilar I, van Dam J. 2013. Conservatism and adaptability during squirrel radiation: what is mandible shape telling us? *PLoS One* 8(4):e61298.

Chutimanitsakun Y, Nipper RW, Cuesta-Marcos A, Cistue L, Corey A, Filichkina T, Johnson EA, Hayes PM. 2011. Construction and application for QTL analysis of a restriction site associated DNA (RAD) linkage map in barley. *BMC Genomics* 12:4.

Collyer ML, Adams DC. 2018. RRPP : An r package for fitting linear models to high- -dimensional data using residual randomization. 2018:1772–79.

Collyer ML, Sekora DJ, Adams DC. 2015. A method for analysis of phenotypic change for phenotypes described by high-dimensional data. *Heredity (Edinb)* 115:357–65.

Cooper WJ, Parsons K, McIntyre A, Kern B, McGee-Moore A, Albertson RC. 2010. Bentho-Pelagic Divergence of Cichlid Feeding Architecture Was Prodigious and

Consistent during Multiple Adaptive Radiations within African Rift-Lakes. *PLoS One* 5(3):e9551.

Cooper WJ, Wernle J, Mann K, Albertson RC. 2011. Functional and Genetic Integration in the Skulls of Lake Malawi Cichlids. *Evol Biol.* 38(3):316-334.

Cooper WJ, Wirgau RM, Sweet EM, Albertson RC. 2013. Deficiency of zebrafish *fgf20a* results in aberrant skull remodeling that mimics both human cranial disease and evolutionarily important fish skull morphologies. *Evol Dev*. 15(6):426-41.

Dumont ER, Dávalos LM, Goldberg A, Santana SE, Rex K, Voigt CC. 2012. Morphological innovation, diversification and invasion of a new adaptive zone. *Proc R Soc B.* 279:1797–1805

Dumont ER, Samadevam K, Grosse IR, Warsi OM, Baird B, Dávalos LM. 2014. Selection for mechanical advantage underlies multiple cranial optima in new world leaf-nosed bats. *Evolution* 68(5):1436-1449.

Ehrenreich IM, Pfennig DW. 2016. Genetic assimilation: a review of its potential proximate causes and evolutionary consequences. *Ann Bot.* 117(5):769-79.

Gibert JM, 2017. The flexible stem hypothesis: Evidence from genetic data. *Dev Genes Evol.* 227:297–307.

Goetz SC, Ocbina PJR, Anderson KV. 2009. The Primary Cilium as a Hedgehog Signal Transduction Machine. *Primary Cilia* 94:199-122.

Goodall C. 1991. Procrustes methods in the statistical analysis of shape. *J R Stat Soc.* 53:285–339.

Gunter HM, Schneider RF, Karner I, Sturmbauer C, Meyer A. 2017. Molecular investigation of genetic assimilation during the rapid adaptive radiations of East African cichlid fishes. *Mol Ecol*. 26(23): 6634-6653.

Gunz P, Mitteroecker P. 2013. Semilandmarks: A method for quantifying curves and surfaces. *Hystrix It J Mamm.* 24(1):103–109.

Haycraft CJ, Banizs B, Aydin-Son Y, Zhang Q, Michaud EJ, Yoder BK. 2005. Gli2 and Gli3 localize to cilia and require the intraflagellar transport protein polaris for processing and function. *PLoS Genet.* 1(4):e53.

Hendrikse JL, Parsons TE, Hallgrimsson B. 2007. Evolvability as the proper focus of evolutionary developmental biology. *Evol Dev*. 9(4):393-401.

Hernandez LP, Bird NC, Staab KL. 2007. Using Zebrafish to Investigate Cypriniform Evolutionary Novelties: Functional Development and Evolutionary Diversification of the Kinethmoid. *J Exp Zool B Mol Dev Evol.* 308:625–41.

Hu Y-N, Albertson RC. 2017. Baby fish working out: an epigenetic source of adaptive variation in the cichlid jaw. *Proc Biol Sci*. 284(1860):20171018.

Irisarri I, Singh P, Koblmüller S, Torres-Dowdall J, Henning F, Franchini P, Fischer C, Lemmon AR, Lemmon EM, Thallinger GG, et al. 2018. Phylogenomics uncovers early hybridization and adaptive loci shaping the radiation of Lake Tanganyika cichlid fishes. *Nat Commun.* 9(1):3159.

Jamniczky HA, Boughner JC, Rolian C, Gonzalez PN, Powell CD, Schmidt EJ, Parsons TE, Bookstein FL, Hallgrimsson B. 2010. Rediscovering Waddington in the post-genomic age. *Bioessays* 32(7):553-558.

Livak KJ, Schmittgen TD. 2001. Analysis of relative gene expression data using real-time quantitative PCR and the 2(-Δ Δ C(T)) Method. *Methods* 25:402–408.

Long F. 2011. Building strong bones: molecular regulation of the osteoblast lineage. *Nat Rev Mol Cell Biol.* 13:27–38.

Manabu S. 2010. Jaw biomechanics and the evolution of biting performance in theropod dinosaurs. *Proc R Soc B.* 277:3327–3333.

Mason JM, Schmitz MA, Muller KM, Arndt KM. 2006. Semirational design of Jun-Fos coiled coils with increased affinity: Universal implications for leucine zipper prediction and design. *Proc Natl Acad Sci USA* 103(24):8989-94.

Mayr E. 1993. What was the evolutionary synthesis? *Trends Ecol Evol.* 8:31-33.

Moczek AP. 2008. On the origins of novelty in development and evolution. *Bioessays* 30(5):432-47.

Mohan S, Timbers TA, Kennedy J, Blacque OE, Leroux MR. 2013. Striated rootlet and nonfilamentous forms of rootletin maintain ciliary function. *Curr Biol.* 23(20):2016-22.

Nei M. 1987. *Molecular Evolutionary Genetics*. Columbia University Press, New York, NY. USA.

Nguyen AM, Jacobs CR. 2013. Emerging role of primary cilia as mechanosensors in osteocytes. *Bone* 54(2):196-204.

Navon D, Male I, Tetrault ER, Aaronson B, Karlstrom RO, Albertson RC. 2020. Hedgehog signaling is necessary and sufficient to mediate craniofacial plasticity in teleosts. *Proc Natl Acad Sci USA* 117(32):19321-19327.

Olsen A, Westneat M. 2015. StereoMorph: an R package for the collection of 3D landmarks and curves using a stereo camera set-up. *Methods Ecol Evol.* 6:351–56

Papachroni KK, Karatzas DN, Papavassiliou KA, Basdra EK, Papavassiliou AG 2009. Mechanotransduction in osteoblast regulation and bone disease. *Trends Mol Med.* 15(5):208-216.

Parnell NF, Hulsey CD, Streelman JT. 2012. The Genetic Basis of a complex functional system. *Evolution* 66(11):3352-66.

Parsons KJ, Robinson BW. 2006. Replicated evolution of integrated plastic responses during early adaptive divergence. *Evolution* 60(4):801-813.

Parsons KJ, Robinson BW. 2007. Foraging performance of diet-induced morphotypes in pumpkinseed sunfish (Lepomis gibbosus) favours resource polymorphism. *J Evol Biol.* 20(2):673-684.

Parsons KJ, Trent Taylor A, Powder KE, Albertson RC. 2014. Wnt signalling underlies the evolution of new phenotypes and craniofacial variability in Lake Malawi cichlids. *Nat Commun.* 5:3629.

Parsons KJ, Concannon M, Navon D, Wang J, Ea I, Groveas K, Campbell C, Albertson RC. 2016. Foraging environment determines the genetic architecture and evolutionary potential of trophic morphology in cichlid fishes. *Mol Ecol.* 25(24):6012-6023.

Pfennig DW, Wund MA, Snell-Rood EC, Cruickshank T, Schlichting CD, Moczek AP. 2010. Phenotypic plasticity's impacts on diversification and speciation. *Trends Ecol Evol.* 25(8):459-467.

Pigliucci M. 2005. Evolution of phenotypic plasticity: where are we going now? *Trends Ecol Evol.* 20(9):481-6.

Pigliucci M. 2007. Do we need an extended evolutionary synthesis? *Evolution* 61(12):2743-9.

Pigliucci M. 2008. Is evolvability evolvable? *Nat Rev Genet.* 9(1):75-82.

Pigliucci M. 2009. An extended synthesis for evolutionary biology. *Ann NY Acad Sci.* 1168:218-28.

Potthoff T. 1984. Clearing and staining techniques. *Ontog Syst Fishes* 1:35–37.

Powder KE, Cousin H, McLinden GP, Albertson RC. 2014. A Nonsynonymous Mutation in the Transcriptional Regulator *lbh* Is Associated with Cichlid Craniofacial Adaptation and Neural Crest Cell Development. *Mol Biol Evol.* 31(12):3113-3124.

Price TD, Qvarnstrom A, Irwin DE. 2003. The role of phenotypic plasticity in driving genetic evolution. *Proc R Soc B* 270(1523):1433-1440.

Qiu N, Xiao Z, Cao L, Buechel MM, David V, Roan E, Quarles LD. 2012. Disruption of Kif3a in osteoblasts results in defective bone formation and osteopenia. *J Cell Sci.* 125(8):1945-57.

R Core Team. 2018. R: A language and environment for statistical computing. R A Lang Environ Stat Comput.

Roberts RB, Hu Y-N, Albertson RC, Kocher TD 2011. Craniofacial divergence and ongoing adaptation via the hedgehog pathway. *Proc Natl Acad Sci USA* 108(32):13194-13199.

Rohlf FJ, Slice DE. 1990. Extensions of the Procrustes method for the optimal superimposition of landmarks. *Syst Zool.* 39:40–59.

Scheiner SM. 1993. Genetics and evolution of phenotypic plasticity. *Anna Rev Ecol Syst.* 24:35-68.

Schneider RF, Meyer A. 2017. How plasticity, genetic assimilation and cryptic genetic variation may contribute to adaptive radiations. *Mol Ecol*. 26(1):330-350.

Schlichting CD, Pigliucci M. *Phenotypic evolution. A reaction norm perspective*. 1998, Suntherland: Sinauer Associates.

Staab KL, Hernandez LP. 2010. Development of the cypriniform protrusible jaw complex in Danio rerio: constructional insights for evolution. *J Morphol*. 271(7):814-25.

Stauffer JRJ, van Snik-Gray E. 2004. Phenotypic plasticity: its role in trophic radiation and explosive speciation in cichlids (Teleostei: Cichlidae). *Animal Biology* 54:137-158.

Taylor WR, Van Dyke GC. 1985. Revised procedures for staining and clearing small fishes and other vertebrates for bone and cartilage study. *Cybium* 9:107–19.

Temiyasathit S, Tang WJ, Leucht P, Anderson CT, Monica SD, Castillo AB, Helms JA, Stearns T, Jacobs CR. 2012. Mechanosensing by the Primary Cilium: Deletion of Kif3A Reduces Bone Formation Due to Loading. *Plos One* 7(3).

Via S, Gomulkiewicz R, Dejong G, Scheiner SM, Schlichting CD, Vantienderen PH. 1995. Adaptive Phenotypic Plasticity - Consensus and Controversy. *Trends Ecol Evol.* 10(5):212-217.

Waddington CH. 1953. Genetic assimilation of an acquired character. *Evolution* 7:118–126.

Waddington CH. 1959. Canalization of Development and Genetic Assimilation of Acquired Characters. *Nature* 183(4676):1654-1655.

Wagner GP, Altenberg L. 1996. Perspective: Complex adaptations and the evolution of evolvability. *Evolution.* 50(3):967-976.

West-Eberhard MJ. 1989. Phenotypic plasticity and the origin of diversity. *Ann. Rev Ecol Evol Syst.* 20:249-278.

West-Eberhard MJ. *Developmental Plasticity and Evolution*. 2003, New York: Oxford University Press.

West-Eberhard MJ. 2005. Developmental plasticity and the origin of species differences. *Proc Natl Acad Sci USA* 102:6543-6549.

Westneat MW. 2004. Evolution of Levers and Linkages in the Feeding Mechanisms of Fishes. *Int Comp Biol.* 44(5):378–389.

Woolfson DN. 2005. The design of coiled-coil structures and assemblies. *Adv Protein Chem.* 70:79-112.

Wund MA, Baker JA, Clancy B, Golub JL, Foster SA. 2008. A test of the "Flexible stem" model of evolution: Ancestral plasticity, genetic accommodation, and morphological divergence in the threespine stickleback radiation. *Am Nat.* 172(4):449-462.

Xiao Z, Zhang S, Mahlios J, Zhou G, Magenheimer BS, Guo D, Dallas SL, Maser R, Calvet JP, Bonewald L, Quarles LD. 2006. Cilia-like structures and polycystin-1 in osteoblasts/osteocytes and associated abnormalities in skeletogenesis and *Runx2* expression. *J Biol Chem.* 281(41):30884-95.

Yang J, Liu X, Yue G, Adamian M, Bulgakov O, Li T. 2002. Rootletin, a novel coiled-coil protein, is a structural component of the ciliary rootlet. *J Cell Biol.* 159(3):431-40.

Yang J, Gao J, Adamian M, Wen XH, Pawlyk B, Zhang L, Sanderson MJ, Zuo J, Makino CL, Li T. 2005. The ciliary rootlet maintains long-term stability of sensory cilia. *Mol Cell Biol.* 25(10):4129-37.

Yuan X, Serra RA, Yang S. 2015. Function and regulation of primary cilia and intraflagellar transport proteins in the skeleton. *Ann N Y Acad Sci.* 1335:78-99.

Zogbaum L, Friend PG, Albertson RC. 2020. Plasticity and genetic basis of cichlid gill arch anatomy reveal novel roles for Hedgehog signaling. *Mol. Ecol.* Dec 5. doi: 10.1111/mec.15766. Online ahead of print.

Supplemental Data

Supplemental Table 1.1. Primer sequences for zebrafish bone markers and the house keeping gene, b-actin.

Danio rerio qRT-PCR Primer Sets	
Gene Name	**Sequence (5'-3)'**
Runx2b For	CAAACACCCAGACCCTCACT
Runx2b Rev	GTATGACCATGGTGGGGAAG
Osx For	GCGTCGATTCTGGAGGAG
Osx Rev	AATCTCGGACTGGACTGGTG
AP For	CAGTGGGAATCGTCACAACAA
AP Rev	CAACACAGTGGGCATAAGCA
Csf1ra For	GGCCAGCATAAGAACATCGT
Csf1ra Rev	CGTCATGGGTTCTGGAAAGT
TRAP For	CGTCCACTGACCACAGGAAGA
TRAP Rev	AAGGATCCTGACGTCTGATTGA
Col10a1 For	CCTGTCTGGCTCATACCACA
Col10a1 Rev	AAGGCCACCAGGAGAAGAAG
Col2a1a For	ATCCCATCATTTCACCTGGA
Col2a1a Rev	TCTGTCCCTTTGCACCAAGT
Ptch1 For	GCCGCATCCCAGGCCAACAT
Ptch1 Rev	CGTCTCGCGAAGCCCGTTGA
Ptch2 For	CATCCCATTCAAGGAGAGGA
Ptch2 Rev	GGCAGGGAATATCAGCAAAA
Gli1 For	GTCATCCGCACCTCTCCAAA
Gli1 Rev	ATGGTGCCCACAGACAGATG
B-Actin For	CAACAGGGAAAAGATGACACAGAT
B-Actin Rev	CAGCCTGGATGGCAACGT

Supplemental Figure 1.1. Amino acid sequence around the coding mutation identified in our genetic cross is highly conserved across African cichlids, but sequence homology begins to breakdown when other perciform and ray-finned fish species are included in the alignment (A-B). Notably, whereas all other African cichlids examined have an Alanine (A) at position 963, *Labeotropheus* has a Valine (V), which is similar to New World cichlids as well as most other perciform species. In fact, all perciforms possess either an A or V, and all fish species possess a non-polar, hydrophobic amino acid at this position (blue shade, B). While considerable sequence variation exists across this stretch of amino acids, the resulting coiled-coil motif is largely conserved, especially toward the N-terminus (C). The V in *Labeotropheus* results in few interruptions (black arrowheads) in heptad repeats (i.e., a-g) compared to other African cichlids (C). This region of Crocc2 is also associated with greater predicted structural variation, which suggests that this

portion of the protein may be less constrained, and/or a target of natural selection. All Crocc2 sequences were obtained from NCBI and the Ensembl genome browser.

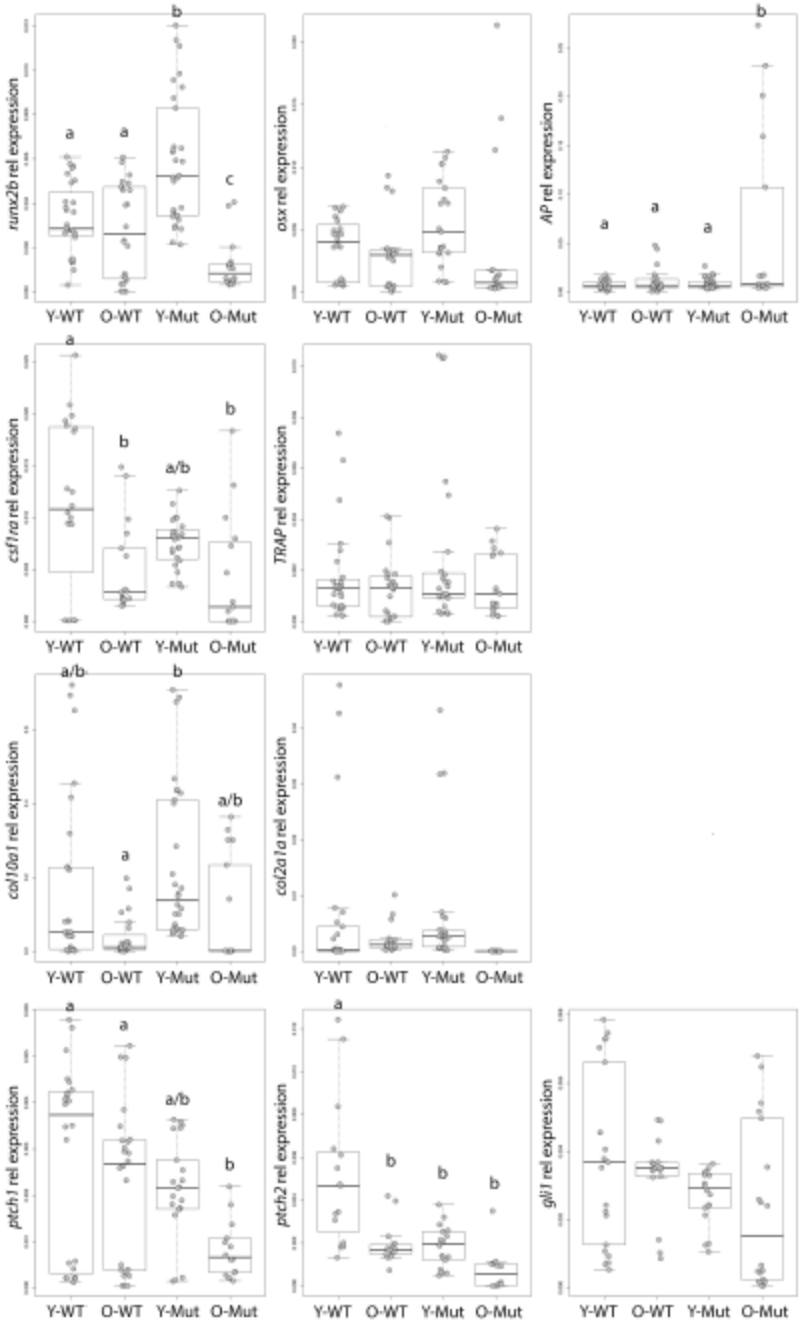

Supplemental Figure 1.2. Expression results from bone marker genes. Full results are shown for quantitative RT-PCR, organized in the same pattern as Table 1. Relative expression levels are shown for young adult WT (Y-WT), old adult WT (O-WT), young adult crocc2 mutants (Y-Mut), and old adult crocc2 mutants (O-Mut). Letters above the box plots refer to statistical groupings as determined by ANOVA followed by a Tukey's multiple comparison test. Graphs with no letters, did not exhibit any significant pair-wise differences.

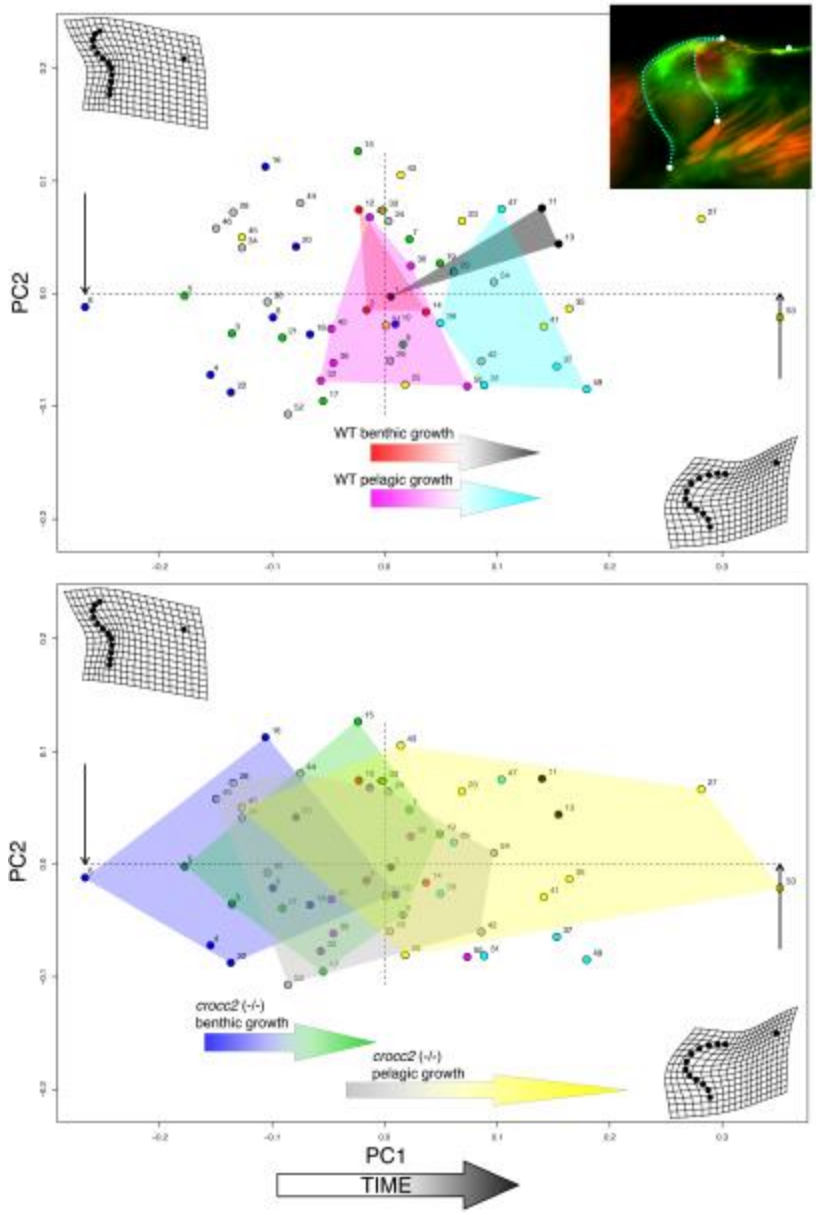

Supplemental Figure 1.3. Shape space from a morphometric analysis on CP shape. PC1 accounts for 63% of the variation, and mainly captures variation in growth over time, such that shape at time 0 (determined using the red fluorochrome, Alizarin Red) is associated with more negative PC1 scores, whereas shape at time 1 (green fluorochrome, Calcein Green) is associated with more positive PC1 scores. PC2 accounts for 17% of the variation in CP shape. The inset at top illustrates the digitizing scheme, with landmarks depicted as white dots and semi-landmarks arrayed along the blue dotted line. Note that each animal is measured twice - once for T0 shape (red), and once for T1 shape (green). In shape space, T1 and T0 are numbered consecutively, such that samples 1 and 2 correspond to individual one at times 1 and 0, respectively.

2. *CHAPTER 2*

CROCC2 PLAYS A KEY DEVELOPMENTAL ROLE IN CELL POLARITY AND CARTILAGE MORPHOGENESIS

AUTHORS: MARY PACKARD[1#], MICHELLE C GILBERT[2#], R CRAIG ALBERTSON[1]

1 Department of Biology, University of Massachusetts, Amherst MA 01003 USA.

2 Graduate Program in Organismic and Evolutionary Biology, University of Massachusetts, Amherst MA 01003 USA.

#Contributed equally to this work

SUBMITTED TO: Developmental Dynamics

FULL CITATION: Packard, M, MC Gilbert, RC Albertson. *In Prep.* CROCC2 plays a key developmental role in cell polarity and cartilage morphogenesis.

Introduction

Phenotypic constraints, whether functionally or genetically imposed, have been an area of interest to biologists for decades.[1,2] From an evolutionary perspective, variation may be considered the fodder upon which natural selection acts[3–5] and constraints affect the degree (or type) of variation that is allowable in a system, thereby influencing future evolutionary trajectories.[1,6–8] Constraints can be variable in strength and broadly placed along a continuum between absolute and relaxed.[9] For example, nearly all mammalian species possess seven cervical vertebrae (e.g., absolute constraint) but the size and shape of these vertebrae can vary substantially between taxa (e.g., relaxed constraint) with greatly elongated cervical vertebrae in giraffes and fused/stunted cervical vertebrae in cetaceans.[10] Furthermore, the concept of constraint is relative and taxon-specific, as within cetaceans, both the number *and* size of cervical vertebrae may be considered stringent.

An important, and longstanding, question in the field is when over ontogeny do constraints manifest.[11] Darwin (1859)[12] correctly noted that variation arising during early development is more likely to have correlative effects on other traits, increasing the probability of deleterious outcomes. Thus, from a developmental (and indeed clinical) perspective, constraints that limit the amount of permissible variation during early developmental stages are essential. For example, the craniofacial skeleton arises within the vertebrate embryo through a highly conserved set of molecular and cellular events.[13–23] Variation in these processes is generally low, and likely selected against, as they can lead to maladaptive and lethal phenotypes.[14,16,24–33] For this reason, it is thought that GWAS (genome wide association studies) on human craniofacial variation have

generally not implicated genes with known roles in early craniofacial development but rather genes that potentially sensitize progenitor cells to receive mechanical input from the environment.[28] However, there is also evidence from non-human vertebrate models to suggest that molecular and cellular shifts during early craniofacial development are associated with the production of adaptive phenotypic variation in adults.[34–39] Thus, craniofacial development and evolution appear to occur within the context of a fine balance between absolute and relaxed constraints on variation.

The ability of precursor cells to sense and respond to mechanical stimuli is essential for proper craniofacial development at multiple stages, and is an important source of variation.[40–44] Cellular and molecular mechanisms underlying mechanosensing are numerous but include primary cilia,[40,45–51] subcellular organelles found on nearly every vertebrate cell type, which are used to sense mechanical and biochemical stimuli and translate that information into biological signals inside the cell.[52] Primary cilia are composed of a microtubule-based axoneme that extends extracellularly (distally), a transition zone that controls trafficking of proteins between the specialized domain of the axoneme and the cell's cytoplasm, a basal body as the microtubule organizing center (MTOC) for the cilium, and a ciliary rootlet that extends proximally into the cell body where it is associated with various proteins, cytoskeleton, organelles, and the nucleus.[53–57] Relative to other ciliary components rootlets are understudied, particularly in the realm of development. Structurally, rootlets are composed almost entirely of the coiled-coil domain-containing protein Rootletin/Crocc/Crocc2 encoded by the ciliary rootlet coiled-coil genes *crocc/crocc2*.[57–59] The coiled-coil domains allow Crocc monomers to homodimerize to form striated filamentous rootlets that can be seen at the ultrastructural

level.[59–61] Studies in mice and fish suggest key roles for Rootletin/Crocc/Crocc2 in cilia maintenance, with cilia becoming lost over time in *Rootletin*[56] and *crocc2* mutants.[62] Work in invertebrate models support a structural role for rootlets in stabilizing the cilium; however, they also suggest more nuanced and direct roles in ciliary function, protein trafficking, and mechanosensing.[57,58,63]

In a recent study, we implicated *crocc2* and the ciliary rootlets in adult fish bone growth, homeostasis, and mechanosensing,[62] later developmental events that are likely related to the presence/absence of cilia. Here we set out to examine roles for this gene in orchestrating early developmental processes, specifically larval zebrafish craniofacial cartilage growth and development. We focus on stages when primary cilia remain present to gain a sense of how this gene may be required for proper formation of the pharyngeal skeleton, beyond its role in ciliary maintenance. Given the importance of the primary cilium in mechanosensing, and of mechanosensing as a source of phenotypic variation, we predict that this mutant may provide insights into the sources of early craniofacial variability and constraint. We present evidence that *crocc2* plays a pivotal role in regulating pharyngeal skeletal shape, as well as levels of shape variation (i.e., disparity). We show further that aberrant cartilage shapes are associated with discrete cell biological features and behaviors. Notably, these cellular defects were largely restricted to areas of direct mechanical input (i.e., muscle insertion). Taken together, our results suggest that rootlets may facilitate the ability of primary cilia to translate micro-environmental stimuli into proper cell behavior and tissue growth. When disrupted, variation increases and thus rootlets may also be instrumental in the regulation of variability in the craniofacial skeleton.

Results

Age-specific effects of the crocc2 mutation on larval craniofacial shape and disparity

Postembryonic development of cartilages and bone involves a complex interplay between numerous cell behaviors, and disruptions in any of these processes can lead to changes in shape or variability (Dash and Trainor, 2020).[64] To examine the effects of the *crocc2* mutant (*crocc2*$^{07/07}$) on craniofacial shape, we performed a geometric morphometric (GM) analysis on the pharyngeal skeleton in the ventral view at 4-, 7-, 12-, and 18-days post fertilization (dpf). Morphological analyses revealed significant differences in shape means between *crocc2*$^{07/07}$ and *crocc2*$^{+/+}$ at 4dpf ($Z = 2.15$; $p = 0.031$) and 12dpf ($Z = 1.88$; $p = 0.048$), and near significant differences at 7dpf ($Z = 1.56$; $p = 0.076$) and 18dpf ($Z = 1.49$; $p = 0.082$). Comparisons of mean shape between heterozygous animals (*crocc2*$^{+/07}$) and *crocc2*$^{+/+}$ siblings were not significant at any time point, nor were differences detected between homozygous mutants and heterozygous animals, except for the 7dpf comparison ($Z = 5.07$; $p = 0.0001$). Deformation grids depicting mean shapes of each genotype over larval development describe both global and local variation, including the relative size of Meckel's cartilage (MC), the positioning of MC relative to the ceratohyal (CH) cartilage, and the width of the branchial region between the left and right hyosymplectic (HS) cartilages (Figure 1).

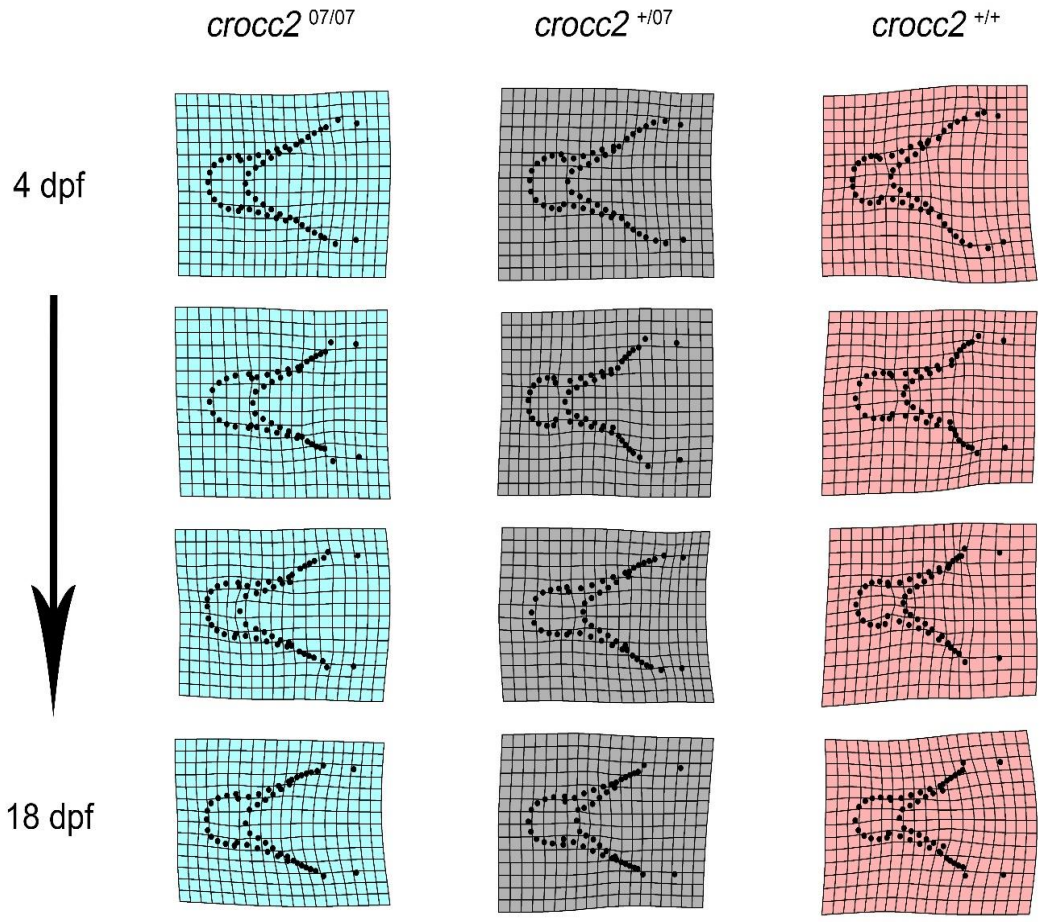

Figure 2.1. Deformation grids suggest differences in the mean shape of larval crocc2 $^{07/07}$ throughout the four time periods investigated. Each genotype (Mutant, blue = crocc2$^{07/07}$, Heterozygous, grey = crocc2$^{+/07}$, Wild-type, red = crocc2$^{+/+}$) is represented by a specific color that can be matched to all geometric morphometric analyses presented here. Top row represents 4dpf, bottom row represents 18dpf. Deformation grids are aligned along the center of their standalone axis for accurate interpretation of morphological differences.

Next, we examined and compared the developmental trajectories of each genotype. Plotting trajectories in principal component (PC) space revealed slight differences in mean shape at each stage, with homozygous mutants exhibiting generally more negative scores, on average, along PC1 and PC2 compared to heterozygous and wild-type siblings at each stage (Figure 2). As a result, the *crocc2$^{07/07}$* developmental

trajectory was shifted in PC space, a pattern that is supported quantitatively by an ANOVA model (i.e., shape ~ size + genotype x age), where each variable had a

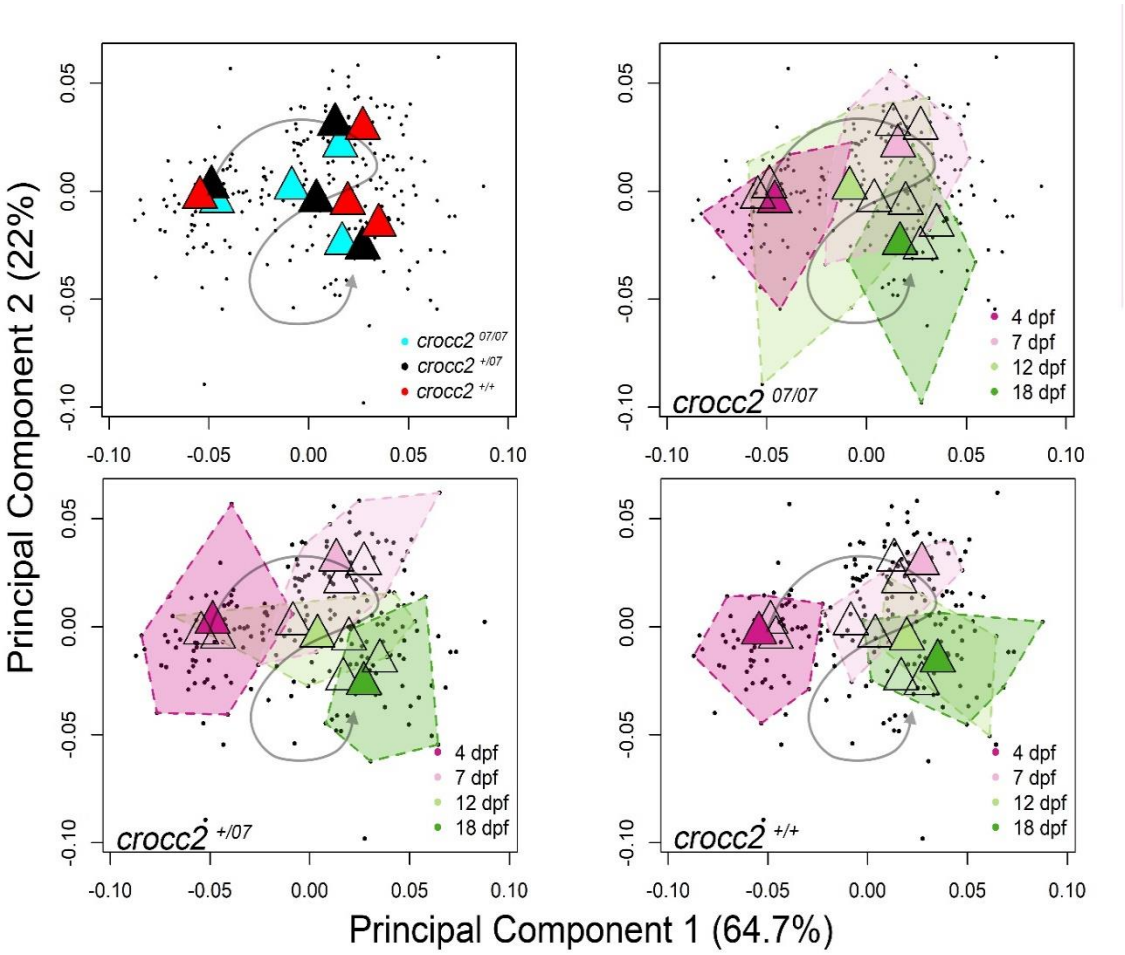

Figure 2.2. Trajectory analysis suggests that mean shapes, and variation around the mean, appear similar at 4dpf, but *crocc2*$^{07/07}$ means diverge at 7dpf, peak at 12dpf, and possibly recover by 18dpf. Grey points represent individual specimens, colored triangles represent the mean shape of genotype:age groups. Top left illustrates the mean paths of all three genotypes (red = *crocc2*$^{+/+}$, black = *crocc2*$^{+/07}$, blue = *crocc2*$^{07/07}$), with time periods progressing from 4dpf to 18dpf along the grey pathway. The remaining three panels highlight morphospace occupancy, for each genotype, throughout early ontogeny. The colors represent the age of the specimens (magenta = 4dpf, light pink = 7dpf, light green = 12dpf, darker green = 18dpf).

significant effect on craniofacial shape, including the genotype-by-age interaction ($Z=3.9354$, $p = 0.0003$). However, pairwise comparisons of path distances, vector correlations, and trajectory shapes revealed no significant differences between genotypes

($p > 0.15$ for all pairwise comparisons). Taken together, these data suggest that shapes are different at each stage (to varying degrees), leading to a shift in developmental trajectories, but that the three genotypes are developing along parallel routes (Figure 2).

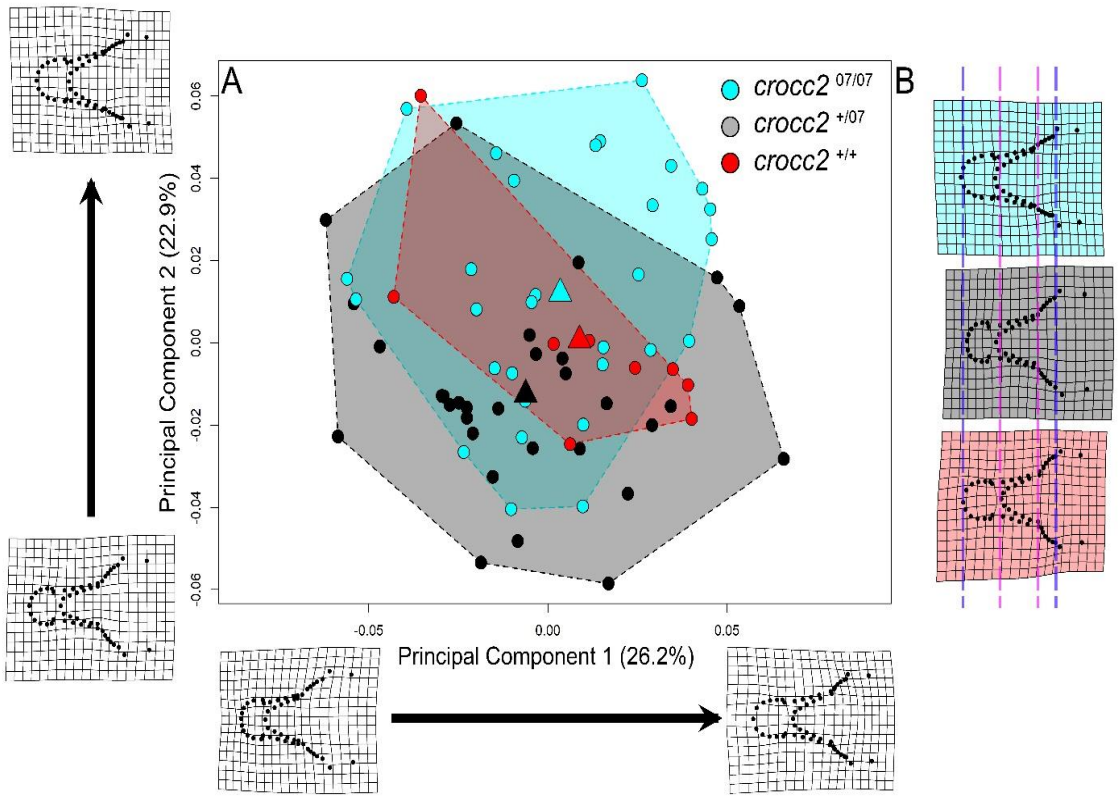

Figure 2.3. Principal component analysis of 7dpf zebrafish larvae shows increased variability and deviation of mean shape in *crocc2*$^{07/07}$. (A) Principal component plot of 7dpf specimens, demonstrating morphospace occupancy by each genotype. Genotypes are color-coded (blue = *crocc2* $^{07/07}$, grey = *crocc2*$^{+/07}$, red = *crocc2*$^{+/+}$), circles represent individual specimens, triangles represent group means, and convex hull boundaries represent the outermost regions of morphospace occupied by each genotype. (B) Mean deformation grids for each genotype, color coded to match the scheme used throughout. These means can be used to visualize the overall differences represented by the triangles in panel A. From left to right, hashed lines represent the anterior margin of Meckel's cartilage, anterior margin of the ceratohyal, the articulation of the palatoquadrate and ceratohyal, and the posterior margin of the hyosymplectic. Deformation grids were aligned via the posterior margin of the hyosymplectic to aid in *relative* comparisons.

Finally, we compared magnitudes of shape variation between genotypes, and found differences at 7dpf, but not at other ages. Specifically, we found that Procrustes

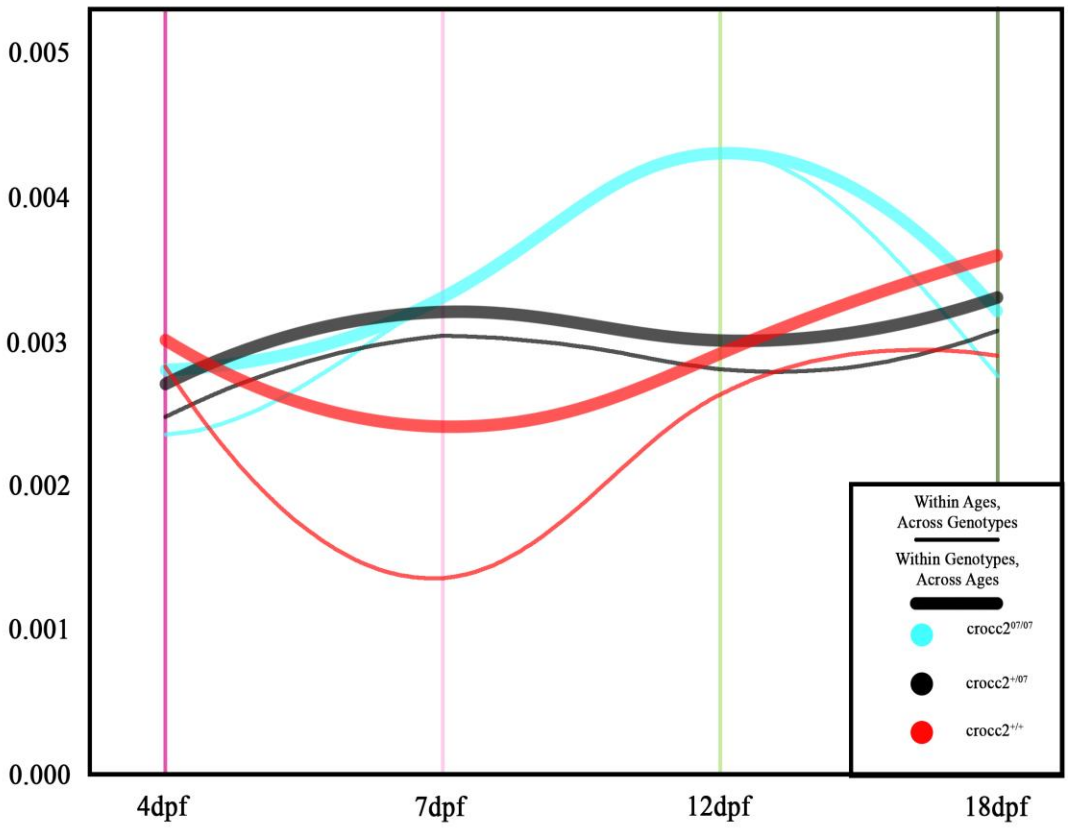

each stage. Thin lines represent variances calculated within ages for each genotype. The trends for each calculation are the same, and show that variances are the same across all genotypes at 4 and 18dpf, but display opposite patterns in wild-type and mutant siblings between these two stages. Specifically, variance decreases in wild-type animals (consistent with canalization) and increases in animals with the mutant allele (consistent with a loss of canalization).

variances in both homozygous mutants and heterozygous animals at 7dpf were over twice that in wild-type siblings (*crocc2*$^{07/07}$= 0.00332 versus *crocc2*$^{+/+}$ = 0.00136, p = 0.0006; *crocc2*$^{+/07}$= 0.00304 versus *crocc2*$^{+/+}$ = 0.00136, p = 0.0041). Procrustes variances in homozygous mutants and heterozygous animals did not differ from one another (p = 0.494). This quantitative metric was evident in the 7dpf PC plot (Figure 3 A), where mean shapes were similar (Figure 3B), but the distribution of individuals was nearly three times greater in *crocc2*$^{07/07}$ and *crocc2*$^{+/07}$ compared to *crocc2*$^{+/+}$. When examining shape

variance within genotypes over time, other notable trends emerged (Figure 4). Specifically, in wild-type animals, variance decreased between 4-7dpf (0.0030 vs. 0.0024), returned to 4dpf levels by 12dpf (0.0029), and increased again at 18dpf (0.0036).

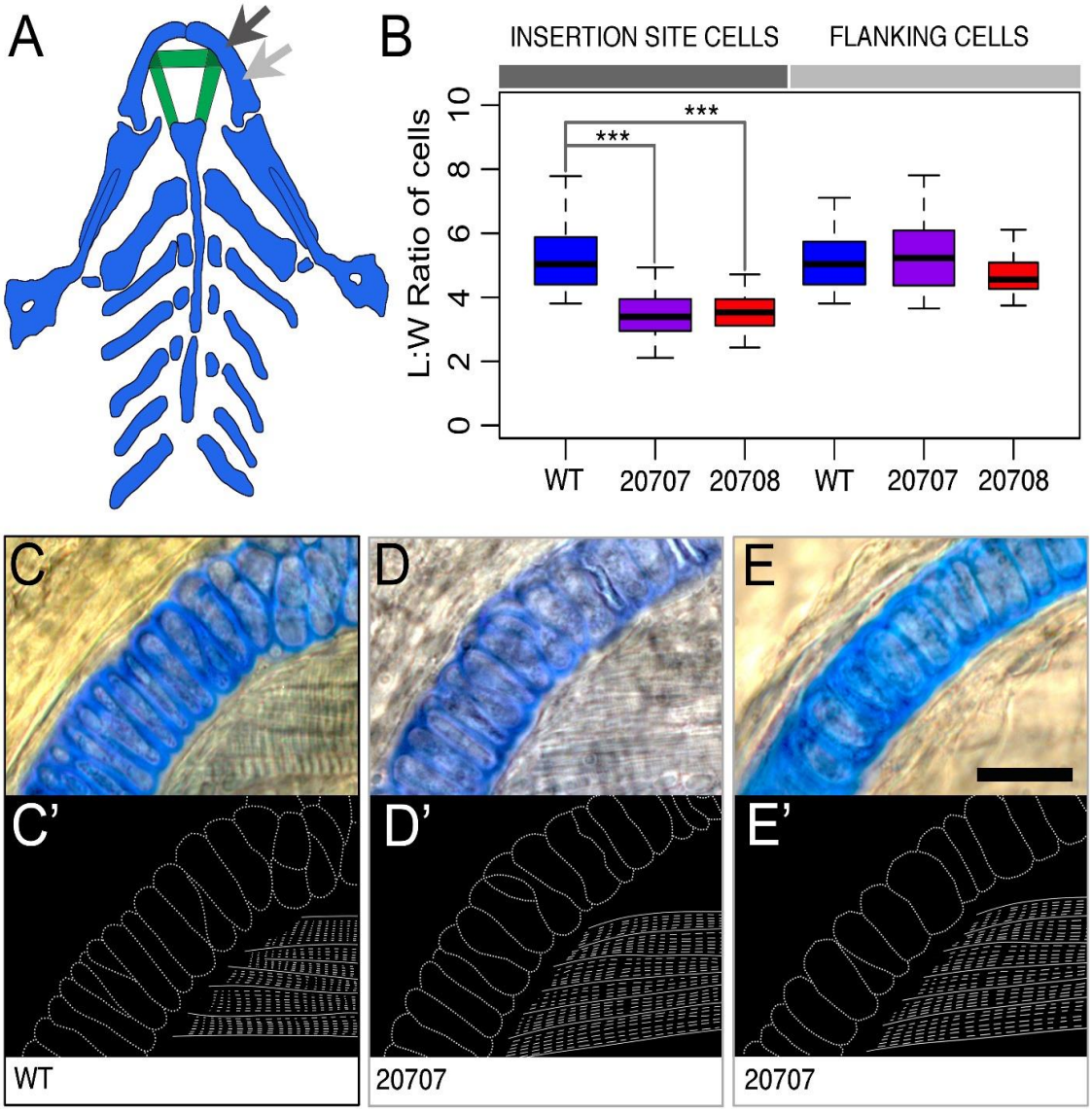

Figure 2.5. Cell phenotypes in early larval cartilage elements are influenced by soft tissue insertion sites. (A) At 5dpf, the zebrafish mandibular skeleton is composed primarily of cartilages (blue) with functional muscles (green) and ligaments that insert into the cartilages. At the cellular level, we focused on Meckel's cartilage (MC) at regions of soft tissue insertion (dark grey arrow) and flanking region cells (light grey arrow). Individual Alcian blue-dyed larval cartilage cells (representative examples shown in C-E) were compared between crocc2$^{+/+}$ (WT), crocc2$^{07/07}$ (20707) and crocc2$^{08/08}$ (20708). Panels in C'-E' show tracings of the examples to highlight muscle positions relative to individual cells and demarcate individual cell shapes. (B) Box plots show a significant reduction in cellular L:W ratio specific to only the insertion

site cells in both of the crocc2 alleles (*** = p<0.0001). In contrast, there was no difference in L:W ratio between crocc2$^{+/+}$ and either crocc2 allele at the flanking region cells. Scale Bar = 20μm.

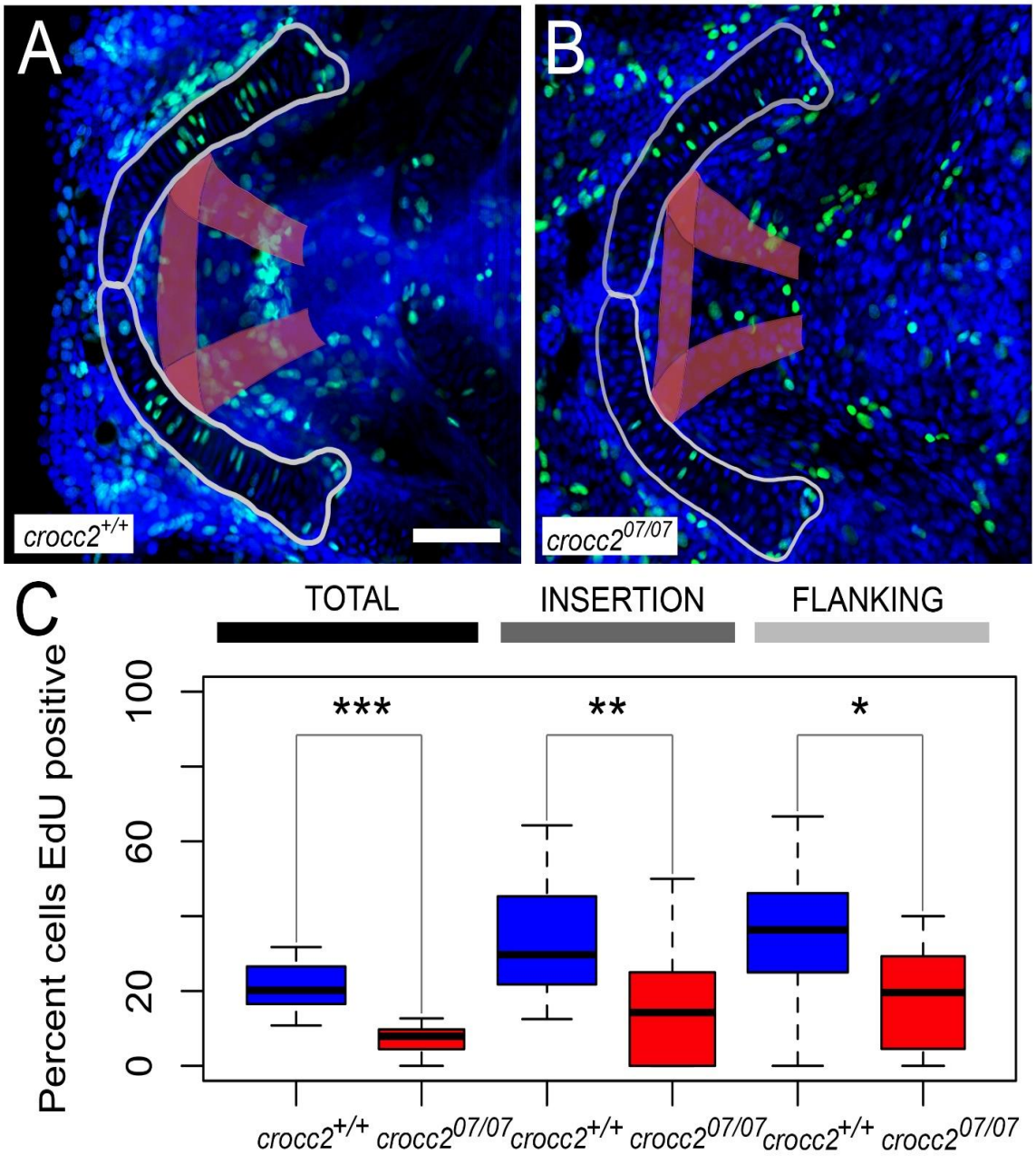

Figure 2.6. Cell proliferation is disrupted across MC in *crocc2$^{07/07}$* in 6dpf larvae. (A-B) EdU fluorescence (green) indicates cells that underwent mitotic division between 5.5 and 6dpf in (A) *crocc2$^{+/+}$* and (B) *crocc2$^{07/07}$*. Individual cells can be identified by their cell nuclei (DAPI, blue). MC elements are delineated in grey and the position of the muscles and their insertion sites is shown by the red overlay. (C) Box plots show the percentage of cells that are positive for EdU in *crocc2$^{+/+}$* (blue) and *crocc2$^{07/07}$*(red) across MC, at insertion site cells, and at flanking cells with mutant alleles showing significant reductions in proliferation across MC at both insertion and flanking regions. (* = p < 0.05; ** = p < 0.01; *** = p < 0.0001). Scale bar = 50 μm.

Thus, variation is reduced in wild-type animals between 4-7dpf, and then steadily increases from 7-18dpf. Alternatively, in homozygous mutants disparity increased between 4-12dpf, before returning to a near wild-type value by 18dpf. Heterozygous animals exhibited an intermediate pattern, whereby shape variance increased between 4-7dpf, but returned to a wild-type value by 12dpf, earlier than in homozygous mutants (Figure 4).

Together, our shape analyses show that the *crocc2* mutation results in subtle differences in craniofacial shape at all stages, and a marked increase in shape variation at 7dpf that recovers by 18dpf. Thus, *crocc2* appears to function in canalizing craniofacial development and growth across these early larval stages. Since cartilage growth is orchestrated by discrete cellular behaviors,[18,22,65–69] we next examined chondrocyte phenotypes in *crocc2* mutants.

Early larval crocc2 mutants exhibit aberrant cartilage cell shape in areas subjected to mechanical input.

The shape of individual chondrocytes can provide important clues about cellular activity and/or maturation state.[65,70–73] We therefore quantified cell shape in early larval cartilages, focusing on MC at 5dpf. Furthermore, to assess putative roles for mechanical input we drew a distinction between MC cells at sites of direct muscle insertion ("insertion site") and the region immediately adjacent and proximal to this region ("flanking site"). Figure 5A shows a simplified schematic of the larval mandible at 5dpf,

a time where the functional mandibular skeleton is primarily made up of cartilage (blue), and soft tissue (e.g., muscles, green). As expected,[22] by 5dpf wild-type chondrocytes were organized as elongated stacks of cells (Figure 5C, C'), and we found no difference in the L:W ratio of chondrocytes between the insertion sites and flanking regions (Figure 5B, blue boxes; n = 30, p = 0.999). In comparison, the L:W ratio at the insertion sites significantly differed between wild-type zebrafish (blue, n = 30) and animals that were homozygous for two *crocc2* mutant alleles (*crocc2*$^{07/07}$ vs. *crocc2*$^{+/+}$ p < 0.0001, purple, n = 40; *crocc2*$^{08/08}$ vs. *crocc2*$^{+/+}$ p < 0.0001, red, n = 27). However, cells in the flanking region showed no difference in L:W ratio between *crocc2*$^{+/+}$ and both mutant lines (*crocc2*$^{07/07}$, p = 0.8956; *crocc2*$^{08/08}$, p = 0.4769). Differences in cartilage cell shape appeared to be largely due to an increase in cell width (Figure 5C-E; p < 0.005 for both *crocc2*$^{07/07}$ and *crocc2*$^{08/08}$ vs. *crocc2*$^{+/+}$), with little to no change in the length of cells (Figure 5C-E; p = 0.072 for *crocc2*$^{07/07}$ and p = 0.068 for *crocc2*$^{08/08}$ vs. *crocc2*$^{+/+}$). Cartilage cell shapes between the mutant alleles did not differ at either the insertion site (for L:W ratio, p = 0.9672) or flanking sites (for L:W ratio, p = 0.0781) (Figure 5B). Finally, cells at the insertion site for both *crocc2* alleles were significantly more rounded than flanking cells (ie: lower L:W ratio, Figure 5B; p < 0.001 for each comparison). These results suggest that *crocc2* is necessary, specifically at the insertion site, to maintain proper cartilage cell shape. Since both mutant alleles exhibited similar cellular phenotypes, we focused on *crocc2*$^{07/07}$ moving forward.

Crocc2 *mutant larvae exhibit reduced cell proliferation*

Following convergence and extension of MC cells, growth during the larval period occurs primarily by way of cell division.[65,72] We therefore compared proliferation

in *crocc2*$^{07/07}$and *crocc2*$^{+/+}$ larvae using ethynyl deoxyuridine (EdU). The wild-type pattern of proliferation that resulted from an overnight EdU pulse from 5.5-6dpf is shown

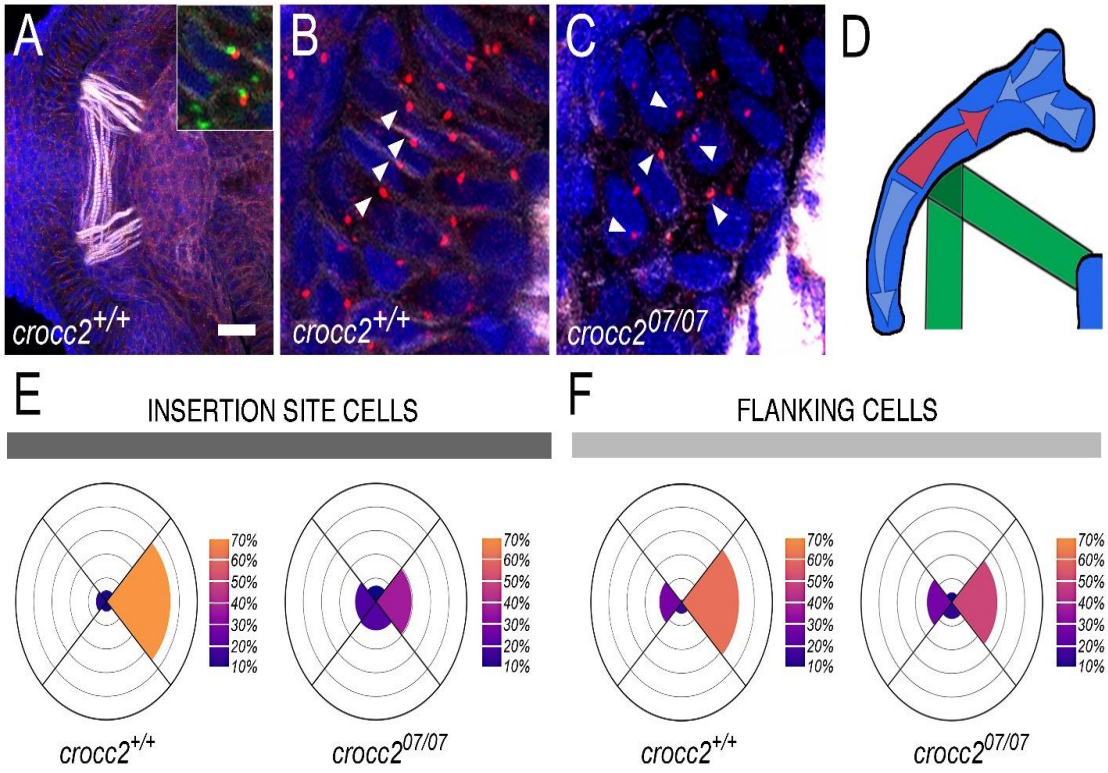

Figure 2.7. Crocc2 serves to maintain planar cell polarity across the muscle insertion sites. (A) Low magnification confocal projection showing muscle fibers (white, phalloidin) inserting into bilateral MC elements. Individual cells are visible by staining of cortical actin at cell boundaries (white, phalloidin), and cell nuclei (blue, DAPI). Ciliary basal bodies (BBs) are labelled (red, anti-gamma-Tubulin). The insert in (A) shows a high magnification of co-labelling between the ciliary axoneme label (green, anti-Acetylated alpha Tubulin) and BBs (red). (B-C) High magnification of muscle insertion site cells of 66hpf *crocc2*$^{+/+}$ and *crocc2*$^{07/07}$ larvae with white arrowheads indicating BB positions relative to each individual cell. (B) *crocc2*$^{+/+}$ animals show BBs primarily positioned on the most proximal side of each cell. (C) At *crocc2*$^{07/07}$ muscle insertion site cells, BB positions appear to be randomized. (D) Polarity map showing the characteristic orientation of PCP (arrows) across regions of MC in wild type samples. Note the switch in polarity (start of red arrow) at the distal-most edge of the muscle (green) insertion site. (E-F) Circular histograms (Roseplots) with quadrants representing cell surface positions (top = rostral; bottom = caudal; right = proximal; left = distal). (E) At muscle insertion sites, the majority of *crocc2*$^{+/+}$ BBs are on the proximal side of the cell (70%) and in *crocc2*$^{07/07}$ the polarity is more randomized. (F) At flanking sites BBs are oriented proximally in *crocc2*$^{+/+}$ and this orientation is disrupted in *crocc2*$^{07/07}$, albeit to a lesser degree than in insertion site cells. Scale bar = 20 μm in A, 7 μm in the insert in A, and 5 μm in B and C.

in Figure 6A. Twenty percent of cells in *crocc2*$^{+/+}$ (n = 28, blue boxes) show EdU fluorescence with an equal proportion showing EdU signal between the insertion and

flanking regions (Figure 6A, C; p = 0.9835). In *crocc2*$^{07/07}$ (n = 21, red boxes) there was a marked reduction in the overall percentage of EdU fluorescence-positive cells across the entirety of MC (Figure 6B, C) (p < 0.0001). Differences in proliferation between *crocc2*$^{+/+}$ and *crocc2*$^{07/07}$ were observed at both insertion (Figure 6C, p = 0.0089) and flanking sites (Figure 6C, p = 0.0262). Similar levels of proliferation were observed between the insertion and flanking regions in mutant animals (p = 0.9261). Taken together, these data reveal a requirement for *crocc2* in cell proliferation across MC.

Crocc2 *mutant larvae exhibit randomized cell polarity*

Planar Cell Polarity (PCP), the coordination of cell polarities to align in the same direction across a tissue, plays an important role in regulating cell behaviors and phenotypes, and is necessary for proper tissue and organ development.[74–78] Given the abnormal shape of MC chondrocytes in *crocc2* mutants, we set out to determine the state of planar cell polarity (PCP). PCP is established by 66hpf in MC and organized into domains[22,72] where regions of soft tissue insertion correlate with a switch in the direction of polarity (Figure 7D, red arrow). To assess tissue polarity across the cells of MC, we identified individual cells and muscle insertion sites (Figure 7A-C) by labeling cell boundaries and muscle fibers (white, phalloidin), cell nuclei (blue, DAPI), and MTOCs/ciliary basal bodies (BBs) (red, anti-gamma-Tubulin) and quantifying BB positioning relative to each cell as in Le Pabic et al (2014) and Ling et al., (2017).[22,72] The inset in Figure 6A shows the colocalization of basal bodies (red), with a ciliary axoneme immunolabel (green: anti-Acetylated alphaTubulin, AaT), demonstrating that anti-gT puncta in MC cells correspond to ciliary MTOCs. In agreement with previous

reports,[22] we found ciliary BBs within both insertion site and flanking site cells MC were largely positioned proximally in wild-types (Figure 7B arrowheads, E, and F; Red arrow in 7D). However, in mutant insertion site cells, the orientation of primary cilia was randomized (Figure 7C arrowheads, E), a pattern that was statistically distinct from wild-type siblings ($X^2 = 37.717$, $p < 0.001$). Although the randomization phenotype in mutants appears more severe at the insertion site compared to flanking cells, polarity in mutant cells from the flanking region was also distinct from wild-type (Figure 7F) ($X^2 = 12.90$, $p = 0.005$). These results support an important role for *crocc2* in the establishment and/or maintenance of PCP.

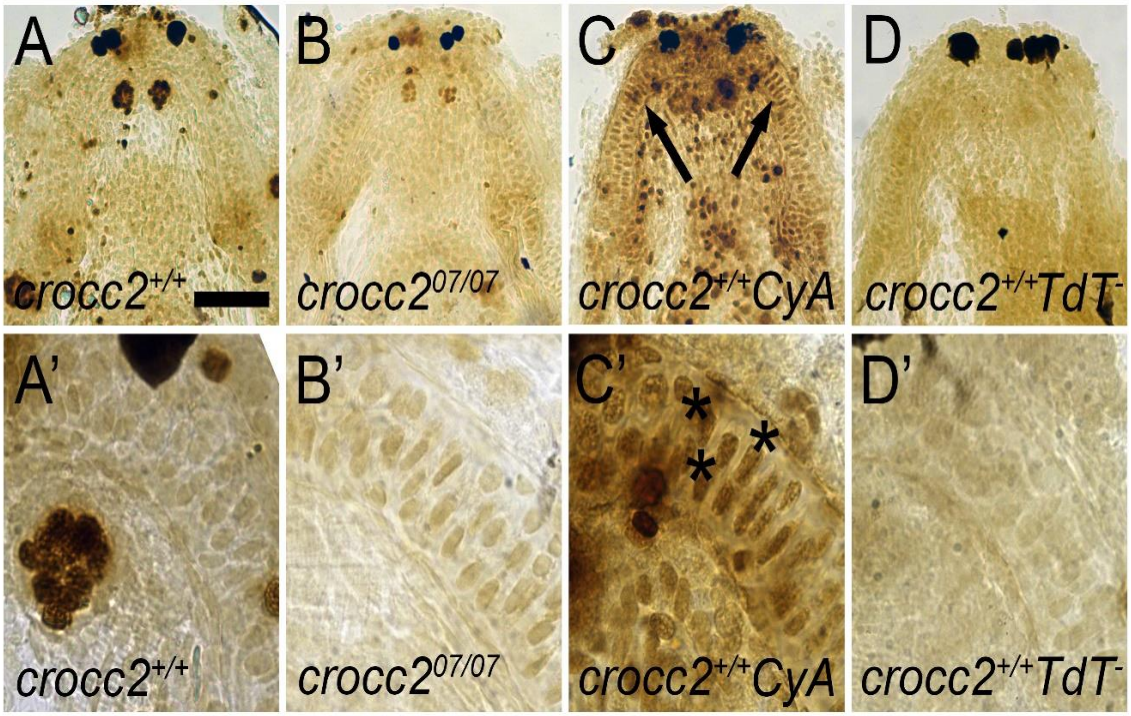

Figure 2.8. TUNEL staining shows no increase in apoptotic cell death in *crocc2*$^{07/07}$ larval cartilages. (A-D) Low and (A'-D') high magnification ventral views of 7dpf larval mandibles showing dark staining in apoptotic cells as detected using the TUNEL method. In the wild type (*crocc2*$^{+/+}$; A and A') a few darkly labelled cells are seen throughout the mandible as compared to no TUNEL staining in the negative control *crocc2*$^{+/+}$ samples that were not exposed to the TUNEL reaction enzyme (TdT$^-$; D and D'). In the positive control samples (CyA; C and C'), *crocc2*$^{+/+}$ larva incubated in cyclopamine show numerous darkly stained cells both throughout the mandible and in MC cells (black arrows in C and *s in C'). MC cells in *crocc2*$^{07/07}$ (B and B') do not exhibit TUNEL staining. Scale Bar = 50 μm for A-D and 10 μm for A'-D'.

Crocc2 *mutant larvae do not exhibit increased cell death*

Cell death is a critical part of organismal development.[79–84] During endochondral bone formation, in particular, terminally differentiated chondrocytes become hypertrophic, whereby they adopt a more circular and enlarged shape, before undergoing programmed apoptotic cell death. The abnormally circular and large cells we observed in 5dpf mutants, coupled with the decrease in cell proliferation is consistent with cells prematurely entering a hypertrophic state. In addition, decreased cell proliferation in mutants could be due to cell death. We therefore sought to ascertain whether *crocc2* mutants exhibited increased cell death by labelling larval cartilages using TUNEL staining at 5dpf and 7dpf. While positive control, cyclopamine (CyA) treated fish, showed a clear increase in TUNEL labeled cells within and around MC (Figure 8C, C', n=14), the amount of labeling in homozygous mutants (Figure 8B, B', n=10) was indistinguishable from that in wild-type siblings (Figure 8A, A', n = 12) and negative control samples (Figure 8D, D', n=6). Thus, we did not detect signs of abnormal apoptosis in *crocc2* mutants.

Crocc2 *mutant larvae exhibit normal bone patterning*

Craniofacial bone formation depends on proper patterning of the cartilaginous template.[64,85–87] Within MC, it has been shown that a population of osteoblasts originates from within the cartilage to give rise to the overlying dentary bone.[88] We have also recently demonstrated that *crocc2* mutants exhibit aberrant bone shape as adults, particularly the lower jaw.[62] Given these lines of evidence, we sought to understand whether dentary bone formation and/or patterning was affected in homozygous mutants.

Using Alizarin Red staining and fluorescence microscopy, we found little difference in the size or positioning of the dentary bone in wild-type and mutant siblings (Figure 9).

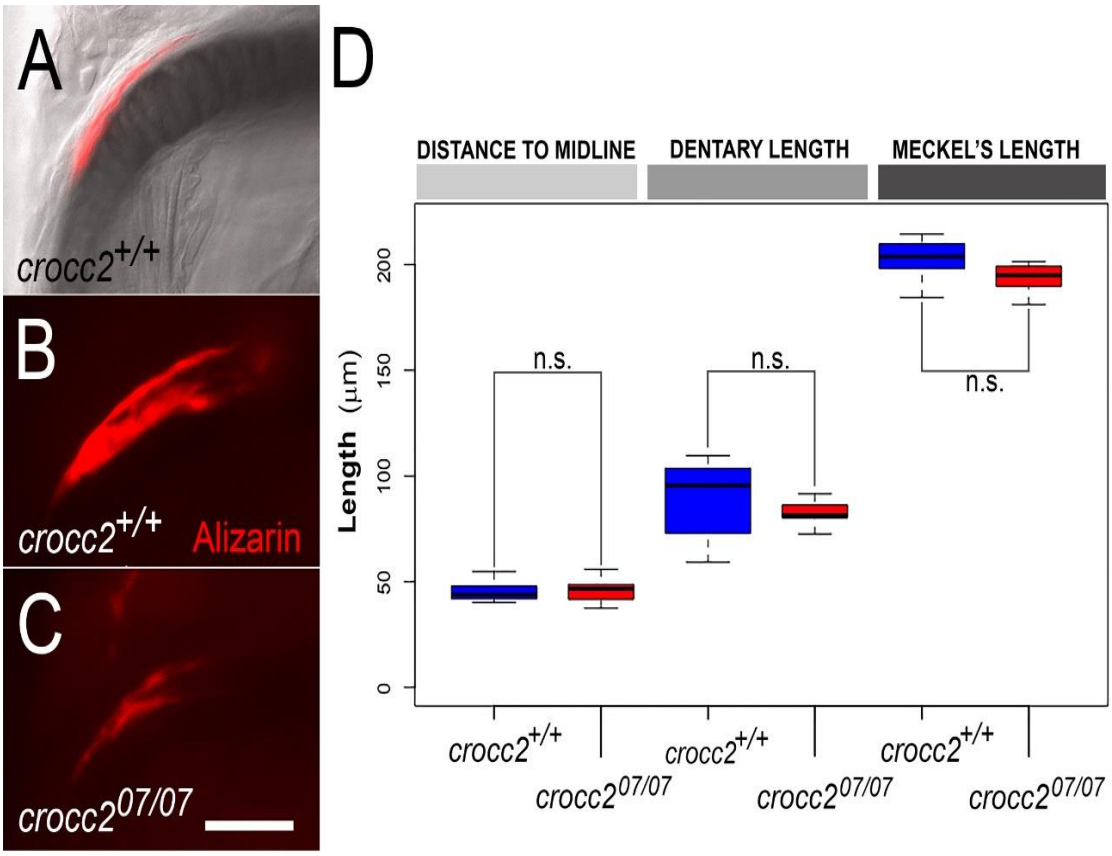

Figure 2.9. Patterning of nascent dentary bone shows no difference between *crocc2*$^{+/+}$ and *crocc2*$^{07/07}$at 5dpf, despite differences in mineralization. (A) A single optical section showing Alizarin Red fluorescence overlying an Alcian Blue dye-labelled MC cartilage element (greyscale) in *crocc2*$^{+/+}$ and (B) a projected confocal image of total Alizarin fluorescence (red) at a single *crocc2*$^{+/+}$ MC element. Each demonstrate the characteristic arch morphology and placement of the newly forming dentary bone alongside MC as of 5dpf. (C) A representative projected confocal image of total Alizarin in *crocc2*$^{07/07}$ demonstrates how the dentary, although it is less mineralized compared to age matched *crocc2*$^{+/+}$ samples, shows the same overall patterning of bone position and length as in wild-type (B). (D) Box plots under the light grey line demonstrate no significant difference (n.s.) in the average distance from the MC midline to the start of the distal edge of the dentary between *crocc2*$^{+/+}$ (B, blue box in D) and *crocc2*$^{07/07}$ (C, red box in D). Box plots under the medium grey line in D show the dentary bone extends the same overall length between the two genotypes. Under the dark grey line box plots show no difference in the average overall length of the MC elements measured. Scale bar = 50 μm.

Specifically, at 5dpf there was no difference between wild-type (Figure 9B, n = 12) and mutant (Figure 9C, n = 7) in the total length of the dentary (Figure 9D, p = 0.613), or in

the location of the dentary relative to the midline of MC (Figure 9D, $p = 0.892$). However, despite the observation that *crocc2* mutant osteoblasts appear to deposit bone in a largely wild-type pattern, we noted apparent differences in the extent of mineralization between genotypes, whereby mutants exhibited bones with reduced, and generally aberrant, Alizarin Red staining (Figure 9C). Whether this phenotype is due to a developmental delay or other, primary mechanism, remains to be determined.

Discussion

Reduced canalization in a developmental program can be maladaptive at the individual level but it can also contribute to greater phenotypic variation, and thus increase evolvability, at the population-level. Here, we demonstrate a requirement for *crocc2* at early larval stages in regulating zebrafish cartilage cell shape, proliferation, and polarity. These cell-specific phenotypes are associated with aberrant pharyngeal cartilage shapes, and increased variability at later larval stages. We hypothesize that these *crocc2* phenotypes are associated with a reduced ability of cartilage cells to sense and/or respond to the mechanical environment, as defects are most pronounced at the point of muscle insertion. Our model specifically postulates a mechanosensing role for Crocc2 in the ciliary rootlets (Figure 10, step 1), which in turn influences the orientation of cell polarity at the site of muscle insertion with subsequent downstream effects on cartilage morphogenesis (Figure 10).[44,53–55,57–59,61,89–102]

Functions for* crocc2 *during cartilage development

We propose that the cartilage defects described for *crocc2* mutants are based, at least in part, on impaired mechanosensing (Figure 10). This assertion is based on several lines of evidence. First, we note that cell-level defects in *crocc2* mutants are more conspicuous at the point on muscle insertion on MC compared to adjacent regions, and

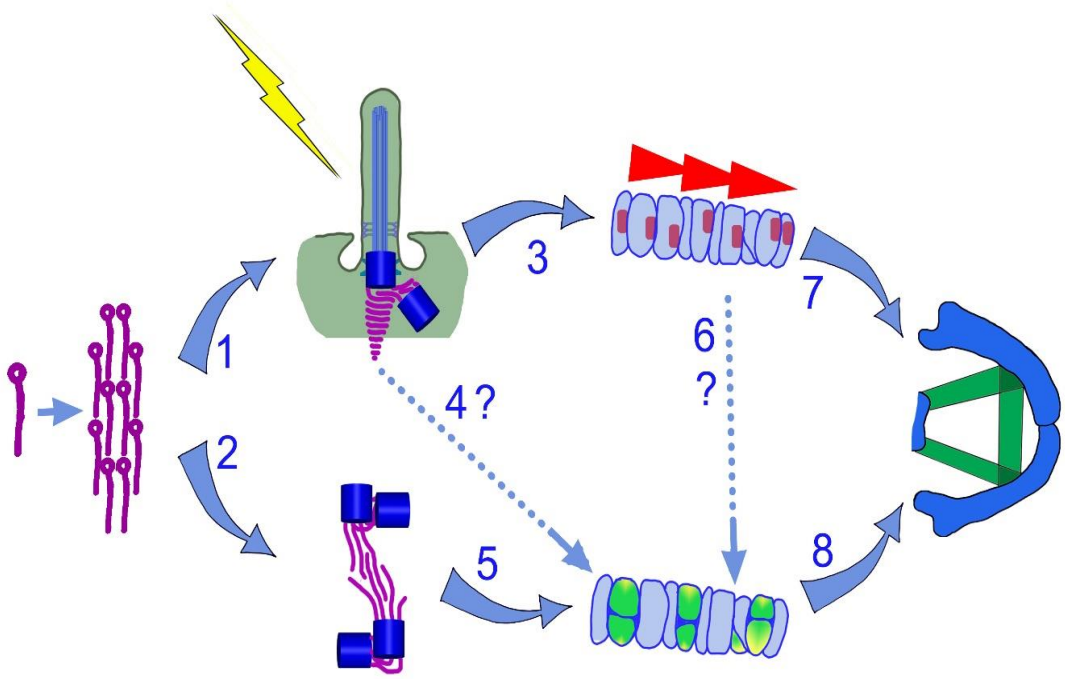

Figure 2.10. **Model for Crocc2 roles in the nexus between mechanical signals and morphogenesis.** Crocc2 plays a role in regulating the formation of the zebrafish mandible. At the protein level, wild-type Crocc2 dimerizes and self-assembles into elongated striated filaments (magenta)[59,61] that can play two roles in cells. (Step 1) As the major constituent of ciliary rootlets, Crocc2 is responsible for rootlet structure.[57–59] These rootlet assemblies extend proximally from the base of a cilium toward subcellular organelles and structures inside the cell, including the cell's nucleus.[53–55,57,59] (Step 2) Crocc2 also serves as a linker protein at centrioles connecting centrosomes during mitotic cell division where absence of linker proteins can play a role in the timing and efficiency of mitotic cell division.[90–94] In the cilium, we propose that as soft tissue insertion sites receive mechanical stimulation from muscles and ligaments, Crocc2 plays a role in mechanotransduction. We have demonstrated one outcome of this is that Crocc2 influences the orientation of PCP across developing cartilage tissue (Step 3). Specifically, as a direct result of *crocc2* mutation, we see PCP is most disrupted in cartilage cells across the sites where muscle and ligamentous forces are exerted upon developing cartilage.[44,95–98] In addition, although it remains to be demonstrated exactly how Crocc2 plays a role in cell proliferation, another possibility is that Crocc2 at ciliary rootlets directly influences chondrocyte proliferation through signal transduction pathways (eg: Wnt/Hh, Step 4).[99,100] Crocc2 might also play a role at the level of the centrosome, influencing the efficacy of cell proliferation (Step 5).[94] Further, PCP mechanisms serve to orient the positions of dividing cells and through interaction with PCP-partner proteins, Crocc2 may even influence cell proliferation through a PCP-

dependent mechanism (Step 6).[101,102] Thus, determining whether Crocc2 at the rootlets plays direct or indirect roles in cell proliferation will require additional research. The outcomes of aberrant cell behaviors in *crocc2* mutants are dysmorphic and variable cartilages (Steps 7 and 8).

finite element analysis (FEA) in zebrafish confirms that stress is concentrated in this region of the larval cartilage.[44] Proper craniofacial development in general requires mechanosensory input, and impaired or manipulated mechanical environments result in both cell- and tissue-level dysmorphologies.[41,42,73,95,96,103,104] In cichlid fishes, variation in naturally occurring jaw movements during early larval development influences skeletal development by altering rates of bone deposition - the higher the frequency of jaw opening ("gaping"), the more bone that is deposited at the point of ligamentous insertion. When the system is manipulated by either changing the behavior (i.e., increasing gaping frequency), or by physically severing the connection between the ligament and bone, the rate of bone growth changes in a predicted manner.[41] Similar experiments were performed in zebrafish larvae, at earlier developmental stages, where genetic mutants as well as a paralysis model were used to increase or reduce jaw movements.[95,96] Under these conditions, the investigators noted conspicuous changes in both cell and cartilage shapes. Furthermore, while not mentioned in the study,[96] the data clearly show increased variability in MC shape in lines characterized by reduced jaw movements, consistent with results presented in our study. Finally, direct roles for ciliary rootlets in mechanosensing come from studies in invertebrate models. *Drosophila* embryos in which the *crocc/crocc2* homolog, *Rootletin,* was knocked out possessed normal cilia, but lacked rootlets, and exhibited severely compromised mechanosensory function in sensory neurons.[57,63] How *crocc2/Rootletin* regulates mechanosensing remains an open question, with several possibilities, including compromised ciliary function, signal transduction, protein

trafficking, and/or integration between the rootlets, cytoskeleton, and subcellular structures including the nucleus.[48,55,57,89] In all, rootlet biology seems to be a rich but largely untapped area of research.

Mechanical forces that arise during morphogenesis are necessary to orient PCP, the polarized organization of cells across a tissue.[75,76,105,106] This notion is supported by observations of tensions serving to orient PCP in *Drosophila* wing blade cells,[75] and the overall timing of the stabilization of PCP in the zebrafish pharyngeal skeleton, which corresponds to the time of soft tissue integration with cartilages.[22,107] PCP is crucial for orienting cell shapes, positioning the direction of cell divisions, controlling cell rearrangements, and directing the positioning of subcellular structures including the MTOCs of primary cilia.[75,76,108,109] Accordingly, PCP plays important roles in skeletal morphogenesis.[22,72,85,108,110] In zebrafish, conserved members of PCP molecular networks are expressed in larval cartilages, and disruption of PCP leads to a failure of the chondrocytes to properly stack, which is critical for the elongation of cartilage elements.[22,65] The cartilage phenotypes in zebrafish PCP mutants are similar to those observed here in that they display abnormal cell shapes, shorter elements, and MTOCs that are not aligned across the long axis of the cartilage providing support for the notion that mechanotransduction via the rootlets can regulate PCP (Figure 10, step 3). While a connection between rootlets and PCP has been documented in *Xenopus*, where the orientation of ciliary rootlets was observed to be reversed in cells adjacent to those where PCP was disrupted,[109] our data suggest that defective rootlets also lead to disrupted PCP. Notably, the observation that MC polarity is randomized in *crocc2* mutants, while muscles remain intact and functioning, provides further support for the hypothesis that

impaired mechanosensing may be a root cause of this defect. Along these lines, it would be informative to know whether PCP is disrupted in the paralysis models described above.

The relationship between Crocc2 and cell proliferation is a more complex question since this protein also plays key roles in cell division. In particular, Rootletin/Crocc filaments link together the centrioles of the centrosome (Figure 10, step 2) when cells enter the cell cycle,[90–93] and thus could influence proliferation by regulating the duration of the cell cycle[94] or in stabilizing the orientation of the mitotic spindle. Further, through interaction with PCP-partner proteins such as the Scribble interaction module, it is possible that Crocc2 could influence cell proliferation through a PCP-dependent mechanism (Figure 10, step 6).[101] Whether reduced cell proliferation in *crocc2* mutants is due to a role for Crocc2 at the primary cilium[111] (Figure 10, step 4) and/or at the centrosome (Figure 10, step 5) remains an open question.

Crocc2 at rootlets may also regulate signal transduction events that begin at the level of the ciliary axoneme via effectors like Hh or Wnts,[25,38,39,112,113] signals that are implicated in myriad developmental processes including chondrocyte proliferation and maturation.[72,88,114–116] Exactly how Crocc2 regulates signal transduction is not known, but numerous ultrastructural studies have revealed that rootlets associate with vesicular packages and organelles such as mitochondria, golgi, and nuclei.[53–55,59,117,118] In addition, a direct association between ciliary rootlet protein Rootletin and the nuclear membrane-associated protein Nesprin1/SYNE1has been demonstrated via co-immunoprecipitation and co-localization studies in NIH3t3 cells and co-localization studies in mouse photoreceptor cells and neural ependymal cells.[54,118] These observations raise the

interesting possibilities that Crocc2 might participate in protein and mRNA trafficking to facilitate signal transduction.[57,63,119,120] It may also be possible that Crocc2 can impact signal transduction through cytoskeletal interactions. For example, ciliary rootlet cytoskeletal structures have been shown to associate with the sub-apical actin cytoskeleton in *Xenopus* multi-ciliated cells and with actin filaments *in vitro.*[56,121,122] Further, Rootletin and Nesprins have been shown to associate with several kinesins, suggesting a potential link between the rootlet and microtubules.[48,89,89,123–125] Thus, the potential for ciliary rootlets to play an active role in cell signaling is another important question to explore in future studies.

Cilia play critical roles in a number of developmental and maintenance processes, including bone formation and regulation, as evidenced by the multitude of skeletal defects associated with human ciliopathies,[15,126–130] and the animal models used to study them.[23,131–133] Using the same *crocc2* line examined here, we demonstrated a role for this gene in regulating the sensitivity of adult bone to respond to mechanical input,[62] consistent with known roles for cilia in bone remodeling.[23,134,135] We linked this adult phenotype to a loss of cilia overtime, which has also been documented in mouse *Rootletin* mutants.[56] Here we examined bone formation, but at an earlier stage when mutant cartilages still possess cilia.[62] We did not observe bone patterning defects in *crocc2* mutants, which suggests that osteogenic inductive signals from the cartilage remain largely intact. This assertion is supported by gene expression analyses in *crocc2* mutants, which showed that the osteogenic network was similar to that in wild-type siblings early (i.e., juvenile stage) but became mis-regulated over time.[62] This is not to say that a *crocc2* bone phenotype is not present, as the dentary bone appears to exhibit

reduced mineralization (Figure 9). It is possible that this phenotype may be related to that described in adults and arises due to impaired mechanosensing formation.[41] If true, this would suggest that bone dysmorphologies previously documented in adult *crocc2* mutants[41] may arise due to a combination of impaired ciliary function and the absence of cilia. Such insights would also be consistent with the observation that different, naturally occurring, predicted structural variants of Crocc2 are associated with different sensitivities of bone to mechanical input among cichlid fishes.[41]

Evolutionary implications of altered canalization in development

Darwin (1859)[12] predicted that an increase in variation at early developmental stages would increase the likelihood of maladaptive outcomes, and thus constraint should be an important feature of organismal development. While phenotypic constraints can limit possible adaptive peaks that a population can reach,[1,6,7] limiting evolutionary potential, they also work to prevent phenotypic variability from meandering along maladaptive axes, and are therefore likely to be maintained by stabilizing selection.[136–139] When the finely tuned symphony of developmental processes and constraints is disrupted, the resulting range of phenotypic outcomes can expand, leading to the production of adaptive, maladaptive, or possibly lethal phenotypes.[30,32,33,139,140] Since the production of the same phenotype over development may be considered adaptive or maladaptive, depending on the lineage in which it appears,[141] understanding how phenotypic variation is modulated over time and phylogeny remains an important challenge in development and evolution.[142]

As a hub of mechanosensing and signal transduction, the primary cilium is an excellent candidate for regulating levels of cellular- and tissue-level variation. While this organelle has garnered much attention in the realm of developmental biology and clinical genetics,[47,143–146] it has not been on the radar of evolutionists or practitioners of evo-devo. In a previous study, we associate allelic variation at *crocc2* with adaptive phenotypic variation in adult bone shape in cichlid fishes.[41] Here, we report increased morphological variation in *crocc2* mutants during the early stages of ontogeny, when wild-type populations experience a reduction in morphological variation (Figure 4). Differences in variation between animals with wild-type vs mutant *crocc2* alleles are most prominent at 7 and 12dpf, and suggest that this gene plays a role in canalizing craniofacial shape variation at this stage. The timing of observed differences in variation is notable, as 5-7dpf is when the yolk become fully absorbed and animals rely on exogenous feeding.[147] This pattern suggests the interesting possibility that mechanical input associated with feeding may serve to decrease variance in the feeding apparatus in wild-type animals. This is also the general window of development when species-specific differences in cartilages begin to take shape in other lineages.[34,148–151] While even earlier developmental stages (e.g., neural crest cell migration)[37,152] have been implicated in the development of species-specific jaw shapes, we suggest that as craniofacial development increasingly relies on the integration of inductive cues from both the intercellular (e.g., signal transduction) and external (e.g., kinematic) environment, there are more ways by which patterns or magnitudes of variation may be altered. Thus, as development unfolds, a focus upon the interaction between genetic and environmental effects (i.e., GxE) is warranted. To this end, we suggest the ciliary rootlets, in general, and *crocc2*, in particular, are

excellent candidates for such GxE effects, as they appear to be important mediators of cellular mechanosensing, and positioned at the nexus of development and evolution.[57,62,63]

Methods

Husbandry

Zebrafish were reared in 2.8-L plastic aquarium tanks and fed a diet of rotifers from 5 to 12dpf. Then, they were fed Gemma Micro-300 (Skretting, Westbrook, ME) and brine shrimp (Artemia International, Fairview, TX). Immediately prior to experiments, larvae were euthanized using Tricaine-S (MS-222; Syndel USA, formerly Western Chemical, Inc, Ferndale, WA). All zebrafish work was performed humanely according to standards of good animal care practice using protocols approved by the University of Massachusetts, Amherst, Institutional Animal Care and Use Committee (IACUC protocols).

Mutant Alleles

The Zebrafish International Resource Center (ZIRC; University of Oregon, Eugene, OR) provided *crocc2* allelic variants used in this study: *20707* and *20708.* Both came from an ENU mutagenesis screen in the Stemple lab.[153] *20707* (*crocc2*$^{07/07}$) encodes a premature stop codon mapped to exon 8 (at 272aa). *20708* (*crocc2*$^{08/08}$) contains a C>T nonsense mutation in exon 14 that creates a premature stop at 585 aa. Zebrafish genome assembly GRCz11 from the UCSC Genome Browser was used to identify map positions.[154] Lines were outcrossed to a wild-type zebrafish stock (AB) for several generations to eliminate any second site mutation from the ENU screen. Crosses for experiments were performed by in-crossing genotypic carriers of the allele of interest. Resulting progeny included homozygous mutant (*crocc2*$^{07/07}$ or *crocc2*$^{08/08}$),

heterozygotes (*crocc2*$^{+/07}$ or *crocc2*$^{+/08}$), and wild-type sibling controls (*crocc2*$^{+/+}$). Following euthanization, larvae were genotyped by digesting the tail of each larva in 15µl HotShot Lysis Buffer at 95ºC for 30 minutes.[155] Digests were immediately neutralized and cDNA was PCR amplified from genomic DNA. Purification and sequencing was performed through Psomagen Boston, MA.

Histology

Larvae were euthanized at 4, 7, 12, and 18dpf for geomorphometric analysis and at 5 and 7dpf for cell morphology and Alizarin Red deposition assessments. Briefly: heads were fixed at 4ºC overnight in 4% PFA pH 7.4 and cleared and stained using a modified, acid-free staining method using Alcian Blue dye to visualize the cartilaginous skeleton and Alizarin Red bone staining.[156]

Alcian staining was imaged for geometric morphometric analyses using a Leica M165 FC microscope and DFC450 5 Megapixel color digital camera (Leica Camera AG, Wetzlar, Germany). For cell morphology, larvae were prepared in 3 independent experiments and either whole mounted or the pharyngeal skeleton was dissected and flat mounted onto glass slides. Imaging of individual cells was performed with a Leica DM1000 slide scope and Leica DFC450C camera. Insertion site cells are the population of cells immediately adjacent to the sites of soft tissue (muscle and ligament) insertion and the flanking cells were defined as the cells in a region immediately proximal to the insertion site cells. The proximal region length was chosen to match the average length of the insertion site. For bone deposition imaging, multi-channel Z-stack images were acquired using a Zeiss ApoTome running Axiovision 4.8.2. Measurements were taken using Fiji 1.53e software.

Geomorphometric Analysis

Geometric morphometric data were collected using Stereomorph[146] in R.[157,158] We characterized the pharyngeal skeleton using 18 fixed and 34 semi (sliding) – landmarks.[159,160]. Morphological data were aligned via generalized Procrustes superimposition[161] and analyzed via ANOVA to test for significance in mean shape among homozygous and heterozygous genotype comparisons within age groups. These analyses involved the comparison of a null model `(shape ~ size)` to a full model `(shape ~ size + genotype)` to control for differences of size among individuals of identical age groups. We calculated differences in morphological disparities between and among Genotype:Age groups using the function `morphol.disparity` which quantifies differences in Procrustes variances.[162] Additionally, we quantified phenotypic trajectories through the progression of different ages `(Shape ~ Genotype * Age, ~ Centroid Size)` using the function `trajectory.analysis`. This function evaluates phenotypic trajectories via ANOVA and calculates differences in trajectory path and magnitude.[162–164] Statistical analyses relied on a randomized residual permutation procedure (RRPP) that subjected landmark data to 10,000 random permutations.[162,164,165] Lastly, principal component analysis (PCA), we mapped ontogenetic trajectories onto morphospace using the first two principal component axes. All morphological analyses were performed using Geomorph v3.0.[166,167]

Immunohistochemistry

Anti-gamma tubulin (gT) was used to label Microtubule Organizing Centers (MTOCs)/Basal Bodies of primary cilia (1:500; Sigma T6557) and anti-acetylated alpha tubulin (AaT) was used to view primary ciliary axonemes (1:500; Sigma T6793) in

euthanized 66-72hpf larvae. For T6793, amplification involved donkey anti-mouse Biotin (1:100) and Alexa 488 Streptavidin Conjugate (1:1000) (Jackson Immunoresearch, Westgrove, PA). Donkey anti-Rabbit Alexa 594 was used to visualize gT antibodies. Briefly, animals were euthanized and fixed 1.5h at room temperature in 4% PFA in PBS at pH 7.4. Samples were permeabilized 20 minutes in acetone at -20˚C and then in 1% Triton X-100 in PBS for 1 hour. Samples were blocked using 5% normal donkey serum (Jackson Immunoresearch) in 0.1% Triton X-100 in PBS. All washes were performed in 0.1% PBS-Tween 20, pH 7.4. Samples were then dissected and flat mounted, ventral side up, using Vectashield mounting medium with DAPI (H-1200; Vector Labs, Burlingame, CA) and imaged using a Zeiss LSM 710 confocal system running Zeiss Zen Black software. Final image analysis was performed in Zen Blue (Lite 3.0) and measurements were taken using Fiji 1.53e.

EdU Cell Proliferation Assay

DNA-synthesis based cell proliferation assay larvae were selected at 5.5dpf and incubated overnight in 3.3mM EdU (Invitrogen Click-it Kit C10337) and 1% DMSO (Invitrogen D12345) in aquaria water. The following day (6dpf), larvae were euthanized and tails used for genotyping as above. Heads were fixed overnight at 4C in fresh 4% PFA, washed in 0.5% Triton X-100 in PBS (PBTx), permeabilized and blocked 1h at RT in 3% BSA in PBTx and rinsed in PBS. Fresh EdU cocktail reagent containing AlexaFluor 488 dye for 30 minutes at room temperature. Samples were then washed 3X in 3% BSA in PBTx and re-fixed 30 minutes in fresh 4% PFA at room temperature before washes in PBTx. Overnight incubations in 25% glycerol preceded further

dissection and flat mounting onto slides in Vectashield containing DAPI. Samples were imaged using the Zeiss 710 LSM Confocal and images were evaluated in Zen Lite 3.0.

TUNEL Cell Death Assay

For apoptotic cell death analysis, 5 and 7dpf larvae were processed using an ApopTag Plus Kit (S7101; MilliporeSigma, Burlington, MA). For positive controls, a subset of *crocc2*$^{+/+}$ were incubated in 100uM Cyclopamine (CyA; Toronto Chemical) in aquaria water for 24h at 28.5˚C, to induce cell death.[168,169] Samples were fixed overnight at 4C in 4% PFA in PBS, washed 3X in 0.1% Tween-20 in PBS (PBT), dehydrated in a methanol series and stored at -20˚C. Larvae were later rehydrated, permeabilized in 5ug/ml Proteinase K (30min for 5dpf; 45min for 7dpf), followed by 1:2 Acetone:Ethanol for 10min at -20˚C. Three percent (3%) hydrogen peroxide in PBS for 5 minutes at room temperature was used to quench endogenous peroxidase. Samples were pooled by genotype and incubated one hour at room temperature in Equilibration Buffer before the Reaction Mix at 37˚C overnight. TdT enzyme was omitted from a subset of *crocc2*$^{+/+}$ (negative controls). Afterward, Stop/Wash buffer was applied and samples were blocked three hours in 10mg/ml BSA, 2% Fetal Bovine Serum (FBS), 2% heat-inactivated lamb serum, and 1% DMSO, in 0.1% Triton X-100[150], before primary antibody incubations at 4˚C overnight in undiluted Anti-Dig-peroxidase from the kit. The next day, peroxidase substrate was used to develop the color reaction. Samples were incubated in 25% glycerol

in PBT for 4h, mounted in 25% glycerol, and stored at 4°C. Mandibles were flat mounted, ventral side up and imaged using the Leica camera as above.

Statistical analysis

Tukey's HSD test was used to test for significance in Alcian, Alizarin, and EdU Assays and polarity assessments were examined for significance using the Chi-sq (X^2) test for goodness of fit using RStudio version 1.2.5033 for Mac OSX.

Literature Cited

1. Wright S. The roles of mutation, inbreeding, crossbreeding and selection in evolution. Sixth International Congress on Genetics. 1932;1(6):356-366.

2. Jacob F. Evolution and tinkering. Science. 1977;196(4295):1161-1166.

3. Lande R, Shannon S. The Role of genetic variation in adaptation and population persistence in a changing environment. Evolution. 1996;50(1):434-437.

4. Smith PF, Konings A, Kornfield I. Hybrid origin of a cichlid population in Lake Malawi: Implications for genetic variation and species diversity. Molecular Ecology. 2003;12(9):2497-2504. doi:10.1046/j.1365-294X.2003.01905.x

5. Collin H, Fumagalli L. Evidence for morphological and adaptive genetic divergence between lake and stream habitats in European minnows (*Phoxinus phoxinus*, Cyprinidae). Molecular Ecology. 2011;20(21):4490-4502. doi:10.1111/j.1365-294X.2011.05284.x

6. Wagner G. The influence of variation and developmental constraints on the rate of multivariate phenotypic evolution. Journal of Evolutionary Biology. 1988;1(1):45-66. doi:10.1046/j.1420-9101.1988.1010045.x

7. Arnold SJ. Constraints on phenotypic evolution. The American Naturalist. 1992;140:S85-S107.

8. Schluter D. Adaptive radiation along genetic lines of least resistance. Evolution. 1996;50(5):1766-1766. doi:10.2307/2410734

9. Klingenberg CP. Developmental Constraints, Modules, and Evolvability. Variation. Published online 2005:219-247.

10. Narita Y, Kuratani S. Evolution of the vertebral formulae in mammals: A perspective on developmental constraints. Journal of Experimental Zoology Part B: Molecular and Developmental Evolution. 2005;304(2):91-106. doi:10.1002/jez.b.21029

11. Cheverud JM. Quantitative genetics and developmental constraints on evolution by selection. Journal of Theoretical Biology. 1984;110(2):155-171. doi:10.1016/S0022-5193(84)80050-8

12. Darwin C. On the Origin of Species.; 1859.

13. Murillo-Rincón AP, Kaucka M. Insights into the complexity of craniofacial development from a cellular perspective. Frontiers in cell and developmental biology. 2020;8:620735-620735. doi:10.3389/fcell.2020.620735

14. Crump JG, Maves L, Lawson ND, Weinstein BM, Kimmel CB. An essential role for Fgfs in endodermal pouch formation influences later craniofacial skeletal patterning. Development. 2004;131(22):5703-5716. doi:10.1242/dev.01444

15. Schock EN, Brugmann SA. Neural crest cells utilize primary cilia to regulate ventral forebrain morphogenesis via Hedgehog-dependent regulation of oriented cell division. Developmental Biology. 2017;431(2):168-178. doi:10.1016/j.ydbio.2017.09.026

16. Creuzet S, Schuler B, Couly G, Le Douarin NM. Reciprocal relationships between Fgf8 and neural crest cells in facial and forebrain development. Proceedings of the National Academy of Sciences of the United States of America. 2004;101(14):4843-4847. doi:10.1073/pnas.0400869101

17. Swartz ME, Nguyen V, McCarthy NQ, Eberhart JK. Hh signaling regulates patterning and morphogenesis of the pharyngeal arch-derived skeleton. Developmental Biology. 2012;369(1):65-75. doi:10.1016/j.ydbio.2012.05.032

18. Mork L, Crump G. Zebrafish Craniofacial Development. A window into early patterning. Current Topics in Developmental Biology. 2015;115:235-269. doi:10.1016/bs.ctdb.2015.07.001

19. Schneider RA, Hu D, Helms JA. From head to toe: Conservation of molecular signals regulating limb and craniofacial morphogenesis. Cell and Tissue Research. 1999;296(1):103-109. doi:10.1007/s004410051271

20. Xavier GM, Seppala M, Barrell W, Birjandi AA, Geoghegan F, Cobourne MT. Hedgehog receptor function during craniofacial development. Developmental Biology. 2016;415(2):198-215. doi:10.1016/j.ydbio.2016.02.009

21. Echevarría-Andino ML, Allen BL. The hedgehog co-receptor boc differentially regulates shh signaling during craniofacial development. Development. 147(23) doi:10.1101/2020.02.04.934497

22. Le Pabic P, Ng C, Schilling TF. Fat-dachsous signaling coordinates cartilage differentiation and polarity during craniofacial development. Mullins MC, ed. PLoS Genetics. 2014;10(10):e1004726-e1004726. doi:10.1371/journal.pgen.1004726

23. Bonatto Paese CL, Brooks EC, Aarnio-Peterson M, Brugmann SA. Ciliopathic micrognathia is caused by aberrant skeletal differentiation and remodeling. Development (Cambridge, England). 2021;148(4). doi:10.1242/dev.194175

24. Gebuijs IGE, Raterman ST, Metz JR, et al. Fgf8a mutation affects craniofacial development and skeletal gene expression in zebrafish larvae. Biology Open. 2019;8(9). doi:10.1242/bio.039834

25. Tobin JL, Di Franco M, Eichers E, et al. Inhibition of neural crest migration underlies craniofacial dysmorphology and hirschsprung's disease in bardet-biedl syndrome. Proceedings of the National Academy of Sciences of the United States of America. 2008;105(18):6714-6719. doi:10.1073/pnas.0707057105

26. Li X, Young NM, Tropp S, et al. Quantification of shape and cell polarity reveals a novel mechanism underlying malformations resulting from related FGF mutations

during facial morphogenesis. Human Molecular Genetics. 2013;22(25):5160-5172. doi:10.1093/hmg/ddt369

27. Hu D, Young NM, Li X, Xu Y, Hallgrımsson B, Marcucio RS. A dynamic shh expression pattern, regulated by shh and bmp signaling, coordinates fusion of primordia in the amniote face. Development (Cambridge). 2015;142(3):567-574. doi:10.1242/dev.114835

28. Green RM, Feng W, Phang T, et al. Tfap2a-dependent changes in mouse facial morphology result in clefting that can be ameliorated by a reduction in Fgf8 gene dosage. DMM Disease Models and Mechanisms. 2015;8(1):31-43. doi:10.1242/dmm.017616

29. Green RM, Fish JL, Young NM, et al. Developmental nonlinearity drives phenotypic robustness. Nature Communications. 2017;8(1). doi:10.1038/s41467-017-02037-7

30. Riley BM, Mansilla MA, Ma J, et al. Impaired FGF signaling contributes to cleft lip and palate. Proceedings of the National Academy of Sciences of the United States of America. 2007;104(11):4512-4517. doi:10.1073/pnas.0607956104

31. Creuzet S, Couly G, Le Douarin NM. Patterning the neural crest derivatives during development of the vertebrate head: Insights from avian studies. Journal of Anatomy. 2005;207(5):447-459. doi:10.1111/j.1469-7580.2005.00485.x

32. Griffin JN, Compagnucci C, Hu D, et al. Fgf8 dosage determines midfacial integration and polarity within the nasal and optic capsules. Developmental Biology. 2013;374(1):185-197. doi:10.1016/j.ydbio.2012.11.014

33. Abu-Issa R, Smyth G, Smoak I, Yamamura KI, Meyers EN. Fgf8 is required for pharyngeal arch and cardiovascular development in the mouse. Development. 2002;129(19):4613-4625.

34. Albertson RC, Streelman JT, Kocher TD, Yelick PC. Integration and evolution of the cichlid mandible: The molecular basis of alternate feeding strategies. Proceedings of the National Academy of Sciences of the United States of America. 2005;102(45):16287-16292. doi:10.1073/pnas.0506649102

35. Abzhanov A, Protas M, Grant BR, Grant PR, Tabin CJ. Bmp4 and morphological variation of beaks in Darwin's finches. Science. 2004;305(5689):1462-1465. doi:10.1126/science.1098095

36. Mallarino R, Grant PR, Grant BR, Herrel A, Kuo WP, Abzhanov A. Two developmental modules establish 3D beak-shape variation in Darwin's finches. Proceedings of the National Academy of Sciences of the United States of America. 2011;108(10):4057-4062. doi:10.1073/pnas.1011480108

37. Powder KE, Cousin H, McLinden GP, Craig Albertson R. A nonsynonymous mutation in the transcriptional regulator lbh is associated with cichlid craniofacial adaptation and neural crest cell development. Molecular Biology and Evolution. 2014;31(12):3113-3124. doi:10.1093/molbev/msu267

38. Parsons KJ, Trent Taylor A, Powder KE, Albertson RC. Wnt signalling underlies the evolution of new phenotypes and craniofacial variability in Lake Malawi cichlids. Nature communications. 2014;5(1):3629-3629. doi:10.1038/ncomms4629

39. Young NM, Chong HJ, Hu D, Hallgrímsson B, Marcucio RS. Quantitative analyses link modulation of sonic hedgehog signaling to continuous variation in facial growth and shape. Development. 2010;137(20):3405-3409. doi:10.1242/dev.052340

40. Du W, Bhojwani A, Hu JK. FACEts of mechanical regulation in the morphogenesis of craniofacial structures. International Journal of Oral Science. 2021;13(1):4-4. doi:10.1038/s41368-020-00110-4

41. Hu Y, Albertson RC. Baby fish working out: An epigenetic source of adaptive variation in the cichlid jaw. Proceedings of the Royal Society B: Biological Sciences. 2017;284(1860). doi:10.1098/rspb.2017.1018

42. Navon D, Male I, Tetrault ER, Aaronson B, Karlstrom RO, Craig Albertson R. Hedgehog signaling is necessary and sufficient to mediate craniofacial plasticity in teleosts. Proceedings of the National Academy of Sciences of the United States of America. 2020;117(32):19321-19327. doi:10.1073/pnas.1921856117

43. Dietrich K, Fiedler I, Kurzyukova A, et al. Skeletal biology and disease modeling in zebrafish. Journal of Bone and Mineral Research. Published online 2021. doi:10.1002/jbmr.4256

44. Lawrence EA, Kague E, Aggleton JA, Harniman RL, Roddy KA, Hammond CL. The mechanical impact of col11a2 loss on joints; col11a2 mutant zebrafish show changes to joint development and function, which leads to early-onset osteoarthritis. Philosophical Transactions of the Royal Society B: Biological Sciences. 2018;373(1759). doi:10.1098/rstb.2017.0335

45. Hoey DA, Downs ME, Jacobs CR. The mechanics of the primary cilium: An intricate structure with complex function. Journal of Biomechanics. 2012;45(1):17-26. doi:10.1016/j.jbiomech.2011.08.008

46. Nguyen AM, Jacobs CR. Emerging role of primary cilia as mechanosensors in osteocytes. Bone. 2013;54(2):196-204. doi:10.1016/j.bone.2012.11.016

47. Temiyasathit S, Tang WJ, Leucht P, et al. Mechanosensing by the primary cilium: Deletion of Kif3A reduces bone formation due to loading. PLoS. 2012;7(3):1-9. doi:10.1371/journal.pone.0033368

48. Kirby TJ, Lammerding J. Emerging views of the nucleus as a cellular mechanosensor. Nature Cell Biology. 2018;20(4):373-381. doi:10.1038/s41556-018-0038-y

49. Vaughan TJ, Mullen CA, Verbruggen SW, McNamara LM. Bone cell mechanosensation of fluid flow stimulation: a fluid–structure interaction model characterising the role integrin attachments and primary cilia. Biomechanics and Modeling in Mechanobiology. 2015;14(4):703-718. doi:10.1007/s10237-014-0631-3

50. Pala R, Alomari N, Nauli S. Primary cilium-dependent signaling mechanisms. International Journal of Molecular Sciences. 2017;18(11):2272-2272. doi:10.3390/ijms18112272

51. Cheong SS, Akram KM, Matellan C, et al. The planar polarity component vangl2 is a key regulator of mechanosignaling. Frontiers in cell and developmental biology. 2020;8:577201-577201. doi:10.3389/fcell.2020.577201

52. Elliott KH, Brugmann SA. Sending mixed signals: Cilia-dependent signaling during development and disease. Developmental Biology. 2019;447(1):28-41. doi:10.1016/j.ydbio.2018.03.007

53. Gilliam JC, Chang JT, Sandoval IM, et al. Three-dimensional architecture of the rod sensory cilium and its disruption in retinal neurodegeneration. Cell. 2012;151(5):1029-1041. doi:10.1016/j.cell.2012.10.038

54. Potter C, Zhu W, Razafsky D, et al. Multiple isoforms of nesprin1 are integral components of ciliary rootlets. Current Biology. 2017;27(13):2014-2022.e6. doi:10.1016/j.cub.2017.05.066

55. Tachi S, Tachi C, Lindner HR. Influence of ovarian hormones on formation of solitary cilia and behavior of the centrioles in uterine epithelial cells of the rat. Biology of Reproduction. 1974;10(4):391-403. doi:10.1095/biolreprod10.4.391

56. Yang J, Gao J, Adamian M, et al. The Ciliary Rootlet Maintains Long-Term Stability of Sensory Cilia. Molecular and Cellular Biology. 2005;25(10):4129-4137. doi:10.1128/MCB.25.10.4129-4137.2005

57. Chen JV, Kao LR, Jana SC, et al. Rootletin organizes the ciliary rootlet to achieve neuron sensory function in Drosophila. The Journal of Cell Biology. 2015;211(2):435-453. doi:10.1083/jcb.201502032

58. Mohan S, Timbers TA, Kennedy J, Blacque OE, Leroux MR. Striated rootlet and nonfilamentous forms of rootletin maintain ciliary function. Current biology: CB. 2013;23(20):2016-2022. doi:10.1016/j.cub.2013.08.033

59. Yang J, Liu X, Yue G, Adamian M, Bulgakov O, Li T. Rootletin, a novel coiled-coil protein, is a structural component of the ciliary rootlet. The Journal of cell biology. 2002;159(3):431-440. doi:10.1083/jcb.200207153

60. Garcia G, Reiter JF. A primer on the mouse basal body. Cilia. 2016;5(1). doi:10.1186/s13630-016-0038-0

61. Ko D, Kim J, Rhee K, Choi HJ. Identification of a structurally dynamic domain for oligomer formation in rootletin. Journal of Molecular Biology. 2020;432(13):3915-3932. doi:10.1016/j.jmb.2020.04.012

62. Gilbert MC, Tetrault E, Packard M, Navon D, Albertson RC. Ciliary rootlet coiled-coil 2 (crocc2) is associated with evolutionary divergence and plasticity of cichlid jaw shape. Mol Biol Evol. 2021;38(8):3078-3092. doi:10.1093/molbev/msab071

63. Styczynska-Soczka K, Jarman AP. The *Drosophila* homologue of rootletin is required for mechanosensory function and ciliary rootlet formation in chordotonal sensory neurons. Cilia. 2015;4(1):9-9. doi:10.1186/s13630-015-0018-9

64. Dash S, Trainor PA. The development, patterning and evolution of neural crest cell differentiation into cartilage and bone. Bone. 2020;137. doi:10.1016/j.bone.2020.115409

65. Eames B, DeLaurier A, Ullmann B, et al. FishFace: interactive atlas of zebrafish craniofacial development at cellular resolution. BMC Developmental Biology. 2013;13(1):23-23. doi:10.1186/1471-213X-13-23

66. Yang L, Tsang KY, Tang HC, Chan D, Cheah KSE. Hypertrophic chondrocytes can become osteoblasts and osteocytes in endochondral bone formation. Proceedings of the National Academy of Sciences of the United States of America. 2014;111(33):12097-12102. doi:10.1073/pnas.1302703111

67. Han S, Park HR, Lee EJ, et al. Dicam promotes proliferation and maturation of chondrocyte through Indian hedgehog signaling in primary cilia. Osteoarthritis and Cartilage. 2018;26(7):945-953. doi:10.1016/j.joca.2018.04.008

68. Man-Ger Sun M, Beier F. Chondrocyte hypertrophy in skeletal development, growth, and disease. doi:10.1002/bdrc.21062

69. Hall J, Jheon AH, Ealba EL, et al. Evolution of a developmental mechanism: Species-specific regulation of the cell cycle and the timing of events during craniofacial osteogenesis. Developmental Biology. 2014;385(2):380-395. doi:10.1016/j.ydbio.2013.11.011

70. Cooper KL, Oh S, Sung Y, Dasari RR, Kirschner MW, Tabin CJ. Multiple phases of chondrocyte enlargement underlie differences in skeletal proportions. Nature. 2013;495(7441):375-378. doi:10.1038/nature11940

71. Merkes C, Turkalo TK, Wilder N, et al. Ewing sarcoma ewsa protein regulates chondrogenesis of meckel's cartilage through modulation of sox9 in zebrafish. Sabaawy HE, ed. PLOS ONE. 2015;10(1):e0116627-e0116627. doi:10.1371/journal.pone.0116627

72. Ling IT, Rochard L, Liao EC. Distinct requirements of wls, wnt9a, wnt5b and gpc4 in regulating chondrocyte maturation and timing of endochondral

ossification. Developmental Biology. 2017;421(2):219-232. doi:10.1016/j.ydbio.2016.11.016

73. Felsenthal N, Zelzer E. Mechanical regulation of musculoskeletal system development. Development (Cambridge). 2017;144(23):4271-4283. doi:10.1242/dev.151266

74. Borovina A, Superina S, Voskas D, Ciruna B. Vangl2 directs the posterior tilting and asymmetric localization of motile primary cilia. Nature Cell Biology. 2010;12(4):407-412. doi:10.1038/ncb2042

75. Aigouy B, Farhadifar R, Staple DB, et al. Cell flow reorients the axis of planar polarity in the wing epithelium of *Drosophila*. Cell. 2010;142(5):773-786. doi:10.1016/j.cell.2010.07.042

76. Mlodzik M. Planar cell polarity: moving from single cells to tissue-scale biology. Development (Cambridge, England). 2020;147(24). doi:10.1242/dev.186346

77. Jussila M, Ciruna B. Zebrafish models of non-canonical Wnt/planar cell polarity signalling: fishing for valuable insight into vertebrate polarized cell behavior. Wiley Interdisciplinary Reviews: Developmental Biology. 2017;6(3):e267-e267. doi:10.1002/wdev.267

78. Ciruna B, Jenny A, Lee D, Mlodzik M, Schier AF. Planar cell polarity signalling couples cell division and morphogenesis during neurulation. Published online 2006. doi:10.1038/nature04375

79. Wong FK, Marín O. Developmental cell death in the cerebral cortex. Annual Review of Cell and Developmental Biology. 2019;35:523-542. doi:10.1146/annurev-cellbio-100818-125204

80. Voss AK, Strasser A. The essentials of developmental apoptosis. F1000Research. 2020;9. doi:10.12688/f1000research.21571.1

81. Montero JA, Lorda-Diez CI, Hurle JM. Confluence of cellular degradation pathways during interdigital tissue remodeling in embryonic tetrapods. Frontiers in Cell and Developmental Biology. 2020;8. doi:10.3389/fcell.2020.593761

82. Fuchs Y, Steller H. Live to die another way: Modes of programmed cell death and the signals emanating from dying cells. Nature Reviews Molecular Cell Biology. 2015;16(6):329-344. doi:10.1038/nrm3999

83. Li M, Liao L, Tian W. Extracellular vesicles derived from apoptotic cells: an essential link between death and regeneration. Frontiers in Cell and Developmental Biology. 2020;8. doi:10.3389/fcell.2020.573511

84. Ghose P, Shaham S. Cell death in animal development. Development (Cambridge). 2020;147(14). doi:10.1242/dev.191882

85. Galea GL, Zein MR, Allen S, Francis-West P. Making and shaping endochondral and intramembranous bones. Dev Dyn. 2021;250(3):414-449. doi:10.1002/dvdy.278

86. Aghajanian P, Mohan S. The art of building bone: emerging role of chondrocyte-to-osteoblast transdifferentiation in endochondral ossification. Bone Res. 2018;6:19. doi:10.1038/s41413-018-0021-z

87. Svandova E, Anthwal N, Tucker AS, Matalova E. Diverse fate of an enigmatic structure: 200 years of meckel's cartilage. Front Cell Dev Biol. 2020;8:821. doi:10.3389/fcell.2020.00821

88. Hammond CL, Schulte-Merker S. Two populations of endochondral osteoblasts with differential sensitivity to Hedgehog signalling. Development. 2009;136(23):3991-4000. doi:10.1242/dev.042150

89. Yang J, Li T. The ciliary rootlet interacts with kinesin light chains and may provide a scaffold for kinesin-1 vesicular cargos. Experimental cell research. 2005;309(2):379-389. doi:10.1016/j.yexcr.2005.05.026

90. Bahe S, Stierhof YD, Wilkinson CJ, Leiss F, Nigg EA. Rootletin forms centriole-associated filaments and functions in centrosome cohesion. Journal of Cell Biology. 2005;171(1):27-33. doi:10.1083/jcb.200504107

91. Hossain D, Shih SYP, Xiao X, White J, Tsang WY. Cep44 functions in centrosome cohesion by stabilizing rootletin. Journal of cell science. 2020;133(4). doi:10.1242/jcs.239616

92. Yang J, Adamian M, Li T. Rootletin interacts with C-Nap1 and may function as a physical linker between the pair of centrioles/basal bodies in cells. Molecular Biology of the Cell. 2006;17(2):1033-1040. doi:10.1091/mbc.E05-10-0943

93. Vlijm R, Li X, Panic M, et al. STED nanoscopy of the centrosome linker reveals a CEP68-organized, periodic rootletin network anchored to a C-Nap1 ring at centrioles. Proceedings of the National Academy of Sciences. 2018;115(10):E2246-E2253. doi:10.1073/pnas.1716840115

94. Kaseda K, McAinsh AD, Cross RA. Dual pathway spindle assembly increases both the speed and the fidelity of mitosis. Biology Open. 2012;1(1):12-18. doi:10.1242/bio.2011012

95. Shwartz Y, Farkas Z, Stern T, Aszódi A, Zelzer E. Muscle contraction controls skeletal morphogenesis through regulation of chondrocyte convergent extension. Developmental Biology. 2012;370(1):154-163. doi:10.1016/j.ydbio.2012.07.026

96. Brunt LH, Roddy KA, Rayfield EJ, Hammond CL. Building finite element models to investigate zebrafish jaw biomechanics. Journal of Visualized Experiments. 2016;2016(118). doi:10.3791/54811

97. McGurk PD, Swartz ME, Chen JW, Galloway JL, Eberhart JK. In vivo zebrafish morphogenesis shows Cyp26b1 promotes tendon condensation and musculoskeletal patterning in the embryonic jaw. PLoS Genetics. 2017;13(12). doi:10.1371/journal.pgen.1007112

98. Kague E, Hughes SM, Lawrence EA, et al. Scleraxis genes are required for normal musculoskeletal development and for rib growth and mineralization in zebrafish. FASEB Journal. 2019;33(8):9116-9130. doi:10.1096/fj.201802654RR

99. Brunt LH, Begg K, Kague E, Cross S, Hammond CL. Wnt signalling controls the response to mechanical loading during zebrafish joint development. Development. 2017;144(15):2798-2809. doi:10.1242/dev.153528

100. Ohba S. Hedgehog signaling in skeletal development: Roles of Indian hedgehog and the mode of its action. International Journal of Molecular Sciences. 2020;21(18):1-17. doi:10.3390/ijms21186665

101. Milgrom-Hoffman M, Humbert PO. Regulation of cellular and PCP signalling by the Scribble polarity module. Seminars in Cell and Developmental Biology. 2018;81:33-45. doi:10.1016/j.semcdb.2017.11.021

102. VanderVorst K, Hatakeyama J, Berg A, Lee H, Carraway KL. Cellular and molecular mechanisms underlying planar cell polarity pathway contributions to cancer malignancy. Semin Cell Dev Biol. 2018;81:78-87. doi:10.1016/j.semcdb.2017.09.026

103. Tao H, Zhu M, Lau K, et al. Oscillatory cortical forces promote three-dimensional cell intercalations that shape the murine mandibular arch. Nature Communications. 2019;10(1). doi:10.1038/s41467-019-09540-z

104. Wang X, Mao JJ. Chondrocyte proliferation of the cranial base cartilage upon in vivo mechanical stresses. Journal of Dental Research. 2002;81(10):701-705. doi:10.1177/154405910208101009

105. Aw WY, Devenport D. Planar cell polarity: global inputs establishing cellular asymmetry. Current Opinion in Cell Biology. 2017;44:110-116. doi:10.1016/j.ceb.2016.08.002

106. Collinet C, Lecuit T. Programmed and self-organized flow of information during morphogenesis. Nat Rev Mol Cell Biol. 2021;22(4):245-265. doi:10.1038/s41580-020-00318-6

107. Chen JW, Galloway JL. The development of zebrafish tendon and ligament progenitors. Development (Cambridge). 2014;141(10):2035-2045. doi:10.1242/dev.104067

108. Huybrechts Y, Mortier G, Boudin E, Van Hul W. WNT signaling and bone: Lessons from skeletal dysplasias and disorders. Front Endocrinol (Lausanne). 2020;11:165. doi:10.3389/fendo.2020.00165

109. Mitchell B, Stubbs JL, Huisman F, Taborek P, Yu C, Kintner C. The PCP pathway instructs the planar orientation of ciliated cells in the *Xenopus* larval skin. Current Biology. 2009;19(11):924-929. doi:10.1016/j.cub.2009.04.018

110. Gao B, Yang Y. Planar cell polarity in vertebrate limb morphogenesis. Curr Opin Genet Dev. 2013;23(4):438-444. doi:10.1016/j.gde.2013.05.003

111. Sorokin SP. Reconstructions of centriole formation and ciliogenesis in mammalian lungs. Journal of Cell Science. 1968;3:207-230.

112. Hu D, Marcucio RS. A SHH-responsive signaling center in the forebrain regulates craniofacial morphogenesis via the facial ectoderm. Development. 2009;136(1):107-116. doi:10.1242/dev.026583

113. Brugmann SA, Goodnough LH, Gregorieff A, et al. Wnt signaling mediates regional specification in the vertebrate face. Development. 2007;134(18):3283-3295. doi:10.1242/dev.005132

114. St-Jacques B, Hammerschmidt M, McMahon AP. Indian hedgehog signaling regulates proliferation and differentiation of chondrocytes and is essential for bone formation. Genes and Development. 1999;13(16):2072-2086. doi:10.1101/gad.13.16.2072

115. Sisson BE, Dale RM, Mui SR, Topczewska JM, Topczewski J. A role of glypican4 and wnt5b in chondrocyte stacking underlying craniofacial cartilage morphogenesis. Mechanisms of Development. 2015;138:279-290. doi:10.1016/j.mod.2015.10.001

116. Corbit KC, Shyer AE, Dowdle WE, Gaulden J, Singla V, Reiter JF. Kif3a constrains β-catenin-dependent Wnt signalling through dual ciliary and non-ciliary mechanisms. Nature Cell Biology. 2008;10(1):70-76. doi:10.1038/ncb1670

117. Olsson R. The relationship between ciliary rootlets and other cell structures. Journal of Cell Biology. 1962;15(3) :doi:10.1083/jcb.15.3.596

118. Joukov V, De Nicolo A. The Centrosome and the primary cilium: the yin and yang of a hybrid organelle. Cells. 2019;8(7):701-701. doi:10.3390/cells8070701

119. Czaplinski K. Understanding mRNA trafficking: Are we there yet? Seminars in Cell and Developmental Biology. 2014;32:63-70. doi:10.1016/j.semcdb.2014.04.025

120. Blower MD. Molecular insights into intracellular RNA localization. Int Rev Cell Mol Biol. 2013;302:1-39. doi:10.1016/B978-0-12-407699-0.00001-7

121. Antoniades I, Stylianou P, Skourides PA. Making the connection: ciliary adhesion complexes anchor basal bodies to the actin cytoskeleton. Dev Cell. 2014;28(1):70-80. doi:10.1016/j.devcel.2013.12.003

122. Werner ME, Hwang P, Huisman F, Taborek P, Yu CC, Mitchell BJ. Actin and microtubules drive differential aspects of planar cell polarity in multiciliated cells. J Cell Biol. 2011;195(1):19-26. doi:10.1083/jcb.201106110

123. Yang J, Andre P, Ye L, Yang YZ. The Hedgehog signalling pathway in bone formation. International journal of oral science. 2015;7(2):73-79. doi:10.1038/ijos.2015.14

124. Wilson MH, Holzbaur ELF. Nesprins anchor kinesin-1 motors to the nucleus to drive nuclear distribution in muscle cells. Development 2015; 142(1): 218-228. doi:10.1242/dev.114769

125. Fridolfsson HN, Ly N, Meyerzon M, Starr DA. UNC-83 coordinates kinesin-1 and dynein activities at the nuclear envelope during nuclear migration. Dev Biol. 2010;338(2):237-250. doi:10.1016/j.ydbio.2009.12.004

126. Ware SM, Aygun MG, Hildebrandt F. Spectrum of clinical diseases caused by disorders of primary cilia. Proceedings of the American Thoracic Society. 2011;8(5):444-450. doi:10.1513/pats.201103-025SD

127. Zaghloul NA, Brugmann SA. The emerging face of primary cilia. Genesis. 2011;49(4):231-246. doi:10.1002/dvg.20728

128. Geister KA, Camper SA. Advances in skeletal dysplasia genetics. Annu Rev Genomics Hum Genet. 2015;16:199-227. doi:10.1146/annurev-genom-090314-045904

129. Handa A, Voss U, Hammarsjö A, Grigelioniene G, Nishimura G. Skeletal ciliopathies: a pattern recognition approach. Japanese Journal of Radiology. 2020;38(3):193-206. doi:10.1007/s11604-020-00920-w

130. Huber C, Cormier-Daire V. Ciliary disorder of the skeleton. American Journal of Medical Genetics, Part C: Seminars in Medical Genetics. 2012;160 C(3):165-174. doi:10.1002/ajmg.c.31336

131. Ibarra BA, Atit R. What do animal models teach us about congenital craniofacial defects? Advances in Experimental Medicine and Biology. 2020;1236:137-155. doi:10.1007/978-981-15-2389-2_6

132. Schock EN, Chang CF, Youngworth IA, Davey MG, Delany ME, Brugmann SA. Utilizing the chicken as an animal model for human craniofacial ciliopathies. Dev Biol. 2016;415(2):326-337. doi:10.1016/j.ydbio.2015.10.024

133. Adel Al-Lami H, Barrell WB, Liu KJ. Micrognathia in mouse models of ciliopathies. Biochem Soc Trans. 2016;44(6):1753-1759. doi:10.1042/BST20160241

134. Temiyasathit S, Jacobs CR. Osteocyte primary cilium and its role in bone mechanotransduction. Ann N Y Acad Sci. 2010;1192:422-428. doi:10.1111/j.1749-6632.2009.05243.x

135. Martín-Guerrero E, Tirado-Cabrera I, Buendía I, Alonso V, Gortázar AR, Ardura JA. Primary cilia mediate parathyroid hormone receptor type 1 osteogenic actions in osteocytes and osteoblasts via Gli activation. J Cell Physiol. 2020;235(10):7356-7369. doi:10.1002/jcp.29636

136. Fisher RA. The possible modification of the response of the wild type to recurrent mutations. Am Nat. 1928;62(679):115-126.

137. Waddington CH. Canalization of development and genetic assimilation of acquired characters. Nature. 1959;183(4676):1654-1655. doi:10.1038/1831654a0

138. Charlesworth B, Lande R, Slatkin M. A Neo-Darwinian commentary on macroevolution. Evolution. 1982;36(3):474-498. doi:10.1111/j.1558-5646.1982.tb05068.x

139. Gibson G, Hogness DS. Effect of polymorphism in the Drosophila regulatory gene Ultrabithorax on homeotic stability. Science. 1996;271(5246):200-203. doi:10.1126/science.271.5246.200

140. Bailey AP, Bhattacharyya S, Bronner-Fraser M, Streit A. Lens specification is the ground state of all sensory placodes, from which FGF promotes olfactory identity. Dev Cell. 2006;11(4):505-517. doi:10.1016/j.devcel.2006.08.009

141. Albertson RC, Cresko W, Detrich HW, Postlethwait JH. Evolutionary mutant models for human disease. Trends in Genetics. 2009;25(2):74-81. doi:10.1016/j.tig.2008.11.006

142. Hallgrimsson B. Variation: A Central Concept in Biology. Academic Press; 2005.

143. Cortés CR, Metzis V, Wicking C. Unmasking the ciliopathies: Craniofacial defects and the primary cilium. Wiley Interdisciplinary Reviews: Developmental Biology. 2015;4(6):637-653. doi:10.1002/wdev.199

144. Goetz SC, Anderson KV. The primary cilium: A signalling centre during vertebrate development. Nature Reviews Genetics. 2010;11(5):331-344. doi:10.1038/nrg2774

145. Rohatgi R, Milenkovic L, Scott M. Patched1 regulates hedghog signaling at the primary cilium. Science. 2007;317:372-377.

146. Berbari NF, O'Connor AK, Haycraft CJ, Yoder BK. The primary cilium as a complex signaling center. Current Biology. 2009;19(13):R526-R535. doi:10.1016/j.cub.2009.05.025

147. Westerfield M. The Zebrafish Book; A Guide for the Laboratory Use of Zebrafish (*Danio Rerio*). 5th ed. University of Oregon Press; 2007.

148. Le Pabic P, Cooper WJ, Schilling TF. Developmental basis of phenotypic integration in two Lake Malawi cichlids. EvoDevo. 2016;7(1):3-3. doi:10.1186/s13227-016-0040-z

149. Powder KE, Milch K, Asselin G, Albertson RC. Constraint and diversification of developmental trajectories in cichlid facial morphologies. EvoDevo. 2015;6(1):25-25. doi:10.1186/s13227-015-0020-8

150. Abzhanov A, Kuo WP, Hartmann C, Rosemary Grant B, Grant PR, Tabin CJ. The calmodulin pathway and evolution of elongated beak morphology in Darwin's finches. Published online 2006. doi:10.1038/nature04843

151. Mansfield JH, Abzhanov A. Hox expression in the american alligator and evolution of archosaurian axial patterning. J Exp Zool (Mol Dev Evol). 2010;314:629-644. doi:10.1002/jez.b.21364

152. Schneider RA, Richard Schneider CA. Neural crest and the origin of species-specific pattern. Genesis 2018; 56(6-7): doi:10.1002/dvg.23219

153. Kettleborough RNW, Busch-Nentwich EM, Harvey SA, et al. A systematic genome-wide analysis of zebrafish protein-coding gene function. Nature. 2013;496(7446):494-497. doi:10.1038/nature11992

154. Lee BT, Barber GP, Benet-Pagès A, et al. The UCSC Genome Browser database: 2022 update. Nucleic Acids Res. 2022;50(D1):D1115-D1122. doi:10.1093/nar/gkab959

155. Truett GE, Heeger P, Mynatt RL, Truett AA, Walker JA, Warman ML. Preparation of PCR-quality mouse genomic DNA with hot sodium hydroxide and tris (HotSHOT). Biotechniques. 2000;29(1):52, 54. doi:10.2144/00291bm09

156. Walker M, Kimmel C. A two-color acid-free cartilage and bone stain for zebrafish larvae. Biotechnic & Histochemistry. 2007;82(1):23-28. doi:10.1080/10520290701333558

157. Westneat A, Olsen A. StereoMorph: an R package for the collection of 3D landmarks and curves using a stereo camera set-up. Methods in Ecology and Evolution. 2015;6:351-356.

158. Olsen A, Haber A. StereoMorph: Stereo Camera Calibration and Reconstruction. Published 2017. https://cran.r-project.org/web/packages/StereoMorph/index.html

159. Rohlf FJ, Slice D. Extensions of the Procrustes method for the optimal superimposition of landmarks. Systematic Biology. 1990;39(1):40-59. doi:10.2307/2992207

160. Gunz P, Mitteroecker P. Semilandmarks: a method for quantifying curves and surfaces. Hystrix, the Italian Journal of Mammalogy. 2013;24(1):103-109. doi:10.4404/hystrix-24.1-6292

161. Goodall C. Procrustes methods in the statistical analysis of shape. Journal of the Royal Statistical Society Series B (Methodological). 1991;53(2):285-339.

162. Collyer ML, Sekora DJ, Adams DC. A method for analysis of phenotypic change for phenotypes described by high-dimensional data. Heredity (Edinb). 2015;115(4):357-365. doi:10.1038/hdy.2014.75

163. Collyer M, Adams D. Phenotypic trajectory analysis: Comparison of shape change patterns in evolution and ecology. Hystrix. 2013;40. doi:10.4404/hystrix-24.1-6298

164. Adams DC, Collyer ML. Phylogenetic ANOVA: Group-clade aggregation, biological challenges, and a refined permutation procedure. Evolution. 2018;72(6):1204-1215. doi:10.1111/evo.13492

165. Collyer ML, Adams DC. Analysis of two-state multivariate phenotypic change in ecological studies. Ecology. 2007;88(3):683-692. doi:10.1890/06-0727

166. Adams DC. A generalized K statistic for estimating phylogenetic signal from shape and other high-dimensional multivariate data. Syst Biol. 2014;63(5):685-697. doi:10.1093/sysbio/syu030

167. Dawe HR, Adams M, Wheway G, et al. Nesprin-2 interacts with meckelin and mediates ciliogenesis via remodelling of the actin cytoskeleton. Journal of Cell Science. 2009;122(15):2716-2726. doi:10.1242/jcs.043794

168. Teraoka H, Dong W, Okuhara Y, et al. Impairment of lower jaw growth in developing zebrafish exposed to 2,3,7,8-tetrachlorodibenzo-p-dioxin and reduced hedgehog expression. Aquatic Toxicology. 2006;78(2):103-113. doi:10.1016/j.aquatox.2006.02.009

169. Male I, Tuba Ozacar A, Fagan RR, et al. Hedgehog signaling regulates neurogenesis in the larval and adult zebrafish hypothalamus. bioRxiv. Published online 2019:740613-740613. doi:10.1101/740613

3. CHAPTER 3

RAPID MORPHOLOGICAL CHANGE IN MULTIPLE CICHLID ECOTYPES FOLLOWING THE DAMMING OF A MAJOR CLEARWATER RIVER IN BRAZIL

AUTHORS: Michelle C Gilbert[1], Alberto Akama[2], Cristina Cox Fernandes[3,4], R Craig Albertson[4]

1 Graduate Program in Organismic and Evolutionary Biology, University of Massachusetts, Amherst MA 01003 USA.

2 Museu Paraense Emílio Goeldi, Belém, PA, Brazil

3 Instituto Nacional de Pesquisas da Amazônia, Manaus, Brazil

4 Department of Biology, University of Massachusetts, Amherst MA 01003 USA.

PUBLISHED IN: Evolutionary Applications

FULL CITATION: M Gilbert, A Akama, CC Fernandez, RC Albertson. 2020. Rapid morphological change in multiple cichlid ecotypes following the damming of a major clearwater river in Brazil. *Evolutionary Applications.* 13: 2754-2771

Abstract

While anthropogenic disturbances can have damaging effects on biodiversity, they also offer an opportunity to understand how species adapt to new environments and may even provide insights into the earliest stages of evolutionary diversification. With these topics in mind, we explored the morphological changes that have occurred across several cichlid species following the damming of the Tocantins River, Brazil. The Tocantins was once a large (2,450km), contiguous river system; however, upon closure of the Tucuruí Hydroelectric Dam in 1984, a large (~2,850km^2), permanent reservoir was established. We used geometric morphometrics to evaluate changes in native cichlids, comparing historical museum specimens collected from the Tocantins to contemporary specimens collected from the Tucuruí reservoir. Six species across five genera were included to represent distinct ecomorphs, from large piscivores to relatively small opportunistic omnivores. Notably, statistically significant changes in shape and morphological disparity were observed in all species. Moreover, the documented changes tended to be associated with functionally relevant aspects of anatomy, including head, fin, and body shape. Our data offer insights into the ways cichlids have responded, morphologically, to a novel lake environment and provide a robust foundation for exploring the mechanisms through which these changes have occurred.

Introduction

Anthropogenic alterations to an ecosystem can provide opportunities for studying how populations respond to rapid ecological change. Over the past 80 years, there has been mounting evidence that modifications to waterways can have immediate, and lasting, ecological consequences that may result in varying degrees of habitat destruction and fragmentation (Trautman, 1939; Allan & Flecker, 1993; Lau, Lauer, & Weinman,

2006; Helfman, 2007; Geladi et al., 2019). Dam and reservoir construction, in particular, can have long reaching ecological effects on fish communities (Agostinho, Pelicice, & Gomes, 2008), including shifts in local fish assemblages (Platania, 1991), impeding the movement of migrating species (Dugan et al., 2010; Liermann, Nilsson, Robertson, & Ng, 2012) and disrupting the reproductive success of species that depend on the flow of water for egg dispersal (Platania & Altenbach, 1998; Alò & Turner, 2005). Further, there is significant concern that such drastic changes increase the risk of extirpation or extinction of local populations, due to reduced genetic diversity (Nei, Maruyama, & Chakraborty, 1975; Higgins & Lynch, 2001; Alò & Turner, 2005).

With the human population continuing to increase, so too is the demand for energy. To meet these needs, there is an increasing reliance on exploiting lotic freshwater systems, with over 3700 dams either currently under construction or planned, many of which are in developing countries (Zarfl, Lumsdon, Berlekamp, Tydecks, & Tockner, 2014; Winemiller et al., 2016). The Tocantins river is one such system that is increasingly being utilized to meet the energy demands of a growing population. Historically characterized by fast flowing rapids, sand and rock covered waterbeds, and rich seasonal floodplains (de Mérona, 1987), the Tocantins is one of the largest clearwater rivers in South America. With a total length of roughly 2450km, the Tocantins River passes through four Brazilian states and serves as the major drainage for both the Tocantins and Araguaia watersheds. Over the past 30 years, the Tocantins River has seen increased anthropogenic activity, including deforestation, agriculture, and the construction of numerous dams. The Tucuruí Hydroelectric Dam is the largest and oldest of these, and its construction has resulted in the establishment of a large (2850km^2)

permanent reservoir, stretching nearly 70km in length and 40km wide (ELETROBRÁS/DNAEE, 1997).

Since the completion and subsequent closure of the Tucuruí Hydroelectric Dam in 1984, the Tocantins River has experienced drastic hydrological, ecological, and geomorphological changes (Fearnside, 2001). For instance, the once historic rapids and streams that characterized the system have disappeared from the surrounding area, which in turn has affected the abundance and variety of food sources available to native fishes (Araújo-Lima, Agostinho, & Fabré, 1995). Alterations such as these may create opportunities for fishes that are inclined to be trophic generalists (Angermeier, 1995; Wilson et al., 2008), while greatly impairing trophic specialists that rely on specific habitats for various life stages, behaviors, and feeding ecologies. Changes in the local fish assemblages within the reservoir have already been observed, including a reported 20% reduction in species diversity since 1984 (Santos, Jégu, & de Mérona, 1984; Santos, de Mérona, Juras, & Jégu, 2004).

Habitat destruction and fragmentation are a significant threat to biodiversity (Vitousek, Mooney, Lubchenco, & Melillo, 1997), and such rapid ecological alterations require populations to adapt or face local extinction. Indeed, habitat fragmentation can spur the contemporary evolution of populations and has even been shown to result in increased speciation and rapid genetic divergence in natural systems (Dias, Cornu, Oberdorff, Lasso, & Tedesco, 2013). Generally speaking, fishes are well known to be capable of quickly responding to rapid ecological shifts (Rüber & Adams, 2001; Hulsey, Hendrickson, & García de León, 2005; Collyer, Hall, Smith, & Hoagstrom, 2015), including anthropogenic change (Candolin, 2009; Franssen, 2011; Franssen, Harris,

Clark, Schaefer, & Stewart, 2013). However, there remains a pressing need to evaluate native fish species that have been subjected to such rapid changes to assess if, how, and why populations respond to sudden human-induced change.

Cichlids (Cichliformes:Cichlidae) are a highly diverse and well-studied family of fishes that have repeatedly undergone extensive adaptive radiations (López-Fernández, Honeycutt, & Winemiller, 2005; Arbour & López-Fernández, 2013), and are well known to adapt quickly to ecological change, especially those that influence the foraging environment (Wimberger, 1991, 1992; Muschick, Barluenga, Salzburger, & Meyer, 2011). Native cichlid populations in and around the Tocantins River and Tucuruí reservoir exhibit a wide range of life history strategies, breeding, and food preferences. Such diversity allows for the exploration and assessment of several foraging ecomorphs, from large, piscivorous predators to small mud sifters. This system, and the alterations it has experienced, provides a unique opportunity to examine how large-scale alterations to an aquatic system can spur incidents of rapid adaptation in complex fish communities.

In this study, we compared the morphology of six cichlid species collected from the Tucuruí reservoir in 2018 (post-dam) to that of cichlids collected at the same locality prior to or just after the closure of the Tucuruí Hydroelectric Dam in 1984 (pre-dam). Our primary aim is to acquire insights into if, and how, the cichlid community has adapted, in terms of shape, during the past 34-48 years to this novel environment. While traditional morphometrics can provide a direct and intuitive link to specific, functionally relevant characters, species rarely change in just one trait, and adaptation often involves subtle, coordinated shifts across a suite of characters (Rohlf & Marcus, 1993; D. C. Adams, Rohlf, & Slice, 2004). By focusing on geometry, geometric morphometrics complements

and extends traditional linear measures to provide a more holistic understanding of variation in organismal shape (Zelditch, Swiderski, Sheets, & Fink, 2012). Further, by using species that represent different ecotypes we will be able to assess the extent to which feeding behavior and ecology can predict the magnitude or pattern of anatomical change. Our hope is that this study will provide insights as to how species respond to rapid environmental change, especially anthropogenic change, and how it may affect the Amazon.

Our overarching hypothesis is that the formation of the Tucuruí reservoir has induced shifts in habitat and foraging behavior and concomitant changes in the anatomy of resident cichlid populations as they adapt to novel environmental conditions. This study represents a first step toward assessing this hypothesis. Given the varied ecologies, foraging behaviors, and life histories of species included in our analysis, a number of more specific predictions arise from this study. *Cichla* are large piscivorous fishes, capable of easily navigating a lotic system. Proposed similarities between *C. kelberi* and *C. pinima* included prognathous lower jaws and maxillae that extended below the middle of the orbit. We expected contemporary specimens of *Cichla* to converge on a phenotype that includes deeper heads and bodies to reflect the change to a large, deep lentic system (Collin & Fumagalli, 2011; Gaston & Lauer, 2015). Our analyses also included four smaller species: two foraging generalists (*G. neambi* and *S. jurupari***)**, and two specialists (*C. spectabilis* and *H. efasciatus*). Broadly speaking, habitat degradation and global change are drivers of the observed replacement of specialists by generalists (Clavel, Julliard, & Devictor, 2011). In principle, generalists should be more resilient than specialists to ecological changes that influence resource availability (Vázquez &

Simberloff, 2002), a scenario that has been widely observed in numerous taxa, including fishes (Angermeier, 1995; Wilson et al., 2008). Thus, we predicted that *G. neambi* and/or *S. jurupari* would exhibit changes in shape and potentially morphological disparity as a result of the introduction of new niche space from flooded riparian and altered hydrology. *C. spectabilis* are ambush predators that consume a variety of prey items including arthropods and smaller fishes. *H. efasciatus* also consume a variety of food items but are inclined towards being a frugivore. Given the relatively narrow feeding repertoires of these two species, we expected to observe less conspicuous changes in their shapes.

Materials and Methods

Study Site:

The Tocantins river presents several dams along its course, such as the Serra da Mesa and Lageado, but the Tucuruí is the largest with the most substantial impact (Akama, 2017). The Tucuruí reservoir (Figure 1; Supplemental 1) covers more than 2.875 km^2, 400 km upstream from the river mouth (de Mérona, Santos, & Almeida, 2001; Santos et al., 2004). Its shape is dendritic with a maximum depth of 75m close to the dam and a mean depth of 17m, with some shallow areas that can become exposed during the dry season (G. dos Santos et al., 2004). Fish inventories were conducted prior to closure in 1980-1982, specimens from which are housed in the *Instituto Nacional de Pesquisas da Amazônia* (INPA) fish collection. Before this, during the 1970's, expeditions in Pará state (Expedição Permanente na Amazônia, "Permanent Expedition to Amazon") also collected in pristine areas of the Tocantins river, with specimens housed at the *Museu de Zoologia da Universidade de São Paulo* (MZUSP). Many of these specimens were used in this study.

Figure 3.1. Google Earth imagery (Landsat/Copernicus) of Tucuruí Hydroelectric dam vicinity, before (left; December 1984) and after (right; December 2016) dam construction. Scale bar represents ~48.3 km (30 miles).

Fish Collections:

To investigate whether native cichlid populations have experienced a rapid change in trophic and body shape morphology, we compared museum specimens (Supplemental Table 1) collected in the region ≤ 1984 to fishes collected from the Tucuruí reservoir in 2018. However, *Cichla pinima* samples were from 1987, collected shortly after the dam was closed, and just as the reservoir appears to have reached its current size (Supplemental Figure 1). Issues for comparing fixed museum specimens with fresh specimens were considered. However, such comparisons are not uncommon in

evolutionary studies and while fixation can influence overall specimen size, the effects on shape have been shown to be minimal (Gaston & Lauer, 2015; Larochelle, Pickens, Burns, & Sidlauskas, 2016). Further, the aspects of shape we assessed tended to be associated with specific bony elements (e.g., jaw length, orbit size, anal fin insertion) that would presumably be less prone to the effects of fixation. Contemporary specimens were obtained fresh from the Association of Fisherman in Tucuruí and directly from fishermen at the margin of Tucuruí reservoir, March 2018, and imaged in the field, apart from *Geophagus neambi* which were collected in January of 2018. Specimens were obtained from multiple fisherman and, therefore, came from multiple collection events around the reservoir. Since nearly all contemporary specimens were collected from local vendors, viscera (including gonads) were often not present, making it impossible to include sex as a trait in our study. These specimens were accessioned in the fish collection at Museu Paraense Emílio Goeldi (MPEG) in Belém, PA, Brazil. In total, we examined six species across five genera that encompassed a range of trophic ecologies.

Study Taxa (Ecology):

Cichla kelberi and *C. pinima.* The peacock basses are large, piscivorous fishes that are commercially important and widely distributed throughout the Amazon basin. *Cichla* species have been reported to rapidly colonize, and undergo population expansion, within dammed sections of rivers (G. Santos, 1995; G. Santos & Oliveira Jr, 1999). This is likely because they will readily consume a wide variety of fish species (Williams, Winemiller, Taphorn, & Balbas, 1998; Novaes, Caramaschi, & Winemiller, 2004; Rosemara Fugi, Luz-Agostinho, & Agostinho, 2008). Further, while cannibalism is a common phenomenon in this genus (*e.g., C. monoculus, C. kelberi*), it has been reported

to occur more frequently in systems affected by dam operation (Novaes et al., 2004; Rosemara Fugi et al., 2008).

Geophagus neambi. G. neambi is a recently described species (Lucinda et al. 2010) from the Tocantins drainage. Across the genus *Geophagus*, a range of reproductive strategies are utilized, including mouthbrooding (e.g., *G. steindachneri*) and substrate spawning (e.g., *G. brasiliensis*), the former which may create functional constraints on how trophic morphology is allowed to change. The diet of certain *Geophagus* species, (*i.e., G. brasiliensis*) suggest a generalist/opportunistic diet that includes gastropods, vegetation, and fish scales (Bastos, Condini, Varela, & Garcia, 2011). Previous studies have shown *Geophagus* species to be phenotypically plastic, both in terms of jaw and body shape morphology, when presented with different diets (Wimberger, 1991, 1992). Further, a related species, *G. surinamensis* (possibly misidentified *G. neambi*), was found to have shifted from an ancestrally omnivorous diet to one more characteristic of a detritivore, whereas within the Tucuruí reservoir this species appeared to adopt an unspecialized carnivorous diet (de Mérona et al., 2001).

Satanoperca jurupari. Formerly named *Geophagus jurupari*, *S. jurupari* is widely distributed throughout the Amazon Basin and is generally characterized by a more omnivorous diet. In the Lake Tucuruí system, *S. jurupari* was classified as a broad invertivore prior to the closure of the Tucuruí Hydroelectric Dam, but has since been found to consume more of an omnivore diet both within Lake Tucuruí and downstream of the dam (de Mérona et al., 2001). Reproductive behavior includes mouth brooding following ~24 hours of substrate spawning (Reid & Atz, 1958). Further, parents have been observed to actively move nest sites in response to changing water levels for the

first 24 hours post spawning (Cichocki, 1976). Much like *Geophagus,* mouth brooding behavior in this genus may create constraints on the functional aspects of trophic morphology and the degree to which it can respond to different feeding regimes.

Caquetaia spectabilis. Caquetaia species are carnivorous predators, well known for their extreme jaw protrusion, which is reported to be an adaptation that enhances foraging efficiency on elusive prey (Waltzek & Wainwright, 2003). Altered hydrologic cycles have been reported to influence the activity and feeding behavior of *C. spectabilis*, notably during dry or low periods where individuals seem to become increasingly sedentary and feed on a greater variety of food items (Röpke, Ferreira, & Zuanon, 2014).

Heros efasciatus. H. efasciatus is an omnivore, and one of few cichlid species that acts a frugivore, especially during flood periods when it is able to exploit riparian zones and floodplains (Favero, Pompeu, & Prado-Valladares, 2010). *H. efasciatus* spawn during October and December, presumably so that the eggs will hatch during the flood season (Favero et al., 2010). Fecundity of individuals has been reported to be low (Favero et al., 2010), suggesting that populations could be highly susceptible to rapid ecological change.

Data Collection:

We photographed the left-lateral surface of museum and field collected specimens using a tripod and digital camera (Olympus E520). A scale bar was included alongside each photograph to later scale landmark data and dorsal, caudal, anal, and pelvic fins were pinned when they obscured the body profile. A range of sizes were available from museum collections, whereas sizes from freshly collected specimens tended to be larger (Supplemental Table 1). Since sample sizes from the museum were often limited, all museum specimens in workable condition were included, and size effects were later

corrected for mathematically (see below). Here, workable condition is defined as lacking conspicuous bending and severe tissue deformation. Total sample sizes for all species:year groups are given in figure legends.

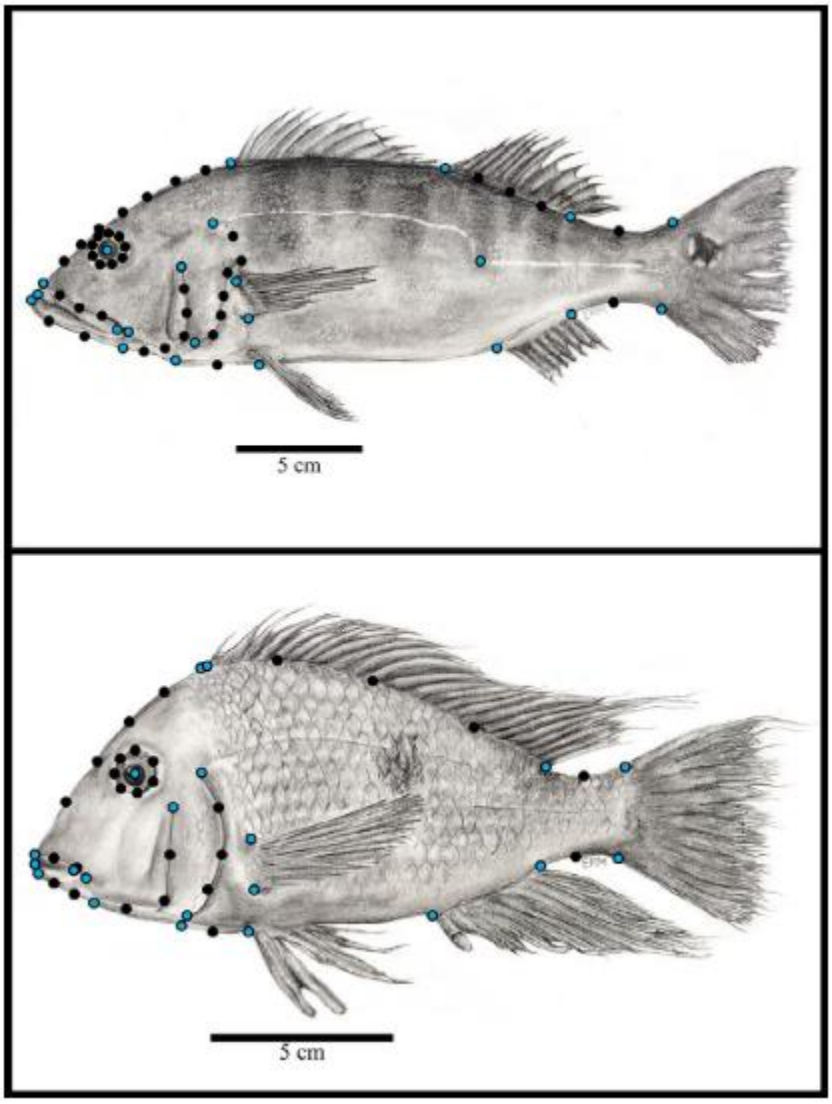

Figure 3.2. Anatomical landmarks used for geometric morphometric analysis. Large, blue circles represent fixed landmarks, small black circles represent semi/sliding landmarks. Cichla (top). A total of 60 landmarks were used, 22 of which were fixed landmarks, including one fixed landmark at the beginning of the second lateral line. Other cichlids (bottom). A total of 48 landmarks were used, 21 of which were fixed landmarks. Fixed landmarks include premaxillary groove, end of nape, insertion of dorsal fin (second dorsal for Cichla), end of dorsal fin, upper and lower ends of the caudal peduncle, insertion and end of anal fin, beginning of breast and insertion of pelvic fin, pectoral fin insertion, opercle & preopercle beginning and end, lower jaw insertion and anterior tip, tip and posterior end of premaxilla, posterior end of maxillary groove, center of the eye, and insertion of the lower lateral line (Cichla only). Illustrations hand-drawn by Emma R Masse.

Landmark configurations for *Cichla* consisted of 22 “fixed” anatomical landmarks and 38 sliding semi-landmarks. For the remaining species, the landmark configurations consisted of 21 “fixed” anatomical landmarks and 27 sliding semi-landmarks (Figure 2). We used a greater number of landmarks in *Cichla* because they possess two distinct dorsal fins, as opposed to the more continuous dorsal fins seen in the remaining four genera. They also exhibited interesting patterns of variation in the positioning of the lateral canal along the body that we wished to quantify. While fixed landmarks correspond to homologous anatomical points of interest, semi-landmarks allow for more nuanced variation found in complex structures, such as curves, to be “captured” and quantified. Being allowed to slide along curves during a generalized Procrustes analysis (GPA; Rohlf and Slice 1990), semi-landmarks allow for the minimizing of Procrustes distances between landmarks of curves and permit one to quantify the curvature of complex structures (Gunz & Mitteroecker, 2013). Landmarking provided X, Y Cartesian coordinates that we used to generate Procrustes residuals during GPA. GPA works by mathematically removing the effects of size, scale, and orientation to allow for one to determine mean shapes (Goodall, 1991) to generate said Procrustes residuals around the mean that reflect specimen variation. All specimens were digitized using STEREOMORPH (Olsen & Westneat, 2015).

In addition to collecting 2-D geometric morphometric data, we also collected four linear measures across all specimens, pre- and post-dam. This was done as a supplement of our geometric morphometric data to assess possible changes in specific traits with explicit ecological relevance. Linear measurements were taken digitally using TPSdig software (v2.2; Rohlf 2016) and consisted of body depth (indicator of maneuverability

and swimming speed), jaw length (relevance to prey capture mechanism and preference), caudal peduncle length (indicator of swimming performance, e.g., cruising or non-cruising), and eye diameter (pertinent to prey preference). Supplemental Figure 2 illustrates how and where each measurement was taken. We calculated slopes from linear measurements within species groups and used ANOVA on least squared means to compare pre/post-dam values, allowing us to determine if trajectories were parallel or divergent. We also corrected for allometric effects via linear regression where linear traits were the dependent variable and standard length was the predictor variable.Residuals were subjected to Welch Two Sample t-tests to test for pair-wise significance (pre- vs post-dam) for all species, with the exception of *Cichla* which we subjected to a Tukey Honest Significant Difference test in order to make comparisons between the two species and year collected. While the comparison of residual, size corrected values assumes that slopes are parallel (McCoy, Bolker, Osenberg, Miner, & Vonesh, 2006), we chose to proceed with such comparisons even in the few cases where slopes are obviously divergent. To this end, we encourage the results of our linear measures to be used a merely as a supplement to the geometric morphometric methods.

Geometric Morphometric Analyses:

GPA aligned coordinate data were subjected to various statistical tests to assess differences between ≤1984 collections and our 2018 collection. Comparisons of shape were performed within cichlid genera. We chose this taxonomic level, as cichlid genera are generally defined by eco-morphological differences. *Cichla* was the only genus containing two species, and represented the only instance of a 4-way comparison. All other comparisons were between a single species at two different times. We conducted a

Procrustes ANOVA among each genus to determine the effect of each variable, as well as interaction terms, on shape [e.g., `(shape ~ centroid size * year)`]. Both R^2 and Z-scores were used to assess and compare variables and interaction terms. In all analyses, the null model consisted of shape and the effect of size alone `(shape ~ centroid size)`, while the full model also included the date collected as the independent variable `(shape ~ centroid size + year)`. In this way, we are able to evaluate the effects of year on shape while also accounting for any effects that may be associated with allometry. The only exception being in *Cichla*, where the full model used the interaction term `species:year` in place of year alone. All statistical tests, when appropriate, utilized a randomized residual permutation procedure (RRPP), ultimately subjected to 10,000 random permutations, and were done using `GEOMORPH` (Adams, Collyer, & Sherratt, 2015; Adams, Collyer, & Kaliontzopoulou, 2018) in R (R Core Team, 2018). RRPP is a method that randomizes the residual values from a null model to compare the statistics associated with a full model (Collyer & Adams, 2007; Collyer, Sekora, & Adams, 2015). We also performed tests of morphological disparity (i.e., variation in geometric shape) utilizing Procrustes variances (Collyer, Sekora, et al., 2015). For the purpose of significance testing, $\alpha = 0.05$ was used for all analyses.

For visualization of our data, we performed a principal component analysis (PCA) on the allometry corrected Procrustes residuals. We generated convex hulls using the first three principal components to project the region of morphospace that each species:year group occupied. This not only allowed for us to visually assess the region of overlap between years within a species group, but also provided a visual representation of changes in shape that we observed in many of our groups.

Results

Cichla species

For all species, we initially tested the effect of size, year, and the interaction of size with year, with the exception of *Cichla,* which contained a third variable distinguishing species. We then quantified both mean morphological shape and disparity within and between species collected before and after closure of the dam (Table 1&2). An initial Procrustes ANOVA revealed that no interactions were meaningful and that the effect of year alone (R^2 = 0.069; Z = 4.25; P = <0.0001) was comparable to or greater than the effect of size (R^2 = 0.088 ; Z = 4.20; P = <0.0001) alone (Supplemental Table 2). Pre-dam species comparisons (pre-dam *C. kelberi* vs *C. pinima*) revealed no significant differences in shape (p = 0.3683) or morphological disparity (p = 0.9098). A post-dam comparison showed a significant difference in the shape of *C. kelberi* and *C. pinima* (p = 0.0002), but not a difference in disparity (p = 0.5181). Across years and within species (*C. kelberi* pre-dam vs post dam; *C. pinima* pre-dam vs post-dam), shape was significantly different for both species (*C. kelberi*, p = 0.0001; *C. pinima*, p = 0.0269). Further, the post-dam collection showed significant increases in disparity for both species, *C. kelberi* (p = 0.0147, Procrustes Variance: pre-dam = 0.00063, post-dam = 0.00130) and *C. pinima* (p = 0.0593; Procrustes Variance: pre-dam = 0.00066, post-dam = 0.00116).

Deformation grids of pre-dam *Cichla* showed that both species were relatively long and possessed slender bodies. Pre-dam specimens of *Cichla kelberi* possessed somewhat larger heads than their *C. pinima* counterparts, but differences were not significant. Deformation grids of post-dam *Cichla* (Figure 3) illustrate morphological

differences between the two species, with contemporary *C. kelberi* possessing deeper bodies and heads. This is in contrast to the elongated bodies and heads observed in post-dam *C. pinima*.

Table 3.1. Pairwise comparisons of shape between species:year groups.

	Cichla kelberi, ≤1984	*Cichla kelberi*, 2018	*Cichla pinima*, 1987	*Cichla pinima*, 2018
Cichla kelberi, ≤1984	–	5.4862	0.2287	2.1289
Cichla kelberi, 2018	0.0001	–	6.1372	5.0857
Cichla pinima, 1987	0.3683	0.0001	–	2.2114
Cichla pinima, 2018	0.0307	0.0002	0.0269	–

Note i: Effect sizes (Z-scores) are above, p values below diagonal. (-) indicates diagonal.

Table 3.2. Pairwise comparisons of morphological disparity between species:year groups.

	Cichla kelberi, ≤1984	*Cichla kelberi*, 2018	*Cichla pinima*, 1987	*Cichla pinima*, 2018
Cichla kelberi, ≤1984	–	0.00066	0.00004	0.00053
Cichla kelberi, 2018	0.0147	–	0.00064	0.00015
Cichla pinima, 1987	0.9098	0.0171	–	0.00049
Cichla pinima, 2018	0.0467	0.5181	0.0593	–
Absolute Variance	0.0006	0.0013	0.0007	0.0012

Note ii: Note: Effect sizes (Z-scores) are above, p-values below diagonal. (–) indicates diagonal. Absolute variance for each group provided in the last row

The first three principal component axes (Figure 3) accounted for 58% of the total variance in shape. PC1 accounted for 25.6% of the variance. Negative scores along this axis were associated with elongated bodies, smaller heads, and a more anteriorly elongated second lateral line, while positive scores were associated with shorter bodies,

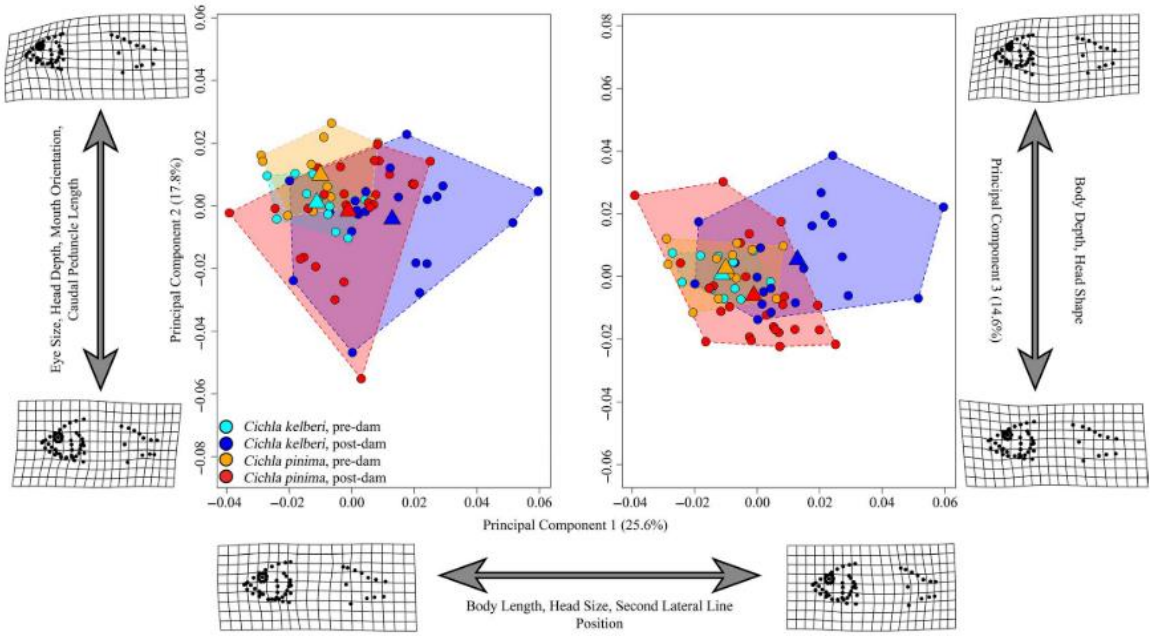

Figure 3.3. *Cichla* principal component plot (X-axis = PC1 (25.6%), Y-axis-left = PC2 (17.8%), Y-axis-right = PC3 (14.6%)) indicating regions of morphospace occupied by each of the four species:year groups, as illustrated by colored convex hulls. Circles indicate individuals, and triangle represents the mean shape of each group within morphospace. Deformation grids are indicative of the minimum and maximum shape values for respective axes. Post-dam collections showed significant increases in disparity for both species, *C. kelberi* (p = .0147, Procrustes Variance: pre-dam = 0.00063, post-dam = 0.00130) and *C. pinima* (p = .0593; Procrustes Variance: pre-dam = 0.00066, post-dam = 0.00116). Pre-, post-dam sample sizes: *Cichla kelberi*, n = 11, 21. *Cichla pinima*, n = 12, 25.

relatively deeper heads, and a shorter second lateral line. Pre-dam specimens exhibited more negative PC1 scores on average, whereas post-dam specimens occupied the full range of this axis. PC2 accounted for 17.8% of the variance. Negative scores on this axis were associated with larger eyes, deep heads, superiorly oriented mouths, and short caudal peduncles. In contrast, positive scores were associated with comparatively narrow heads, terminally positioned mouths, and longer caudal peduncles. Similar to PC1, pre-dam specimens were largely restricted to one end of this axis (i.e., positive PC2 scores), whereas post-dam specimens spanned most of this axis of shape space. PC3 accounted for 14.6% of the variance and captured variation in body and head size. *Cichla* with negative PC3 scores had slender bodies and robust heads, while *Cichla* with positive

scores can be characterized as having a deep body and narrow head. Mean shapes along this axis were largely similar between groups, however, post-dam specimens occupied a greater amount of shape space. Contrary to our predictions, our results suggest that contemporary *C. kelberi* and *C. pinima* are not converging on a single "reservoir" eco-morph, but instead appear to be spreading into distinct regions of morphospace. We had predicted that both *Cichla* species would develop deeper bodies and larger mouths in response to the change to a lentic system. Our prediction was accurate only for *C. kelberi*, and opposite to what we observed in *C. pinima*, which appear to have developed more streamlined bodies over time. Further, pre-dam specimens are highly constrained in morphospace on both PC1 axes and mean population shapes appear to be similar. However, post-dam population means for both *C. kelberi* and *C. pinima* appear much how Kullander & Ferreira (2006) had described them with *C. kelberi* having a deeper body (~33% of its standard length) compared to *C. pinima* (~28% of its standard length) (Kullander & Ferreira, 2006). In more general terms, *Cichlia* species found in river systems tend to vary in head size and body depth, which may correspond to differences in micro-habitat preference (e.g., fast flowing or more stagnant water).

Tests of allometry on geometric morphometric data failed to reject ($p = 0.2412$; Supplemental Table 3) the null hypothesis that allometries were parallel, indicating that there has been no significant alteration of allometric trajectories over the past ~ 34 years since the Tucuruí dam was constructed. Across our four linear measurements, only two showed significant differences between species (Supplemental Table 4). Both body depth and eye diameter differed between species, regardless of whether they were collected before or after the dam was closed. No significant differences were detected

within species over time; however, trajectory analyses revealed significant differences in both jaw length and eye diameter. Slopes for *C. kelberi* (Supplemental Figure 3) jaw length were significantly different ($p = 0.0353$), with pre-dam specimens exhibiting accelerated jaw growth. Slopes also differed for eye diameter in both *C. kelberi* ($p = 0.0013$) and *C. pinima* ($p = 0.0002$), with accelerated eye size development in pre-dam specimens. However, we note that size distributions for pre- and post-dam specimens were different, especially for *C. kelberi*, which suggests that differences in slopes should be interpreted with caution, especially those results following size corrected residuals.

Geophagus neambi

An initial Procrustes ANOVA revealed that no interactions were meaningful and that the effect of year alone ($R^2 = 0.114$; $Z = 3.87$; <0.0001) was comparable to the effect of size ($R^2 = 0.130$; $Z = 3.8781$; $P = <0.0001$) alone (Supplemental Table 2). *G. neambi* pre/post-dam groups had significantly different shapes ($p = 0.0003$), but disparity was not different between the two groups ($p = 0.1681$; Procrustes Variance: pre-dam = 0.0010, post-dam = 0.0012). Deformation grids of mean shapes revealed that pre-dam *G. neambi* have larger eyes and jaws, and more rounded pre-orbital region of the skull compared to post-dam specimens. These data are consistent with our prediction that foraging generalists would be susceptible to anatomical change over time in this system.

The first three principal component axes (Figure 4) accounted for 59% of the total variance. PC1 explained 29.3% of the variance and was associated with relative head and body size and shapes. Negative PC1 scores represented relatively smaller jaws, acutely angled faces, and larger bodies. On average, post-dam specimens exhibited negative PC1 scores compared to pre-dam specimens. PC2 accounted for 17.9% of the variance and was primarily associated with variation in head size. *G. neambi* with negative PC2 scores

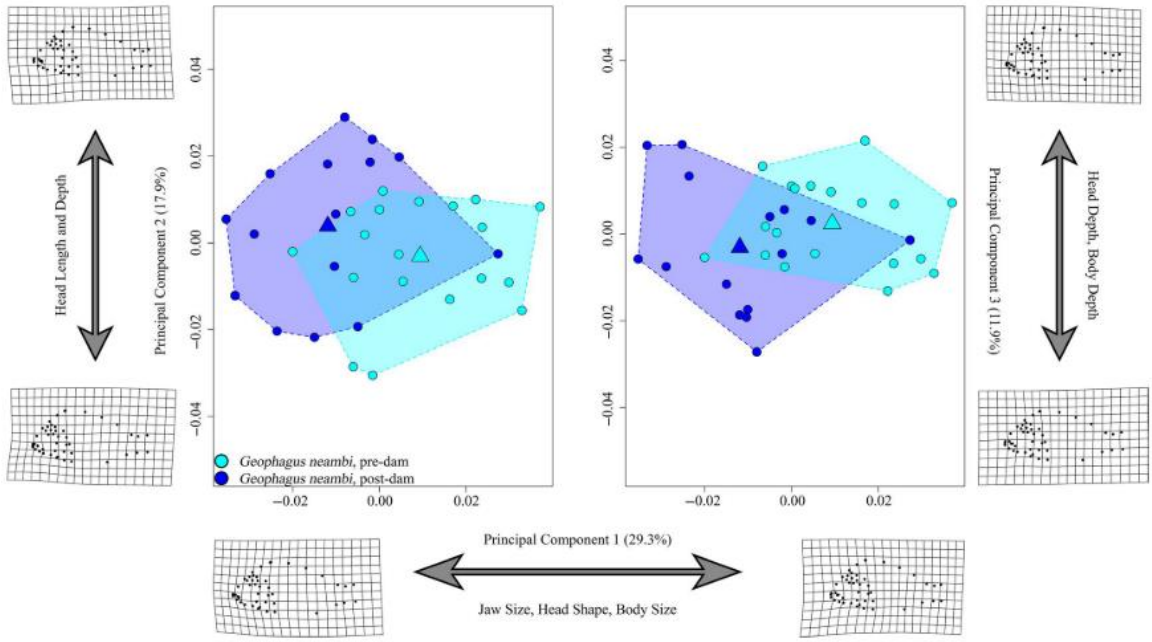

Figure 3.4. *Geophagus neambi* principal component plot (X-axis = PC1 (29.3%), Y-axis-left = PC2 (17.9%), Y-axis-right = PC3 (11.9%)) indicating regions of morphospace occupied by each year group, as illustrated by colored convex hulls. Circles indicate individuals, and triangle represents the mean shape of each group within morphospace. Deformation grids are indicative of the minimum and maximum shape values for respective axes. Morphological disparity test reveals no significant (p = .1681) reduction in disparity between pre/post-dam groups (Procrustes variance = 0.00096 and 0.00117, respectively). Pre-, post-dam sample sizes: n = 19, 15.

possessed relatively short and deep heads. Pre/post-dam specimens exhibited considerable overlap along this axis. PC3 explained 11.9% of the variance and captured variation in body depth and head profile, with negative scores associated with animals that possessed more shallow head profiles and less deep bodies. Similar to PC2, pre/post-dam specimens exhibited overlapping distributions along this axis.

Tests of allometry on geometric morphometric data rejected (p = 0.0312; Supplemental Table 3) the null hypothesis that allometries were parallel, suggesting that there has been an alteration of allometric trajectories over the ~ 34 years since the Tucuruí dam was constructed. Linear models on measurements revealed that body depth (p = 0.0120) and jaw length (p = 0.0284) were significantly different from pre-dam *G. neambi* (Supplemental Table 5). Pre-dam *G. neambi* possessed both deeper bodies and

longer jaws than the contemporary specimens. Neither caudal peduncle ($p = 0.2983$), nor eye diameter ($p = 0.4967$) was significantly different between the pre/post-dam group. Slopes between pre/post-dam (Supplemental Figure 4) collections were significantly different for both jaw length ($p = 0.0012$) and body depth ($p = 0.0049$). In both cases, pre-dam *G. neambi* experienced accelerated growth relative to their post-dam counterparts. Similar to the *Cichla* data presented above, these data should also be interpreted with care. In this case, pre- and post-dam specimens had similar size distributions, but size ranges were limited, meaning that slopes were highly dependent upon a handful of individuals at the periphery of the distributions. Given that slopes were divergent and that sampling was not uniform across size ranges, we caution the interpretation of results from size corrected linear measures.

Satanoperca jurupari

Procrustes ANOVA revealed that no interactions were meaningful and that the effect of year alone ($R^2 = 0.165$; $Z = 5.22$; $P = <0.0001$) was greater than the effect of size ($R^2 = 0.088$; $Z = 3.70$; <0.0001) alone (Supplemental Table 2). Pre/post-dam groups had significantly different shapes ($p = <0.0001$), but differences in disparity between the two groups was not significant ($p = 0.1306$; Procrustes Variance: pre-dam = 0.0008, post-dam = 0. 0007). Deformation grids of mean shapes revealed conspicuous differences in head shape. In particular, pre-dam *S. jurupari* possessed an elongated preorbital regions of the skull, upturned jaws, smaller eyes, and larger opercles, compared to post-dam specimens. Differences were also apparent in the size and shape of the caudal peduncle. Similar to *G. neambi*, these data were consistent with our predictions with respect to trophic generalists.

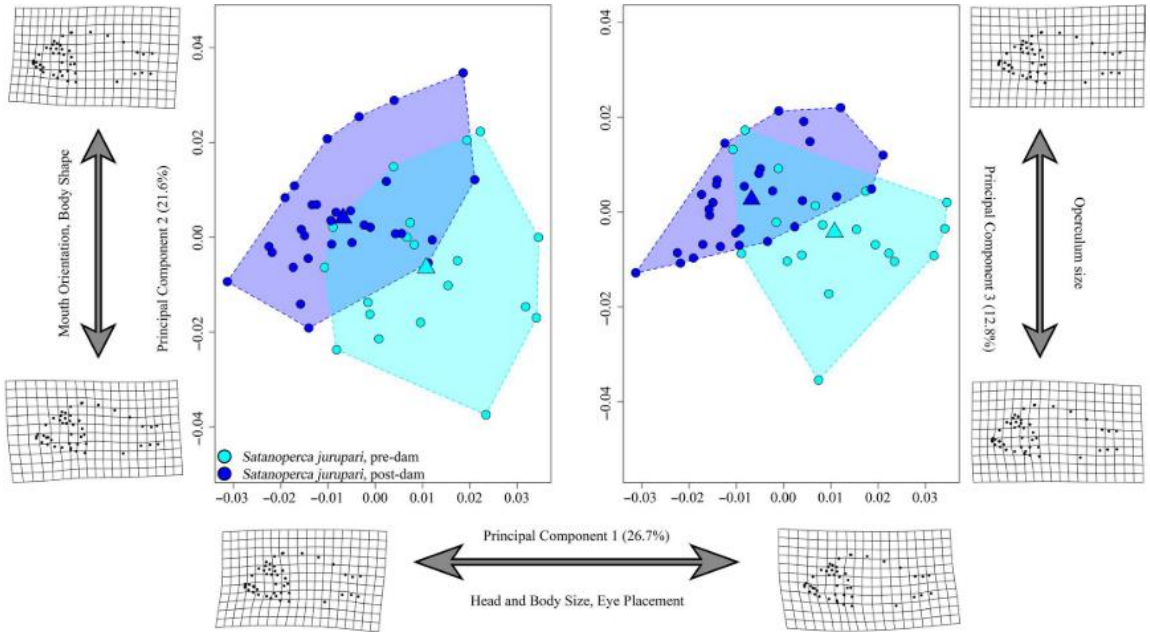

Figure 3.5. *Satanoperca jurupari* principal component plot (X-axis = PC1 (26.7%), Y-axis-left = PC2 (21.6%), Y-axis-right = PC3 (12.8%)) indicating regions of morphospace occupied by each year group, as illustrated by colored convex hulls. Circles indicate individuals, and triangle represents the mean shape of each group within morphospace. Deformation grids are indicative of the minimum and maximum shape values for respective axes. Morphological disparity test reveals no significant ($p = .1306$) change in disparity between pre/post-dam groups (Procrustes variance = 0.00084 and 0.00067, respectively). Pre-, post-dam sample sizes: n = 19, 30.

The first three principal component axes (Figure 5) accounted for 61.1% of the total variance. PC1 accounted for 26.7%, and described variation in head and body size, as well as eye placement. Negative scores were associated with short, rounded faces and more ventrally positioned eyes. Post-dam specimens exhibited more negative PC1 scores on average. PC2 accounted for another 21.6% of the variance and described variation in mouth orientation and body shape. Negative scores were associated with a more terminally positioned mouth, and a slender body with a more pronounced posterior tapering toward the tail. In contrast, positive scores were associated with a more upturned mouth, and rounded body shape. Post-dam specimens exhibited more positive PC2 scores. PC3 accounted for 12.8% of the variance and largely described variation in the opercular region of the skull. *S. jurupari* with negative scores tended to have larger

opercles, whereas specimens with positive scores possessed smaller opercles. Post-dam specimens exhibited slightly more positive PC3 scores on average.

Tests of allometry on geometric morphometric data failed to reject ($p = 0.1026$; Supplemental Table 3) the null hypothesis that allometries were parallel, indicating that there has been no significant alteration of allometric trajectories over the past ~ 34 years since the Tucuruí dam was constructed. Across all four linear measurements, we observed no significant difference in absolute group means (Supplemental Figure 4; Supplemental Table 5). Additionally, we found no significant differences among slope trajectories in any comparison.

Caquetaia spectabilis

Procrustes ANOVA revealed that interaction between size and year was meaningful ($R^2 = 0.056$; $Z = 2.71$; $P = 0.0051$) and that, despite being significant, the effect of year alone ($R^2 = 0.040$; $Z = 1.84$; $P = 0.039$) was less meaningful than the effect of size ($R^2 = 0.167$; $Z = 4.49$; <0.0001) alone (Supplemental Table 2). Pre/post-dam groups were significant at alpha=90% in terms of both shape ($p = 0.0935$) and disparity ($p = 0.0604$; Procrustes Variance: pre-dam = 0.0009, post-dam = 0.0007). Deformation grids of mean shapes suggested that pre-dam *C. spectabilis* possess slightly more upturned mouths, shallower bodies and anteriorly positioned eyes and pectoral fins compared to post-dam specimens. Thus, while subtle differences were noted, pre- and post-dam *C. spectabilis* specimens were not as divergent as the two generalist species, which is largely consistent with our predictions.

The first three PC axes (Figure 6) accounted for 54.3% of the total variance. PC1 accounted for 28.3% and was largely associated with differences in mouth orientation and body size. Negative PC1 scores were associated with a slightly shorter mouth and

shorter, deeper bodies. The distribution of pre- and post-dam specimens overlapped along this axis. PC2 accounted for 15.1% of the variance and was predominantly associated with eye size and body shape and head length, with negative scores associated with relatively small eyes, short, rounded bodies and shorter heads. Post-dam specimens exhibited slightly more negative PC2 scores on average. PC3 accounted for 10.8% of the variance and was associated with variation in head and caudal peduncle size, as well as positioning of the pectoral fin base. Negative scores along this axis were associated with small heads and caudal peduncles, and a larger pectoral fin base. Pre- and post-dam specimens overlapped along this axis.

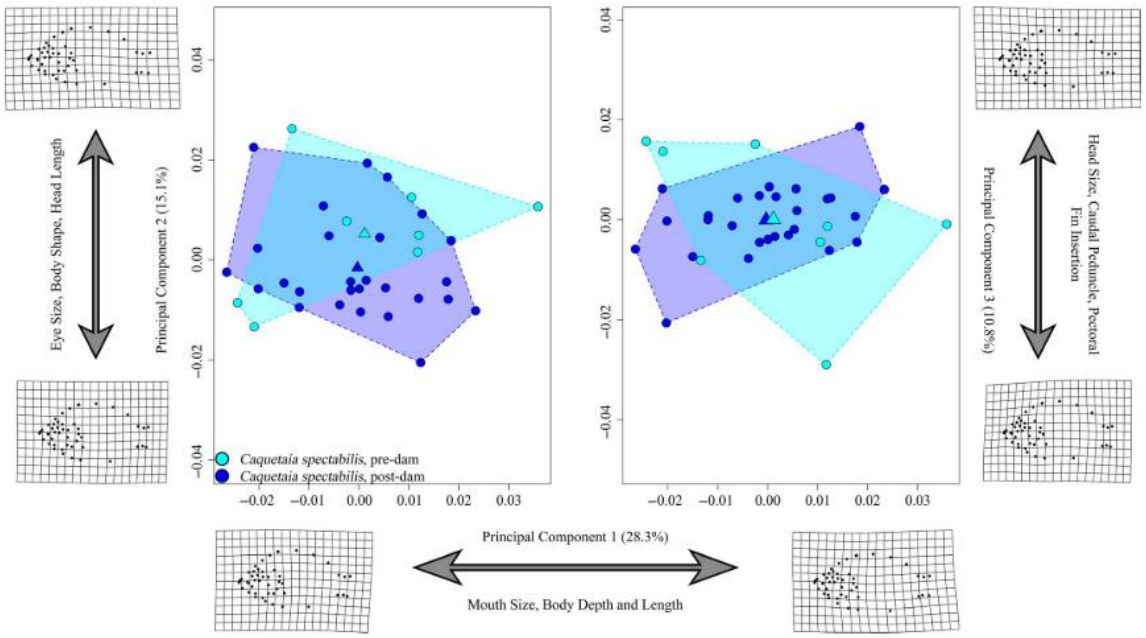

Figure 3.6. *Caquetaia spectabilis* principal component plot (X-axis = PC1 (28.3%), Y-axis-left = PC2 (15.1%), Y-axis-right = PC3 (10.8%)) indicating regions of morphospace occupied by each year group, as illustrated by colored convex hulls. Circles indicate individuals, and triangle represents the mean shape of each group within morphospace. Deformation grids are indicative of the minimum and maximum shape values for respective axes. Morphological disparity test reveals a significant (p = .0604) reduction in disparity between pre/post-dam groups (Procrustes variance = 0.00092 and 0.00067, respectively). Pre-, post-dam sample sizes: n = 8, 26.

Tests of allometry on geometric morphometric data rejected ($p = 0.0110$; Supplemental Table 3) the null hypothesis that allometries were parallel, indicating that there has been a significant alteration of allometric trajectories since the Tucuruí dam was constructed. No significant differences in group means were observed across all four linear measures (Supplemental Figure 4; Supplemental Table 5). Additionally, we detected no significant differences among slope trajectories in any comparison.

Heros efasciatus

Procrustes ANOVA revealed that interaction between size and year was not meaningful ($R^2 = 0.027$; $Z = 2.88$; $P = 0.0045$) and that, despite being significant, the effect of year alone ($R^2 = 0.045$; $Z = 3.66$; $P = 0.0002$) was less meaningful than the effect of size ($R^2 = 0.439$; $Z = 5.72$; $P = <0.0001$) alone (Supplemental Table 2). Pre/post-dam groups showed significant differences in both shape ($p = 0.0103$) and disparity ($p = 0.0025$; Procrustes Variance: pre-dam = 0.00115, post-dam = 0.00061). Notably, post-dam specimens exhibited lower levels of morphological disparity than pre-dam *H. efasciatus.* Deformation grids of mean group shapes showed that pre-dam *H. efasciatus* have relatively larger eyes, smaller jaws, deeper heads and bodies, dorsal fin insertions behind operculum (post dam specimens appear to have dorsal fins that insert just above the operculum), and a shorter caudal fin base. These results were not consistent with our predictions regarding trophic specialists.

The first three PC axes (Figure 7) accounted for 52.1% of the total variance. PC1 accounted for 21.2%, and explained variation in head, mouth, and body size. Negative scores were associated with shallow bodies and longer faces. Post-dam specimens were largely restricted to one end of this axis (i.e., negative scores on average), whereas pre-dam specimens occupied the full range of PC1 scores. PC2 accounted for 17.7% of the

variance, and describes variation nape length, dorsal fin insertion, and eye size. Negative scores were associated with relatively smaller eyes and operculum, dorsal fin insertion just above the opercle (as opposed to positive scores that represent a more posterior dorsal fin insertion), and size of the pectoral fin base. Pre- and post-dam specimens overlapped along this axis but pre-dam specimens trended towards more positive scores while post-dam specimens trended toward more negative scores. PC3 accounted for 13.1% of the variance, and was associated with eye position, body length, mouth size, and preopercle angle. Negative scores were associated with more ventrally positioned eyes, shorter bodies, and longer mouths, and a more rounded (as opposed to angular) preopercle. While both pre- and post-dam specimens occupied a wide range of the observed PC3 scores, pre-dam specimens had a somewhat larger occupancy, leaving post-dam specimens to occupy a central position.

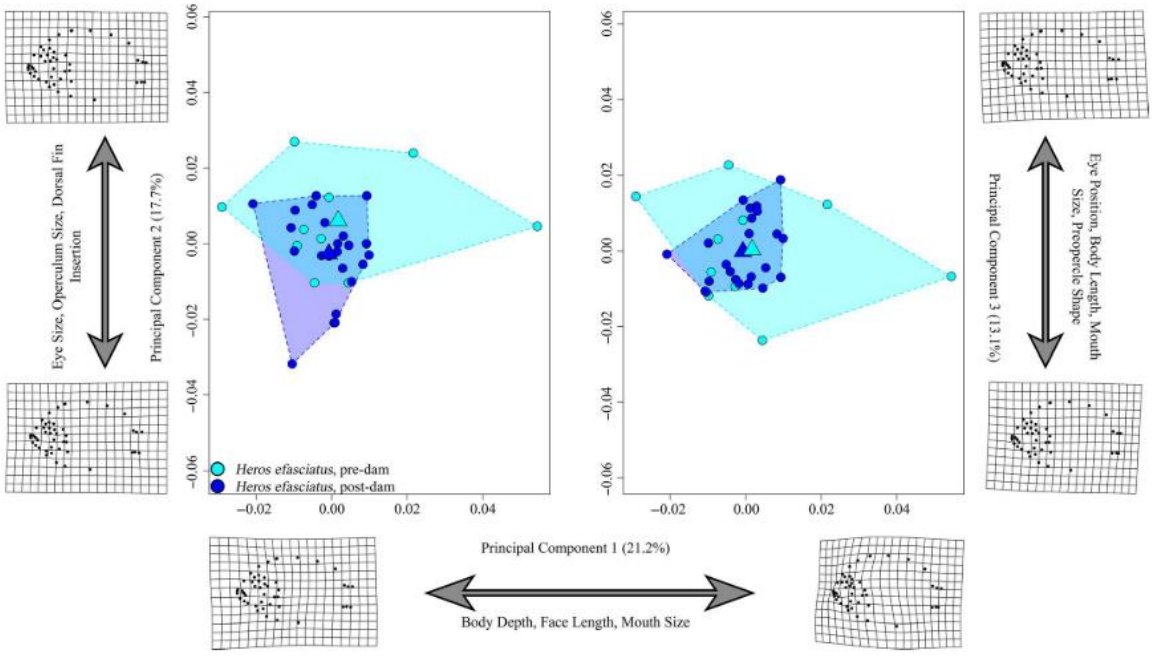

Figure 3.7. *Heros efasciatus* principal component plot (X-axis = PC1 (21.5%), Y-axis-left = PC2 (17.9%), Y-axis-right = PC3 (14.5%)) indicating regions of morphospace occupied by each year group, as illustrated by colored convex hulls. Circles indicate individuals, and triangle represents the mean shape of each group within morphospace. Deformation grids are indicative of the minimum and maximum shape values for respective axes. Morphological disparity test reveals a significant (p = .0025) reduction in disparity

between pre/post-dam groups (Procrustes variance = 0.00115 and 0.00061, respectively). Pre-, post-dam sample sizes: n = 10, 23.

Tests of allometry on geometric morphometric data reject ($p = 0.0045$; Supplemental Table 3) the null hypothesis that allometries were parallel, indicating that there has been a significant alteration of allometric trajectories. No significant differences in absolute group means were observed across all four linear measures (Supplemental Figure 4; Supplemental Table 5). Despite allometric differences in shape being detected, we found no significant difference among slope trajectories for our four linear measures.

Discussion

The capacity of fishes to quickly respond to rapid environmental change, 'natural' or anthropogenic, is well documented (Rüber & Adams, 2001; Candolin, 2009; Franssen, 2011). However, the present scenario offers a unique opportunity to explore how large-scale environmental alterations can alter evolutionary trajectories and spur evolutionary divergence, especially in one of the most biologically diverse regions on the planet that is under increasing pressure from anthropogenic exploitation. The formation of the Tucuruí reservoir brought about dramatic changes that altered the local ecosystem from shallow, clearwater rapids to a deep, silty reservoir. While such operatic changes can be detrimental to fish populations (Fearnside, 2001; Alò & Turner, 2005; Agostinho et al., 2008), they can also spur instances of speciation (Dias et al., 2013). This study provides insight into not just how cichlid populations respond to large-scale ecological changes, but also how different ecotypes respond to an altered landscape. We describe extensive morphological changes across the body for all cichlid species examined, regardless of ecotype, over the course of ~34 years following a major ecological change. While a subset of our data are limited to what is available from small historical collections, they ultimately suggest that cichlid species are experiencing rapid morphological change in

response to large-scale modifications of their environment. These findings are especially notable, as they stands in contrast to results recently presented by Geladi et al. (2019), which document little to no morphological change in characid species in response to damming. Thus, among two of the largest families of fishes worldwide, with especially high levels of biodiversity in the Neotropics, each appears to respond differently to major anthropogenic change, underscoring our limited ability to predict how different lineages will respond to similar ecological disturbances.

Anatomical changes are observed across cichlid ecomorphs

The peacock basses (e.g., *Cichla* species) are widespread throughout the Amazon basin, play important roles as large piscivorous predators (Williams et al., 1998; R Fugi, Agostinho, & Hahn, 2001; Sharpe, De León, González, & Torchin, 2017), and are economically important for both food and recreation. Despite being native to the Amazon basin, these species have been widely introduced to numerous non-native systems where they play prominent roles in the decline of native fishes (Kovalenko, Dibble, Agostinho, Cantanhêde, & Fugi, 2010; Sharpe et al., 2017).

The construction of the Tucuruí Dam, and subsequent formation of the Tocantins reservoir has likely aided the establishment and success of local *Cichla* species, which have been reported to require stable water levels and adequate littoral zones for reproduction (Williams, Winemillar, Taphorn, & Balbas, 1998). *Cichla* are large bodied cichlids that are capable of traveling extremely long distances (Hoeinghaus, Layman, Arrington, & Winemiller, 2003), and have an evolutionary history largely shaped by the historical hydrology of South America (Willis, Nunes, Montaña, Farias, & Lovejoy, 2007). Our geometric morphometric data show that both *Cichla kelberi* and *C. pinima*

appear morphologically similar in pre-dam collections with semi-elongate bodies. They also exhibit indifferent disparities and are constrained to a relatively narrow region of morphospace (Figure 3). However, post-dam specimens appear to have experienced changes in morphology that not only pushed the two species apart in morphospace and distinguished them from the historical collections, but also resulted in a near identical, two-fold increase in disparity (Table 2). The divergence in shape that we observed in these two species may be due to the altered riverine state of the area and the introduction of a deep, lentic environment. It has been well documented that lentic environments promote the development of deep bodies, whereas lotic environments promote more streamlined body shape in fishes (Collin & Fumagalli, 2011; Gaston & Lauer, 2015; Geladi et al., 2019) that are more efficient in reducing drag when navigating such environments (Gosline, 1971). Mathematically, compressed, deep bodied objects (*e.g.*, fish) should be less capable of navigating waters characterized by high flow, owing to increased drag (Batchelor, 1967; Lamb, 1975). This is conversely true for more streamlined shapes, which are predicted to generate less drag in fluidic space and are therefore more energetically efficient. This appears to be the case for one of our species, *Cichla kelberi*, where contemporary collections exhibit a relatively deep, robust overall body shape compared to pre-dam specimens. In contrast, the local *C. pinima* population appears to have responded in the opposite way, exhibiting more streamlined bodies compared to historic collections. This apparent divergence in body shape between *Cichla* species is consistent with ecological character displacement, a hypothesis that may be tested in the future. Sympatric *Cichla* species have previously been shown to consume different ichthyofauna. In one study, *C. temensis* were found to consume primarily

characid fishes, while sympatric *C. orinocensis* largely consumed other cichlids (Williams, Winemillar, Taphorn, & Balbas, 1998). Thus, the different reaction of these two species, *C. kelberi* and *C. pinima*, could indicate that niche space across the reservoir is being partitioned to reduce the effects of competition between two large, predatory fishes. In addition, differences in the growth trajectories of specific functionally relevant traits, such as eye and jaw size, are consistent with niche shifts over life history within the reservoir that are distinct from those in ancestral riverine populations.

We had predicted that generalists and specialists would respond differently to large-scale ecological changes. While cichlids in general are renowned for their flexibility in foraging behavior (Liem & Osse, 1975; Hulsey et al., 2005), they may be arrayed along axes of ecomorphology related to foraging (Wainwright, Osenberg, & Mittelbach, 1991; Hahn & Cunha, 2005; Cooper et al., 2010). Accordingly, the four smaller species included here were chosen based on their placement along a continuum between foraging generalist and specialist. Consistent with our prediction, both generalist species, *Geophagus neambi* and *Satanoperca jurupari*, experienced significant deviations in shape but not disparity, effectively shifting position, but not distribution, in morphospace (Figures 4 & 5). Both species experienced changes across the body, but the most striking shifts were largely associated with head morphology, including changes in eye size and placement, jaw length, skull dimensions, and opercle sizes. These shifts are predicted to be associated with alterations in feeding behavior and kinematics and are consistent with the observation that both *G. neambi* and *S. jurupari* have atypical diets within the reservoir (de Mérona et al., 2001). Notably, the anatomical changes documented here effectively make the two species appear more similar than they were historically. *G. neambi* developed smaller eyes, smaller jaws, and less rounded jaws, while *S. jurupari* developed larger eyes, a shorter preorbital region of the head, and more rounded jaws. Thus, *G. neambi* and *S.*

jurupari appear to be converging on a common head shape, which predicts that similar feeding strategies are being employed by these two closely related species within the reservoir.

In contrast to our prediction, both specialist species, *Caquetaia spectabilis* and *Heros efasciatus*, also exhibited changes in body and head shape morphology. In addition, both appear to have experienced a reduction in morphological disparity. This could suggest that selective pressures experienced in the altered environment are working to canalize phenotypic variation in these species, generally reducing observed phenotypic variance. The fact that we saw relatively low R^2 values and Z scores associated with mean shapes, but more obvious differences in disparity, supports the hypothesis that these two species (*H. efasciatus* and *C. spectabilis*) are experiencing phenotypic canalization centered around the mean shape of their respective populations. A similar trend in a reduction of morphological variation has been reported for *Cyprinella lutrensis* (Cypriniformes:Cyprinidae) in reservoirs when compared to stream dwelling populations (Franssen, 2011), as well as for characid fishes (Geladi et al., 2019).

Possible mechanisms of morphological change

While it is impossible to explicitly connect changes in cichlid morphology detected here to the construction of the Tucuruí dam, there are many reasons to assume that it has played an important role. For instance, it is well established that dam construction will introduce dramatic changes to the hydrology of the immediate area (Miller, 1961; Maingi & Marsh, 2002; de Mérona, Vigouroux, & Tejerina-Garro, 2005; Dugan et al., 2010), thereby altering the ecology of residing taxa, and possibly creating a foundation for ecological opportunity by introducing novel ecological niches to the system (Schluter, 2000; Losos, 2010). Furthermore, species diversity has been shown to be reduced in this area following construction of the Tucuruí dam (G. dos Santos et al., 2004), which has likely opened up additional resources to the remaining species, possibly leading to new selection regimes (Roughgarden, 1972; Lahti et al., 2009).

A likely mechanism contributing to some of the changes documented here is phenotypic plasticity, which refers to the capacity for a single genotype to express various morphological, physiological, and/or behavioral phenotypes under different ecological conditions. Plasticity can allow populations to quickly adapt and persist when faced with new ecological challenges (Ghalambor, McKay, Carroll, & Reznick, 2007), including the formation of a large reservoir. The present study does not present information directly regarding plasticity in cichlids, but plasticity has been well documented in fishes (Lindsey, 1981; Robinson & Parsons, 2002; Alexander & Adams, 2004; Lema & Nevitt, 2006; Garduño-Paz, Couderc, & Adams, 2010), and is especially notable within the feeding apparatus (Wainwright et al., 1991; Alexander & Adams, 2004; Parsons et al., 2016). Furthermore, plasticity in body and head shape has been well documented in cichlids (Chapman, Galis, & Shinn, 2000; Muschick et al., 2011), including Geophagini cichlids (Wimberger, 1991, 1992). An important topic for future investigation will be to determine the extent to which phenotypic plasticity has contributed to shape differences documented here. Such insights will not only inform a better understanding of short-term adaptation to novel environments, but they may also contribute to an understanding of longer-term patterns of evolutionary divergence. This is because plasticity has the capacity to influence longer-term patterns of evolution by biasing the phenotypic variation that is exposed to selection (West-Eberhard, 1989, 2003). Thus, by recapitulating a river-to-lake transition that has occurred repeatedly across many fish lineages, including cichlids, the Tucuruí system may provide insights into how plasticity has contributed to the earliest stages of adaptive radiations, a topic that has largely been a matter of theory and deduction.

Genetic mechanisms can also underlie short-term changes in phenotype, mainly via the sorting of ancestral alleles. For instance, selection may act against alleles that are maladapted to the new lacustrine system, resulting in a different distribution of phenotypes in the new environment (Yoder et al., 2010). Interspecific hybridization can further alter the genetic pool through the random sorting of alleles, leading to the development of novel phenotypes (Salzburger, Baric, & Sturmbauer, 2002; Smith, Konings, & Kornfield, 2003). Transgressive segregation is an especially potent mechanism, whereby novel combinations of alleles in a hybrid population can lead to the expression of extreme phenotypic variation within just a couple of generations (Bell & Travis, 2005). Therefore, hybridization, coupled with ecological change not unlike that observed in the Tucuruí region, has the potential to lead to conspicuous shifts in morphology in a brief period of time. Morphological trends in *Cichla* are consistent with these factors, including a divergence in shape over time, as well as a drastic increase in morphological disparity. Changes in ecologically relevant shape are consistent with a shift in niche space, while expanded disparity suggests that *Cichla* species within the Tucuruí reservoir may be hybridizing. Indeed, many of the diagnostic characteristics of *Cichla* species were unreliable for our contemporary collections, including traditional meristics, coloration, and lateral line patterning. Approximately 10% of *Cichla* specimens collected from the reservoir in 2018, exhibited a mosaic of features, and were excluded from our analyses due to the inability to properly key them to species. Contemporary *Cichla* collections overlap with historical collections in shape-space, however the expansion of variation that we observe in *C. kelberi* and *C. pinima* is consistent with transgressive segregation, and is similar to documented cases of this phenomenon in East

African cichlids (Albertson & Kocher, 2005). By acting on standing genetic variation, selection has the capacity to quickly alter patterns of phenotypic variation (Lande & Shannon, 1996; Smith et al., 2003; Collin & Fumagalli, 2011), and is credited for contributing to ongoing species divergence in old world cichlid radiations (Kocher, 2004; Burress, 2014; Malinsky et al., 2018).

Finally, changes in growth trajectories can explain the emergence of new morphological forms, as well as increased morphological diversity (Mina, 2001; Collyer et al., 2005; Réveillac et al., 2015; Simonsen et al., 2017). Since we did not set out to specifically address this question, our experimental design is limited with respect to these types of analyses (e.g., in general, our samples only included one life-history stage – adult). In spite of this caveat, we observed significant differences in allometric trajectories, based on our geometric morphometric data, for three of our five genera (*Caquetaia spectabilis, Heros efasciatus,* and *Geophagus neambi*). Furthermore, for at least one linear measure, slopes were significantly different between pre- and post-dam *Cichla* and *Geophagus.* For both geometric and linear traits, when differences were noted, the trend was consistent, with accelerated growth noted for the pre-dam population relative to its post-dam counterpart. This is apart from the global shape of *Geophagus neambi,* where post-dam slope was steeper than pre-dam *G. neambi*. We found almost no significant difference across our linear measures despite observing significant differences in shape. Because geometric morphometric data are measuring global shape change, comprised of relative (and often subtle) changes across the entire body, they are more sensitive to detecting mean differences than any single linear measure. They also enable intuitive interpretations of the results via deformation grids (Thompson, 1917). From

these interpolations, we may identify which regions of the body are varying more than other regions. While it can be more difficult to ascribe specific functional relevance to these types of changes, as compared to the length of a lever arm, for example, they are biologically relevant and represent pertinent organismal change (Rohlf & Marcus, 1993; D. C. Adams et al., 2004; Zelditch et al., 2012). Taken together, the allometric deviations in post-dam collections that we document here could be due to a number of ecological changes that reservoir formation has brought to the region – including changes to turbidity, primary productivity, reproduction and feeding strategies, community composition, and predator-prey dynamics. This will be an interesting line of future investigation.

As with most experiments, there are limitations to the conclusions that may be considered. Here we relied heavily on historical collections, which were limited in terms of quality (inadequately preserved for geometric morphometric analyses), quantity, and size distributions. We acknowledge these shortcomings and the difficulties in some of the analyses concerning our linear measures and size corrected values, but feel confident nevertheless in our overall interpretations, and our conclusion that cichlid species are undergoing rapid phenotypic change (in levels and patterns of variation) in response to the novel environment within the Tucuruí reservoir. How this has occurred remains an open question. As a first step, future research should aim to determine the extent to which the morphological changes documented here are genetically determined versus the product of phenotypic plasticity.

Predicting outcomes?

The construction of the Tucuruí dam has resulted in pronounced changes to the hydrology of the immediate area, establishing a foundation for ecological opportunity by

introducing the local ichthyofauna to novel niches. Among those changes, the most obvious is the transition from a fast-flowing riverine system, to a deep, stagnant reservoir, significantly altering the flow regime and hydrodynamics of the system. Morphological changes in fishes following such alterations in flow regimes have been recorded in other taxa following impoundment (Kristjansson, Skulason, Noakes, & Kristjánsson, 2002; Haas, Blum, & Heins, 2010; Franssen, 2011; Perkin & Bonner, 2011; Franssen et al., 2013), and these can mimic adaptive divergence from river to lake systems (Langerhans, Layman, Langerhans, & Dewitt, 2003). In particular, when examining adaptation from systems with high flow to a system with no/low flow, stereotypical morphological shifts are often cited (Webb, 1984), including changes in body depth (Brinsmead & Fox, 2002; Langerhans et al., 2003; Collyer, Novak, & Stockwell, 2005; Haas et al., 2010; Cureton II & Broughton, 2014; B. A. I. Santos & Araújo, 2015; Collyer, Hall, et al., 2015), mouth orientation (Langerhans et al., 2003; Franssen et al., 2013), size and location of paired/medial fin attachment sites (Brinsmead & Fox, 2002; Aguirre, Shervette, Navarrete, Calle, & Agorastos, 2013; Cureton II & Broughton, 2014; B. A. I. Santos & Araújo, 2015), and eye size and placement (Aguirre et al., 2013). These shifts are almost certainly due to adaptations to novel flow regimes themselves, as well as to novel prey items that may be found within them. Notably, many of these changes are reported, in one or more species, here in our comparison between contemporary (reservoir) and historical (riverine) specimens from Tucuruí. Although the speed at which anthropogenic changes occur is much greater than what is typically witnessed in natural systems, it is possible that the two events can inform one another. For example, understanding the mechanisms that underlie adaptive radiations may allow investigators to predict the types

of morphological changes that may arise in lineages subjected to impoundment, which in turn may be applied to develop a more holistic picture of the long-term environmental consequences. In addition, knowledge gleaned from studying the immediate effects of damming may provide a glimpse into the early stages of adaptive radiations, a topic that is largely a matter of theory and speculation. Thus, it is important to note that several dams built in the Amazon Basin, like the Xingu and Madeira Rivers dams, should also adopt similar studies monitoring how the fishes will adapt to a new environment. The outcome could lead to a better understanding of how environmental changes acts through time and space over resilient species.

Conclusions

The significant changes to the Tocantins, a product of deforestation, large-scale agriculture, and the construction of the Tucuruí Hydroelectric Dam, have altered the ecological dynamics of the systems culminating with the Tucuruí reservoir. The historic fast flowing, clearwater rapids have been replaced by an extensive, deep, lentic system with high levels of turbidity and sediment deposition. Using a combination of museum specimens prior to the construction of the dam and contemporary specimens collected 34 or more years after the reservoir had been established, this study shows that native cichlid populations have undergone dramatic morphological changes in a short period of time, likely as a result of the reservoir formation. The closure of the dam has already resulted in a dramatic reduction in ichthyofauna diversity (dos Santos et al., 1984, 2004), possibly reducing competition for remaining species that now have access to an expanded array of ecological niches. The construction of the Tucuruí Hydroelectric Plant has allowed for a unique opportunity to witness how fish populations respond to sudden, large-scale alteration to an ecosystem. This study provides evidence that ecologically related traits

are changing in response to hydrological alteration, changes that are not limited to generalists alone, but apparent to varying degrees in all taxa investigated. Given the high number of dams constructed in the Amazon, particularly on the Tocantins, this study adds to the growing literature of what we can expect to occur within resident fish communities, notably in one of the most diverse freshwater fish communities on Earth.

Author contributions

CCF and RCA conceived the project. AA, CCF and RCA collected, processed and imaged specimens. MCG performed the morphological analyses and analyzed linear traits. MCG, CCF, and RCA interpreted the morphometric results. MCG and RCA interpreted results from linear measurements. MCG and RCA wrote the first draft of the manuscript. All authors contributed to manuscript revisions.

Acknowledgements

The authors are deeply indebted to Fernanda AG de Andrade from Instituto Federal do Pará – Tucurui for providing us with laboratory space and to Jacyra Oliver, Luiza Baruch, and Sandro Souza for assistance with processing the specimens. The collections, curators, and managers at MZUSP, Oswaldo Oyakawa and Alessio Datovo, and Lúcia Rapp Py-Daniel at the INPA fish collection. Michael L Collyer for help with R code to generate polygon plots. The Natural History Collections at the University of Massachusetts for providing travel funds. We also thank members of the Albertson lab for thoughtful comments and suggestions on the data presented here.

Data archiving statement

Data for this study are available at: to be completed after manuscript is accepted for publication.

Literature cited

Adams, D. C., Collyer, M. L., & Sherratt, E. (2015). geomorph: Software for geometric morphometric analysis. Retrieved from http://cran.r-project.org/web/packages/geomorph/index.html

Adams, D. C., Rohlf, F. J., & Slice, D. E. (2004). Geometric morphometrics : Ten years of progress following the ‘ revolution ’. *Italian Journal of Zoology*, *71*(January 2015), 5–16. doi:10.1080/11250000409356545

Adams, D., Collyer, M. L., & Kaliontzopoulou, A. (2018). Geomorph: Software for geometric morphometric analysis. R package version 3.0.6. Retrieved from https://cran.r-project.org/package=geomorph

Agostinho, A., Pelicice, F., & Gomes, L. (2008). Dams and the fish fauna of the Neotropical region : impacts and management related to diversity and fisheries. *Brazilian Journal of Biology*, *68*(4), 1119–1132.

Aguirre, W. E., Shervette, V. R., Navarrete, R., Calle, P., & Agorastos, S. (2013). Morphological and Genetic Divergence of Hoplias microlepis (Characiformes: Erythrinidae) in Rivers and Artificial Impoundments of Western Ecuador. *Copeia*, *2013*(2), 312–323. doi:10.1643/CI-12-083

Akama, A. (2017). Impacts of the hydroelectric power generation over the fish fauna of the Tocantins river, Brazil: Marabá dam, the final blow. *Oecologia Australis*, *21*(3), 222–231. doi:10.4257/oeco.2017.2103.01

Albertson, R. C., & Kocher, T. D. (2005). Genetic architecture sets limits on transgressive segregation in hybrid cichlid fishes. *Evolution*, *59*(3), 686–690.

Alexander, G. D., & Adams, C. E. (2004). Exposure to a common environment erodes inherited between-population trophic morphology differences in Arctic charr. *Journal of Fish Biology*, *64*, 253–257. doi:10.1111/j.1095-8649.2004.00276.x

Allan, J. D., & Flecker, A. S. (1993). Biodiversity conservation in running waters. *BioScience*, *43*(1), 32–43. doi:10.2307/1312104

Alò, D., & Turner, T. F. (2005). Effects of habitat fragmentation on effective population size in the endangered Rio Grande silvery minnow. *Conservation Biology*, *19*(4), 1138–1148. doi:10.1111/j.1523-1739.2005.00081.x

Angermeier, P. L. (1995). Ecological attributes of extinction-prone species: loss of freshwater fishes of Virginia. *Conservation Biology*, *9*(1), 143–158. Retrieved from https://www.jstor.org/stable/pdf/2386396.pdf

Araújo-Lima, C., Agostinho, A., & Fabré, N. (1995). Trophic aspects of fish communities in Brazilian rivers and reservoirs. In *Limnology in Brazil* (pp. 105–136). Rio de Janeiro: Brazilian Academy of Sciences.

Arbour, J. H., & López-Fernández, H. (2013). Ecological variation in South American geophagine cichlids arose during an early burst of adaptive morphological and functional evolution. *Proceedings of the Royal Society B: Biological Sciences*, *280*(1763), 20130849–20130849. doi:10.1098/rspb.2013.0849

Bastos, R. F., Condini, M. V., Varela, A. S., & Garcia, A. M. (2011). Diet and food consumption of the pearl cichlid Geophagus brasiliensis (Teleostei: Cichlidae): Relationships with gender and sexual maturity. *Neotropical Ichthyology*, *9*(4), 825–830. doi:10.1590/S1679-62252011005000049

Batchelor, G. (1967). *An introduction to fluid dynamics*. New York: Cambridge University Press.

Bell, M. A., & Travis, M. P. (2005). Hybridization, transgressive segregation, genetic covariation, and adaptive radiation. *Trends in Ecology and Evolution*, *20*(7), 358–361. doi:10.1016/j.tree.2005.03.015

Brinsmead, J., & Fox, M. G. (2002). Morphological variation between lake- and stream-dwelling rock bass and pumpkinseed populations. *Journal of Fish Biology*, *61*, 1619–1638. doi:10.1006/jfbi.2002.2179

Burress, E. D. (2014). Cichlid fishes as models of ecological diversification: patterns, mechanisms, and consequences. *Hydrobiologia*, *748*(1), 7–27. doi:10.1007/s10750-014-1960-z

Candolin, U. (2009). Population responses to anthropogenic disturbance: Lessons from three-spined sticklebacks Gasterosteus aculeatus in eutrophic habitats. *Journal of Fish Biology*, *75*(8), 2108–2121. doi:10.1111/j.1095-8649.2009.02405.x

Chapman, L. G., Galis, F., & Shinn, J. (2000). Phenotypic plasticity and the possible role of genetic assimilation: Hypoxia-induced trade-offs in the morphological traits of an African cichlid. *Ecology Letters*, *3*(5), 387–393. doi:10.1046/j.1461-0248.2000.00160.x

Cichocki, F. (1976). *Cladistic history of cichlid fishes and reproductive strategies of the American genera Acarichthys, Biotodoma and Geophagus. Ph.D. Thesis*. University of Michigan.

Clavel, J., Julliard, R., & Devictor, V. (2011). Worldwide decline of specialist species: toward a global functional homogenization? *Frontiers in Ecology and the Environment*, *9*(4), 222–228. doi:10.1890/080216

Collin, H., & Fumagalli, L. (2011). Evidence for morphological and adaptive genetic divergence between lake and stream habitats in European minnows (Phoxinus phoxinus, Cyprinidae). *Molecular Ecology*, *20*(21), 4490–4502. doi:10.1111/j.1365-294X.2011.05284.x

Collyer, M. L., & Adams, D. C. (2007). Analysis of two-state multivariate phenotypic change in ecological studies. *Ecology*, *88*(3), 683–692. doi:10.1890/06-0727

Collyer, M. L., Hall, M. E., Smith, M. D., & Hoagstrom, C. W. (2015). Habitat-morphotype associations of Pecos pupfish (Cyprinodon pecosensis) in isolated habitat complexes. *Copeia*, *2015*, 181–199. doi:10.1643/OT-14-084

Collyer, M. L., Novak, J. M., & Stockwell, C. A. (2005). Morphological Divergence of Native and Recently Established Populations of White Sands Pupfish (Cyprinodon tularosa). *Copeia*, *2005*(1), 1–11.

Collyer, M. L., Sekora, D. J., & Adams, D. C. (2015). A method for analysis of phenotypic change for phenotypes described by high-dimensional data. *Heredity*, *115*(4), 357–365. doi:10.1038/hdy.2014.75

Cooper, W. J., Parsons, K., McIntyre, A., Kern, B., McGee-Moore, A., & Albertson, R. C. (2010). Bentho-pelagic divergence of cichlid feeding architecture was prodigious and consistent during multiple adaptive radiations within African Rift-Lakes. *PLoS ONE*, *5*(3). doi:10.1371/journal.pone.0009551

Cureton II, J. C., & Broughton, R. E. (2014). Rapid morphological divergence of a stream fish in response to changes in water flow. *Biology Letters*, *10*, 8–11. Retrieved from http://dx.doi.org/10.1098/rsbl.2014.0352

de Mérona, Bernard, Mendes Dos Santos, G., & Goncçalves de Almeida, R. (2001). Short term effects of Tucuruí Dam (Amazonia, Brazil) on the trophic organization of fish communities. *Environmental Biology of Fishes*, *60*(4), 375–392. doi:10.1023/A:1011033025706

de Mérona, Bernard, Vigouroux, R., & Tejerina-Garro, F. L. (2005). Alteration of fish diversity downstream from Petit-Saut Dam in French Guiana. Implication of ecological strategies of fish species. *Hydrobiologia*, *551*(1), 33–47. doi:10.1007/s10750-005-4448-z

Dias, M. S., Cornu, J. F., Oberdorff, T., Lasso, C. A., & Tedesco, P. A. (2013). Natural fragmentation in river networks as a driver of speciation for freshwater fishes. *Ecography*, *36*(6), 683–689. doi:10.1111/j.1600-0587.2012.07724.x

Dugan, P. J., Barlow, C., Agostinho, A. A., Baran, E., Cada, G. F., Chen, D., … Winemiller, K. O. (2010). Fish migration, dams, and loss of ecosystem services in the mekong basin. *Ambio*, *39*(4), 344–348. doi:10.1007/s13280-010-0036-1

ELETROBRÁS/DNAEE. (1997). *Manual de Inventário Hidrelétrico de Bacias Hidrográficas*. Brasília.

Favero, J. M. del, Pompeu, P. dos S., & Prado-Valladares, A. C. (2010). Biologia reprodutiva de Heros efasciatus Heckel, 1840 (Pisces, Cichlidae) na Reserva de Desenvolvimento Sustentável Amanã-AM, visando seu manejo sustentável. *Acta*

Amazônica, *40*(2), 373–380.

Fearnside, P. M. (2001). Environmental impacts of Brazil's Tucuruı´ Dam: Unlearned lessons for hydroelectric development in Amazonia. *Environmental Management*, *27*(3), 377–396. doi:10.1007/s002670010156

Franssen, N. R. (2011). Anthropogenic habitat alteration induces rapid morphological divergence in a native stream fish. *Evolutionary Applications*, *4*(6), 791–804. doi:10.1111/j.1752-4571.2011.00200.x

Franssen, N. R., Harris, J., Clark, S. R., Schaefer, J. F., & Stewart, L. K. (2013). Shared and unique morphological responses of stream fishes to anthropogenic habitat alteration. *Proceedings of the Royal Society B: Biological Sciences*, *280*(1752), 20122715. doi:10.1098/rspb.2012.2715

Fugi, R, Agostinho, a a, & Hahn, N. S. (2001). Trophic morphology of five benthic-feeding fish species of a tropical floodplain. *Revista Brasleira de Biologia*, *61*(1), 27–33. doi:10.1590/S0034-71082001000100005

Fugi, Rosemara, Luz-Agostinho, K. D. G., & Agostinho, A. A. (2008). Trophic interaction between an introduced (peacock bass) and a native (dogfish) piscivorous fish in a Neotropical impounded river. *Hydrobiologia*, *607*(1), 143–150. doi:10.1007/s10750-008-9384-2

Garduño-Paz, M. V., Couderc, S., & Adams, C. E. (2010). Habitat complexity modulates phenotype expression through developmental plasticity in the threespine stickleback. *Biological Journal of the Linnean Society*, *100*(2), 407–413. doi:10.1111/j.1095-8312.2010.01423.x

Gaston, K. A., & Lauer, T. E. (2015). Morphometric variation in bluegill Lepomis macrochirus and green sunfish Lepomis cyanellus in lentic and lotic systems. *Journal of Fish Biology*, *86*(1). doi:10.1111/jfb.12581

Geladi, I., De León, L. F., Torchin, M. E., Hendry, A. P., González, R., & Sharpe, D. M. T. (2019). 100-year time series reveal little morphological change following impoundment and predator invasion in two Neotropical characids. *Evolutionary Applications*, *12*(7), 1385–1401. doi:10.1111/eva.12763

Ghalambor, C. K., McKay, J. K., Carroll, S. P., & Reznick, D. N. (2007). Adaptive versus non-adaptive phenotypic plasticity and the potential for contemporary adaptation in new environments. *Functional Ecology*, *21*(3), 394–407. doi:10.1111/j.1365-2435.2007.01283.x

Goodall, C. (1991). Procrustes methods in the statistical analysis of shape. *Journal of the Royal Statistical Society*, *53*(2), 285–339.

Gosline, W. A. (1971). *Functional Morphology and Classification of Teleostean Fishes*. Honolulu: University Press of Hawaii.

Gunz, P., & Mitteroecker, P. (2013). Semilandmarks: A method for quantifying curves and surfaces. *Hystrix*, *24*(1). doi:10.4404/hystrix-24.1-6292

Haas, T. C., Blum, M. J., & Heins, D. C. (2010). Morphological responses of a stream fish to water impoundment. *Biology Letters*, *6*, 803–806. doi:10.1098/rsbl.2010.0401

Hahn, N. S., & Cunha, F. (2005). Feeding and trophic ecomorphology of Satanoperca

pappaterra (Pisces, Cichlidae) in the Manso Reservoir, Mato Grosso State, Brazil. *Brazilian Archives of Biology and Technology*, *48*(6), 1007–1012. doi:10.1590/S1516-89132005000800017

Helfman, G. (2007). *Fish Conservation: A guide to understanding and restoring global aquatic biodiversity and fishery resources*. Washington, D.C.: Island Press.

Higgins, K., & Lynch, M. (2001). Metapopulation extinction caused by mutation accumulation. *Proceedings of the National Academy of Science*, *98*(5), 2928–2933.

Hoeinghaus, D. J., Layman, C. A., Arrington, D. A., & Winemiller, K. O. (2003). Movement of Cichla species (Cichlidae) in a Venezuelan floodplain river. *Neotropical Ichthyology*, *1*(2), 121–126. doi:10.1590/s1679-62252003000200006

Hulsey, C. D., Hendrickson, D. A., & García De León, F. J. (2005). Trophic morphology, feeding performance and prey use in the polymorphic fish Herichthys minckleyi. *Evolutionary Ecology Research, 7*, 303–324.

Kocher, T. D. (2004). Adaptive evolution and explosive speciation: the cichlid fish model. *Nature Reviews Genetics*, *5*(4), 288–298. doi:10.1038/nrg1316

Kovalenko, K. E., Dibble, E. D., Agostinho, A. A., Cantanhêde, G., & Fugi, R. (2010). Direct and indirect effects of an introduced piscivore, Cichla kelberi and their modification by aquatic plants. *Hydrobiologia*, *638*, 245–253. doi:10.1007/s10750-009-0049-6

Kristjansson, B. K., Skulason, S., Noakes, D. L. G., & Kristjánsson, B. (2002). Rapid

divergence in a recently isolated population of threespine stickleback (Gasterosteus aculeatus L.). *Evolutionary Ecology Research*, *4*, 659–672. Retrieved from http://cat.inist.fr/?aModele=afficheN&cpsidt=14395917%5Cn%3CGo to ISI%3E://WOS:000177011200003

Kullander, S. O., & Ferreira, E. J. G. (2006). A review of the South American cichlid genus Cichla, with descriptions of nine new species (Teleostei: Cichlidae). *Ichthyological Exploration of Freshwaters*, *17*(4), 289–398.

Lahti, D. C., Johnson, N. A., Ajie, B. C., Otto, S. P., Hendry, A. P., Blumstein, D. T., … Foster, S. A. (2009). Relaxed selection in the wild. *Trends in Ecology and Evolution*, *24*(9), 487–496. doi:10.1016/j.tree.2009.03.010

Lamb, H. (1975). *Hydrodynamics*. New York: Dover.

Lande, R., & Shannon, S. (1996). The Role of genetic variation in adaptation and population persistence in a changing environment. *Evolution*, *50*(1), 434–437.

Langerhans, R. B., Layman, C. A., Langerhans, A. K., & Dewitt, T. J. (2003). Habitat-associated morphological divergence in two Neotropical fish species, 689–698.

Larochelle, C. R., Pickens, F. A. T., Burns, M. D., & Sidlauskas, B. L. (2016). Long-term isopropanol storage does not alter fish morphometrics. *Copeia*, *104*(2), 411–420. doi:10.1643/CG-15-303

Lau, J. K., Lauer, T. E., & Weinman, M. L. (2006). Impacts of channelization of stream habitats and associated fish assemblages in east central Indiana. *American*

Midland Naturalist, *156*(2), 319–330.

Lema, S. C., & Nevitt, G. a. (2006). Testing an ecophysiological mechanism of morphological plasticity in pupfish and its relevance to conservation efforts for endangered Devils Hole pupfish. *The Journal of Experimental Biology*, *209*(Pt 18), 3499–509. doi:10.1242/jeb.02417

Liem, K. F., & Osse, J. (1975). Biological versatility, evolution, and food resource exploitation in African cichlid fishes. *American Zoologist*, *15*(2), 427–454.

Liermann, C. R., Nilsson, C., Robertson, J., & Ng, R. Y. (2012). Implications of dam obstruction for global freshwater fish diversity. *BioScience*, *62*(6), 539–548. doi:10.1525/bio.2012.62.6.5

Lindsey, C. C. (1981). Stocks are chameleons: Plasticity in gill rakers of coregonid fishes. *Canadian Journal of Fisheries and Aquatic Sciences*, *38*, 1497–1506.

López-Fernández, H., Honeycutt, R. L., & Winemiller, K. O. (2005). Molecular phylogeny and evidence for an adaptive radiation of geophagine cichlids from South America (Perciformes: Labroidei). *Molecular Phylogenetics and Evolution*, *34*(1), 227–244. doi:10.1016/j.ympev.2004.09.004

Losos, J. B. (2010). Adaptive Radiation, Ecological Opportunity, and Evolutionary Determinism. *The American Naturalist*, *175*(6), 623–639. doi:10.1086/652433

Maingi, J. K., & Marsh, S. E. (2002). Quantifying hydrologic impacts following dam construction along the Tana River, Kenya. *Journal of Arid Environments*, *50*(1), 53–79. doi:10.1006/jare.2000.0860

Malinsky, M., Svardal, H., Tyers, A. M., Miska, E. A., Genner, M. J., Turner, G. F., & Durbin, R. (2018). Whole-genome sequences of Malawi cichlids reveal multiple radiations interconnected by gene flow. *Nature Ecology and Evolution*, *2*(12), 1940–1955. doi:10.1038/s41559-018-0717-x

McCoy, M. W., Bolker, B. M., Osenberg, C. W., Miner, B. G., & Vonesh, J. R. (2006). Size correction: Comparing morphological traits among populations and environments. *Oecologia*, *148*(4), 547–554. doi:10.1007/s00442-006-0403-6

Mérona, B. (1987). Aspectos ecológicos da ictiofauna no Baixo Tocantins. *Acta Amazônica*, *1*, 109–124.

Miller, R. R. (1961). *Man and the Changing fish fauna of the American Southwest*. Alma: Michigan Academy of Science, Arts, and Letters.

Mina, M. V. (2001). Morphological diversification of fish as a consequence of the divergence of ontogenetic trajectories. *Ontogenez*, *32*(6), 471–476. doi:10.1023/A:1012842221732

Muschick, M., Barluenga, M., Salzburger, W., & Meyer, A. (2011). Adaptive phenotypic plasticity in the Midas cichlid fish pharyngeal jaw and its relevance in adaptive radiation. *BMC Evolutionary Biology*, *11*(1), 116. doi:10.1186/1471-2148-11-116

Nei, M., Maruyama, T., & Chakraborty, R. (1975). The Bottleneck effect and genetic variability in populations. *Evolution*, *29*(1), 1–10.

Novaes, J. L. C., Caramaschi, É. P., & Winemiller, K. O. (2004). Feeding of Cichla monoculus Spix, 1829 (Teleostei: Cichlidae) during and after reservoir formation

in the Tocantins River, Central Brazil. *Acta Limnologica Brasiliensia*, *16*(1), 41–49. doi:10.5829/idosi.mejsr.2016.24.04.23231

Olsen, A., & Westneat, M. (2015). StereoMorph: an R package for the collection of 3D landmarks and curves using a stereo camera set-up. *Methods in Ecology and Evolution*, *6*, 351–356.

Parsons, K. J., Concannon, M., Navon, D., Wang, J., Ea, I., Groveas, K., … Albertson, R. C. (2016). Foraging environment determines the genetic architecture and evolutionary potential of trophic morphology in cichlid fishes. *Molecular Ecology*, *25*(24). doi:10.1111/mec.13801

Perkin, J. S., & Bonner, T. H. (2011). Long-term changes in flow regime and fish assemblage composition in the Guadelupe and San Marcos rivers of Texas. *River Research and Applications*, *27*, 566–579. doi:10.1002/rra

Platania, S. (1991). Fishes of the Rio Chama and Upper Rio Grande , New Mexico , with preliminary comments on their longitudinal distribution. *The Southwestern Naturalist*, *36*(2), 186–193.

Platania, S. P., & Altenbach, C. S. (1998). Reproductive strategies and egg types of seven Rio Grande Basin cyprinids. *Copeia*, *1998*(3), 559–569.

R Core Team. (2018). R: A language and environment for statistical computing. *R: A Language and Environment for Statistical Computing*. Vienna, Austria: R Foundation for Statistical Computing. Retrieved from http://www.r-project.org/.

Reid, M., & Atz, J. (1958). Oral incubation in the cichlid fish Geophagus jurupari.

Zoologica, *43*, 77–88.

Robinson, B. W., & Parsons, K. J. (2002). Changing times, spaces, and faces: tests and implications of adaptive morphological plasticity in the fishes of northern postglacial lakes. *Canadian Journal of Fisheries and Aquatic Sciences*, *59*(11), 1819–1833. doi:10.1139/f02-144

Rohlf, F. J. (2016). tpsDig, digitize landmarks and outlines, version 2.22. Department of Ecology and Evolution: State University of New York at Stony Brook.

Rohlf, F. J., & Marcus, L. F. (1993). A revolution in morphometrics. *Trends in Ecology and Evolution*, *8*(4), 129–132. doi:10.1016/0169-5347(93)90024-J

Rohlf, F. J., & Slice, D. E. (1990). Extensions of the Procrustes method for the optimal superimposition of landmarks. *Systematic Zoology*, *39*(1), 40–59.

Röpke, C. P., Ferreira, E., & Zuanon, J. (2014). Seasonal changes in the use of feeding resources by fish in stands of aquatic macrophytes in an Amazonian floodplain, Brazil. *Environmental Biology of Fishes*, *97*, 401–414. doi:10.1007/s10641-013-0160-4

Roughgarden, J. (1972). The Evolution of niche width. *The American Naturalist*, *106*(952), 683–718.

Rüber, L., & Adams, D. C. (2001). Evolutionary convergence of body shape and trophic morphology in cichlids from Lake Tanganyika. *Journal of Evolutionary Biology*, *14*, 325–332. doi:10.1046/j.1420-9101.2001.00269.x

Salzburger, W., Baric, S., & Sturmbauer, C. (2002). Speciation via introgressive

hybridization in East African cichlids? *Molecular Ecology*, *11*, 619–625. doi:10.1046/j.0962-1083.2001.01438.x

Santos, B. A. I., & Araújo, F. G. (2015). Evidence of morphological differences between Astyanax bimaculatus (Actinopterygii : Characidae) from reaches above and below dams on a tropical river. *Environmental Biology of Fishes*, *98*, 183–191. doi:10.1007/s10641-014-0248-5

Santos, G. dos, Jégu, M., & Mérona, B. de. (1984). Catálogo de peixes comerciais do Baixo Rio Tocantins. *Projeto Tucuruí*, 83.

Santos, G. dos, Mérona, B. de, Juras, A., & Jégu, M. (2004). Peixes do Baixo Rio Tocantins: 20 anos depois da Usina Hidroelétrica Tucuruí, 215.

Santos, G. (1995). Impactos da hidrelétrica Samuel sobre as comunidades de peixes do Rio Jamari (Rondônia, Brasil). *Acta Amazônica*, *25*, 247–280.

Santos, G., & Oliveira Jr, A. (1999). A Pesca no reservatório da hidrelétrica de Balbina (Amazonas, Brasil). *Acta Amazônica*, *29*, 147–163.

Schluter, D. (2000). *The Ecology of Adaptive Radiation*. Oxford University Press.

Sharpe, D. M. T., De León, L. F., González, R., & Torchin, M. E. (2017). Tropical fish community does not recover 45 years after predator introduction. *Ecology*, *98*(2), 412–424. doi:10.1002/ecy.1648

Smith, P. F., Konings, A., & Kornfield, I. (2003). Hybrid origin of a cichlid population in Lake Malawi: Implications for genetic variation and species diversity. *Molecular Ecology*, *12*(9), 2497–2504. doi:10.1046/j.1365-294X.2003.01905.x

Thompson, D. (1917). *On growth and form*. Cambridge, U.K.: Cambridge University Press.

Trautman, M. (1939). The Effects of man-made modifications on the fish fauna in Lost and Gordon Creeks , Ohio , between 1887-1938. *The Ohio Journal of Science*, *39*(5), 275–288.

Vázquez, D. P., & Simberloff, D. (2002). Ecological specialization and susceptibility to disturbance: conjectures and refutations. *The American Naturalist*, *159*(6), 606–623. doi:10.1086/339991

Vitousek, P. M., Mooney, H. a, Lubchenco, J., & Melillo, J. M. (1997). Human Domination of Earth' s Ecosystems. *Science*, *277*(5325), 494–499. doi:10.1126/science.277.5325.494

Wainwright, P. C., Osenberg, C. W., & Mittelbach, G. G. (1991). Trophic Polymorphism in the pumpkinseed sunfish (Lepomis-Gibbosus Linnaeus) - effects of environment on ontogeny. *Functional Ecology*, *5*(1), 40–55. doi:10.2307/2389554

Waltzek, T. B., & Wainwright, P. C. (2003). Functional morphology of extreme jaw protrusion in Neotropical cichlids. *Journal of Morphology*, *257*, 96–106. doi:10.1002/jmor.10111

Webb, P. W. (1984). Body form, locomotion and foraging in aquatic vertebrates. *American Zoologist*, *24*(1), 107–120. doi:10.1093/icb/24.1.107

West-Eberhard, M. J. (1989). Phenotypic plasticity and the origins of diversity. *Annual Review of Ecology and Systematics*, *20*, 249–278.

doi:10.1146/annurev.es.20.110189.001341

West-Eberhard, M. J. (2003). *Developmental Plasticity and Evolution*. New York, NY: Oxford University Press.

Williams, J. D., Winemiller, K. O., Taphorn, D. C., & Balbas, L. (1998). Ecology and Status of Piscivores in Guri, an Oligotrophic Tropical Reservoir. *North American Journal of Fisheries Management*, *18*(2), 274–285. doi:10.1577/1548-8675(1998)018<0274:EASOPI>2.0.CO;2

Willis, S. C., Nunes, M. S., Montaña, C. G., Farias, I. P., & Lovejoy, N. R. (2007). Systematics, biogeography, and evolution of the Neotropical peacock basses Cichla (Perciformes: Cichlidae). *Molecular Phylogenetics and Evolution*, *44*(2007), 291–307. doi:10.1016/j.ympev.2006.12.014

Wilson, S. K., Burgess, S. C., Cheal, A. J., Emslie, M., Fisher, R., Miller, I., … Sweatman, H. P. A. (2008). Habitat utilization by coral reef fish: implications for specialists vs. generalists in a changing environment. *Journal of Animal Ecology*, *77*, 220–228. doi:10.1111/j.1365-2656.2007.0

Wimberger, P. H. (1991). Plasticity of jaw and skull morphology in the neotropical cichlids Geophagus brasiliensis and Geophagus steindachneri. *Evolution*, *45*(7), 1545–1563. doi:10.2307/2409778

Wimberger, P. H. (1992). Plasticity of fish body shape. The effects of diet, development, family and age in two species of Geophagus (Pisces: Cichlidae). *Biological Journal of the Linnean Society*, *45*, 197–218.

Winemiller, K. O., McIntyre, P. B., Castello, L., Fluet-Chouinard, E., Giarrizzo, T., Nam, S., … Sáenz, L. (2016). Balancing hydropower and biodiversity in the Amazon, Congo, and Mekong. *Science*, *351*(6269), 128–129. doi:10.1126/science.aac7082

Yoder, J. B., Clancey, E., Des Roches, S., Eastman, J. M., Gentry, L., Godsoe, W., … Harmon, L. J. (2010). Ecological opportunity and the origin of adaptive radiations. *Journal of Evolutionary Biology*, *23*(8), 1581–1596. doi:10.1111/j.1420-9101.2010.02029.x

Zarfl, C., Lumsdon, A. E., Berlekamp, J., Tydecks, L., & Tockner, K. (2014). A global boom in hydropower dam construction. *Aquatic Sciences*, *77*(1), 161–170. doi:10.1007/s00027-014-0377-0

Zelditch, M. L., Swiderski, D., Sheets, H., & Fink, W. (2012). *Geometric Morphometrics for Biologists: A Primer*. Amsterdam: Elsevier/Academic Press.

Supplemental Data

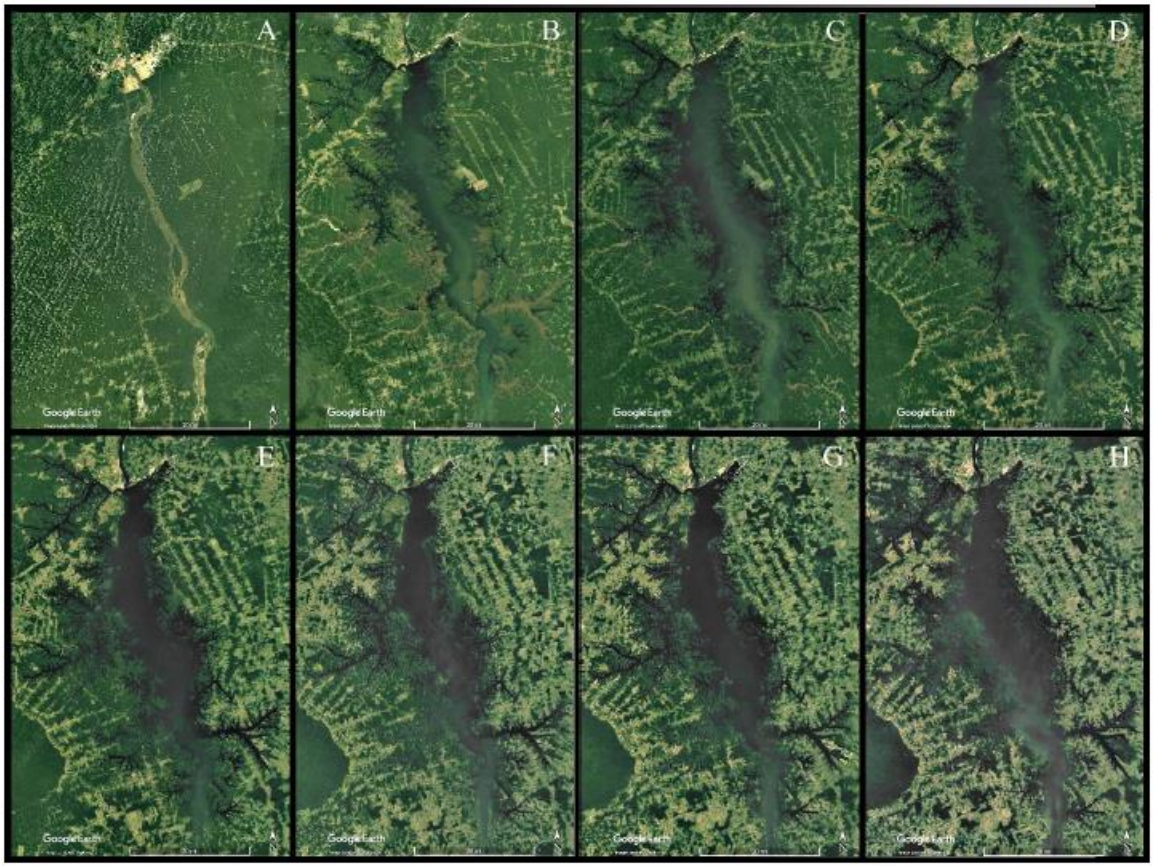

Supplemental Figure 3.1. Google Earth Landsat/Copernicus imagery of Tucuruí Hydroelectric dam vicinity over the past 32 years since closure. **A)**1984 **B)**1988 **C)**1993 **D)**1996 **E)**2001 **F)**2006 **G)**2008 **H)**2016. All images are taken to scale and scale bars represent ~32.2 kilometers (20 miles).

Supplemental Table 3.1. Museum accession numbers for all lots examined and included and included in all analyses.

Species	Lot #	Year	n
Cichla kelberi	MPEG 38519	2018	21/21
Cichla kelberi	INPA-ICT 24061	1980	2/2
Cichla kelberi	MZUSP 46067	1970	1/1
Cichla kelberi	MZUSP 50594	1970	1/1
Cichla kelberi	MZUSP 50595	1970	2/2
Cichla kelberi	MZUSP 50599	1970	3/6
Cichla kelberi	MZUSP 63139	1970	2/2
Cichla pinima	MZUSP 38409	1987	12/12
Cichla pinima	MPEG 38520	2018	25/25
Geophagus neambi	MZUSP 40927	1970	1/1
Geophagus neambi	MZUSP 44835	1970	3/3
Geophagus neambi	MZUSP 44954	1970	2/2
Geophagus neambi	MZUSP 44956	1970	1/15
Geophagus neambi	MZUSP 44958	1970	3/9
Geophagus neambi	MZUSP 44959	1970	5/7
Geophagus neambi	MZUSP 44965	1970	3/43
Geophagus neambi	MZUSP 44966	1970	1/23
Geophagus neambi	MPEG 36753	2018	8/15
Geophagus neambi	MPEG 37099	2018	7/16
Satanoperca jurupari	MZUSP 44194	1970	1/10
Satanoperca jurupari	MZUSP 44217	1970	5/11
Satanoperca jurupari	MZUSP 44233	1970	4/7
Satanoperca jurupari	MZUSP 44234	1970	1/1
Satanoperca jurupari	MZUSP 44235	1970	2/77
Satanoperca jurupari	MZUSP 44236	1970	2/11
Satanoperca jurupari	MZUSP 44237	1970	4/12
Satanoperca jurupari	MPEG 38526	2018	30/30
Caquetaia spectabilis	MZUSP 45823	1970	1/5
Caquetaia spectabilis	MZUSP 45824	1970	1/5
Caquetaia spectabilis	MZUSP 45825	1970	2/8
Caquetaia spectabilis	MZUSP 45827	1970	1/3
Caquetaia spectabilis	MZUSP 45828	1970	1/2
Caquetaia spectabilis	MZUSP 45830	1970	2/2
Caquetaia spectabilis	MPEG 38517	2018	26/27
Heros efasciatus	INPA 9441	1980	9/9
Heros efasciatus	INPA 9463	1980	1/1
Heros efasciatus	MPEG 38525	2018	23/23

Note i. Museum abbreviations are as follows, **MPEG**: Museu Paraense Emílio Goeldi; **MZUSP**: Museu de Zoologia da Universidade de São Paulo; **INPA**: Instituto Nacional de Pesquisas da Amazônia. (n) represents the number of specimens used against the number of specimens available in the lot.

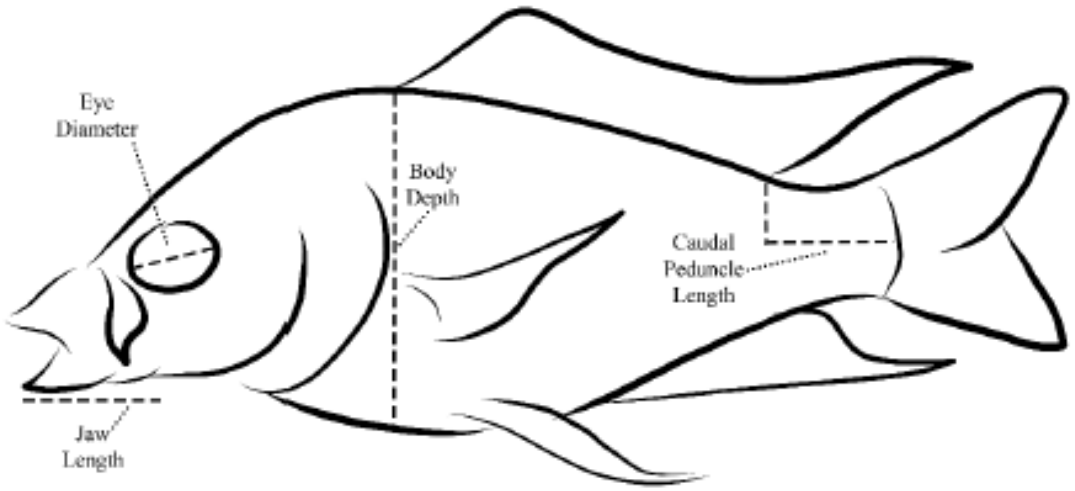

Supplemental Figure 3.2. Simple outline sketch of *Caquetaia spectabilis* detailing the four linear measurements taken across all cichlid specimens. Body depth was measured from the insertion of the spinous dorsal fin to the breast. Caudal Peduncle length was measured from the end of the soft dorsal fin to the end of the caudal peduncle proper. Jaw length was measured from the tip of dentary to the posterior margin of the articular. Eye diameter was measured as a straight line through the center of the orbit.

Supplemental Table 3.2. Results from ANOVA testing for effect strength on variables of interest and the interaction terms between them. For significance testing $\alpha = 0.05$.

	R^2	F-Stat	Z-score	P
Cichla sp.				
Log(CS)	0.08813	7.2760	4.2025	<0.0001
Species	0.04312	3.5595	3.3165	0.0002
Year (Dam)	0.06908	5.0726	4.2535	<0.0001
Log(CS):Species	0.01805	1.4902	1.5486	0.0622
Log(CS):Year	0.00551	0.4551	-0.8932	0.8122
Species:Year	0.03000	2.4766	2.7724	0.0029
Log(CS):S:Y	0.00722	0.5931	-0.2583	0.5990
Geophagus neambi				
Log(CS)	0.13029	5.4467	3.8781	<0.0001
Year (Dam)	0.11415	4.7718	3.8720	<0.0001
Log(CS):Year	0.03794	1.5860	1.8546	0.0312
Satanoperca jurupari				
Log(CS)	0.08751	5.4065	3.6992	<0.0001
Year (Dam)	0.16451	10.1634	5.2245	<0.0001
Log(CS):Year	0.01960	1.2110	1.2853	0.1026
Caquetaia spectabilis				
Log(CS)	0.16748	7.0506	4.4890	<0.0001
Year (Dam)	0.04041	1.7014	1.8435	0.0385
Log(CS):Year	0.05576	2.3474	2.7149	0.0051
Heros efasciatus				
Log(CS)	0.43942	26.0597	5.7212	<0.0001
Year (Dam)	0.04470	2.6508	3.6592	0.0002
Log(CS):Year	0.02687	1.5938	2.8757	0.0045

Supplemental Table 3.3. Results from ANOVA, regressing centroid size against predicted shape (Shape ~ Centroid Size + Dam) across between pre/post dam genera. For significance testing, $\alpha = 0.05$.

	R^2	P
Cichla	0.03317	0.2412
Caquetaia	0.0489	0.0110
Geophagus	0.0375	0.0312
Heros	0.02687	0.0045
Satanoperca	0.0196	0.1026

Supplemental Table 3.4. Results from Tukey Honest Significant Differences test on residuals of linear measurements (X ~ Standard Length) across four anatomically functional traits. Absolute differences in means above diagonal, p-values below. For significance testing, $\alpha = 0.05$.

	C. kelberi, pre	*C. kelberi*, post	*C. pinima*, pre	*C. pinima*, post
			Body Depth	
C. kelberi, pre	-	0.1408	0.6852	0.8418
C. kelberi, post	0.5942	-	0.5444	0.7010
C. pinima, pre	<0.0001	<0.0001	-	0.1566
C. pinima, post	<0.0001	<0.0001	0.4553	-
			Jaw Length	
C. kelberi, pre	-	0.0935	0.2618	0.0827
C. kelberi, post	0.8481	-	0.1683	0.0107
C. pinima, pre	0.1888	0.4412	-	0.1780
C. pinima, post	0.8804	0.9994	0.3595	-
			Caudal Peduncle Length	
C. kelberi, pre	-	0.0431	0.0665	0.1506
C. kelberi, post	0.9748	-	0.0234	0.1076
C. pinima, pre	0.9382	0.9954	-	0.0841
C. pinima, post	0.4371	0.5545	0.8205	-
			Eye Diameter	
C. kelberi, pre	-	0.0059	0.1906	0.1681
C. kelberi, post	0.9984	-	0.1846	0.1622
C. pinima, pre	<0.0001	<0.0001	-	0.0224
C. pinima, post	<0.0001	<0.0001	0.9140	-

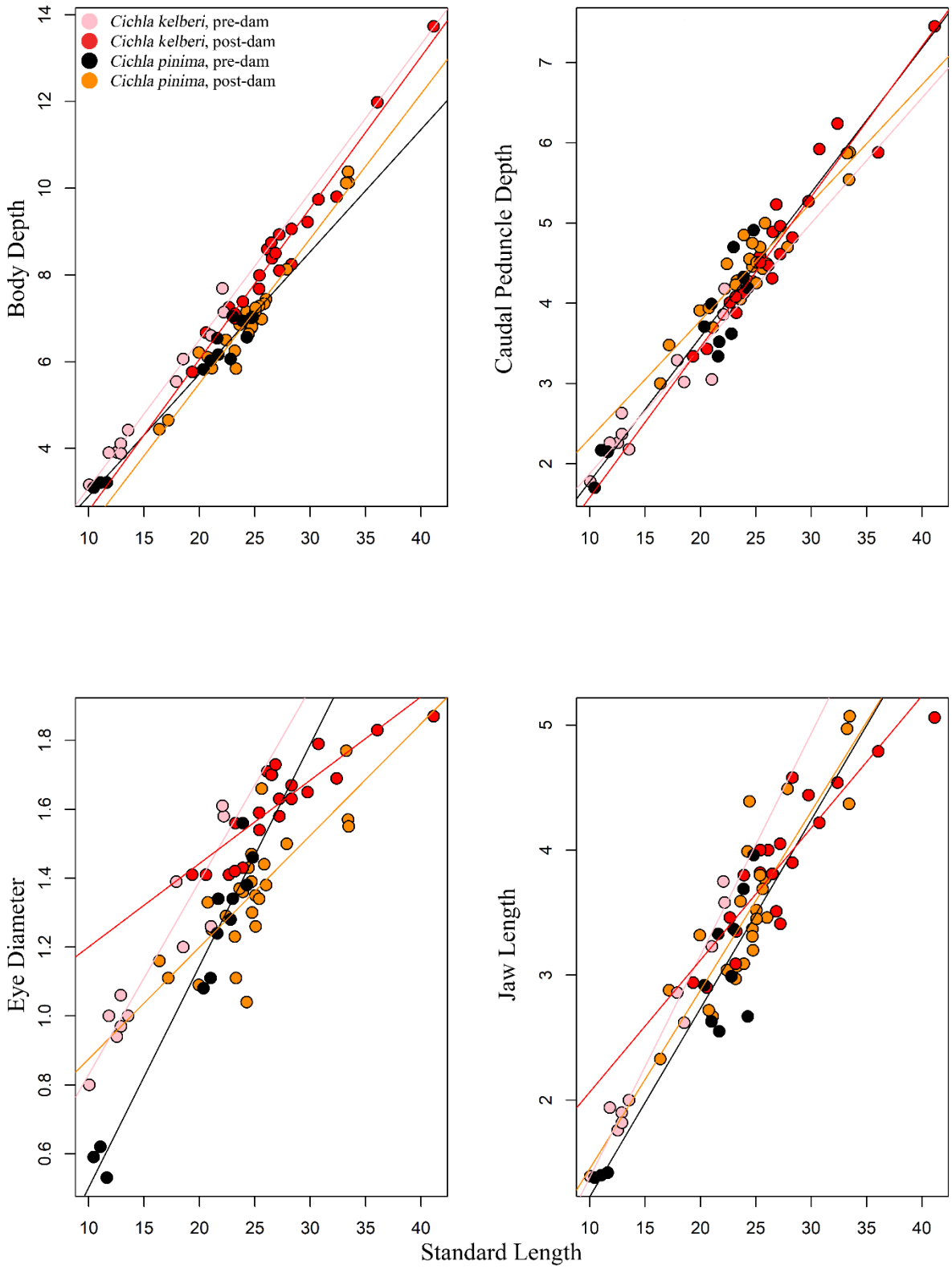

Supplemental Figure 3.3. Four traits of interest (body depth, caudal peduncle depth, eye diameter, and jaw length) regressed against standard length among the two Cichla species between the two year groups.

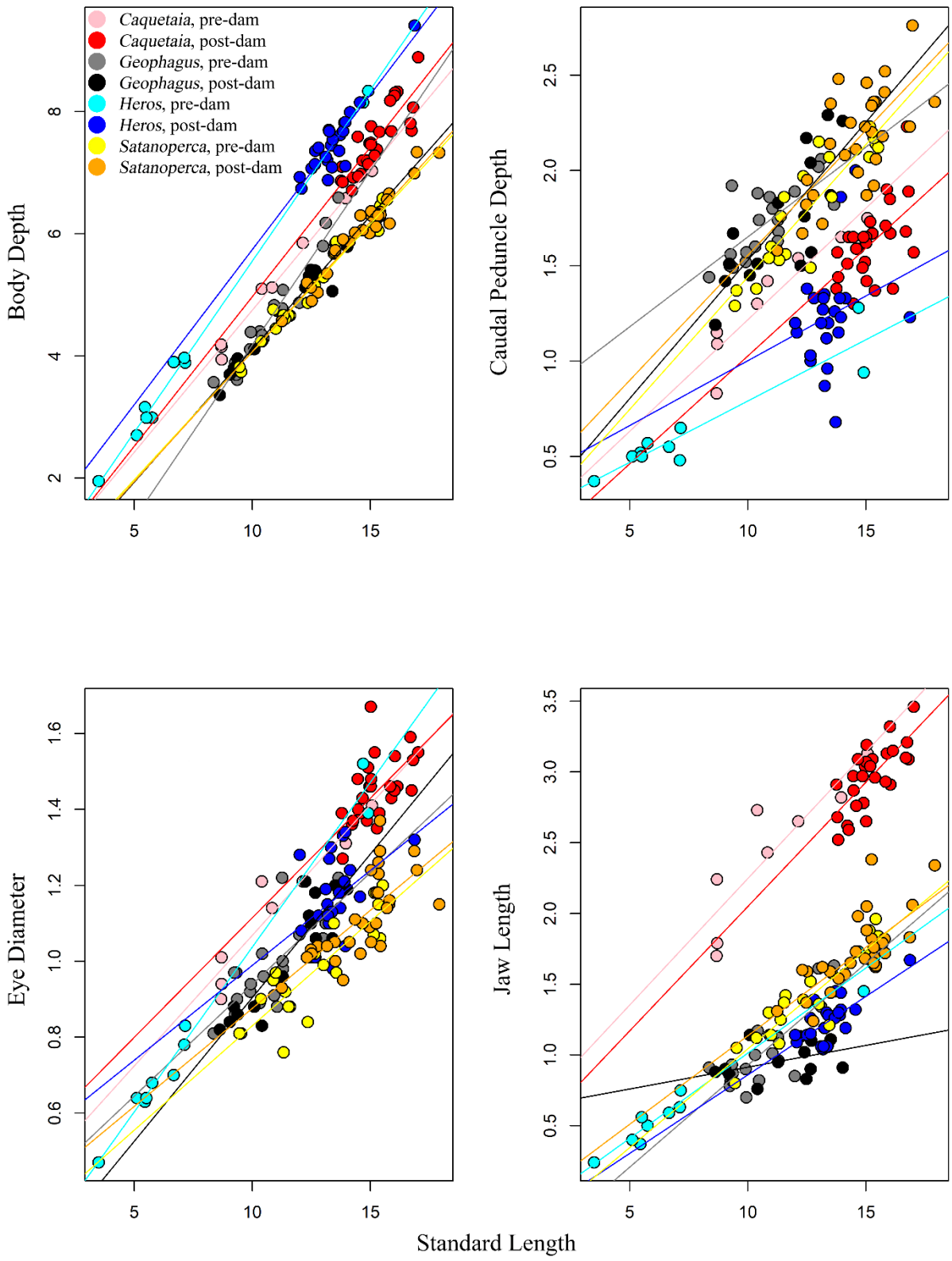

Supplemental Figure 3.4. Four traits of interest (body depth, caudal peduncle depth, eye diameter, and jaw length) regressed against standard length for the four remaining species between year groups.

Supplemental Table 3.5. Results from t- tests on residuals of linear measurements (X ~ Standard Length) across four anatomically functional traits. For significance testing, $\alpha = 0.05$.

	Absolute Difference in Means	P-Value
	Geophagus neambi	
Body Depth	0.2004	0.0120
Jaw Length	0.1274	0.0284
Caudal Peduncle Length	0.0665	0.2983
Eye Diameter	0.0162	0.4967
	Satanoperca jurupari	
Body Depth	0.0216	0.6838
Jaw Length	0.0287	0.5182
Caudal Peduncle Length	0.0618	0.2149
Eye Diameter	0.0243	0.2517
	Caquetaia spectabilis	
Body Depth	0.1195	0.1694
Jaw Length	0.0799	0.4129
Caudal Peduncle Length	0.0783	0.1938
Eye Diameter	0.0093	0.7161
	Heros efasciatus	
Body Depth	0.0173	0.7889
Jaw Length	0.0718	0.1185
Caudal Peduncle Length	0.0892	0.2141
Eye Diameter	0.0592	0.1084

4. CHAPTER 4

SUBSTRATE TYPE INDUCES PLASTIC RESPONSES IN THE CRANIOFACIAL MORPHOLOGY OF A WINNOWING CICHLID

Michelle C. Gilbert[1], Sofia Piggott[2], R. Craig Albertson[2]

1 Organismic and Evolutionary Biology Graduate Program, University of Massachusetts, Amherst, MA 01003

2 Biology Department, Morrill Science Center, University of Massachusetts, 611 North Pleasant Street, Amherst, MA 01003

SUBMITTED TO: Hydrobiologia

FULL CITATION: Gilbert, M, S Piggott, RC Albertson. *In review*. Muscle and bone plasticity in a winnowing, South American cichlid.

Abstract

Understanding how local populations respond to specific changes in the environment can help us better predict how populations respond to such change. With this topic in mind, we followed up on a previous study by exploring the capabilities of a Geophagini cichlid, known for its unique feeding strategy, to mount a plastic response. We exposed *Satanoperca daemon*, a winnowing cichlid, to three different substrate types, two of which encouraged winnowing behaviors and a third that prevented winnowing entirely. Using geometric morphometrics, we quantified aspects of craniofacial anatomy to test for morphological differences between the treatments and to test for the integration of different traits across the head. We found significant differences across our experimental populations in both shape and disparity. We report evidence in support of wide-spread integration across craniofacial traits. A notable exception to this pattern was the epibranchial lobe, a structure unique to the Geophagini, which exhibited more modular variation. Since anthropogenic alterations such as the damming of rivers can impact substrate type, these data offer insights into how Geophagini cichlids may respond to environmental change. In addition, this work further illuminates the functional morphology of winnowing foraging behaviors.

Introduction

The Cichlidae contain an enormous diversity of fishes that have exploited different niches, environments, and behaviors. Cichlids are distributed in both Africa, South America, India, and Madagascar and have been the focus of study for decades becoming a modern model for understanding complex evolutionary and ecological processes and for digging into evo-devo concepts (Muschick et al. 2012; Arbour and

López-Fernández 2013; Feilich 2016; Mcgee et al. 2016; Powder and Albertson 2016; Navon et al. 2020). Much of the work regarding adaptive radiations has focused on African cichlids (Turner 2007), undoubtedly due to the nature of the rift lake system. However, it has been shown that South American cichlids have also gone through rapid radiation events, most notably within the Geophagini clade (López-Fernández et al. 2013, Burress et al. 2018, 2022). Due to its importance in allowing populations to respond to rapid environmental shifts (citations?), as well as its proclivity to influence the evolutionary patterns and trajectories of populations, the capability to exhibit plasticity is a key mechanism in understanding adaptive radiations (West-Eberhard 1989, 2003).

Plasticity in cichlids has been extensively noted and includes numerous aspects of craniofacial morphology (Chapman et al. 2000; Muschick et al. 2011). Because of this, plasticity has become incorporated as a key concept of how the diversity of cichlids has arisen, particularly through the feeding apparatus representing a flexible stem (West-Eberhard 1989, 2003). This extends to the South American cichlids where plasticity has been demonstrated in the Geophagini cichlid genus *Geophagus* (Wimberger 1991, 1992, 1993). The Geophagini cichlids are so named (i.e., “earth eating”) due to their unique behavior of winnowing, a process of taking in mouthfuls of sediment and sifting out detritus and invertebrates. Unique to the geophagine cichlids is a highly modified epibranchial lobe on the first gill arch that is speculated to have evolved to facilitate winnowing and mouthbrooding behaviors (López-Fernández et al. 2012; Weller et al. 2022), although the exact role is unknown.

The epibranchial lobe possesses some degree of variation tied to diet and ecomorphology (López-Fernández et al. 2012). However, it is unknown how specific

aspects of the morphology of the epibranchial lobe associate with different substrates and/or prey items. Further, the degree to which the epibranchial lobe is plastic remains largely unknown. Previously published work detailed substantial morphological change in the winnowing cichlid species *Satanoperca jurupari* and *Geophagus neambi* following the damming of a major river system, suggesting that radical environmental alterations had a substantial effect on the cranial morphology of this species (Gilbert et al. 2020).

Because the alteration of a riverine system to a lacustrine system can substantially alter sediment type (Trautman 1939; Allan and Flecker 1993; Lau et al. 2006; Helfman 2007), we sought to understand if different substrates (i.e., rock, sand, or substrate-free) could induce a plastic morphological change in a winnowing cichlid. Specifically, we exposed the winnowing geophagine cichlid, Satanoperca daemon, to alternate substrate types and quantified and compared morphological variation across a suite of foraging-related traits. We predicted that the population exposed to larger sediments would develop deeper heads, larger muscles, and altered oral cavities, including the epibranchial lobes, to sift through the heavy, coarse substrate. Next, we tested for correlations between various craniofacial traits to identify sets of traits that exhibited an integrated plastic response. We predicted that functionally related traits, such as the oral jaws and adductor muscles as well as the oral cavity and epibranchial lobes, would covary. Together, these results will aid in discerning how winnowing species may adapt their feeding architecture in response to rapid environmental change. In addition, levels of phenotypic integration across various aspects of foraging anatomy, may provide further insights into the kinematics of winnowing behavior including roles for the novel epibranchial lobe.

Methods

Experimental design

We obtained wild caught *Satanoperca daemon* juveniles from local importers who specialized in acquiring fishes from the Central and South Americas. Upon arrival, we parsed fish into one of three different 40-gallon aquaria. To evaluate the effect of substrate composition on winnowing morphology, we modified the substrate in each tank. Tank one contained no substrate and fish were fed twice daily with bloodworms provided on the surface of the water. The lack of substrate in this tank prevented winnowing from occurring at all, even when food was absent. Tank two possessed sand substrate, fish were fed twice daily with bloodworms that had been covered with sand in a 2" deep Pyrex dish. Tank three possessed a substrate comprised of aquarium gravel and fish were fed twice daily with bloodworms that had been covered with identical gravel in a 2" deep Pyrex dish. Since *Satanoperca* had been previously observed to winnow casually, even outside of feeding hours, tanks two and three had substrate in their tanks continuously to reinforce winnowing behaviors even while food was absent. However, tank one never possessed substrate of any kind to prevent the mechanical process of

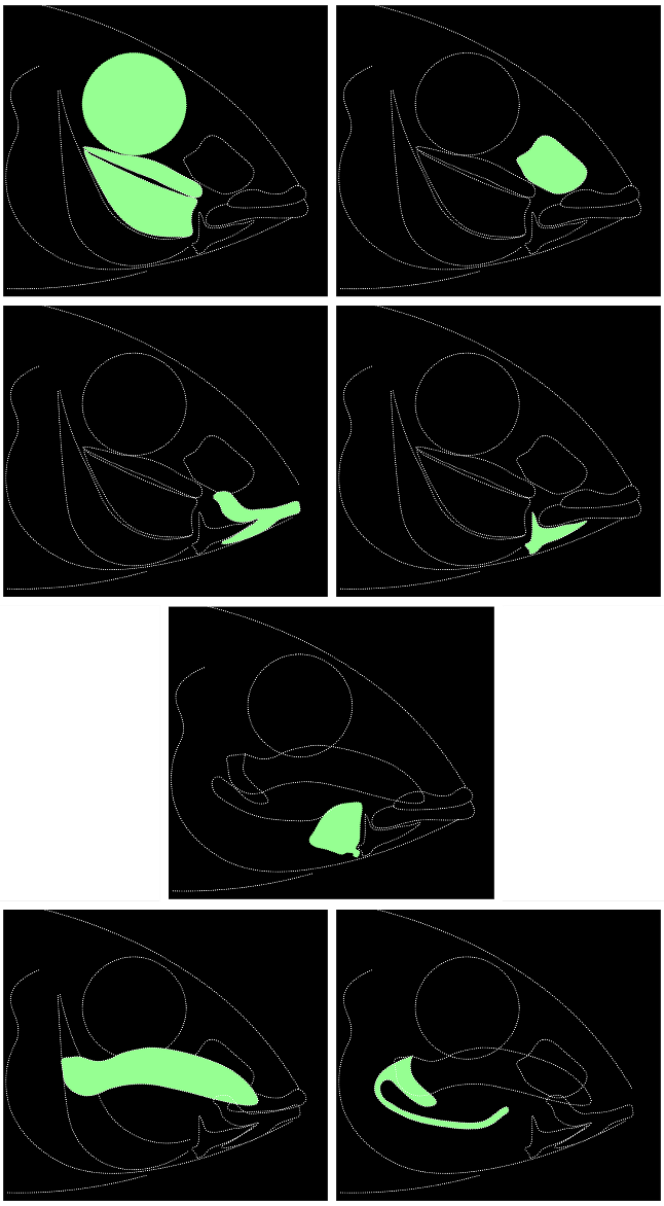

Figure 4.1. Graphical illustration of the various aspects of anatomy that were assessed in this study. **A)** Orbit and *Adductor mandibularis*, **B)** Lacrymal, **C)** Dentary, **D)** Anguloarticular, **E)** Quadrate, **F)** Oral cavity, **G)** First gill arch and epibranchial lobe.

winnowing entirely. This experiment was kept active for 27 weeks and were fixed following MS-222 (Tricaine methane sulfonate) overdose coupled with ice shock.

Specimen preparation and data collection

Fixed fish were stained using an alizarin solution in 75% EtOH to visualized osteological elements but preserve muscle integrity and morphology for data acquisition. We then carefully dissected all specimens to reveal the *adductor mandibularis pars malaris* (A1) and *par rictalis* (A2), and subsequent layers of muscles and bone were systematically removed, and collected, to ensure imagery of the dentary, angulo-articular, lachrymal, first epibranchial, and buccal cavity (including parasphenoid and hyoglossal – pharyngeal jaws; Figure 1).

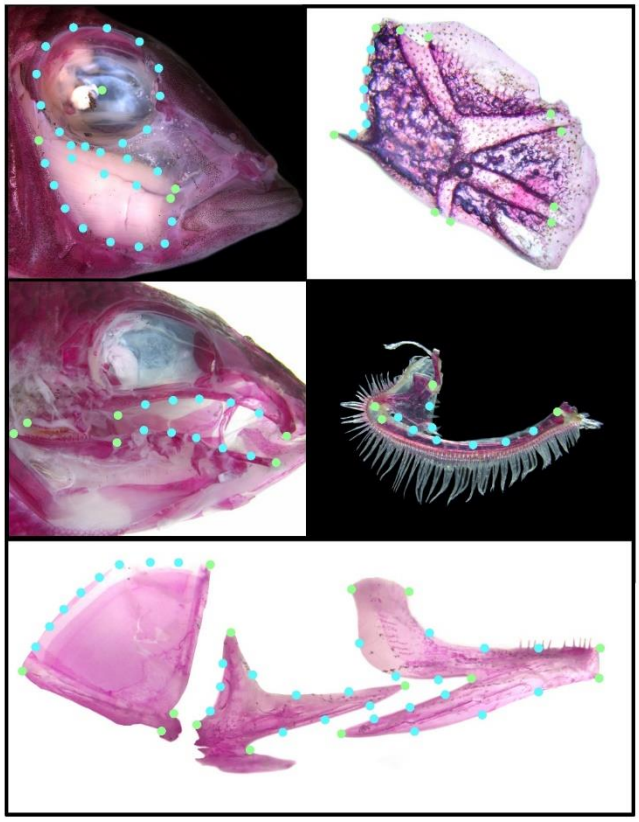

Figure 4.2. Landmark configurations for each aspect of anatomy that we digitized.

We collected two-dimensional geometric morphometric data for the aforementioned structures using STEREOMORPH (Olsen and Westneat 2015) in R (R

Core Team 2018). In total, we collected morphometric data across 7 unique image sets. **For *Adductor mandibularis* and the orbit,** five fixed and 24 semi-landmarks, 12 of which formed a continuous curve. **Lachrymal**, 10 fixed and six semi-landmarks. **Anguloarticular,** four fixed and nine semi-landmarks. **Quadrate**, four fixed landmarks and eight semi-landmarks. **Dentary,** six fixed and 12 semi-landmarks. **For the first gill arch, including the epibranchial,** four fixed and 10 semi-landmarks. **For the oral cavity,** six fixed and 10 semi-landmarks. See Figure 2.

Geometric Morphometric Analyses

Unless otherwise stated, all analyses here were conducted using GEOMORPH (Adams et al. 2014, 2018). All geometric morphometric data were initially put through a generalized Procrustes analysis (Goodall 1991) utilizing bending energy. Using a Procrustes ANOVA, we tested for differences in mean shape between treatment groups within each GM dataset [e.g., (shape ~ centroid size + treatment)]. Following the initial Procrustes ANOVA, we conducted post-hoc pairwise comparisons using the function pairwise in the RRPP package (Collyer and Adams 2018). Lastly, using the GEOMORPH function two.b.pls (Rohlf and Corti 2000; Adams and Collyer 2016, 2019), we tested for correlations between each of the different anatomical elements included in this study.

Results

Foraging environment induces mean shape differences for numerous traits

Our feeding treatments had a significant effect on 6/7 components investigated (Table 1), the one exception being the anguloarticular ($P = 0.138$) and quadrate ($P = 0.986$). When compared to the *z*-score of centroid size, the effect of treatment had the

greatest influence on the oral cavity (z = 3.245 compared to CS, z = 1.957), whereas it had the lowest effect on the quadrate (z = -2.089 compared to CS, z = 2.946). Post-hoc pairwise comparisons (Table 2) show pelagic treated fish differing significantly from both sand and rock treated populations (P = 0.013, 0.001 respectively) in orbit and adductor mandibulae shapes. Pelagic treated fish also differed in both dentary and oral cavity shapes when compared to rock treated fish (P = 0.018, 0.002).

Table 4.1. Results of Procrustes ANOVA across all eight anatomical elements testing for the effect of treatment or centroid size. **AM, O** = *Adductor mandibularis* and orbit, **LAC** = lachrymal, **AA =** anguloarticular, **D** = dentary, **Q** = quadrate, **GA** = first gill arch and epibranchial lobe, **OC** = oral cavity. For significance testing, $\alpha = 0.05$.

	RSQ	Z	P
AM, O			
CS	0.2471	4.9481	**0.0001**
TR	0.0928	3.5694	**0.0003**
LAC			
CS	0.2942	5.1016	**0.0001**
TR	0.0388	1.6197	0.0528
AA			
CS	0.1152	3.1433	**0.0003**
TR	0.0627	1.0924	0.1380
D			
CS	0.1488	3.8882	**0.0001**
TR	0.0720	2.2501	**0.0064**
Q			
CS	0.1378	2.9465	**0.0016**
TR	0.0112	-2.0894	0.9856
GA			
CS	0.0628	1.6573	**0.0379**
TR	0.1027	1.8120	**0.0255**
OC			
CS	0.0555	1.9570	**0.0187**
TR	0.1473	3.2450	**0.0004**

Table 4.2. Pairwise comparisons of shape across treatment groups. Z scores above, p-values below diagonal. Abbreviations same as Table 1.

	Pelagic	***Rock***	***Sand***	***Pelagic***	***Rock***	***Sand***
		AM, O			***Lac***	
Pelagic		**4.0063**	**2.7111**		0.5908	0.7973
Rock	**0.0011**		-0.1117	0.2516		0.2988
Sand	**0.0133**	0.4916		0.2047	0.3425	
		AA			***D***	
Pelagic		0.3396	1.4616		**2.3468**	0.7017
Rock	0.3363		0.1548	**0.018**		1.6532
Sand	0.0876	0.398		0.2368	0.0604	
		Q			***GA***	
Pelagic		-1.2756	-1.6939		1.5764	1.2330
Rock	0.9466		-0.9756	0.0755		**1.9564**
Sand	0.9944	0.8584		0.1219	**0.0426**	
		OC				
Pelagic		**3.76857**	1.4429			
Rock	**0.0016**		**3.88693**			
Sand	0.0892	**0.0012**				

Deformation grids of treatment groups suggest that our sand winnowing population often appears as an intermediate phenotype between pelagic feeding fish and rock winnowing fish (Figure 3). Overall, the rock winnowing population can be characterized by substantially larger adductor muscles relative to the orbit, a gracile coronoid process, truncated but stout epibranchial lobes, an evenly curved parasphenoid, and a sloping hyoglossal and hyoid creating a relatively large oral cavity. The pelagic feeding population is characterized by reduced adductor muscles relative to the orbit, a somewhat robust coronoid process (compared to the robust sand winnowing population), elongated epibranchial lobes, and a substantially smaller oral cavity.

Foraging environment induces few differences in morphological disparity between populations

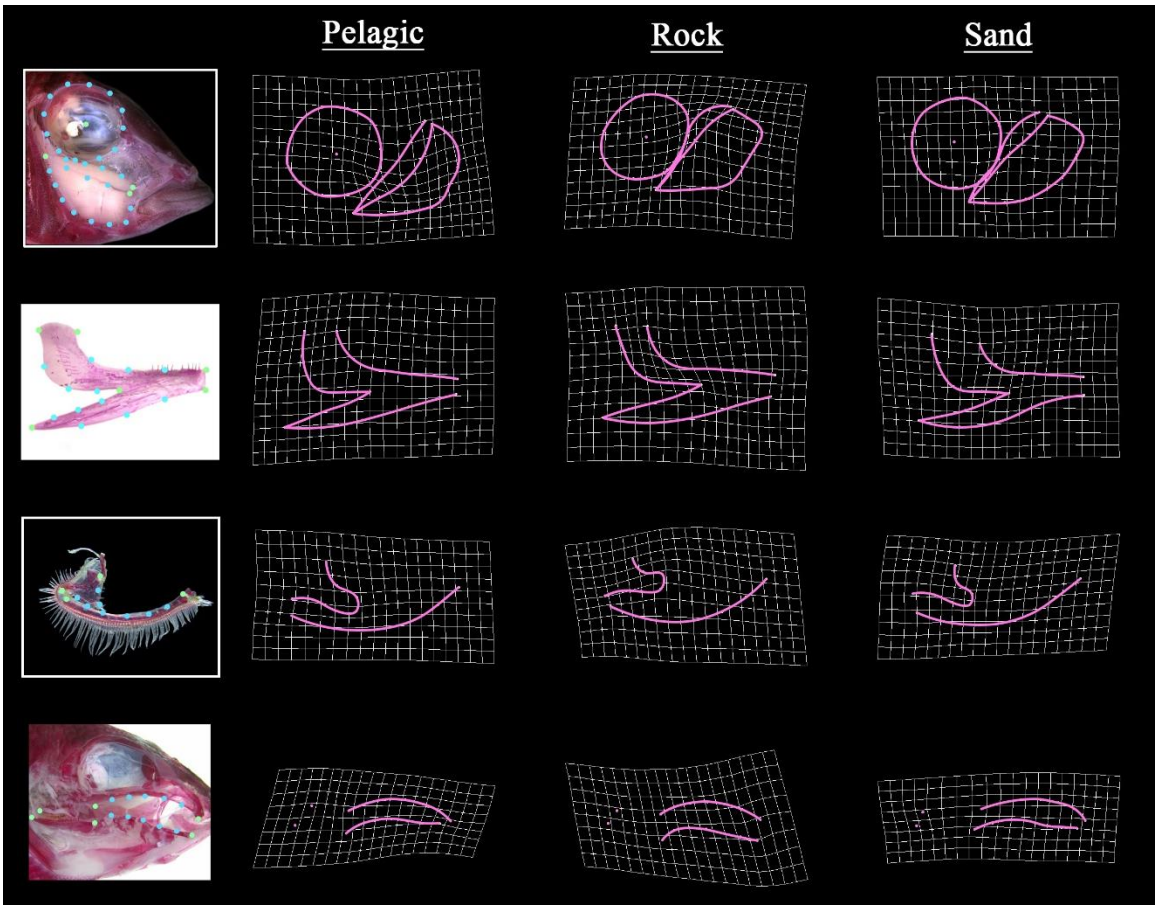

Figure 4.3. Deformation grid matrix of the three different feeding treatments. Graphical examples of traits in the left column. Curves are outlined on deformation grids in pink, fixed landmarks not associated with curves are represented by pink circles. Lachrymal, anguloarticular, and quadrate were not included since no significant pairwise comparison existed in our dataset.

Across all seven anatomical components, only two comparisons showed significantly different levels of disparity (Table 3). The sand winnowing population had significantly more variance ($\sigma 2$ = 0.00467) in lachrymal shape than both the pelagic feeding population ($\sigma 2$ = 0.00261, P = 0.0161) and rock winnowing population ($\sigma 2$ = 0.00285, P = 0.0418). Furthermore, the rock winnowing population had significantly less variance ($\sigma 2$ = 0.00110) than pelagic fed fish ($\sigma 2$ = 0.00169, P = 0.013) and sand treated fishes ($\sigma 2$ = 0.00157, P = 0.0532).

Table 4.3. Pairwise comparisons of shape disparity across treatment groups. Differences in absolute values above, p-values below diagonal. Abbreviations same as Table 1. |***Var***| = Absolute variance.

	Pelagic	***Rock***	***Sand***	***Pelagic***	***Rock***	***Sand***
		AM, O			***Lac***	
Pelagic		0.00004	0.00072		0.00024	0.00206
Rock	0.9281		0.00067	0.8105		0.00181
Sand	0.1082	0.1661		**0.0161**	0.0418	
		AA			***D***	
Pelagic		0.00193	0.00111		0.00011	0.00036
Rock	0.0559		0.00083	0.8539		0.00047
Sand	0.2442	0.4148		0.5291	0.435	
		Q			***GA***	
Pelagic		0.00023	0.00012		0.00043	0.00058
Rock	0.4250		0.00036	0.7722		0.00101
Sand	0.6487	0.1911		0.6789	0.4692	
		OC				
Pelagic		0.00064	0.00226			
Rock	0.706		0.00161			
Sand	0.0816	0.2673				

Orbit and Adductor shape is correlated with numerous other traits whereas the epibranchial lobe is largely modular

We implemented numerous partial least squares tests to assess the degrees of integration between each aspect of anatomy (Figure 4; Supplemental Table 1). Because quadrate shape was statistically the same across all three test populations, this component was not included in the PLS assay. Of the 15 partial least squares tests, seven revealed a significant correlation. The trait that had the fewest significant shape correlations was the first gill arch including the epibranchial lobe, which only correlated with oral cavity shape (R^2 = 0.2972, P = 0.022). The orbit/*adductor mandibulae* had the greatest number of significant shape correlations (4/5 tests being significant). Of these, the strongest correlation, and also the strongest correlation of all trait comparisons, was with the lachrymal (R^2 =0.6727, P < 0.0001).

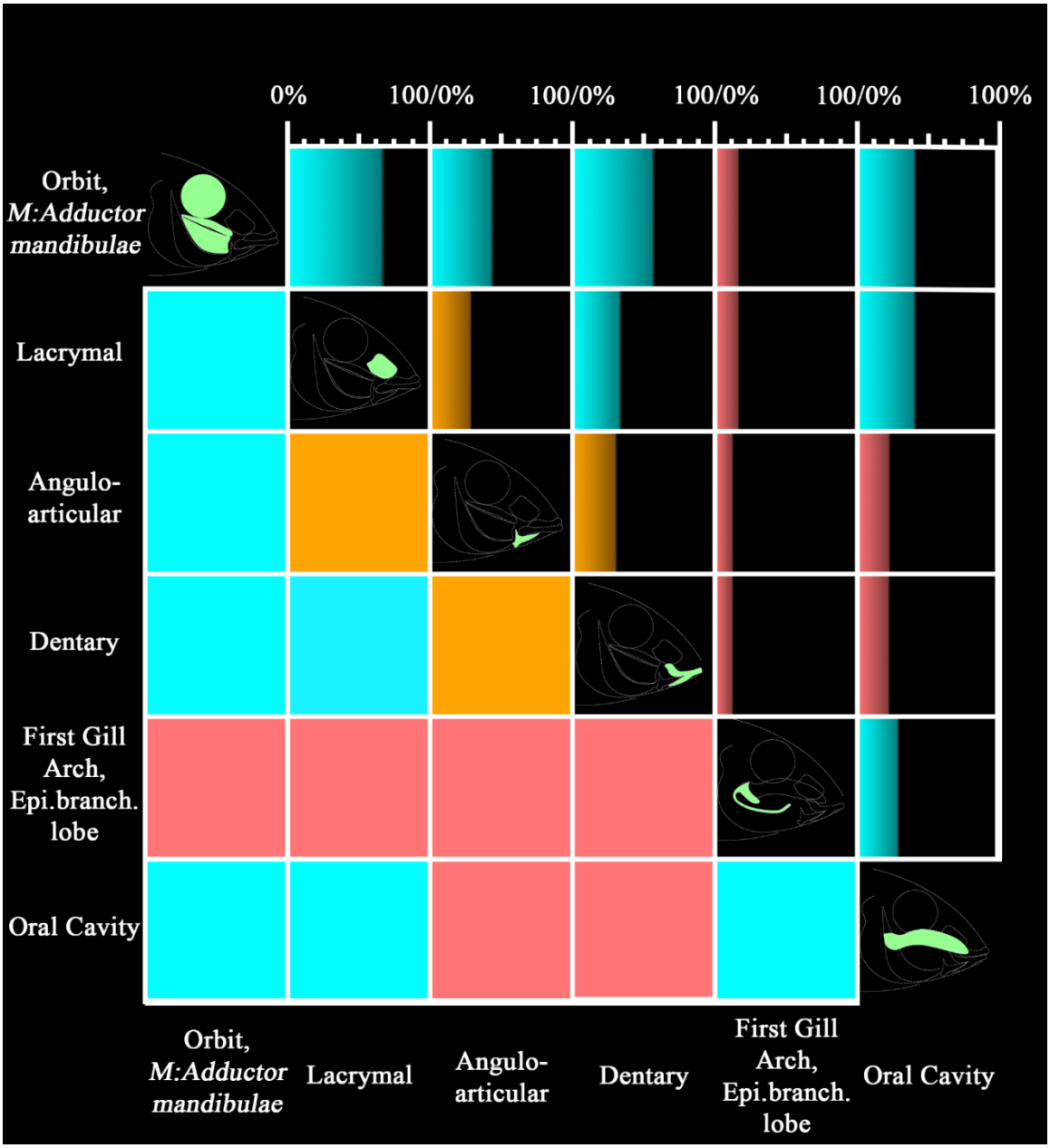

Figure 4.4. Graphical scatterplot matrix illustrating the results of various partial least squares tests to assess degrees of correlation between two anatomical units (or complexes). R^2 values are depicted as percentages above the diagonal, while the p-values are below. Cyan colored squares represent significant correlations ($P \leq 0.05$), orange represent near significant comparisons ($0.05 < P \leq 0.10$), and pink represents insignificant comparisons ($P > 0.10$).

Discussion

Substrate size induces plasticity in winnowing cichlid anatomy

The results of morphological analyses on multiple elements of craniofacial anatomy suggest that different substrate composition alone is sufficient to induce plastic responses in various aspects of feeding morphology in the winnowing cichlid *Satanoperca daemon.* Winnowing, a behavior that utilizes suction feeding to bring large amounts of sediment into the oral cavity, parsing of sediments and food items, and subsequent ejection of sediment (Weller et al. 2017) is an underexplored feeding strategy. While common among the Geophagini cichlids, it is rare across the Cichlidae family. Comparisons of mean morphological shape across three different foraging environments shows that winnowing in rocky sediments induces the most drastic changes. Of 7 significant pairwise differences in mean shape, 6 involved the rock treatment. Only a single pairwise comparison, muscles + orbit, was significant for sand vs pelagic treatments.

Lab-based results are similar to patterns of morphologic change following a major anthropogenic disturbance

The changes in a system from riverine to lacustrine are typically accompanied by substantial changes to the local environment, including shifts in sediment composition (Trautman 1939; Allan and Flecker 1993; Lau et al. 2006; Helfman 2007), alterations that followed the construction of the Tucuruí Hydroelectric Dam in 1984 (Araújo-Lima et al. 1995; ELETROBRÁS/DNAEE 1997; Fearnside 2001). Our previous work in this study documented statistically significant differences in the gross morphology within two Geophagini cichlids, *Geophagus neambi* and *Satanoperca jurupari* (Gilbert et al. 2020). We speculated that changes in sediment, from rocky to silty, had influenced the

morphology of the Geophagini, possibly through phenotypic plasticity. It is also possible that a relatively deeper reservoir habitat would provide greater opportunity for pelagic modes of feeding (e.g., ram/suction). Here, we show that substrate type alone (including substrate-free habitat) is indeed sufficient to induce morphological change in a closely related winnowing cichlid. It is therefore possible that the changes in craniofacial morphology that we reported in 2020 was, at least in part, due to substantial alterations of the substrate. However, we did not previously report on specific elements of craniofacial anatomy and next steps should work to directly compare anatomical elements of specimens from the two studies. The trend of effectively shifting mean shape values in phenotypic space but keeping interpopulation variation consistent was also consistent with our previous paper (Gilbert et al. 2020), where we reported differences in whole body shape means, but not disparity, among cichlid species.

Morphological plasticity in fishes, especially cichlids, has been heavily documented (Chapman et al. 2000; Alexander and Adams 2004; Lema and Nevitt 2006; Muschick et al. 2011) and others have reported plasticity in related taxa, such as *Geophagus brasiliensis* and *steindachneri* (Wimberger 1991, 1992). To our knowledge, this is the first report of sediment-induced morphological plasticity in a winnowing cichlid. Understanding the mechanical forces that have precipitated these changes will be an important topic for future study.

Functional Implications of Plastic Changes

The differences observed in morphology are likely related to the effort required to suction and process substrates of radically different size. *Satanoperca* that winnowed rock, compared to the non-winnowers (pelagic), had substantially larger adductor

muscles, larger buccal cavities, and parasphenoids that arced higher. These traits could be associated with the cycling motions of the jaw when winnowing is occurring and room to generate increased water flow and turbulence to parse food items out of substrate (Van Wassenbergh et al. 2015; Brooks et al. 2018; Weller et al. 2022). Winnowers had shorter epibranchial lobes and with more room between the lobe itself and rest of the gill arch. This is intuitive, given that this is the area where food items are being parsed from substrate. Anecdotal evidence in support of direct contact between substrate and the epibranchial lobe includes the observation that rock sifting cichlids possessed gill rakers that were generally more mineralized than those from other treatments (gill raker number did not vary between treatments). Finally, we found no correlation in morphology between the first gill arch/epibranchial lobe with the other traits, consistent with a modular plastic response relative to other aspects of the head (Cheverud 1996; Cheverud et al. 1997; Klingenberg 2008; Navon et al. 2021).

Modular vs integrated plasticity and paths of least evolutionary resistance

The subdivision of different biological systems into different modules is hypothesized to facilitate the evolvability of various traits (Wagner et al. 2007; Larouche et al. 2018; Zelditch and Goswami 2021). Modular traits are often evolutionarily decoupled, allowing the two or more traits to evolve independently from one another to serve multiple, even disparate, functions (Cheverud 1996). The independence of traits from one another can be explained by the weakening of evolutionary constraints between them (Jacob 1977; Wagner and Misof 1993; Klingenberg 2005; McGhee 2007; Hallgrimsson et al. 2009; Sheftel et al. 2013). Indeed, it has been hypothesized for some

time that the evolution of novel traits is in part the result of an increasingly modular system developing (Prum 2005; Kuratani 2009; Niwa et al. 2010; Gilbert et al. 2021). Thus, it is plausible that an increasingly modular system can lead to increased rates of evolution in lineages, thereby promoting speciation in diverse, complex environments (West-Eberhard 1989, 2003; Foote 1997).

Challenging fishes with various foraging environments provides excellent opportunities to quantify magnitudes of both shape variation and covariation, thereby enabling assessments of phenotypic integration (Conith et al. 2020; Navon et al 2021). We document various levels of integration across craniofacial traits. On one end of the spectrum, the first gill arch including the epibranchial lobe is relatively modular, only covarying with the oral cavity. On the other end of the spectrum, orbit-*adductor mandibulae* shape is integrated with most other traits, suggesting that these traits have the potential to co-evolving along an evolutionary path of least resistance (Schluter 1996; Foote 1997; Conith and Albertson 2021).

We hypothesize that the morphological decoupling of the first gill arch from other craniofacial elements and its plasticity have allowed, in part, for the Geophagini cichlids to take advantage of a novel niche environment. Given phenotypic plasticity can lead to the evolution of phenotypic novelties (Moczek 2008), it is possible that this mechanism underlies the evolution of the epibranchial lobe (a novelty specific to Geophagini cichlids), and that its decoupled, modular nature allowed it to be modified without influencing other aspects of the head. Further, these attributes of the epibranchial lobe may support the hypothesis put forth by Weller and colleagues (2022), which states that winnowing provided the anatomical, functional, and behavioral framework for

mouthbrooding to evolve. Specifically, we speculate that the retention of modularity and plasticity in the epibranchial lobe paved the way for multifunctionality to evolve in certain lineages, including the co-option of this functional complex for mouthbrooding, without altering other aspects of prey capture and processing.

LITERATURE CITED

Adams, D. C., and M. L. Collyer. 2019. Comparing the strength of modular signal, and evaluating alternative modular hypotheses, using covariance ratio effect sizes with morphometric data. Evolution (N. Y). 73:2352–2367.

Adams, D. C., and M. L. Collyer. 2016. On the comparison of the strength of morphological integration across morphometric datasets. Evolution (N. Y). 70:2623–2631.

Adams, D. C., M. L. Collyer, and E. Otarola-Castillo. 2014. Geomorph Software for geometric morphometric analysis.

Adams, D., M. L. Collyer, and A. Kaliontzopoulou. 2018. Geomorph: Software for geometric morphometric analysis. R package version 3.0.6.

Allan, J. D., and A. S. Flecker. 1993. Biodiversity conservation in running waters. Bioscience 43:32–43.

Alexander, G. D., and C. E. Adams. 2004. Exposure to a common environment erodes inherited between-population trophic morphology differences in Arctic charr. J. Fish Biol. 64:253–257.

Araújo-Lima, C., A. Agostinho, and N. Fabré. 1995. Trophic aspects of fish communities in Brazilian rivers and reservoirs. Pp. 105–136 in Limnology in Brazil. Brazilian Academy of Sciences, Rio de Janeiro.

Arbour, J. H., and H. López-Fernández. 2013. Ecological variation in South American geophagine cichlids arose during an early burst of adaptive morphological and functional evolution. Proc. R. Soc. B Biol. Sci. 280:20130849–20130849.

Brooks, H., G. E. Haines, M. Carly Lin, and S. Laurie Sanderson. 2018. Physical modeling of vortical cross-step flow in the American paddlefish, Polyodon spathula. PLoS One 13:1–25.

Burress, E. D., F. Alda, A. Duarte, M. Loureiro, J. W. Armbruster, and P. Chakrabarty. 2018. Phylogenomics of pike cichlids (Cichlidae: *Crenicichla*): the rapid ecological speciation of an incipient species flock. J. Evol. Biol. 31:14–30.

Burress, E. D., L. Piálek, J. Casciotta, A. Almirón, and O. Říčan. 2022. Rapid parallel morphological and mechanical diversification of South American Pike Cichlids (*Crenicichla*). Syst. Biol. 0:1–14.

Chapman, L. G., F. Galis, and J. Shinn. 2000. Phenotypic plasticity and the possible role of genetic assimilation: Hypoxia-induced trade-offs in the morphological traits of an African cichlid. Ecol. Lett. 3:387–393.

Cheverud, J. M. 1996. Developmental integration and the evolution of pleiotropy. Am. Zool. 36:44–50.

Cheverud, J. M., E. J. Routman, and D. J. Irschick. 1997. Pleiotropic effects of individual gene loci on mandibular morphology. Evolution (N. Y). 51:2006–2016.

Collyer, M. L., and D. C. Adams. 2018. RRPP: An r package for fitting linear models to high- - dimensional data using residual randomization. 2018:1772–1779.

Conith, A. J., and R. C. Albertson. 2021. The cichlid oral and pharyngeal jaws are evolutionarily and genetically coupled. Nat. Commun. 12:1–11. Springer US

ELETROBRÁS/DNAEE. 1997. Manual de Inventário Hidrelétrico de Bacias Hidrográficas. Brasília.

Fearnside, P. M. 2001. Environmental impacts of Brazil's Tucuruı´ Dam: Unlearned lessons for hydroelectric development in Amazonia. Environ. Manage. 27:377–396.

Feilich, K. L. 2016. Correlated evolution of body and fin morphology in the cichlid fishes. Evolution (N. Y). 70:2247–2267.

Foote, M. 1997. The evolution of morphological diversity. Annu. Rev. Ecol. Syst. 28:129–152.

Gilbert, M. C., A. Akama, C. Cox, and R. C. Albertson. 2020. Rapid morphological change in multiple cichlid ecotypes following the damming of a major clearwater river in Brazil. 2754–2771.

Gilbert, M. C., A. J. Conith, C. S. Lerose, J. K. Moyer, S. H. Huskey, and R. C. Albertson. 2021. Extreme Morphology, Functional Trade-Offs, and Evolutionary Dynamics in a Clade of Open-Ocean Fishes (Perciformes: Bramidae). Integr. Org. Biol. 3:obab003.

Goodall, C. 1991. Procrustes methods in the statistical analysis of shape. J. R. Stat. Soc. 53:285–339.

Hallgrimsson, B., H. Jamniczky, N. M. Young, C. Rolian, T. E. Parsons, J. C. Boughner, and R. S. Marcucio. 2009. Deciphering the palimpsest: Studying the relationship between morphological integration and phenotypic covariation. Evol. Biol. 36:355–376.

Helfman, G. 2007. Fish Conservation: A guide to understanding and restoring global aquatic biodiversity and fishery resources. Island Press, Washington, D.C.

Jacob, F. 1977. Evolution and tinkering. Science. 196:1161–1166.

Klingenberg, C. P. 2008. Morphological Integration and Developmental Modularity. Annu. Rev. Ecol. Evol. Syst. 39:115–132.

Kuratani, S. 2009. Modularity, comparative embryology and evo-devo: Developmental dissection of evolving body plans. Dev. Biol. 332:61–69. Elsevier Inc.

Larouche, O., M. L. Zelditch, and R. Cloutier. 2018. Modularity promotes morphological divergence in Lau, J. K., T. E. Lauer, and M. L. Weinman. 2006. Impacts of channelization of stream habitats and associated fish assemblages in east central Indiana. Am. Midl. Nat. 156:319–330.ray-finned fishes. Sci. Rep. 8:1–6. Springer US.

Lema, S. C., and G. a Nevitt. 2006. Testing an ecophysiological mechanism of morphological plasticity in pupfish and its relevance to conservation efforts for endangered Devils Hole pupfish. J. Exp. Biol. 209:3499–509.

López-Fernández, H., K. O. Winemiller, C. Montaña, and R. L. Honeycutt. 2012. Diet-morphology correlations in the radiation of south American geophagine cichlids (Perciformes: Cichlidae: Cichlinae). PLoS One 7.

López-Fernández, H., J. H. Arbour, K. O. Winemiller, and R. L. Honeycutt. 2013. Testing for ancient adaptive radiations in neotropical cichlid fishes. Evolution (N. Y). 67:1321–1337.

Mcgee, M. D., B. C. Faircloth, S. R. Borstein, J. Zheng, C. D. Hulsey, P. C. Wainwright,

M. E. Alfaro, W. Pc, and A. M. E. Replicated. 2016. Replicated divergence in cichlid radiations mirrors a major vertebrate innovation. 1–6.

McGhee, G. R. 2007. The geometry of evolution: Adaptive landscapes and theoretical morphospaces. Cambridge University Press, Cambridge.

Moczek, A. P. 2008. On the origins of novelty in development and evolution. BioEssays 30:432–447.

Muschick, M., M. Barluenga, W. Salzburger, and A. Meyer. 2011. Adaptive phenotypic plasticity in the Midas cichlid fish pharyngeal jaw and its relevance in adaptive radiation. BMC Evol. Biol. 11:116. BioMed Central Ltd.

Muschick, M., A. Indermaur, and W. Salzburger. 2012. Convergent Evolution within an Adaptive Radiation of Cichlid Fishes. Curr. Biol. 22:2362–2368. Elsevier Ltd.

Navon, D., I. Male, E. R. Tetrault, B. Aaronson, R. O. Karlstrom, and R. Craig Albertson. 2020. Hedgehog signaling is necessary and sufficient to mediate craniofacial plasticity in teleosts. Proc. Natl. Acad. Sci. U. S. A. 117:19321–19327.

Niwa, N., A. Akimoto-Kato, T. Niimi, K. Tojo, R. Machida, and S. Hayashi. 2010. Evolutionary origin of the insect wing via integration of two developmental modules. Evol. Dev. 12:168–176.

Olsen, A., and M. Westneat. 2015. StereoMorph: an R package for the collection of 3D landmarks and curves using a stereo camera set-up. Methods Ecol. Evol. 6:351–356.

Powder, K. E., and R. C. Albertson. 2016. Cichlid fishes as a model to understand normal and clinical craniofacial variation. Dev. Biol. 415:338–346.

Price, T. D., A. Qvarnström, and D. E. Irwin. 2003. The role of phenotypic plasticity in driving genetic evolution. Proc. R. Soc. B Biol. Sci. 270:1433–1440.

Prum, R. O. 2005. Evolution of the morphological innovations of feathers. J. Exp. Zool. Part B Mol. Dev. Evol. 304:570–579.

R Core Team. 2018. R: A language and environment for statistical computing. R Foundation for Statistical Computing, Vienna, Austria.

Rohlf, F. J., and M. Corti. 2000. Use of two-block partial least-squares to study covariation in shape. Syst. Biol. 49:740–753.

Schluter, D. 1996. Adaptive radiation along genetic lines of least resistance. Evolution (N. Y). 50:1766.

Sheftel, H., O. Shoval, A. Mayo, and U. Alon. 2013. The geometry of the Pareto front in biological phenotype space. 1471–1483.

Trautman, M. 1939. The Effects of man-made modifications on the fish fauna in Lost and Gordon Creeks, Ohio , between 1887-1938. Ohio J. Sci. 39:275–288.

Turner, G. F. 2007. Adaptive radiation of cichlid fish. Curr. Biol. 17:827–831.

Van Wassenbergh, S., N. Z. Potes, and D. Adriaens. 2015. Hydrodynamic drag constrains head enlargement for mouthbrooding in cichlids. J. R. Soc. Interface 12.

Wagner, G. P., and B. Y. Misof. 1993. How can a character be developmentally constrained despite variation in developmental pathways? J. Evol. Biol. 6:449–455.

Wagner, G. P., M. Pavlicev, and J. M. Cheverud. 2007. The road to modularity. Nat. Rev. Genet. 8:921–931.

Weller, H. I., C. D. Mcmahan, and M. W. Westneat. 2017. Dirt-sifting devilfish: winnowing in the geophagine cichlid Satanoperca daemon and evolutionary implications. Zoomorphology 136:45–59. Springer Berlin Heidelberg.

Weller, H., H. López-Fernández, C. D. McMahan, and E. L. Brainerd. 2022. Relaxed

feeding constraints facilitate the evolution of mouthbrooding in Neotropical cichlids. Am. Nat. 199.

West-Eberhard, M. J. 2003. Developmental Plasticity and Evolution. Oxford University Press, New York, NY.

West-Eberhard, M. J. 2005. Developmental plasticity and the origin of species differences. Proc. Natl. Acad. Sci. U. S. A. 102:6543–6549.

West-Eberhard, M. J. 1989. Phenotypic plasticity and the origins of diversity. Annu. Rev. Ecol. Syst. 20:249–278.

Wimberger, P. H. 1993. Effects of Vitamin C Deficiency on Body Shape and Skull Osteology in Geophagus brasiliensis: Implications for Interpretations of Morphological Plasticity Author(s): Peter H. Wimberger Published by: American Society of Ichthyologists and Herpetologis. Copeia 1993:343–351.

Wimberger, P. H. 1992. Plasticity of fish body shape. The effects of diet, development, family, and age in two species of Geophagus (Pisces: Cichlidae). Biol. J. Linn. Soc. 45:197–218.

Wimberger, P. H. 1991. Plasticity of jaw and skull morphology in the neotropical cichlids Geophagus brasiliensis and Geophagus steindachneri. Evolution (N. Y). 45:1545–1563.

Wund, M. A., J. A. Baker, B. Clancy, J. L. Golub, and S. A. Foster. 2008. A test of the "flexible stem" model of evolution: Ancestral plasticity, genetic accommodation, and morphological divergence in the threespine stickleback radiation. Am. Nat. 172:449–462.

Zelditch, M. L., and A. Goswami. 2021. What does modularity mean? Evol. Dev. 23:377–403

5. CHAPTER 5

EXTREME MORPHOLOGY, FUNCTIONAL TRADE-OFFS, AND EVOLUTIONARY DYNAMICS IN A CLADE OF OPEN-OCEAN FISHES (PERCIFORMES: BRAMIDAE)

Michelle C. Gilbert[1], Andrew J. Conith[2], Catherine S. Lerose[2], Joshua K. Moyer[1], Steve H. Huskey[3], R. Craig Albertson[2]

1 Organismic and Evolutionary Biology Graduate Program, University of Massachusetts, Amherst, MA 01003
2 Biology Department, Morrill Science Center, University of Massachusetts, 611 North Pleasant Street, Amherst, MA 01003
3 Biology Department, Western Kentucky University, 1906 College Heights Boulevard, Bowling Green, KY 42101

PUBLISHED IN: Integrative Organismal Biology

FULL CITATION: M Gilbert, AJ Conith, CS Lerose, JK Moyer, SH Huskey, RC Albertson. 2021. Extreme morphology, functional trade-offs, and evolutionary dynamics in a clade of open-ocean fishes (Perciformes: Bramidae). *Integrative Organismic Biology.* 3: obab003

Abstract

When novel or extreme morphologies arise, they are oft met with the burden of functional trade-offs in other aspects of anatomy, which may limit phenotypic diversification and make particular adaptive peaks inaccessible. Bramids (Perciformes: Bramidae) comprise a small family of 20 extant species of fishes, which are distributed throughout pelagic waters worldwide. Within the Bramidae, the fanfishes (*Pteraclis* and *Pterycombus*) differ morphologically from the generally stout, laterally compressed species that typify the family. Instead, *Pteraclis* and *Pterycombus* exhibit extreme anterior positioning of the dorsal fin onto the craniofacial skeleton. Consequently, they possess fin and skull anatomies that are radically different from other bramid species. Here, we investigate the anatomy, development, and evolution of the Bramidae to test the hypothesis that morphological innovations come at functional (proximate) and evolutionary (ultimate) costs. Addressing proximate effects, we find that the development of an exaggerated dorsal fin is associated with neurocrania modified to accommodate an anterior expansion of the dorsal fin. This occurs via reduced development of the supraoccipital crest (SOC), providing a broad surface area on the skull for insertion of the dorsal fin musculature. While these anatomical shifts are presumably associated with enhanced maneuverability in fanfishes, they are also predicted to result in compromised suction feeding, possibly limiting the mechanisms of feeding in this group. Phylogenetic analyses suggest craniofacial and fin morphologies of fanfishes evolved rapidly and are evolutionarily correlated across bramids. Furthermore, fanfishes exhibit a similar rate of lineage diversification as the rest of the Bramidae, lending little support for the prediction

that exaggerated medial fins are associated with phylogenetic constraint. Our phylogeny places fanfishes at the base of the Bramidae and suggests that non-fanfish bramids have reduced medial fins and re-evolved SOCs. These observations suggest that the evolution of novel fin morphologies in basal species has led to the phylogenetic coupling of head and fin shape, possibly predisposing the entire family to a limited range of feeding. Thus, the evolution of extreme morphologies may have carry-over effects, even after the morphology is lost, limiting ecological diversification of lineages.

Introduction

When a novel trait is manifested, it not only must work in the confines of previous constraints (historical contingency), but it also introduces new constraints to the system (Jacob 1977), which can limit evolutionary trajectories by restricting the number of adaptive peaks that can be reached by a lineage (Wright 1932; Arnold 1992; Schluter 1996). Darwin (1859) acknowledged the impact evolutionary histories and developmental processes have on evolutionary trajectories, noting that an interplay of the two results in a "unity of type." Given that organisms use morphological structures to complete numerous ecologically relevant tasks (e.g. feeding, locomotion, reproduction, etc.), and no single phenotype enables optimal performance in all tasks, a structural dilemma exists, forcing evolutionary trajectories to optimize phenotypes via compromise (Arnold 1983). Pareto optimality theory, historically used in the fields of engineering and economics, suggests that a multidimensional phenotype cannot be improved for all tasks at once (McGhee 2007; Kennedy 2010; Shoval et al. 2012) and has been increasingly used in biology to explain evolutionary constraints that limit phenotypic evolution (Farnsworth and Niklast 1995; Sheftel et al. 2013; Tendler et al. 2015). To understand the current and future

evolutionary and phenotypic trajectories of a species, one must consider the trade-offs that have deflected past trajectories to produce the observed phenotype.

Phenotypic trade-offs have been a core component of evolutionary biology for decades (Charnov 1989; Stearns 1989; Leroi et al. 1994; Brodie III and Brodie Jr 1999; Patek and Oakley 2003; Roff and Fairbairn 2007). Specialization and the consequential performance/functional trade-off(s), have been documented across numerous taxa (Toro et al. 2004; Langerhans et al. 2005; Herrel et al. 2009; Herrel and Bonneaud 2012; Holzman et al. 2012; Pelegrin et al. 2017), and, at times, can appear inconspicuous. However, when morphological traits are exaggerated the demand on the system as a whole is greater, forcing trade-offs to be more substantial. Such is the case for *Tropidurus* lizards in Northeastern Brazil, where specialized rock-dwelling ecomorphs are dorsoventrally flattened to aid in traversing narrow rocky crevasses, but suffer from a 66% loss in overall egg capacity (Pelegrin et al. 2017). In the carabid beetle, *Damaster blaptoides*, two diametrically distinct head morphologies are observed, depending on the shell size of resident snails. Konuma and Chiba (2007) report that beetle populations with small heads are able to consume snail prey directly by reaching into the aperture, but this forces the size of mandibles and associated muscles to be significantly reduced. In bony fishes, one would expect extreme jaw protrusion to lead to greater suction feeding capabilities. However, the mechanism of extreme premaxillary protrusion in two cichlid species significantly decreases suction feeding performance and, instead, appears to be an adaptation that optimizes ram feeding on elusive prey (Waltzek and Wainwright 2003). While there are numerous studies that aim to address proximate (e.g., functional, biomechanical) or ultimate (e.g., evolutionary constraints) consequences of such trade-

offs, few are able to connect the two due to the difficulty in resolving long-term evolutionary history with contemporary functional studies. Here, we seek to test the hypothesis that extreme morphological traits result in, not only functional trade-offs, but also long-term evolutionary trade-offs (as constraints). To investigate this, we explore the development, anatomy, and phylogenetic relationships of a unique clade of fishes in the family Bramidae, the fanfishes.

Bramids (Perciformes: Bramidae) are a small family of fishes, comprised of 20 extant species across seven genera. Nearly all bramids are known, or thought, to be migratory, traversing the high seas seasonally for food and reproduction (Mead 1972). Despite this, and having representatives in every major ocean (Mead 1972), they remain uncommon and, in some taxa, quite rare. Much of the contemporary work concerning bramids is isolated to sightings and bycatches that provide new information on their distribution (Gutiérrez et al. 2005; Park et al. 2007; Carvalho-filho et al. 2009; Ali and McNoon 2010; González-lorenzo et al. 2013; Jawad et al. 2014; Lee and Kim 2015; Orr et al. 2018; Lee et al. 2019; Rahangdale et al. 2019), insights to their ecology (Lobo and Erzini 2001; Moteki et al. 2001; Carvalho-filho et al. 2009), and opportunities to obtain mitochondrial sequence data (Chen et al. 2016; Liu et al. 2016; Xu et al. 2018). Within the family, two sister genera, *Pterycombus* and *Pteraclis* (commonly known as fanfishes), stand as outliers, deviating from the generally stout, laterally compressed morphologies that typify the family. Instead, these two genera are characterized by relatively elongate bodies and extreme anterior extensions of dorsal and anal fins, extending well onto the neurocranium and even beyond the orbit in some species. Work detailing the anatomy and evolutionary interrelationships of the family are scarce or limited to a select few taxa

and it is unknown how the exaggeration of the dorsal fin has influenced, if at all, the neurocranium. Mead echoed this in his 1972 monograph, stating "The phyletic unity of these six remains in doubt and this question, together with that of the origin of the group, deserves further study," referring to the six genera that were known at the time, as *Xenobrama* went undescribed until 1989 (Yatsu and Nakamura 1989).

The goal of the present study was to identify possible functional and/or biomechanical trade-offs associated with extreme, morphological adaptations, determine if there are regions of bramid morphology that have been constrained through carry over effects from their evolutionary history, and assess how early during ontogeny these differences are detectable. The unique anatomy of the fanfishes offer an opportunity to investigate how extreme morphologies can not only impose proximate trade-offs in functional morphology, but also constrain evolution and levy evolutionary trade-offs. To this end, we wanted to understand if the extreme dorsal fin morphology in fanfishes has influenced the evolutionary trajectory of the family by introducing phenotypic constraints that deflected historical trajectories or limited diversification.

Methods

Phylogenetic Tree Construction

We utilized the mitochondrial genes for cytochrome oxidase subunit 1 (COI) and Cytochrome B (cytb) retrieved from GenBank (Benson et al. 2013) in keeping with the methods of recent studies of mitochondrial sequence data across the family Bramidae (Chen et al. 2016; Liu et al. 2016; Xu et al. 2018). Accession numbers for all gene data are provided in Supplemental Table 1. Both COI (length ~ 640bp) and cytb (length ~ 1141 bp) were aligned using the AliView v1.25 alignment viewer and editor (Larsson 2014). We constructed a Bayesian, time-calibrated tree of all available bramid taxa listed

on GenBank, encompassing 14/20 known species (n = 43), including a representative of the closely related family Caristiidae (*Caristius macropus*, n = 1), and three representative species from the family Stromateidae (*Peprilus paru*, n = 1; *Peprilus simillimus*, n = 3; *Peprilus triacanthus*, n = 6) as an outgroup.

To conduct a Bayesian, time-calibrated analysis of the Bramidae we constructed an XML input file for BEAST using the BEAUTi v.2.5.1 application (Bouckaert et al. 2014). We used the bModelTest v.1.1.2 application to estimate substitution models for these mitochondrial genes. We selected the default transition-transversion split option, which allows BEAST to average out uncertainty in substitution model selection during the Markov chain Monte Carlo (MCMC) run (Bouckaert and Drummond 2017). Based on AICc fit, bModelTest selected different substitution models for each codon partition. Codon positions for each gene, following gene alignment, are as follows: COI position 1: 121131; COI position 2: 121321; COI position 3: 121134; cytb position 1: 123421; cytb position 2: 123343; cytb position 3: 121123.

We used a log-normal distributed relaxed molecular clock for divergence time estimation and assigned a pure-birth (Yule) model as the branching process. All other parameters we left at their default settings. To estimate divergence times we used a series of fossil calibrations outlined by (Miya et al. 2013). We set the split between Caristiidae and Bramidae (log normal distribution; offset = 56.0, mean = 1, lower = 0.0, upper = 0.72) at 56mya (Bannikov and Tyler 1994; Fierstine et al. 2012), crown Bramidae (log normal distribution; offset = 49.11, mean = 1, lower = 0.0, upper = 2.0) at 49.11mya (Casier 1966; Ellison et al. 1994; Baciu and Bannikov 2003), and crown Stromateidae (log normal distribution; offset = 31.35, mean = 1, lower = 0.0, upper = 5.0) at 31.35mya

(Lenov 1998; Bannikov 2012). Finally, we performed four independent runs for $2x10^7$ generations sampling every 1000 generations using the BEAST v.2.5.1 module (Bouckaert et al. 2014) on the CIPRES Science Gateway v3.3 computing cluster (Miller et al. 2010).

We used Tracer v1.7.1 (Rambaut et al. 2018) to test for convergence of our four runs, and used effective sample size (ESS) to check the true posterior and likelihood distributions. We removed 20% for burn in using Log Combiner v2.5.1 and the maximum clade credibility tree (MCCT) was created using TreeAnnotator v2.5.1 (Drummond et al. 2006).

Morphometric Data Collection

Given the difficulty of acquiring bramid specimens, and the rarity of the fanfishes in general, we utilized the collection of the Museum of Comparative Zoology (MCZ) at Harvard University (Cambridge, MA USA) to obtain representative specimens of the family Bramidae. A single *Eumegistus illustris* was obtained from the Smithsonian National Museum of Natural History (Washington DC, USA), and two specimens of *Pteraclis aesticola* were obtained from the Australian Museum of Natural History (Darlinghurst, Australia). A single intact *Pterycombus petersii* specimen was collected when it was regurgitated by a yellowfin tuna (*Thunnus albacares*) off the coast of Hawaii (see Acknowledgements). The combination of the previous factors limits one's ability to conduct proper kinematic studies. Therefore, we focus on aspects of functional morphology in our questions and interpretations. Details on all lots, adult and juvenile, can be found in Supplemental Table 2. As they were not the focus of this study, we did not collect morphometric data concerning Stromateidae.

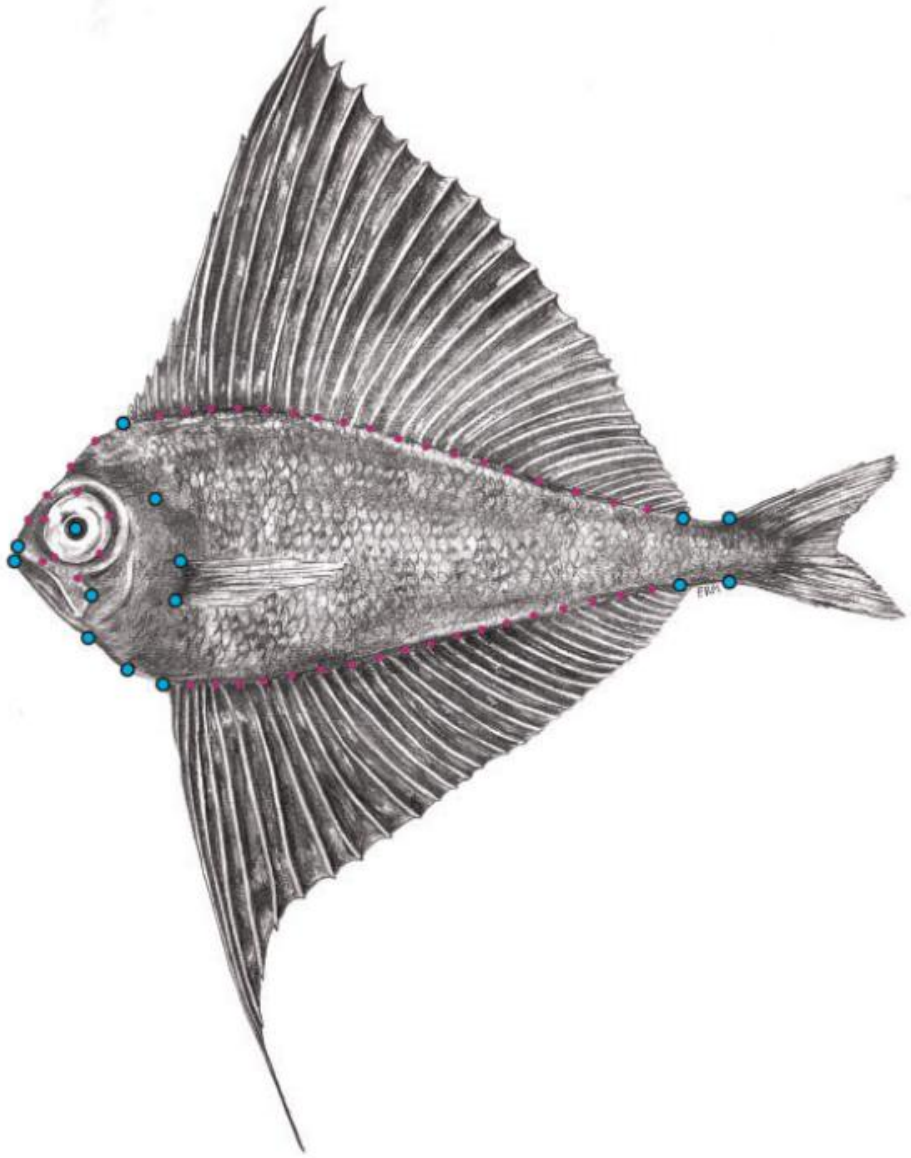

Figure 5.1. Illustration of a fresh *Pterycombus petersii* specimen with the landmark configuration used in this study. In total, we used 62 landmarks, 15 of which were fixed (cyan), the remaining 47 being semi-(sliding)-landmarks (magenta). Fixed landmarks are placed on the: tip of premaxilla, dorsal fin insertions (nape being listed here as the region between tip of premaxilla and dorsal fin insertion), dorsal- and ventral-most point where the caudal peduncle meets the caudal fin, anal fin insertions, pelvic fin insertion, anterior margin of breast (breast is defined as the margin of opercle to pelvic fin insertion), dorsal and ventral pectoral fin insertion, dorsal end of the opercular opening, anterior tip of the dentary, posterior tip of maxilla, and center of the eye. Illustration hand drawn by Emma R. Masse.

We photographed the left-lateral surface of museum specimens, with the exception of two adult *Pteraclis aesticola* and a single *Eumegistus illustris*, for which

photographs were obtained through web portals. All available adults and a number of juveniles representing the available genera were utilized (Supplemental Table 2).

Our morphological landmark configuration (Figure 1) consisted of 15 fixed anatomical landmarks and 47 sliding semi-landmarks and were subjected to generalized Procrustes analysis (Goodall 1991) utilizing bending energy. These data were later parsed into two separate configurations: head and body shape. Our configuration for body shape is largely driven by body depth, length, and fin length, with dorsal and anal fin base length being the primary trait of interest. Head shape configuration was largely driven by nape size, maxilla length and angle, and eye placement. All coordinate data were collected via `STEREOMORPH` (Olsen and Westneat 2015) in R (R Core Team 2018).

Additionally, we collected linear measures of all genera that had 3 or more specimens, focusing specifically on lower jaw (the tip of the dentary to the mandible quadrate joint) and head length (tip of snout to the furthest posterior margin of the operculum). These data were collected from digital photographs using the software package MorphoJ (Klingenberg 2011). We then regressed lower jaw length against head length to look for differences across the Bramidae. These data were log transformed and plotted twice, once to evaluate the family as a whole and once to calculate regression lines for each of the four genera.

Phylogenetic Comparative Methods

The MCCT was pruned of all bramid taxa for which we did not have both morphometric and phylogenetic information (n = 2, *Xenobrama microlepis* and *Brama australis*), leaving 12 bramid taxa and a single representative of Caristiidae, *Caristius sp*. Since we did not have phylogenetic data for *C. macropus*, we matched those data with

morphological data from the only congener we could acquire, *C. fasciatus.* This pruned topology provided the framework for all subsequent comparative analyses.

Using `GEOMORPH` v3.0.6 (Adams et al. 2014, 2018) and `PHYTOOLS` (Revell 2012), the consensus tree and morphometric data were used to generate a phylomorphospace that mapped principal component data for morphology with the phylogenetic relationships intertwined. We used the combination of `two.b.pls` and `phylo.integration` (Rohlf and Corti 2000; Adams and Felice 2014; Collyer et al. 2015; Adams and Collyer 2016, 2018) functions in `GEOMORPH` to assess the association between the head and body configurations. The functions use partial least squares to estimate the degree of covariation between our two variables while the latter does so while also accounting for the phylogeny under a Brownian motion model of evolution. We used two approaches to characterize the Brownian rate of morphological evolution in the Bramidae. First, we used the `compare.evol.rates` function in `GEOMORPH` to assess the rate of morphological evolution between the bramids and fanfish clades. Second, we used the `compare.multi.evol.rates` function in `GEOMORPH` to assess rates of morphological evolution in the head and body configurations independently (Denton and Adams 2015). Both these methods estimate phylogenetically corrected rates based on a distance approach for high-dimensional data sets such as shape (Adams 2014).

We calculated the mean PC1 and PC2 scores for head and body shape across each taxon and then determined rates of trait evolution across the phylogeny. To accomplish this, we utilized routines contained within the BAMM (Bayesian analysis of macroevolutionary mixtures) software package (Rabosky et al. 2013; Rabosky 2014).

BAMM analysis was executed with four reversible jump MCMC simulations for $1x10^7$ generations, sampling every 1,000 generations. Our prior distributions were estimated via `BAMMtools` (Rabosky et al. 2014) in R (R Core Team 2018). This was repeated for PC1 and PC2 means for head (βIntPrior: 317.220 & 2103.425; βShiftPrior: 0.023 & 0.023) and body (βIntPrior: 510.455 & 2410.561; βShiftPrior: 0.023 & 0.023) shape for the entire phylogeny. BAMM output files were then also analyzed with `BAMMtools` (Rabosky et al. 2014).

To investigate further the diversification dynamics of the family Bramidae, we used the gamma (γ) summary statistic to characterize lineage diversification through time (Pybus and Harvey 2000) using the full phylogeny. Given incomplete taxon sampling (six missing taxa; *Brama caribbea*, *B. myersi*, *B. pauciradiata*, *Eumegistus brevorti*, *Pteraclis carolinus*, and *P. velifera*), we assessed γ using the Monte Carlo constant-rates (MCCR) test. This test uses our bramid data to simulate 5000 phylogenies under a constant-rate pure-birth diversification model (the null), before randomly pruning taxa from the simulated trees to mimic incomplete sampling and derive a null distribution of γ statistics. The MCCR test then compares the empirical γ value to the simulated distribution to generate a p-value.

We then compared the fit of four different diversification models to our tree. We assessed two rate-constant models, pure-birth (Yule) and constant-rate birth-death, and two rate-variable models, variable-rate logistic density dependent (DDL) and a variable-rate exponential density dependent (DDX) model of lineage diversification (Rabosky and Lovette 2008). These analyses use Birth-Death likelihoods, which offer an advantage over the γ-statistic alone when background extinction rates are non-zero (Rabosky 2006).

Models were statistically evaluated with the Akaike Information Criterion (AIC). To visually reflect these patterns, we constructed a lineage-through-time (LTT) plot from the MCCT.

We then explicitly tested for differences in the rate of lineage diversification between fanfish and the remaining bramids. We scored the presence or absence of elongated fin morphology as binary characters and estimated state-specific speciation and extinction rates in a Bayesian framework (Fitzjohn 2012). Specifically, we assessed the diversification rate in each group using the binary state speciation and extinction (BiSSE) model from the R package `diversitree` (v.0.9-14). We set exponential priors for each parameter in BiSSe with rate 1/(2r), where r is the trait-independent diversification rate. Maximum likelihood-estimated model parameters served as a starting point. Markov chain Monte Carlo (MCMC) chains were run for 5000 generations, and we discarded the initial 10% as burn-in. To account for incomplete taxon sampling, we used the sampling fraction procedure, which requires the specification of the number of taxa present in each grouping out of the total number of described species in that group (elongated fins absent = 0.73, elongated fins present = 0.6).

Bramid Ontogeny

To determine ontogenetic differences in shape, we used geometric morphometrics to quantify and determine phenotypic trajectories (Collyer and Adams 2013; Collyer et al. 2015). Ontogenetic trajectories can provide valuable insights into the developmental mechanisms and processes that facilitate phenotypic evolution. Specifically, our aim was to determine how early morphological difference arose across the family Bramidae. We assessed two stages of development across four of the seven bramid genera (excluding

Eumegistus, *Xenobrama*¸ and *Pteraclis* due to extreme difficulty in acquiring juvenile and adult specimens) and a very limited sample of *Caristius fasciatus* for outgroup comparisons. We digitized individuals in both developmental stages following the same landmarking scheme as the adults (see Figure 1). Phenotypic trajectories were evaluated via `trajectory.analysis` (Collyer and Adams 2013; Collyer et al. 2015) in `GEOMORPH`. This function evaluates phenotypic trajectories through the use of ANOVA and a RRPP (Collyer and Adams 2018), calculating differences in trajectory path and magnitude. In our model `(Shape ~ Genus * Stage, ~ Centroid Size)`, we included size as a covariate and deemed it to be an outside source of shape variation. These outside sources of variation are accounted for prior to the trajectory defining variables of genera and developmental stage. Using the results from a principal component analysis (PCA), we mapped ontogenetic trajectories into morphospace using the first two principal components.

In addition to geometric morphometrics, *Pterycombus brama* and *Brama dussumieri* larvae were cleared and stained across early and late juvenile stages to identify anatomical differences. Images were captured with both LED backlights and, to take advantage of the fluorescent properties of alizarin, under fluorescent light with a Red Fluorescent Protein (RFP) filter. By using fluorescent lighting and an RFP filter, we were better able to isolate the ossified elements in the craniofacial skeleton and identify anatomical elements of interest.

Craniofacial Anatomy

Because ecological, functional, and behavioral data are limited, we chose to investigate the osteology and myology of the rare *Pterycombus petersii* (see

Acknowledgements) to glean insights into the functional and ecological properties of the genus and, ideally, family. To accomplish this, we used a combination of X-ray micro-computer tomography (μCT) and gross anatomization. We used a Bruker Skyscan 1276 μCT (Bruker microCT, Kontich, Belgium) at the University of Massachusetts Animal Imaging Core (Amherst, MA) to collect high-resolution scans of *P. petersii*. We scanned at 20μm resolution with a 0.25mm aluminum filter. Reconstruction was accomplished with the use of InstaRecon CBR (Bruker, Kontich, Belgium). Z-stack images were oriented and cropped with IrfanView v4.54 (Irfan Skiljan), skeletal anatomy was segmented using Mimics v19 (Materialise NV, Belgium). We then exported mesh models to Geomagic 2014 v1.0 (3D Systems, Rock Hill, SC, USA) to remove noise, and ultimately visualized using MeshLab 2016 (Cignoni et al. 2008).

To better visualize osteological elements and associated muscles, we double stained an intact *Pterycombus petersii* specimen in alcian and alizarin. The alizarin stain was dissolved in a 75% ethanol solution, rather than the typical 0.25-1% potassium hydroxide to preserve muscle integrity, color, and form, specifically to visualize epaxial and dorsal fin musculature attachment points on the neurocranium. Enough alizarin was added to the ethanol solution to turn it a modest orange color. The specimen was stained overnight and rinsed in 95% ethanol the following morning until the solution remained clear. Pigment bleaching and clearing phases were skipped altogether and the specimen was stored in 75% ethanol. We then performed careful dissections across the specimen to identify skeletal elements and muscles of interest, especially those involved in dorsal fin adduction and abduction and muscles associated with feeding [e.g., adductor mandibulae, dilatator opercula, levator arcus palatini (Gosline 1971; Liem and Osse 1975; Westneat

2004; Datovo and Vari 2013)]. Images were recorded using a Leica M165 FC microscope and attached Leica DFC450 camera (Leica Camera AG, Wetzlar, Germany). Post-processing (manipulation of contrast, brightness, and focus image stacking) of all images was conducted in Adobe Photoshop CC 2019 (Adobe Systems, San Jose, CA, USA).

Results

Bramid Phylogeny

To assess the extent to which extreme morphologies have imposed evolutionary constraints in bramids, we first sought to reconstruct the ancestral state in the family. We find that the relationships and divergence times of the bramids included in this study (Figure 2A; Supplemental Figure 1) are congruent with previously published trees (Miya et al. 2013; Chen et al. 2016; Friedman et al. 2019). Nodes are generally well-supported with high posterior probabilities (%PP), especially those associated with genus level relationships (%PP = > 95%). Posterior support between the *Brama* & *Xenobrama* clade and *Taractes* & *Tarachtichthys* clade was lower (%PP = 77%). Support for *Eumegistus* belonging to the *Taractes* clade, as opposed to *Tarachtichthys* was low (%PP = 49%), but support for a *Taractes*, *Tarachtichthys*, *Eumegistus* clade was high (%PP > 95%). *Pteraclis* and *Pterycombus* expressed high posterior support for being part of a single clade (%PP > 95%) and were revealed to be the oldest bramid lineage (%PP > 95%).

Results from the MCCR test suggest diversification rates across the Bramidae have declined through time. The γ test statistic for the MCC tree (-2.38) quantitatively demonstrates significant declines in diversification rates (P = 0.009), and appears robust to missing taxa (γ crit. = -1.92; P = 0.018). The lineage through time (LTT) plot visually

illustrates a rapid increase in lineages early in the clade's history relative to the expectation under a constant-rate pure-birth model (Figure 2B).

We found strong support for a density-dependent pattern of diversification in bramids (Table 1). Specifically, the density-dependent logistic (DDL) model best-fit the pattern of bramid lineage accumulation through time. Competing diversification models were more than four ΔAICc units away. Diversification rate parameter estimates for the

Table 5.1. Diversification models are ranked from best to worst based on AIC weights (wtAIC).

Model	LH	AIC	ΔAIC	wtAIC
DDL	26.56569	57.131	0	0.883
DDX	28.93567	61.871	4.74	0.083
Pure-birth	31.13453	64.269	7.138	0.025
Birth-death	31.13453	66.269	9.138	0.009

Note i: Model comparison demonstrates high support for density-dependent clade growth using a logistic model (DDL). Log likelihood (LH) is also provided for each model, as is the AIC score (AIC), and change in AIC score (DAIC).

DDL model [λ_0 (initial rate) = 0.13, *K* (carrying capacity) = 13.78] suggest an initial burst of diversification followed by a linear decline in speciation rate. Lastly, we found no evidence for differences in state specific diversification rates; both the fanfish and the remaining bramids exhibit similar rates of lineage diversification (Figure 2C; Table S3). These data demonstrate that fanfishes represent the ancestral state, with exaggerated medial fins and laterally compressed body shape morphologies.

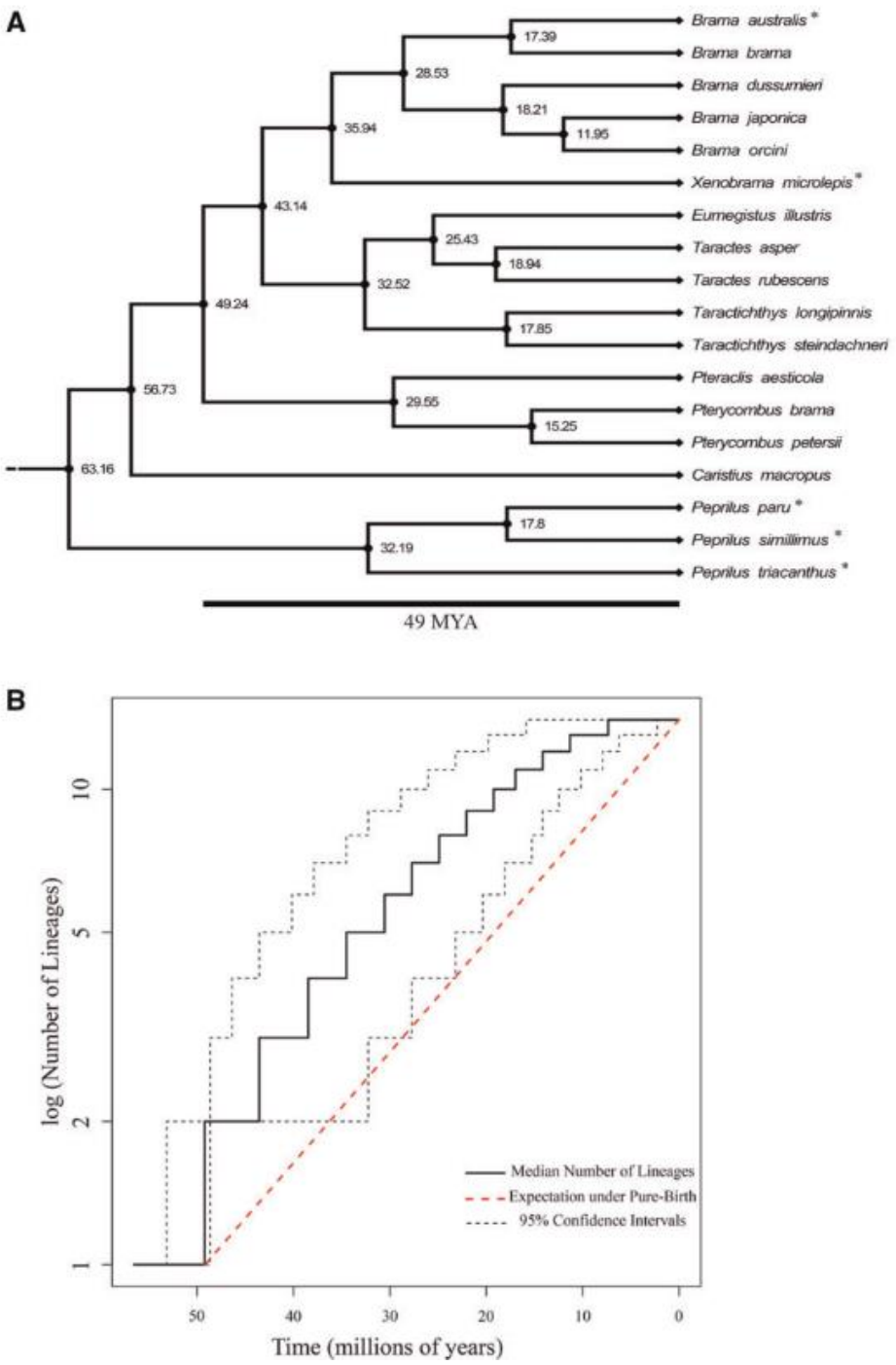

Figure 5.2. (a) Trimmed tree with all bramids with genetic data, including a representative of Caristiidae. Butterfishes (Stromateidae) were used as a reliable outgroup. Asterisks indicate species that were removed from all morphometric analyses due to either genetic or morphological data being unavailable. Values indicate divergence times (mya). (B) Log LTT plot for the Bramidae only, excluding the stromateids and caristiids. Solid black line indicates median lineage though time curve for the consensus tree, and black-dashed lines illustrate 95% confidence intervals of lineages through time derived from a posterior distribution of 1000 phylogenetic trees. Red- dashed line depicts rate of lineage accumulation expected under constant-rate pure-birth diversification (i.e., no extinction). Bramid lineages accumulate quickly relative to a pure-birth model, before hitting a plateau as diversification slows.

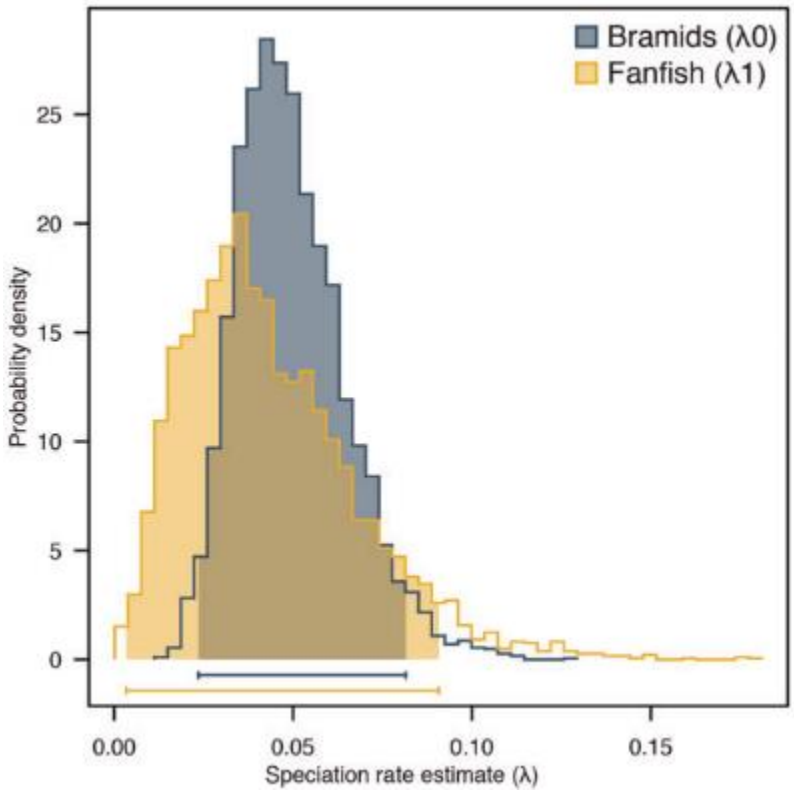

Figure 5.3. State-specific diversification rates between fanfishes and the remaining bramid genera. Both fanfishes and their bramid relatives exhibit substantial overlap in their speciation rate estimate distributions, suggesting similar rates of lineage diversification.

Fanfishes Deviate from Common Bramid Morphospace

We next sought to more formally characterize patterns of morphological divergence across bramids. To this end, we conducted a Procrustes ANOVA to determine the effects of size and species across the available species. Both size and species had significant effects on shape ($P < 0.0001$). Species effects explained a greater proportion of the morphological variance ($R^2 = 0.67$) than did size alone ($R^2 = 0.21$) and much more than the interaction of size and species (`Shape ~ size * species`; $R^2 = 0.02$). Subsequent pairwise comparisons revealed significant differences between nearly all fanfish comparisons with the other bramid taxa, and such comparisons always resulted in the greatest effect sizes (z-scores; Table 2). *Pterycombus brama* possessed the least

number of significantly different comparisons of the fanfishes (only six out of 12 were significant), whereas *Pteraclis aesticola* and *Pterycombus petersii* expressed significantly different shapes in 11/12 and 10/12 comparisons, respectively. Those comparisons which were not significant were between fanfishes. Additionally, *Brama japonica* and *Taractes rubescens* also exhibited 7/12 significant pairwise comparisons.

Table 5.2. Results of Procrustes MANOVA across all available bramid species, including a single representative of Caristiidae (*Caristius fasciatus*).

	B. brama	*B. dussumieri*	*B. japonica*	*B. orcini*	*C. fasciatus*	*E. illustris*	*P. aesticola*	*P. brama*	*P. petersii*	*T. asper*	*T. rubescens*	*T. longipinnis*	*T. steindachneri*
B. brama		0.699	1.177	0.356	1.480	0.106	**7.050**	1.466	**3.138**	0.740	**1.839**	0.463	0.092
B. dussumieri	0.7477		0.943	1.408	1.351	0.747	**5.483**	1.293	**3.592**	0.647	0.003	0.289	0.344
B. japonica	0.9786	0.8628		0.519	**1.585**	0.011	**8.456**	**1.749**	**3.251**	1.273	**3.952**	**2.142**	**2.477**
B. orcini	0.5564	0.9971	0.6673		1.387	0.345	**6.204**	1.381	**2.968**	0.049	1.012	1.007	0.474
C. fasciatus	0.0577	0.0770	**0.0492**	0.0759		0.491	**4.109**	1.324	**2.619**	1.323	1.198	1.469	1.384
E. illustris	0.4094	0.7919	0.3431	0.5550	0.1917		**4.800**	1.523	**2.230**	0.715	0.468	0.615	0.231
P. aesticola	**0.0001**	**0.0003**	**0.0001**	**0.0001**	**0.0121**	**0.0027**		**1.808**	0.888	**7.781**	**8.906**	**8.548**	**9.032**
P. brama	0.0567	0.0783	**0.0400**	0.0733	0.0685	0.0657	**0.0473**		0.051	**2.236**	**2.966**	**1.965**	**2.186**
P. petersii	**0.0168**	**0.0051**	**0.0179**	**0.0211**	**0.0337**	**0.0438**	0.1421	0.3997		**3.398**	**3.567**	**3.975**	**3.601**
T. asper	0.1850	0.7140	0.1020	0.4139	0.0688	0.8350	**0.0001**	**0.0341**	**0.0123**		0.122	**2.380**	1.725
T. rubescens	**0.0544**	0.4207	**0.0013**	0.1331	0.0793	0.6744	**0.0001**	**0.0289**	**0.0091**	0.4641		**3.930**	**5.079**
T. longipinnis	0.2465	0.3070	**0.0349**	0.1261	0.0566	0.1294	**0.0001**	**0.0344**	**0.0068**	**0.0329**	**0.0031**		0.401
T. steindachneri	0.3596	0.5737	**0.0198**	0.2288	0.0606	0.2011	**0.0001**	**0.0326**	**0.0116**	0.0713	**0.0002**	0.5903	

Note ii: MANOVA was conducted with 10,000 permutations of residual values (Randomized Residual Permutation Procedure). Effect sizes are above and P values are below the diagonal. Bolded P values and z scores indicate significant differences in mean shapes between species. For the purpose of significance testing, $\alpha \leq 0.05$.

We next trimmed the MCCT to include only species for which we possessed both mitochondrial and morphological data (Figure 2A). The first two axes of our phylomorphospace, based on this tree, explained 62.9% and 19.6% of variation in our data, respectively (Figure 4). The first principal component (PC) (primarily representing dorsal and anal fin insertion and length, and the size of the nape, or region prior to dorsal fin insertion) completely isolated the fanfishes (*Pteraclis aesticola*, *Pterycombus brama*, *Pterycombus petersii*) from all other bramids, largely attributed to their unique dorsal and

anal fin morphology. On this axis, the fanfishes possessed positive scores, while the other bramids possessed largely negative scores. The second PC axis primarily explained nape

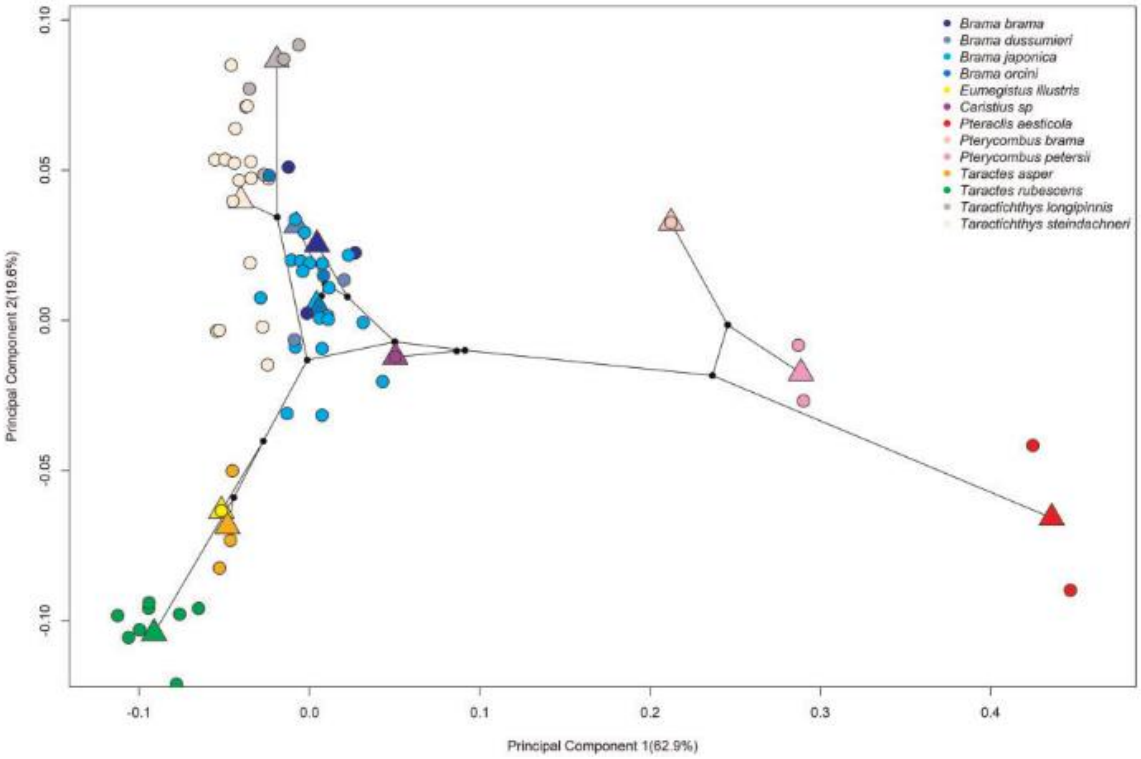

Figure 5.4. Phylomorphospace of overall body shape showing clustering of all bramid genera in negative PC space on PC1, except for the fanfishes, *Pteraclis* and *Pterycombus*, which exhibit positive PC scores on PC1. PC2 mainly separates *Taractes* (negative PC2 scores) from *Taractichthys* (positive PC2 scores). *Caristius* spp (Perciformes: Caristiidae; purple), which represents the closest related family to that of the Bramidae, exhibits a shape that is between the two major groups of bramids. Species are separated by colors, circles represent individual specimens, and triangles represent the mean shape for their respective species. Circles that exist with triangles indicate that a single specimen was available for inclusion in the analysis.

curvature, relative eye size, and body depth, with positive scores representing deeper bodies, relatively smaller eyes, and more rounded napes and negative scores being associated with shallower napes and bodies, and relatively larger eyes. Fanfishes excluded, the second axis tended to isolate genus specific groups, distinguishing the deeper bodied, highly laterally compressed *Tarachtichthys* from the slender, fusiform *Taractes* and the more closely related *Eumegistus*. *Brama* were largely intermediate

along this axis, alongside *Caristius fasciatus* and the fanfishes. In short, four distinct groups are identified in morphospace: highly laterally compressed (*Taractichthys),* highly fusiform (*Taractes, Eumegistus*), intermediate (*Brama*), and elongate + exaggerated medial fins (*Pteraclis, Pterycombus*).

These results show that fanfishes are morphologically unique when compared to the other bramids, as well as to the sister group, and that this difference is driven by their extreme exaggerated medial fin morphology.

Head and Body Shapes are Integrated

A possible outcome of evolutionary constraint is the integration of anatomical units, which in turn can bias the direction of morphological evolution. Since the exaggerated medial fins in fanfishes grossly extend well into the cranial region, we reasoned that this could lead to the evolutionary coupling of these two anatomical regions. Two-block partial least-squares test, without accounting for the phylogeny, revealed that head and body shape were indeed highly integrated (rPLS = 0.8445, P = < 0.0001; Supplemental Figure 2A). Relatively large eyes, heavily reduced nape and breast, smaller opercles, and smaller pectoral fins corresponded to a slender body, elongated dorsal and anal fins, and a small caudal fin base. Conversely, large heads and small eyes, a robust nape and breast, and large opercula corresponded to deeper bodies, relatively shorter dorsal and anal fins, and a more robust caudal fin base. This trend strengthened once we accounted for the phylogeny (rPLS = 0.9829, P = < 0.0001; Supplemental Figure 2B).

These results support our prediction that head and body shapes are related, and that this relationship is likely driven by expanded medial fin architecture. They are also

congruent with patterns reveal by our phylomorphospace, and collectively point to an evolutionary constraint that has biased the direction of morphological evolution in this group.

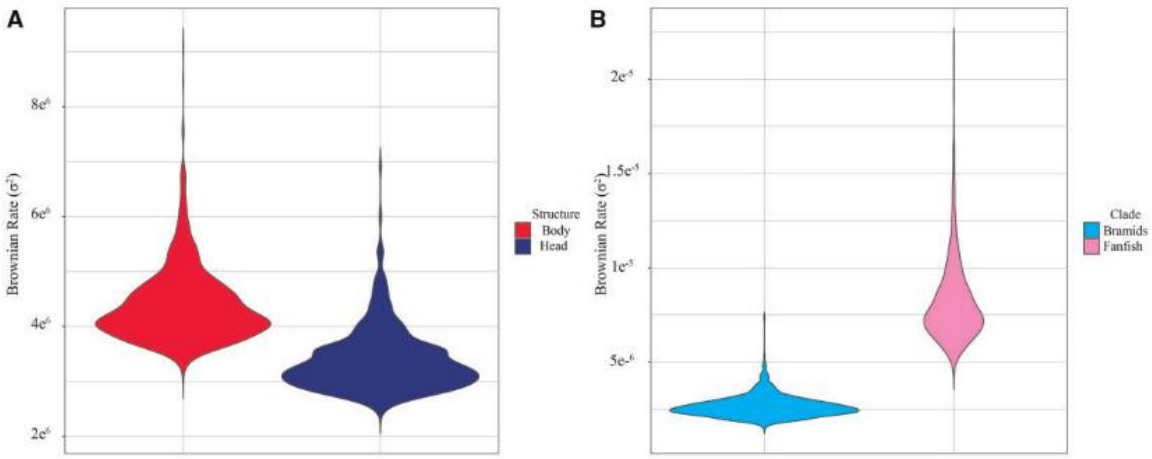

Figure 5.5. Violin plots depicting the Brownian rate of morphological evolution in the Bramidae. (A) Comparing rates of morphological evolution in the head and body regions of the Bramidae. (B) Comparing rates of morphological evolution in the fanfishes and remaining bramids.

Fanfishes Exhibit Faster Rates of Morphological Evolution than other Bramids

To determine whether putative constrains have also influenced rates of morphological evolution, we assessed this parameter in bramids. We found that fanfishes have experienced whole body shape evolution at a rate ~ 2.93 times faster than the sum of the other bramids (Rate = 8.14×10^{-6}, 95% CI = 5.54×10^{-6}, 1.37×10^{-5} versus Rate = 2.66×10^{-6}, 95% CI = 1.87×10^{-6}, 4.15×10^{-6}, P = 0.0099; Figure 5). When head and body shapes were parsed, net rates of morphological evolution between the two units were not significantly different (head rate = 3.38×10^{-6}, 95% CI = 2.67 $\times 10^{-6}$, 4.85×10^{-6}, body rate = 4.38×10^{-6}, 95% CI = 3.54×10^{-6}, 6.10×10^{-6}, observed rate ratio = 1.30, P = 1; Supplemental Figure 3).

We next calculated evolutionary rates for head and body shape independently in an attempt to tease apart any taxon-specific differences with mean PC1 and PC2 scores

representing the traits (Figure 6). For body shape, rates of morphological evolution were generally low across the phylogeny for both PC1 and PC2 scores, with the exception of

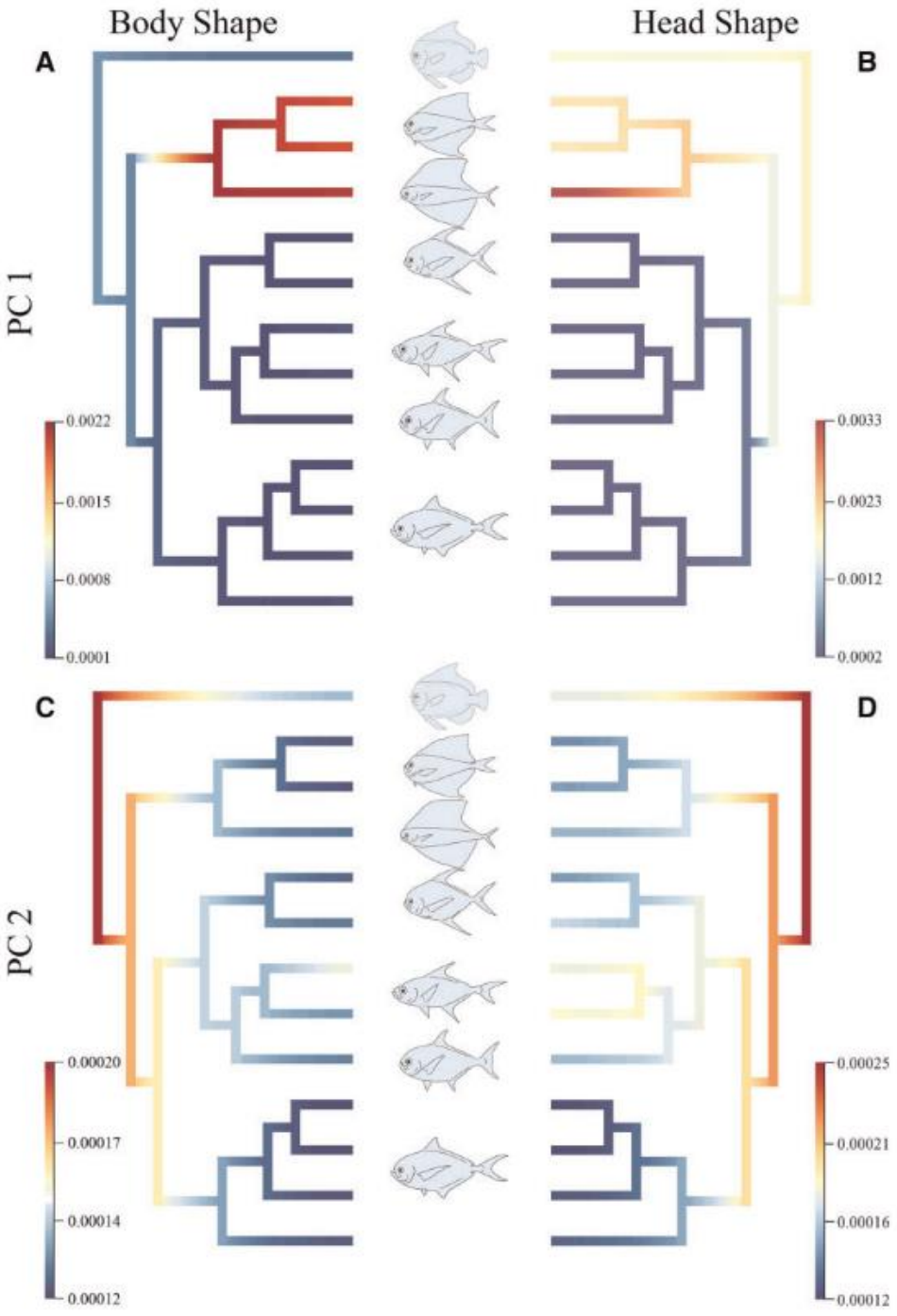

Figure 5.6. Evolutionary rates for mean body and head shape across the family Bramidae, and including a single member of Caristiidae (*Caristus* sp.). PC1 for body (A) and head (B) shape evolution. PC2 for body (C) and head (D) shape evolution. Generalized body shapes for each of the genera included in our analyses are in the center. Genera from top to bottom: *Caristus*, *Pterycombus*, *Pteraclis*, *Taractichthys*, *Taractes*,

Eumegistus, *Brama*. Warm colors indicate faster rates of shape evolution, while cool colors represent slower rates of shape evolution.

the fanfish clade (*Pteraclis* and *Pterycombus*). Fanfish rates were substantially higher than that of all other bramids and *Caristius sp.* for PC1. A similar trend existed for head shape evolution on PC1, with all bramids being characterized by relatively low rates, while fanfishes (notably *Pteraclis*) and *Caristius sp.* were characterized by higher rates of evolution. PC2 showed a different pattern, with body shape evolution appearing to be relatively fast at the base of the clade but slowing within each lineage. Head shape PC2 evolution showed a similar pattern, but with a less dramatic reduction in rates, especially within *Caristius sp.* and *Taractes* clades.

These results are consistent with our integration analysis, and show that rates of evolution in head and body shapes are similar across bramids. Further, they reveal that rates are higher in fanfishes, due to a further elaboration of medial fin morphology, and concomitant shifts in head and body shapes along an evolutionary line of least resistance (Schluter 1996).

Differences in Fanfish Anatomy are Detectable Early in Ontogeny

Since developmental processes can impact the emergence of phenotypic novelties, we sought to determine how early exaggerated fins appear during fanfish ontogeny – e.g., are they pre-patterned in their fully exaggerated form, or are they elaborated over ontogeny? The results of a phenotypic trajectory analysis revealed significant differences in phenotypic trajectory correlations in *Pterycombus* fanfishes compared to the other bramid genera (*Brama*, *Taractes*, and *Taractichthys*) but no significant difference when compared to the manefish genus, *Caristius* (Table 3). The genera *Brama*, *Taractes*, and

Taractichthys exhibited no significant difference in phenotypic trajectory correlations from one another, and, of those, only *Brama* was significantly different from *Caristius*.

The first two axes of morphospace explained 48.2% and 19.1%, respectively, of the total variation (Figure 7). The first axis can largely be attributed to medial fin insertion points and length, eye size, and the relative ratio of head:body size. It was on this axis that fanfishes are isolated from the other bramid taxa, regardless of ontogenetic stage. The second axis primarily explained body length:depth ratio and eye size, with positive scores relating to smaller eyes and longer bodies. The second axis largely separated the two ontogenetic stages across species, with juvenile groups overwhelmingly characterized by having lower scores than their adult counterparts.

Table 5.3. Results comparing phenotypic trajectory correlations among genera between juvenile and adult ontogenetic stages.

	Brama	*Caristius*	*Pterycombus*	*Taractes*	*Taractichthys*
Brama		**2.14**	**2.79**	1.09	1.16
Caristius	**0.040**		1.64	1.81	1.85
Pterycombus	**0.019**	0.072		**2.93**	**1.93**
Taractes	0.134	0.061	**0.015**		−0.46
Taractichthys	0.122	0.058	**0.049**	0.624	

Note iii: Z scores are above and P values are below the diagonal. Bolded P values and z scores indicate significant differences in mean shapes between species. For the purpose of significance testing, $\alpha \leq 0.05$.

Since it was apparent that fanfish juveniles are morphologically distinct from other bramids, we cleared and stained two larval and one juvenile *Pterycombus brama* and three larval *Brama dussumieri* specimens. Given the substantial emphasis that previous analyses had placed on dorsal fin insertion and relative head size, we focused on identifying skeletal differences in these regions between the species at distinct ontogenetic stages. Larval *P. brama* showed an abundance of dorsal pterygiophores that

extended into the caudal neurocranium. They can be seen dorsal to the neurocranium, which consequently lacks a supraoccipital crest (SOC) (Supplemental Figure 3A). At the

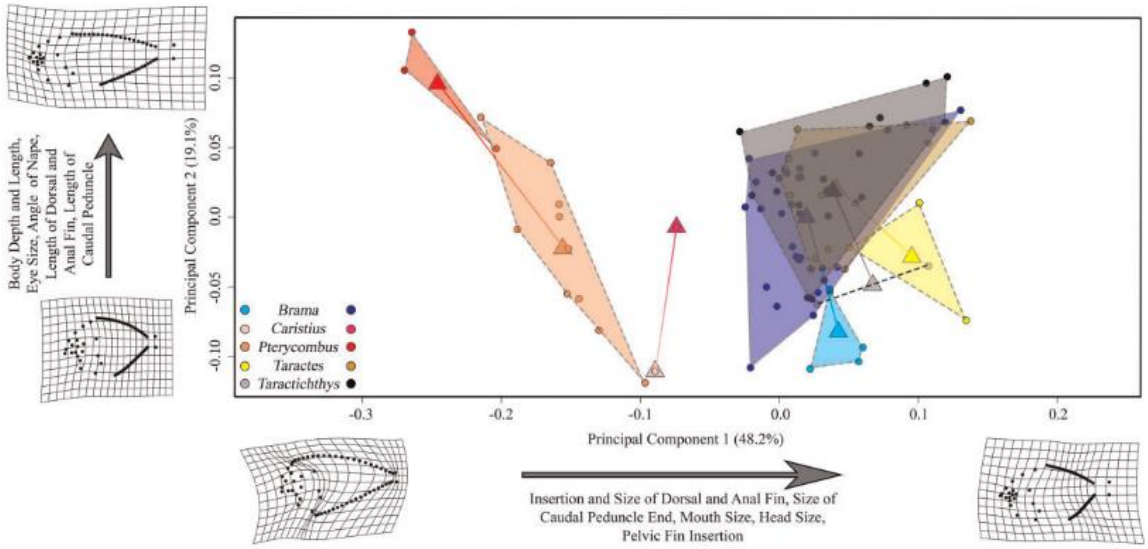

Figure 5.7. Morphospace of available bramid taxa and a juvenile/adult *Caristius* sample, with trajectories imposed for group means. Lighter colors represent juveniles, darker colors represent adults, and gradient-filled lines indicate the trajectory from juvenile to adult. All bramids, with the exception of fanfishes (here, *Pterycombus* spp.), occupy net neutral and positive scores during both juvenile and adult stages. Fanfishes occupy negative scores. Manefish (*Caristius fasciatus*) occupy an intermediate region of morphospace between fanfishes and all other bramids. Triangles represent mean shape values, while circles represent individual specimens. Circles that exist within a triangle indicate that a single specimen was available for use.

juvenile stage, *P. brama* still lack a noticeable SOC, as pterygiophores continue to grow just above the posterior neurocranium (Supplemental Figure 3B). Alternatively, *B. dussumieri* possessed a relatively robust SOC by the late larval stage (Supplemental Figure 3C-D), and pterygiophore development was restricted to posterior of the neurocranium.

These data suggest that key aspects of fanfish anatomy are predisposed to accommodate the formation of an expanded dorsal fin, and thus some of the earliest stages of skeletal development appear to have been altered during the evolution of this trait.

Fanfish Craniofacial Architecture suggests Co-option of Important Elements

Given the results of our developmental analyses, we wanted to examine in greater resolution the anatomical relationship between the dorsal fin and skull in fanfishes.

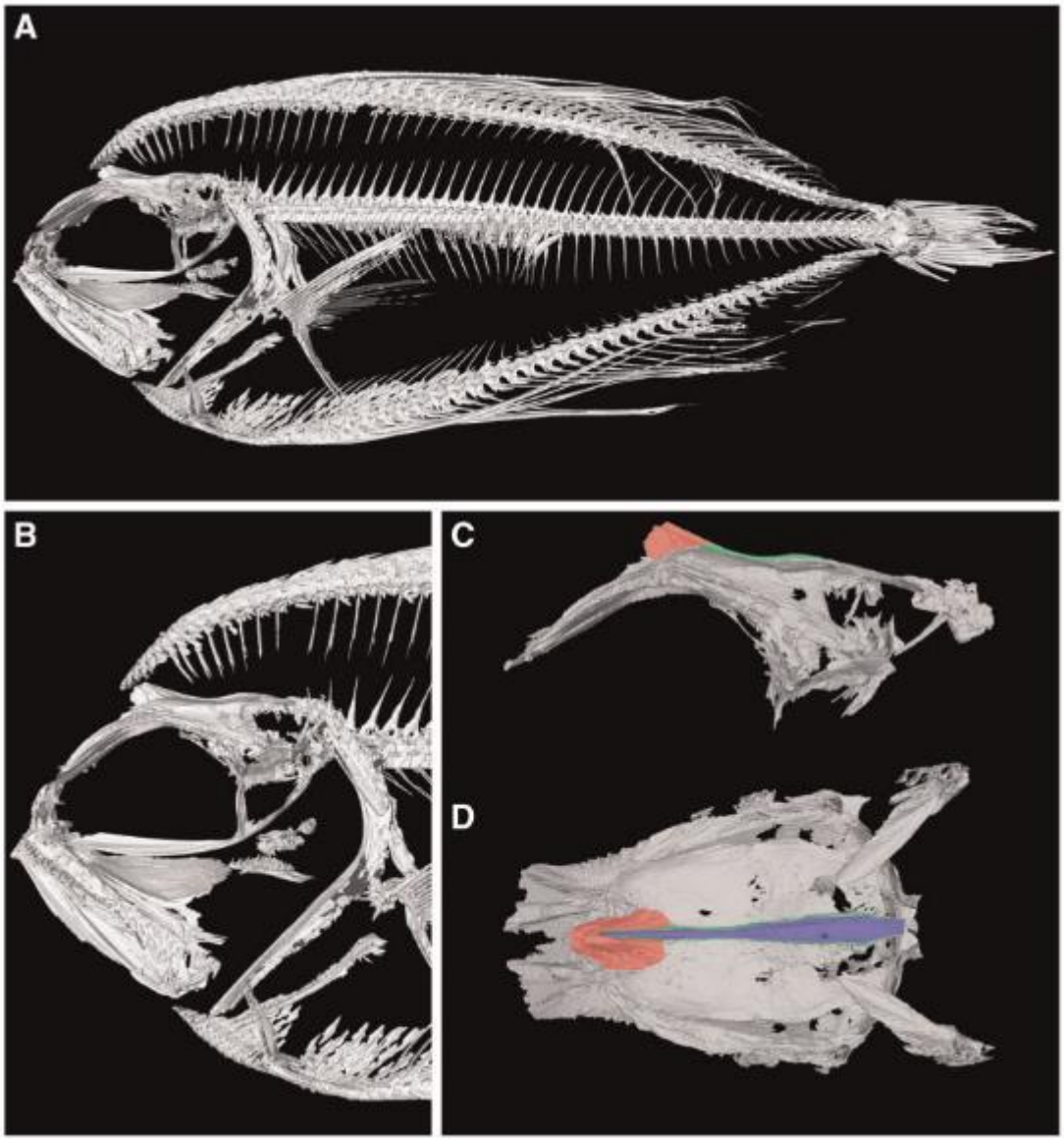

Figure 5.8. Reconstruction from mCT scans of a representative *Pterycombus petersii*, standard length 7.9 cm. (A) High-resolution full body scan. (B) Craniofacial skeleton showing internal elements of the dorsal fin. Lateral (C) and dorsal (D) view of the digitally isolated neurocranium to highlight the substantially altered supraoccipital crest (red), its proximal bifurcation (green), and the deep cleft that accommodates dorsal fin pterygiophores and their associated musculature (blue; not visible in C).

Accordingly, we gathered µCT data from a single adult *Pterycombus petersii* specimen (Figure 8A), collected off the coast of Hawaii in the Fall of 2018 from the stomach of a tuna, *Thunnus albacares.* Again, given the emphasis that previous analyses have place on this region, we focused on the craniofacial skeleton (Figure 8B) to identify osteological elements that may have been altered to accommodate extreme anterior dorsal fin expansion. Consistent with our developmental data, skeletal components of the dorsal fin occupy roughly half the space that would otherwise be available for SOC growth. As a result, the SOC is greatly reduced and restricted to the anterior neurocranium (Figure 8C). The loss of a posterior SOC may lead to a greatly reduced (relative) area for epaxial muscle attachment, something that we hope to address quantitatively in future studies. In addition, there is a bifurcation of the posterior skull that forms a cleft and appears to be associated with the intruding pterygiophores from the dorsal fin (Figure 8D).

Gross dissection of this specimen confirmed a truncated SOC and reduced epaxial muscle attachment (Figure 9). Further, the posterior bifurcation of the skull appears to accommodate pterygiophore growth and function, as the base of anterior pterygiophores extended to the cleft formed by the bifurcation, which is also the site of attachment for the associated dorsal fin musculature. Dorsal fin musculature is highly complex, comprised of a number of muscles, and detailed myological work will be the topic of future investigation.

Another notable aspect of fanfish anatomy includes a lower jaw that extends posteriorly to the caudal margin of the orbit, which predicts a large gape. Further, the ascending arm of the premaxilla is highly reduced, which likely results in limited, or non-existent, premaxillae protrusion (Westneat 1990; Cooper and Westneat 2009), and a jaw

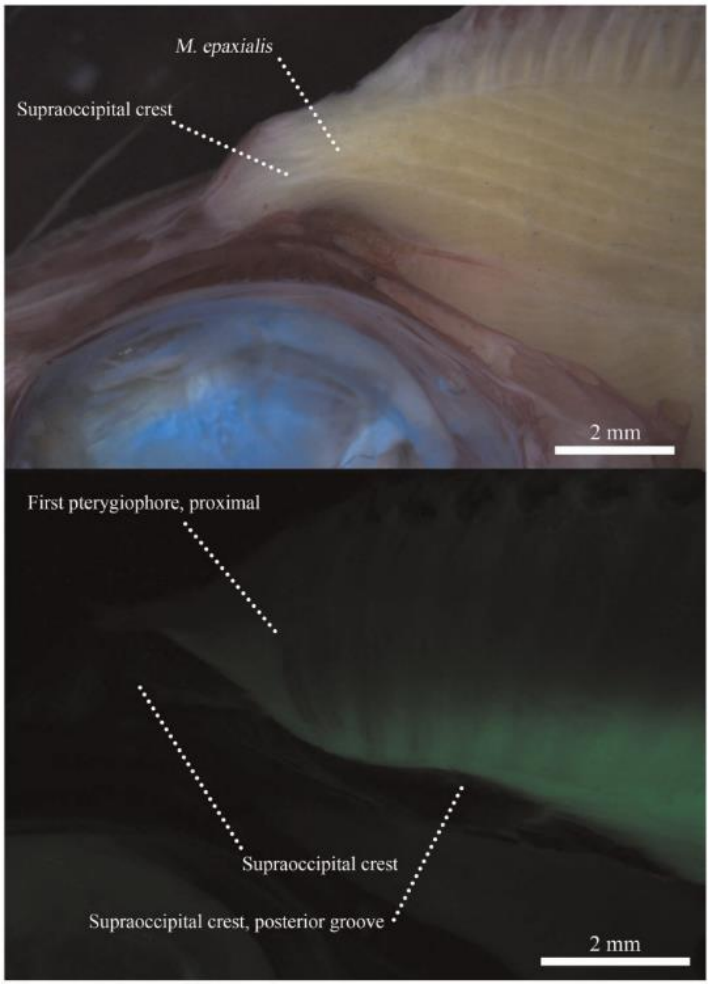

Figure 5.9. (A) Image of alcian and EtOH alizarin stained *Pterycombus petersii*, illustrating epaxial muscle attachment to the supraoccipital crest. (B) Same specimen under fluorescent lighting with GFP filter and epaxial musculature removed. Bright green areas represent endogenous illumination, highlighting connective and muscle tissues originating from the dorsal fin skeleton and inserting on the skull posterior to the supraoccipital crest. Black and low contrast areas indicate bone.

opening mechanism that is primarily driven by rotation of the articular-quadrate joint. The oral jaw anatomy described here appears ubiquitous within the family Bramidae (Supplemental Figure 4A-C; Supplemental Figures 5 A & B) and is similar to what we observe in Caristiidae (Supplemental Figure 4D).

Discussion

While evolution can yield an incredible number of phenotypic outcomes, only a fraction of those destinations are accessible to any given population due to evolutionary constraints. As adaptive phenotypes evolve along one trajectory, the degree to which related traits (e.g., physiological, developmental, morphological, etc.) can diverge and diversify may be limited, canalizing future phenotypic trajectories on an evolutionary scale. Pareto optimality theory echoes this, arguing that no system can be simultaneously improved for all tasks at once and that in order to improve one aspect of a system, a sacrifice, or trade-off, must be made elsewhere (McGhee 2007; Kennedy 2010; Shoval et al. 2012).

Our work on bramids exemplifies not only putative anatomical/morphological constraints (proximate) associated with the development of an exaggerated trait, but also the long term, evolutionary costs (ultimate) in the sense of constraining future lineages to increasingly fewer adaptive peaks (Conway Morris 2003). Using previously deposited mitochondrial DNA sequences, we create the most speciose bramid tree to date, and illustrate genera specific relationships to the outgroup, Caristiidae (manefishes). While our morphometric data are limited to gross form, we quantitatively demonstrate the substantial differences in overall head and body shape, and rates of morphological evolution in fanfishes compared to their bramid relatives. Through this, we also find support for manefishes being relatively intermediate in overall form to what we identify as two divergent bramid sub-groups, the subfamily Ptericlinae (genera *Pteraclis* and *Pterycombus*) and the remaining bramids (genera *Brama*, *Eumegistus*, *Taractes*, *Taractichthys*, and, presumably, *Xenobrama*). Further, to accommodate the exaggerated fin morphology, we identify and present morphological data that illustrate pronounced modifications to the craniofacial skeleton in the Ptericlinae. Many of these modifications, with the exception of the supraoccipital crest, persist among the other bramids, notably the oral jaw architecture of the other bramid taxa that may contribute to the known and predicted feeding ecology of these fishes.

We set out to understand the anatomical and evolutionary constraints associated with extreme dorsal fin morphology in the family Bramidae. The fanfishes, monophyletic and totaling five of the 20 extant bramid species, stand apart from the rest of the family and demonstrate a greatly exaggerated trait that, we predict, would come at a functional cost (Adriaens and Herrel 2009). We also predict that, if this phenotypic trait was ancestral to the family, there would be a detectable evolutionary cost associated with the other bramid lineages (Farnsworth and Niklast 1995; Tendler et al. 2015). What follows is a discussion of our results in the larger overall context of how extreme adaptations can create functional constraints and how those constraints may influence evolutionary trajectories.

Exaggerated Fin Morphology Appears Ancestral and may Constrain Foraging Anatomy in Bramids

The evolutionary relationships within the family Bramidae have been poorly resolved, and the majority of trees include only a small number of bramid taxa (Chen et al. 2016; Liu et al. 2016; Xu et al. 2018). Previous hypotheses suggested that the benthopelagic genus *Eumegsitus* (Bramidae) was the most ancestral (Mead 1972). In his monograph, Mead speculates that the family Caristiidae (typically represented by deep, robust bodies and exaggerated medial fin morphology), may have derived from a *Pteraclis*-like ancestor (Bellottii 1903). However, our study, as well as recent work presented by Miya et al. (2013) and Friedman et al. (2019), suggests that the family Bramidae diverged from caristiids. This assertion is also supported by the fossil record (Casier 1966; Bannikov and Tyler 1994; Ellison et al. 1994; Baciu and Bannikov 2003; Miya et al. 2013), which dates caristiids prior to bramids. If true, it is possible that exaggerated dorsal fin morphology is the ancestral state for the family Bramidae and that the Ptericlinae continued to exaggerate the extreme medial fin morphology present in

manefishes. In this proposed scenario, the last common ancestor to the other bramid lineages likely lost this exaggeration, but maintained, and continued to develop, deeper, robust, body shape morphologies.

While we are able to identify four distinct body shape morphologies within the family Bramidae (Figure 3; the fusiform body shape of *Taractes*, the deep bodies of *Taractichthys*, the intermediate form of *Brama*, and the elongated *Pteraclis*), the most striking anatomical feature remains the relative proportions of the medial fins. In particular, PC1 explained nearly 63% of the total variation and mainly captured variation in medial fin size and position (e.g., the deformation grid describing extreme shape along this axis nearly folds in on itself at the junction between the head and median fins; Figure 3). This is again highlighted in ontogenetic trajectories (Figure 7), where we see a separation of fanfishes from all other bramids along PC1 and noticeable differences in dorsal fin placement early during development. These data suggest that morphological differences between fanfishes and other bramids arise early in development and may therefore be "locked-in". They suggest further that differences in rates of morphological evolution between these two lineages may be linked to alternate developmental patterning mechanisms with respect to the medial fins. Gaining a better understanding of bramid developmental processes and mechanisms will be a fruitful line of future research.

Across fishes, dorsal fin structure is diverse and functions in myriad tasks, including, but not limited to, locomotion (Breder Jr 1926; Loofbourrow 2006; Jagnandan and Sanford 2013), protection (Hoogland et al. 1956), cutwaters, hydrodynamic efficiency (Drucker and Lauder 2001; Nauen and Lauder 2001; Wang et al. 2020),

advertising (Allen and Nicoletto 1997), herding prey (Domenici et al. 2014), generating rapid propulsion and bursts of speed (Gibb et al. 1999; Nauen and Lauder 2001), reducing yaw and roll in fast swimmers (Webb 1984; Weihs 1993; McGowan 1999), and increased maneuverability (Standen and Lauder 2005). For fishes with large, erectable fins, the increased surface area allows for greater deflection of water (Lamb 1975), thereby increasing their ability to change direction. This feature is more common in prey species but can be seen in some predators as well (e.g., Istiophoriformes, *Coryphaena*).

Typically, the dorsal fin begins 3-5 vertebrae caudal to the cranio-vertebral joint following the supraneurals (Thys 1997; Jimenez et al. 2018). This anatomical configuration facilitates cranial elevation during suction feeding, whereby the skull rotates dorsally to facilitate mouth opening, premaxillary protrusion, and hyoid depression (Lauder 1981; Lauder and Liem 1981; Svanbäck et al. 2002; Wainwright et al. 2006; Tegge et al. 2020). Cranial elevation is of great importance to suction-feeding fishes (Carroll and Wainwright 2006; Coughlin and Carroll 2006; Camp and Brainerd 2014; Van Wassenbergh et al. 2015), and thus the predominant insertion point of the dorsal fin usually begins posterior to three to five free-floating interneural bones. Functionally, this void of articulated bones creates a region of "folding" as the epaxial musculature contracts on the posterior region of a fish's skull to elevate the neurocranium (Jimenez et al. 2018). Having a dorsal fin attach directly to the top of the skull, as seen in the fanfishes, eliminates this void, which likely compromises the ability of the skull to rotate about the cranio-vertebral joint, a stereotypical feature of suction-feeding. Ram-feeders also exhibit cranial rotation (Bergert and Wainwright 1997; Ferry-Graham, Wainwright, Darrin Hulsey, et al. 2001; Porter and Motta 2004), but generally to a lesser

degree. Rather, this mode of feeding is more strongly associated with long jaws and the ability to generate large gapes (e.g., mackerels, barracuda, etc.) to engulf evading prey (Ferry-Graham, Wainwright, and Bellwood 2001; Ferry-Graham, Wainwright, Darrin Hulsey, et al. 2001; Porter and Motta 2004). As a whole, the Bramidae possess long lower jaws that are relatively constant in size when regressed against head size (Supplemental 5), consistent with large gapes. Further, long jaws coupled with limited upper jaw protrusion suggests that bramids exhibit a notched, rather than circular, mouth opening, which should compromise suction performance by altering flow dynamics critical to successful suction feeding (Carroll et al. 2004). We suggest that the evolution of a dorsal fin that extends anteriorly into the cranial region and mechanically inhibits skull rotation, while potentially increasing swimming maneuverability, predisposed the lineage toward the ram-feeding end of the ram-suction prey -capture continuum.

In *Pterycombus petersii* (and other fanfishes), we observe a combination of anatomical features consistent with such a trade-off. Firstly, they have extremely large, erectable fins, which suggests they use these fins for evading predators (e.g., tuna) and/or pursuing elusive prey (e.g., cephalopods, myctophids). In addition, they possess modified scales at the base of the medial fins (allowing for complete dorsal and anal fin retraction and concealment), a large aspect ratio of the caudal fin (throughout the family Bramidae and rivaling that of other pelagic cruisers like *Rachycentron canadum*), and symmetrical rows of raised, recurved scale spines (found throughout the family on various bramid species) reminiscent of placoid scales in elasmobranchs known to increase hydrodynamic efficiency (Bechert et al. 1997; Oeffner and Lauder 2012; Wen et al. 2014). Together, these traits suggest that, despite having large, seemingly cumbersome fins, fanfishes have

adapted methods for increasing their hydrodynamic efficiency, enabling them to swim at high cruising speeds, relative to their body size (by retracting their fins and creating an elongate,streamlined body form), and vastly improve their maneuverability when the need arises by erecting their exaggerated fins. The evolution of elaborate fins appears to come with a substantial modification of the occipital region of the skull (Figure 8), including a considerable reduction of the SOC and a bifurcated cleft in the occipital region where the dorsal fin musculature attaches. This novel anatomical modification demonstrates a direct mechanical linkage between the dorsal fin and the neurocranium. A shortened SOC is also notable, as this bone contributes to the in-lever during the action of cranial elevation (Carroll et al. 2004). A short (nearly absent) SOC in fanfishes should therefore result in a short in-lever and less effective mechanical system for suction feeding. While expanded surface area on top of the neurocranium could mitigate the lack of a SOC in fanfishes, this seems unlikely as skull width is not noticeably greater in fanfishes compared to other bramids.

High-speed filming of open water species is challenging, and the manipulation of fixed specimens (e.g., to directly assess jaw protrusion or cranial elevation) is all but impossible. We therefore make all kinematic inferences about bramid foraging with caution. Despite these difficulties, large museum specimens did allow us to take advantage of preservation state, allowing us to make hypotheses about feeding mechanics. Regarding this, of all specimens examined, we make no observation of any fixed museum specimen showing meaningful premaxilla protrusion, but do observe substantial lower jaw depression (Supplemental Figure 6). Nevertheless, teleosts are an exceptionally well-studied kinematic system, with a detailed understanding of the

connection between form and function. (for review, see Liem and Osse 1975). Based on the functional anatomy of bramids as a whole, we hypothesize that this lineage is well adapted to move and forage within the open ocean habitat, but is simultaneously constrained to a narrower realm of niche-space (e.g., most likely strict ram-feeders). If true, this would represent an example of how proximate form-function trade-offs may translate to constrained patterns of morphological evolution.

The Influence of Historical Contingency on Bramid Ecology and Evolution

While the path of evolution is largely unpredictable, future outcomes of a lineage are undoubtedly reliant on the historical states (Gould and Woodruff 1990). In this respect, the numerous small changes that accumulate in lineages create limitations that can render *some* aspects of evolution predictable, or provide a rationale for why certain realms of phenotypic space have not been occupied (Conway Morris 2003). The evolution of the family Bramidae provides an excellent system to explore these ideas.

Events of natural history can be difficult to evaluate and require an adequate record of a lineage's past to assist in making inferences about the contemporary phenotypes that we observe in living taxa (Gould and Woodruff 1990). However, using fossils in conjunction with molecular data can help inform such predictions. For instance, fossils of caristiid [*Exellia proxima*, *E. velifer*; (Bannikov and Tyler 1994)] and bramid [*Paucaichthys neamtensis*, *P. elamensis*; (Baciu and Bannikov 2003); (Přikryl and Bannikov 2014)] relatives show striking similarities in both overall body shape, craniofacial anatomy, and medial fin morphology. Our phylogeny and morphometric analyses, along with the recent phylogenies of others (Miya et al. 2013; Friedman et al. 2019), suggest that caristiids are sister to bramids and possess an intermediate form in terms of gross head and body shape (Figure 4). Taken together, these data suggest that expanded medial

fin morphology was ancestral, and therefore early diversification within this lineage occurred within the context of this exaggerated trait.

We find that bramid evolution was initially marked by rapid diversification, followed by a linear decline in speciation rate. One explanation for an initial burst of diversification could be the exploitation of new resources following the extinction of predatory Mesozoic teleosts (Friedman 2009, 2010). An alternate, though not mutually exclusive, hypothesis may involve a shift in locomotor behavior in the bramid stem lineage. For example, while data are scarce, descriptions of caristiid ecology are largely centered around their seemingly poor swimming ability and mysterious relationship to siphonophores (Janssen et al. 1989; Benfield et al. 2009). This is a striking contrast to the predominately open ocean bramids, which anatomically appear well-adapt at attaining high speeds (Legendre 1924) and are known for their substantial migratory habits (Mead 1972). Thus, it is plausible that the initial burst of diversification we detect in bramids is the result of one lineage losing exaggerated fin morphology entirely, opting for maximizing high speeds, navigating the high seas, and growing to much larger sizes and bulk than fanfishes, while the other lineage maintains exaggerated fins, but evolves a functional work-around to poor swimming performance, enabling it to excel at both maneuverability and speed. Notably, however, in both lineages the evolution of craniofacial shape appears to be relatively constrained, which may be due to an ancestral trade-off between the historical locomotion and foraging architecture that has predisposed the bramid lineage toward ram-feeding. In summary, the story of bramid evolution may be one whereby a lineage takes advantage of ecological opportunity (e.g., Mesozoic extinction) by modulating traits that remain highly evolvable (e.g., medial fins), while experiencing niche-space limitations (e.g., to ram-feeding) due to historical constraints.

Summary and Significance

The evolution of novel traits not only introduces new constraints to a system, but must also work within the confines of previous evolutionary constraints (Jacob 1977; Gould and Woodruff 1990; Losos et al. 1998; Blount et al. 2012), thereby limiting future adaptive peaks to an increasingly narrow field of view (Wright 1932; Arnold 1992; Schluter 1996). Nearly fifty years ago, Mead (1972) remarked that the evolution and phylogenetic relationships within family Bramidae deserved further study. Due to the rarity of several species, this has been a challenging task to accomplish; however, recent work has made progress toward clarifying the phylogenetic relationship among bramids, as well as between bramids and other open ocean lineages. Here, we build upon this work to explore the evolution of exaggerated fins, hypothesize putative tradeoffs between fin and skull functional morphology, and attempt to identify how these may have shaped bramid evolutionary trajectories. To summarize, given the SOC and intraneural bones of other bramids, they (non-fanfish bramids) should be able to generate suction. However, since their ancestral state likely had extreme dorsal fin morphology, and evolved to maximize ram feeding as a consequence, the evolution of the entire family appears to have been constrained. All in all, we are excited by the prospect that this system offers examples of, and provides insight into, how the development of an exaggerated trait can introduce both proximate and ultimate trade-offs in a lineage.

Acknowledgements

The authors are exceedingly grateful to Meaghan H. Sorce and Andrew D. Williston from the Museum of Comparative Zoology at Harvard for their overwhelming support, intellectual discussion, and x-rays used in Supplemental Figure 3. Without the two, this paper would not have been possible. Kerryn Parkinson and Amanda Hay at the Australian Museum for help with acquiring additional bramid specimens, both for this paper and for future work. Art Westwood is acknowledged for catching the tuna that ate, and regurgitated, the initial prickly fanfish

(*Pterycombus petersii*) that spurred the conception of this project (we are also grateful for this tuna and its hard work at capturing the fanfish). Emma R. Masse for beautifully illustrating a reconstructed visual of this fanfish that was used for Figure 1. We are grateful to Gina L. Georgadarellis for assistance with functional concepts from an engineering/hydrodynamics perspective, to Kristen N. Gilbert for help with data input and organization, and to Rene P. Martin for intellectual discussion and discourse. The Albertson Lab is thanked for their support, feedback, and encouragement throughout the various stages of this manuscript. Three anonymous reviewers, whose suggestions improved the overall quality of this manuscript and gave us much to think about for our future work.

Data availability statement

Accession numbers for all specimens, both gene (*Supplemental 1*) and museum (*Supplemental 2*), are provided in the supplemental. Raw data are available as supplemental files.

Declaration of Competing Interests:

The authors declare no competing interests.

References

Adams D, Collyer ML, Kaliontzopoulou A. 2018. Geomorph: Software for geometric morphometric analysis. .

Adams DC. 2014. Quantifying and comparing phylogenetic evolutionary rates for shape and other high-dimensional phenotypic data. Syst Biol 63:166–77.

Adams DC, Collyer ML. 2016. On the comparison of the strength of morphological integration across morphometric datasets. Evolution (N Y) 70:2623–31.

Adams DC, Collyer ML. 2018. Multivariate phylogenetic comparative methods: Evaluations, comparisons, and recommendations. Syst Biol 67:14–31.

Adams DC, Collyer ML, Otarola-Castillo E. 2014. R: package, geomorph: Software for geometric morphometric analysishttp//cranr Proj.

Adams DC, Felice RN. 2014. Assessing trait covariation and morphological integration on phylogenies using evolutionary covariance matrices. PLoS One 9.

Adriaens D, Herrel A. 2009. Functional consequences of extreme morphologies in the craniate trophic system. Physiol Biochem Zool 82:1–6.

Ali AM, McNoon A. 2010. Additions to benthopelagic fish fauna of the Aden Gulf-Arabian Sea (Actinopterygii: Bramidae and Sternoptychidae). J Fish Aquat Sci 5:23–32.

Allen JM, Nicoletto PF. 1997. Response of *Betta splendens* to computer animations of males with fins of different length. Copeia 1997:195–99.

Arnold SJ. 1983. Morphology, performance and fitness. Integr Comp Biol 23:347–61.

Arnold SJ. 1992. Constraints on phenotypic evolution. Am Nat 140:S85–107.

Baciu D, Bannikov AF. 2003. *Paucaichthys neamtensis* gen . et sp . nova-the first discovery of sea breams (Bramidae) in the Oligocene of Romania. Vopr ikhtiologii 43:598–602.

Bannikov AF. 2012. The first record of the genus *Isurichthys* (Perciformes, Ariommatidae) in the Lower Oligocene of the Northern Caucasus. Paleontol J 46:171–76.

Bannikov AF, Tyler JC. 1994. A revision of the Eocene fish family Exelliidae (Perciformes). Paleontol J 28:128–40.

Bechert DW, Bruse M, Hage W, Van Der Hoeven JGT, Hoppe G. 1997. Experiments on drag-reducing surfaces and their optimization with an adjustable geometry. J Fluid Mech 338:59–87.

Bellottii C. 1903. Di un nuovo pteraclide giapponese. Atti della Soc Ital di Sci Nat di

Milano 42:136–39.

Benfield MC, Caruso JH, Sulak KJ. 2009. In situ video observations of two manefishes (Perciformes: Caristiidae) in the Mesopelagic zone of the northern Gulf of Mexico. Copeia 2009:637–41.

Benson DA, Cavanaugh M, Clark K, Karsch-Mizrachi I, Lipman DJ, Ostell J, Sayers EW. 2013. GenBank. Nucleic Acids Res 41:36–42.

Bergert BA, Wainwright PC. 1997. Morphology and kinematics of prey capture in the syngnathid fishes *Hippocampus erectus* and *Syngnathus floridae*. Mar Biol 127:563–70.

Blount ZD, Barrick JE, Davidson CJ, Lenski RE. 2012. Genomic analysis of a key innovation in an experimental *Escherichia coli* population. Nature 489:513–18.

Bouckaert R, Heled J, Kühnert D, Vaughan T, Wu CH, Xie D, Suchard MA, Rambaut A, Drummond AJ. 2014. BEAST 2: A software platform for Bayesian evolutionary analysis. PLoS Comput Biol 10:1–6.

Bouckaert RR, Drummond AJ. 2017. bModelTest: Bayesian phylogenetic site model averaging and model comparison. BMC Evol Biol 17:1–11.

Breder Jr C. 1926. The locomotion of fishes. Zoologica 4:159–291.

Brodie III ED, Brodie Jr ED. 1999. Costs of exploiting poisonous prey: Evolutionary trade-offs in a predator-prey arms race. Evolution (N Y) 53:626–31.

Camp AL, Brainerd EL. 2014. Role of axial muscles in powering mouth expansion during suction feeding in largemouth bass (Micropterus salmoides). J Exp Biol 217:1333–45.

Carroll AM, Wainwright PC. 2006. Muscle function and power output during suction

feeding in largemouth bass, Micropterus salmoides. Comp Biochem Physiol - A Mol Integr Physiol 143:389–99.

Carroll AM, Wainwright PC, Huskey SH, Collar DC, Turingan RG. 2004. Morphology predicts suction feeding performance in centrarchid fishes. J Exp Biol 207:3873–81.

Carvalho-filho A, Marcovaldi G, Sampaio CLS, Paiva MIG, Duarte LAG. 2009. First report of rare pomfrets (Teleostei: Bramidae) from Brazilian waters, with a key to Western Atlantic species. Zootaxa 2290:1–26.

Casier E. 1966. Faune ichthyologique du London Clay. London Trust Br Museum (Natural Hist London.

Charnov EL. 1989. Phenotypic evolution under Fisher's fundamental theorem of natural selection. Heredity (Edinb) 62:113–16.

Chen F, Ma H, Ma C, Zhang H, Zhao M, Meng Y, Wei H, Ma L. 2016. Sequencing and characterization of mitochondrial DNA genome for *Brama japonica* (Perciformes: Bramidae) with phylogenetic consideration. Biochem Syst Ecol 68:109–18.

Cignoni P, Callieri M, Corsini M, Dellepiane M, Ganovelli F, Ranzuglia G. 2008. MeshLab: An open-source mesh processing tool. 6th Eurographics Ital Chapter Conf 2008 - Proc 129–36.

Collyer M, Adams D. 2013. Phenotypic trajectory analysis: comparison of shape change patterns in evolution and ecology. Hystrix 24:75–83.

Collyer ML, Adams DC. 2018. RRPP : An r package for fitting linear models to high- - dimensional data using residual randomization. 2018:1772–79.

Collyer ML, Sekora DJ, Adams DC. 2015. A method for analysis of phenotypic change for phenotypes described by high-dimensional data. Heredity (Edinb) 115:357–65.

Conway Morris S. 2003. Life's Solution Cambridge: Cambridge University Press.

Cooper WJ, Westneat MW. 2009. Form and function of damselfish skulls: Rapid and repeated evolution into a limited number of trophic niches. BMC Evol Biol 9:1–17.

Coughlin DJ, Carroll AM. 2006. In vitro estimates of power output by epaxial muscle during feeding in largemouth bass. Comp Biochem Physiol - A Mol Integr Physiol 145:533–39.

Darwin C. 1859. On the origin of species.

Datovo A, Vari RP. 2013. The Jaw Adductor Muscle Complex in Teleostean Fishes: Evolution, Homologies and Revised Nomenclature (Osteichthyes: Actinopterygii). PLoS One 8.

Denton JSS, Adams DC. 2015. A new phylogenetic test for comparing multiple high-dimensional evolutionary rates suggests interplay of evolutionary rates and modularity in lanternfishes (Myctophiformes; Myctophidae). Evolution (N Y) 69:2425–40.

Domenici P, Wilson ADM, Kurvers RHJM, Marras S, Herbert-Read JE, Steffensen JF, Krause S, Viblanc PE, Couillaud P, Krause J. 2014. How sailfish use their bills to capture schooling prey. Proc R Soc B Biol Sci 281:1–6.

Drucker EG, Lauder G V. 2001. Locomotor function of the dorsal fin in teleost fishes: Experimental analysis of wake forces in sunfish. J Exp Biol 204:2943–58.

Drummond AJ, Ho SYW, Phillips MJ, Rambaut A. 2006. Relaxed phylogenetics and dating with confidence. PLoS Biol 4:699–710.

Ellison R, Knox R, Jolley D, King C. 1994. A revision of the lithostratigraphical classification of the early Palaeogene strata of the London Basin and East Anglia.

Proc Geol Assoc 105:187–97.

Farnsworth KD, Niklast KJ. 1995. Theories of optimization, form and function in branching architecture in plants. Funct Ecol 9:355–63.

Ferry-Graham LA, Wainwright PC, Bellwood DR. 2001. Prey capture in long-jawed butterflyfishes (Chaetodontidae): The functional basis of novel feieding habits. J Exp Mar Bio Ecol 256:167–84.

Ferry-Graham LA, Wainwright PC, Darrin Hulsey C, Bellwood DR. 2001. Evolution and mechanics of long jaws in butterflyfishes (Family Chaetodontidae). J Morphol 248:120–43.

Fierstine H, Huddleston R, Takeuchi G. 2012. Neogene bony fishes of California: a systematic inventory of all published accounts. Calif Acad Sci.

Fitzjohn RG. 2012. Diversitree: Comparative phylogenetic analyses of diversification in R. Methods Ecol Evol 3:1084–92.

Friedman M. 2009. Ecomorphological selectivity among marine teleost fishes during the end-Cretaceous extinction. Proc Natl Acad Sci U S A 106:5218–23.

Friedman M. 2010. Explosive morphological diversification of spiny-finned teleost fishes in the aftermath of the end-Cretaceous extinction. Proc R Soc B Biol Sci 277:1675–83.

Friedman M, Feilich KL, Beckett HT, Alfaro ME, Faircloth BC, Černý D, Miya M, Near TJ, Harrington RC. 2019. A phylogenomic framework for pelagiarian fishes (Acanthomorpha: Percomorpha) highlights mosaic radiation in the open ocean. Proc R Soc B Biol Sci 286.

Gibb AC, Dickson KA, Lauder G V. 1999. Tail kinematics of the chub mackerel

Scomber japonicus: Testing the homocercal tail model of fish propulsion. J Exp Biol 202:2433–47.

González-lorenzo G, González-jiménez JF, Brito A, González JF. 2013. The family Bramidae (Perciformes) from the Canary Islands (Northeastern Atlantic Ocean), with three new records. Cybium 37:295–303.

Goodall C. 1991. Procrustes methods in the statistical analysis of shape. J R Stat Soc 53:285–339.

Gosline WA. 1971. Functional Morphology and Classification of Teleostean Fishes Honolulu: University Press of Hawaii.

Gould SJ, Woodruff DS. 1990. History as a cause of area effects: an illustration from *Cerion* on Great Inagua, Bahamas. Biol J Linn Soc 40:67–98.

Gutiérrez E, Fernandez A, Hernández R. 2005. *Brama caribbea* (Pisces: Bramidae), un nuevo registro para las aguas cubanas. Solenodon 5:78–79.

Herrel A, Bonneaud C. 2012. Trade-offs between burst performance and maximal exertion capacity in a wild amphibian, *Xenopus tropicalis*. J Exp Biol 215:3106–11.

Herrel A, Podos J, Vanhooydonck B, Hendry AP. 2009. Force-velocity trade-off in Darwin's finch jaw function: A biomechanical basis for ecological speciation? Funct Ecol 23:119–25.

Holzman R, Collar DC, Price SA, Darrin Hulsey C, Thomson RC, Wainwright PC. 2012. Biomechanical trade-offs bias rates of evolution in the feeding apparatus of fishes. Proc R Soc B Biol Sci 279:1287–92.

Hoogland R, Morris D, Tinbergen N. 1956. The spines of sticklebacks (*Gasterosteus* and *Pygosteus*) as means of defence against predators (*Perca* and *Esox*). Behaviour

10:205–36.

Jacob F. 1977. Evolution and Tinkering. Science (80-) 196:1161–66.

Jagnandan K, Sanford CP. 2013. Kinematics of ribbon-fin locomotion in the bowfin, *Amia calva*. J Exp Zool Part A Ecol Genet Physiol 319:569–83.

Janssen J, Gibbs RH, Pugh PR. 1989. Association of *Caristius sp.* (Pisces : Caristiidae) with a Siphonophore, *Bathyphysa conifera*. Copeia 1989:198–201.

Jawad LA, Al-Mamry JM, Al-Busaidi HK. 2014. New record of the keeltail pomfret, *Taractes rubescens* (Jordan & Evermann, 1887) (Perciformes : Bramidae) from the Sea of Oman. Int J Mar Sci 4:227–30.

Jimenez YE, Camp AL, Grindall JD, Brainerd EL. 2018. Axial morphology and 3D neurocranial kinematics in suction-feeding fishes. Biol Open 7.

Kennedy MC. 2010. Functional-structural models optimize the placement of foliage units for multiple whole-canopy functions. Ecol Res 25:723–32.

Klingenberg CP. 2011. MorphoJ: an integrated software package for geometric morphometrics. Mol Ecol Resour 11:353–57.

Konuma J, Chiba S. 2007. Trade-offs between force and fit: Extreme morphologies associated with feeding behavior in carabid beetles. Am Nat 170:90–100.

Lamb H. 1975. Hydrodynamics New York: Dover.

Langerhans RB, Layman CA, DeWitt TJ. 2005. Male genital size reflects a tradeoff between attracting mates and avoiding predators in two live-bearing fish species. Proc Natl Acad Sci U S A 102:7618–23.

Larsson A. 2014. AliView: A fast and lightweight alignment viewer and editor for large datasets. Bioinformatics 30:3276–78.

Lauder G V., Liem KF. 1981. Prey capture by *Luciocephalus pulcher*: implications for models of jaw protrusion in teleost fishes. Environ Biol Fishes 6:257–68.

Lauder G V. 1981. Intraspecific functional repertoires in the feeding mechanism of the characoid fishes *Lebiasina, Hoplias* and *Chalceus*. Copeia 1981:154–68.

Lee J, Lee W, Kim J. 2019. First reliable record of the keeltail pomfret *Taractes rubescens* (Bramidae : Perciformes) from Korea. Korean J Fish Aquat Sci 52:283–87.

Lee WJ, Kim JK. 2015. New record of *Brama dussumieri* (Pisces: Bramidae) from Korea, as revealed by morphological and molecular analyses. Fish Aquat Sci 18:311–16.

Legendre R. 1924. *Brama raii* Bl.: sa présence au large des côtes sud de la Bretagne. Bull la Société Zool Fr 49:218–25.

Lenov Y. 1998. Late Eocene-Early Oligocene geological and biotical events on the territory of the former Soviet Union. Part II. The geological and biotical events, Moscow: GEOS.

Leroi AM, Kim SB, Rose MR. 1994. The evolution of phenotypic life-history trade-offs: An experimental study using *Drosophila melanogaster*. Am Nat 144:661–76.

Liem KF, Osse J. 1975. Biological versatility, evolution, and food resource exploitation in African cichlid fishes. Am Zool 15:427–54.

Liu X, Tian S, Li W, Wu F, Dai X. 2016. Complete mitochondrial genome of the *Taractes rubescens* (Perciformes: Bramidae). Mitochondrial DNA 27:2809–10.

Lobo C, Erzini K. 2001. Age and growth of Ray's bream (*Brama brama*) from the south of Portugal. Fish Res 51:343–47.

Loofbourrow H. 2006. Hydrodynamics of balistiform swimming in the picasso triggerfish, *Rhinecanthus aculeatus*.

Losos JB, Jackman TR, Larson A, De Queiroz K, Rodríguez-Schettino L. 1998. Contingency and determinism in replicated adaptive radiations of island lizards. Science (80-) 279:2115–18.

McGhee GR. 2007. The Geometry of evolution: Adaptive landscapes and theoretical morphospaces Cambridge: Cambridge University Press.

McGowan C. 1999. A practical guide to vertebrate mechanics Cambridge, U.K.: Cambridge University Press.

Mead GW. 1972. Bramidae. The Carlsberg Foundation's oceanographical expedition round the World 1928-30 and previous Dana-expeditions. Dana-Report.

Miller MA, Pfeiffer W, Schwartz T. 2010. Creating the CIPRES Science Gateway for inference of large phylogenetic trees. 2010 Gatew Comput Environ Work GCE 2010 1–8.

Miya M, Friedman M, Satoh TP, Takeshima H, Sado T, Iwasaki W, Yamanoue Y, Nakatani M, Mabuchi K, Inoue JG, Poulsen JY, Fukunaga T, Sato Y, Nishida M. 2013. Evolutionary origin of the Scombridae (tunas and mackerels): Members of a Paleogene adaptive radiation with 14 other Pelagic fish families. PLoS One 8:e73535.

Moteki M, Arai M, Tsuchiya K, Okamoto H. 2001. Composition of piscine prey in the diet of large pelagic fish in the eastern tropical Pacific Ocean. Fish Sci 67:1063–74.

Nauen JC, Lauder G V. 2001. Locomotion in scombrid fishes: Visualization of flow around the caudal peduncle and finlets of the chub mackerel *Scomber japonicus*. J

Exp Biol 204:2251–63.

Oeffner J, Lauder G V. 2012. The hydrodynamic function of shark skin and two biomimetic applications. J Exp Biol 215:785–95.

Olsen A, Westneat M. 2015. StereoMorph: an R package for the collection of 3D landmarks and curves using a stereo camera set-up. Methods Ecol Evol 6:351–56.

Orr JW, Tuttle V, Donovan C. 2018. *Pterycombus petersii* (Bramidae: Teleostei): First record for the eastern North Pacific. Northwest Nat 99:236–38.

Park JH, Kim JK, Moon JH, Kim CB. 2007. Three unrecorded marine fish species from Korean waters. Ocean Sci J 42:231–40.

Patek SN, Oakley TH. 2003. Comparative tests of evolutionary trade-offs in a palinurid lobster acoustic system. Evolution (N Y) 57:2082–2100.

Pelegrin N, Mesquita DO, Albinati P, Caldas FLS, de Queiroga Cavalcanti LB, Costa TB, Falico DA, Galdino JYA, Tucker DB, Garda AA. 2017. Extreme specialization to rocky habitats in Tropidurus lizards from Brazil: Trade-offs between a fitted ecomorph and autoecology in a harsh environment. Austral Ecol 42:677–89.

Porter HT, Motta PJ. 2004. A comparison of strike and prey capture kinematics of three species of piscivorous fishes: Florida gar (*Lepisosteus platyrhincus*), redfin needlefish (*Strongylura notata*), and great barracuda (*Sphyraena barracuda*). Mar Biol 145:989–1000.

Přikryl T, Bannikov AF. 2014. A new species of the Oligocene pomfret fish *Paucaichthys* (Perciformes; Bramidae) from Iran. Neues Jahrb für Geol und Paläontologie - Abhandlungen 272:325–30.

Pybus OG, Harvey PH. 2000. Testing macro-evolutionary models using incomplete

molecular phylogenies. Proc R Soc B Biol Sci 267:2267–72.

R Core Team. 2018. R: A language and environment for statistical computing. R A Lang Environ Stat Comput.

Rabosky DL. 2006. Likelihood methods for detecting temporal shifts in diversification rates. Evolution (N Y) 60:1152–64.

Rabosky DL. 2014. Automatic detection of key innovations, rate shifts, and diversity-dependence on phylogenetic trees. PLoS One 9.

Rabosky DL, Grundler M, Anderson C, Title P, Shi JJ, Brown JW, Huang H, Larson JG. 2014. BAMMtools: An R package for the analysis of evolutionary dynamics on phylogenetic trees. Methods Ecol Evol 5:701–7.

Rabosky DL, Lovette IJ. 2008. Density-dependent diversification in North American wood warblers. Proc R Soc B Biol Sci 275:2363–71.

Rabosky DL, Santini F, Eastman J, Smith SA, Sidlauskas B, Chang J, Alfaro ME. 2013. Rates of speciation and morphological evolution are correlated across the largest vertebrate radiation. Nat Commun 4:1–8.

Rahangdale S, Kumar R, Roul SK, Kannan K, Suresh Kumar K, Ranjith L, Manoj Kumar PP. 2019. Filling missing links in bramids distribution along the indian coast with first record of big tooth pomfret, *Brama orcini* (Perciformes: Bramidae) from the east coast of India. Indian J Geo-Marine Sci 48:654–61.

Rambaut A, Drummond AJ, Xie D, Baele G, Suchard MA. 2018. Posterior summarization in Bayesian phylogenetics using Tracer 1.7. Syst Biol 67:901–4.

Revell LJ. 2012. phytools: An R package for phylogenetic comparative biology (and other things). 2Methods Ecol Evol 3:217–23.

Roff DA, Fairbairn DJ. 2007. The evolution of trade-offs: Where are we? J Evol Biol 20:433–47.

Rohlf FJ, Corti M. 2000. Use of two-block partial least-squares to study covariation in shape. Syst Biol 49:740–53.

Schluter D. 1996. Adaptive radiation along genetic lines of least resistance. Evolution (N Y) 50:1766.

Sheftel H, Shoval O, Mayo A, Alon U. 2013. The geometry of the Pareto front in biological phenotype space. Ecol Evol 3:1471–83.

Shoval O, Sheftel H, Shinar G, Hart Y, Ramote O, Mayo A, Dekel E, Kavanagh K, Alon U. 2012. Evolutionary trade-offs, pareto optimality, and the geometry of phenotype space. Science (80-) 336:1157–61.

Standen EM, Lauder G V. 2005. Dorsal and anal fin function in bluegill sunfish *Lepomis macrochirus*: Three-dimensional kinematics during propulsion and maneuvering. J Exp Biol 208:2753–63.

Stearns SC. 1989. Trade-offs in life-history evolution. Funct Ecol 3:259–68.

Svanbäck R, Wainwright PC, Ferry-Graham LA. 2002. Linking cranial kinematics, buccal pressure, and suction feeding performance in largemouth bass. Physiol Biochem Zool 75:532–43.

Tegge S, Hall J, Huskey S. 2020. Spatial and temporal changes in buccal pressure during prey-capture in the trumpetfish (*Aulostomus maculatus*). Zoomorphology 139:85–95.

Tendler A, Mayo A, Alon U. 2015. Evolutionary tradeoffs, Pareto optimality and the morphology of ammonite shells. BMC Syst Biol 9:1–12.

Thys T. 1997. Spatial variation in epaxial muscle activity during prey strike in largemouth bass (Micropterus salmoides). J Exp Biol 200:3021–31.

Toro E, Herrel A, Irschick D. 2004. The evolution of jumping performance in Caribbean Anolis lizards: Solutions to biomechanical trade-offs. Am Nat 164.

Van Wassenbergh S, Day SW, Hernández LP, Higham TE, Skorczewski T. 2015. Suction power output and the inertial cost of rotating the neurocranium to generate suction in fish. J Theor Biol 372:159–67.

Wainwright PC, Huskey SH, Turingan RG, Carroll AM. 2006. Ontogeny of suction feeding capacity in snook, *Centropomus undecimalis*. J Exp Zool 305A:246–52.

Waltzek TB, Wainwright PC. 2003. Functional morphology of extreme jaw protrusion in Neotropical cichlids. J Morphol 257:96–106.

Wang J, Wainwright DK, Lindengren RE, Lauder G V., Dong H. 2020. Tuna locomotion: a computational hydrodynamic analysis of finlet function. J R Soc Interface 17:20190590.

Webb PW. 1984. Form and function in fish swimming. Sci Am 251:72–83.

Weihs D. 1993. Stability of aquatic animal locomotion. Contemp Math 141:443–61.

Wen L, Weaver JC, Lauder G V. 2014. Biomimetic shark skin: Design, fabrication and hydrodynamic function. J Exp Biol 217:1656–66.

Westneat MW. 1990. Feeding mechanics of teleost fishes (Labridae; Perciformes) – a test of 4-bar linkage models. J Morphol 205:269–95.

Westneat MW. 2004. Evolution of levers and linkages in the feeding mechanisms of fishes. Integr Comp Biol 44:378–89.

Wright S. 1932. The roles of mutation, inbreeding, crossbreeding and selection in

evolution. Sixth Int Congr Genet.

Xu L, Wang X, Li H, Du F. 2018. The complete mitochondrial genome of Perciformes fish (*Brama dussumieri*) from South China Sea. Mitochondrial DNA Part B Resour 3:876–77.

Yatsu A, Nakamura I. 1989. *Xenobrama microlepis*, a new genus and species of bramid fish, from the Subantarctic waters of the South Pacific. Japanese J Ichthyol 36:190–95.

Supplemental Data

Supplemental Table 5.1. Accession numbers for mitochondrial gene data retrieved from GenBank.

Species	COI	CytB
Brama australisA	KT455496.1	FJ435626.1
Brama australisB	KT455495.1	FJ435625.1
Brama australisC		FJ435624.1
Brama bramaA	HQ564257.1	DQ197933.1
Brama bramaB	HQ564256.1	
Brama dussumieriA	MH638791.1	
Brama dussumieriB	MH638770.1	
Brama japonicaA	MH638780.1	AY973048.1
Brama japonicaB	MH638779.1	KF546812.1
Brama japonicaC		KF546811.1
Brama japonicaD		KF546810.1
Brama japonicaE		KF546809.1
Brama orciniA	JN312891.1	
Brama orciniB	KY371231.1	
Caristius fasciatusA	KY033875.1	
Caristius fasciatusB	KU176441.1	
Caristius macropus	AP005999.1	AP005999.1
Eumegistus illustrisA	KU943868.1	
Eumegistus illustrisB	AP012497.1	AP012497.1
Peprilus paruA	MH378570.1	
Peprilus paruB	MH378544.1	
Peprilus paruC	MH378516.1	
Peprilus simillimusA	KY570356.1	FJ264431.1
Peprilus simillimusB	KY570355.1	FJ264297.1
Peprilus simillimusC	KT247733.1	FJ264296.1
Peprilus triacanthusA	KF930245.1	
Peprilus triacanthusB	KC015786.1	
Peprilus triacanthusC	KC015784.1	
Peprilus triacanthusD	KC015782.1	
Peprilus triacanthusE	NC_022502.1	NC_022502.1

Peprilus triacanthusF	AP012518.1	AP012518.1
Platyberyx sp	HQ564263.1	
Pteraclis aesticolaA	KU892878.1	
Pteraclis aesticolaB	NC_022487.1	NC_022487.1
Pteraclis aesticolaC	AP012499.1	AP012499.1
Pterycombus bramaA	GU225016.1	
Pterycombus bramaB	GU225017.1	
Pterycombus bramaC	GU225018.1	
Pterycombus bramaD	GU225019.1	
Pterycombus petersiiA	HQ564259.1	
Pterycombus petersiiB	HQ564260.1	
Taractes asperA	GU440550.1	AY973049.1
Taractes asperB	AP012498.1	AP012498.1
Taractes asperC	NC_022486.1	NC_022486.1
Taractes rubescensA	HQ564480.1	
Taractes rubescensB	KY372191.1	
Taractes rubescensC	KY372190.1	
Taractes rubescensD	NC_028079.1	NC_028079.1
Taractes rubescensE	KR349364.1	KR349364.1
Taractichthys longipinnisA	EF609476.1	EF392625.1
Taractichthys longipinnisB	AB639845.1	
Taractichthys steindachneriA	KY372198.1	
Taractichthys steindachneriB	KY372197.1	
Taractichthys steindachneriC	KY372196.1	
Taractichthys steindachneriD	EF609477.1	
Taractichthys steindachneriE	NC_027858.1	NC_027858.1
Taractichthys steindachneriF	KT153629.1	KT153629.1
Xenobrama microlepisA	KX497161.1	
Xenobrama microlepisB	EF609495.1	

Supplemental Table 5.2. Museum prefixes and lot number for each specimen used in morphometric analyses. Museum prefixes: **MCZ** Museum of Comparative Zoology, Harvard College, **USNM** National Museum of Natural History, **AUNMH** Australian Museum of Natural History.

Lot Number	Species	Life Stage
MCZ_Lot_40826_1	*Brama brama*	Juvenile
MCZ_Lot_40826_2	*Brama brama*	Juvenile
MCZ_Lot_40826_3	*Brama brama*	Juvenile
MCZ_Lot_40826_4	*Brama brama*	Juvenile
MCZ_Lot_40826_5	*Brama brama*	Juvenile
MCZ_Lot_46336	*Brama brama*	Adult
MCZ_Lot_46337	*Brama brama*	Adult
MCZ_uncatalogued	*Brama brama*	Adult
MCZ_148287	*Brama dussumieri*	Adult
MCZ_148287_2	*Brama dussumieri*	Adult
MCZ_Lot_44137	*Brama japonica*	Adult
MCZ_Lot_44138	*Brama japonica*	Adult
MCZ_Lot_44142	*Brama japonica*	Adult
MCZ_Lot_44143	*Brama japonica*	Adult
MCZ_Lot_44144	*Brama japonica*	Adult
MCZ_Lot_46327	*Brama japonica*	Adult
MCZ_Lot_46333	*Brama japonica*	Adult
MCZ_Lot_46334	*Brama japonica*	Adult
MCZ_Lot_46335	*Brama japonica*	Adult
MCZ_Lot_46339	*Brama japonica*	Adult
MCZ_Lot_46340	*Brama japonica*	Adult
MCZ_Lot_46341	*Brama japonica*	Adult
MCZ_Lot_46342	*Brama japonica*	Adult
MCZ_Lot_46343	*Brama japonica*	Adult
MCZ_Lot_46344	*Brama japonica*	Adult
MCZ_Lot_46345	*Brama japonica*	Adult
MCZ_Lot_46356	*Brama japonica*	Adult
MCZ_Lot_46357	*Brama japonica*	Adult
MCZ_Lot_46358	*Brama japonica*	Adult
MCZ_Lot_148066_1	*Brama orcini*	Adult
MCZ_Lot_148066_2	*Brama orcini*	Adult
MCZ_Lot_148381	*Caristius fasciatus*	Juvenile
MCZ_Lot_164024	*Caristius fasciatus*	Adult
USNMFIN27271	*Eumgeistus illustris*	Adult
AUMNH - caught by W. Bolliger, New South Wales 2004	*Pteraclis aesticola*	Adult
AUMNH_34777_001	*Pteraclis aesticola*	Adult
MCZ_Lot_55338	*Pteraclis carolinus*	Juvenile
MCZ_148116_1	*Pterycombus brama*	Juvenile
MCZ_Lot_76100	*Pterycombus brama*	Juvenile
MCZ_Lot_76115	*Pterycombus brama*	Juvenile
MCZ_Lot_76104_3	*Pterycombus brama*	Juvenile
MCZ_Lot_76104_4	*Pterycombus brama*	Juvenile
MCZ_Lot_76104_6	*Pterycombus brama*	Juvenile
MCZ_Lot_76111_2	*Pterycombus brama*	Juvenile
MCZ_Lot_76111_3	*Pterycombus brama*	Juvenile
MCZ_Lot_76111_4	*Pterycombus brama*	Juvenile
MCZ_Lot_76112	*Pterycombus brama*	Juvenile
MCZ_Lot_174129	*Pterycombus brama*	Adult
Fresh, custody of MC Gilbert & SH Huskey	*Pterycombus petersii*	SubAdult
MCZ_Lot_59503	*Pterycombus petersii*	Adult
MCZ_Lot_148056	*Taractes asper*	Juvenile

MCZ_Lot_161671	*Taractes asper*	Juvenile
MCZ_Lot_46347	*Taractes asper*	Adult
MCZ_Lot_46348	*Taractes asper*	Adult
MCZ_Lot_46349	*Taractes asper*	Adult
MCZ_Lot _148060	*Taractes rubescens*	Juvenile
MCZ_Lot_39974	*Taractes rubescens*	Adult
MCZ_Lot_44140	*Taractes rubescens*	Adult
MCZ_Lot_44145	*Taractes rubescens*	Adult
MCZ_Lot_46322	*Taractes rubescens*	Adult
MCZ_Lot_46325	*Taractes rubescens*	Adult
MCZ_Lot_46326	*Taractes rubescens*	Adult
MCZ_Lot_46328	*Taractes rubescens*	Adult
MCZ_Lot_46355	*Taractes rubescens*	Adult
MCZ_Lot_57531	*Taractes rubescens*	Adult
MCZ_Lot_46330	*Taractichthys longipinnis*	Adult
MCZ_Lot_46331	*Taractichthys longipinnis*	Adult
MCZ_Lot_96428	*Taractichthys longipinnis*	Adult
MCZ_Lot_131846	*Taractichthys longipinnis*	Adult
MCZ_ Uncatalogued_sp19-3	*Taractichthys longipinnis*	Adult
MCZ_Lot_150538_1	*Taractichthys steindachneri*	Juvenile
MCZ_Lot_150538_2	*Taractichthys steindachneri*	Juvenile
MCZ_Lot_44139	*Taractichthys steindachneri*	Adult
MCZ_Lot_44141	*Taractichthys steindachneri*	Adult
MCZ_Lot_44147	*Taractichthys steindachneri*	Adult
MCZ_Lot_46324	*Taractichthys steindachneri*	Adult
MCZ_Lot_46329	*Taractichthys steindachneri*	Adult
MCZ_Lot_46346	*Taractichthys steindachneri*	Adult
MCZ_Lot_46350	*Taractichthys steindachneri*	Adult
MCZ_Lot_46351	*Taractichthys steindachneri*	Adult
MCZ_Lot_46352	*Taractichthys steindachneri*	Adult
MCZ_Lot_46353	*Taractichthys steindachneri*	Adult
MCZ_Lot_46354	*Taractichthys steindachneri*	Adult
MCZ_Lot_57530	*Taractichthys steindachneri*	Adult
MCZ_Lot_57532	*Taractichthys steindachneri*	Adult
MCZ_Lot_57533	*Taractichthys steindachneri*	Adult
MCZ_Lot_57534	*Taractichthys steindachneri*	Adult
MCZ_Lot_57535	*Taractichthys steindachneri*	Adult
MCZ_Lot_172796	*Taractichthys steindachneri*	Adult

Supplemental Table 5.3. Summary statistics output from the BiSSE analysis. Trait state 0 indicates absence of elongated fins, state 1 indicates presence. Speciation rate (λ0) | Speciation rate (λ1) | Extinction rate (μ0) | Transition rate (q) | Posterior probability (p).

Parameter	lambda0	lambda1	mu0	q01	p
Min.	0.01203	0.0001799	3.00E-08	2.67E-05	-62.57
1stQu.	0.03861	0.0260566	4.64E-03	3.62E-03	-50.37
Median	0.04762	0.0394374	1.11E-02	6.12E-03	-49.15
Mean	0.04963	0.0438941	1.53E-02	7.39E-03	-49.51
3rdQu.	0.05858	0.05777	2.14E-02	9.89E-03	-48.25
Max.	0.12866	0.1810267	1.10E-01	4.36E-02	-46.84

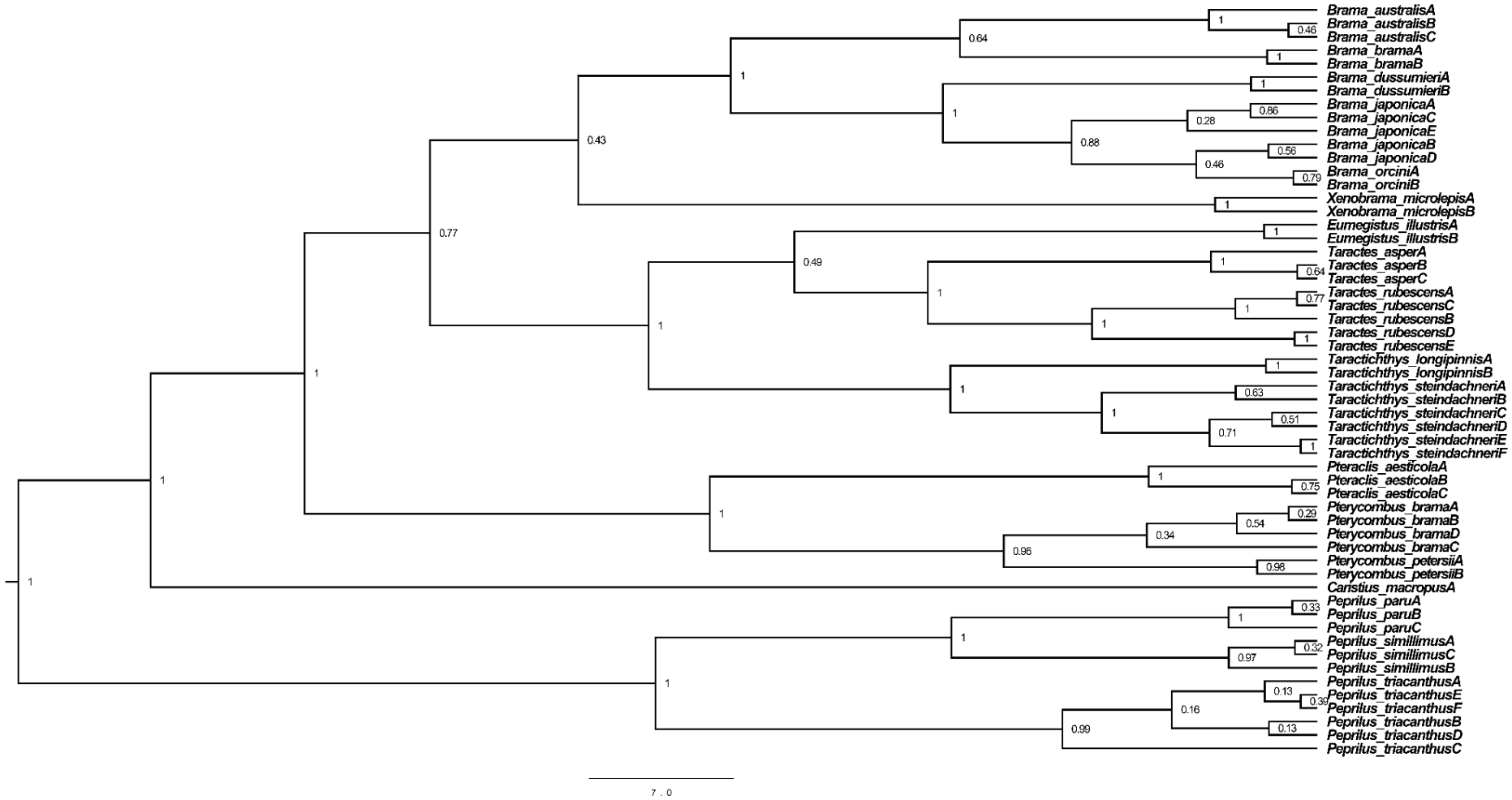

Supplemental Figure 5.1. Consensus of the most parsimonious topologies of the combined 640bp COI and 1141 Cytb. Values for posterior support are provided at the base of each node. For additional details, see main text.

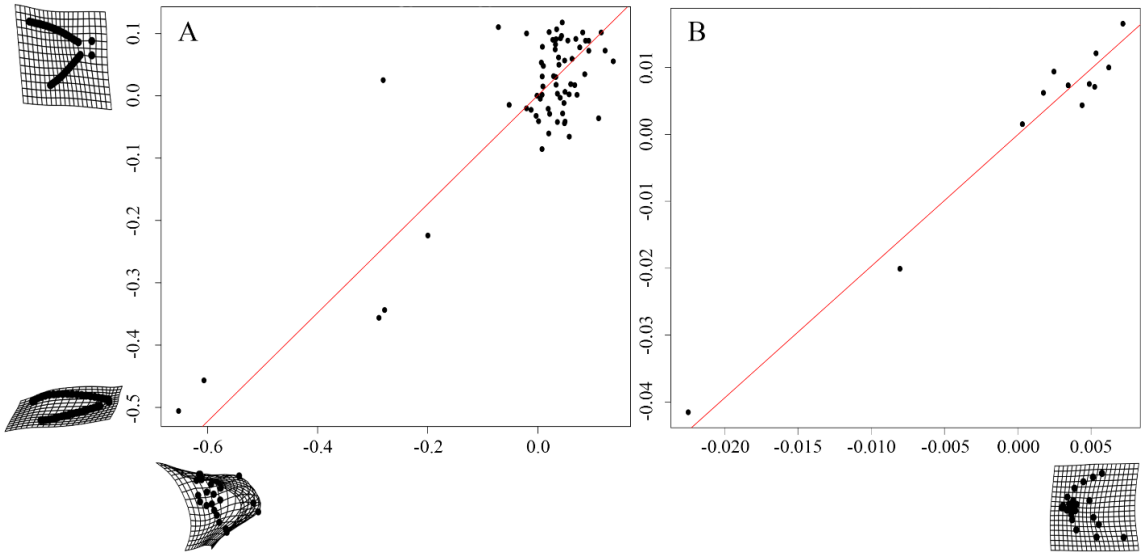

Supplemental Figure 5.2. Linear regression of two block partial least squares test assessing the integration of head (x-axis) and body (y-axis) shape. Covariation of head and body shape among **(A)** individuals, without accounting for the phylogeny, and **(B)** after accounting for the phylogeny.

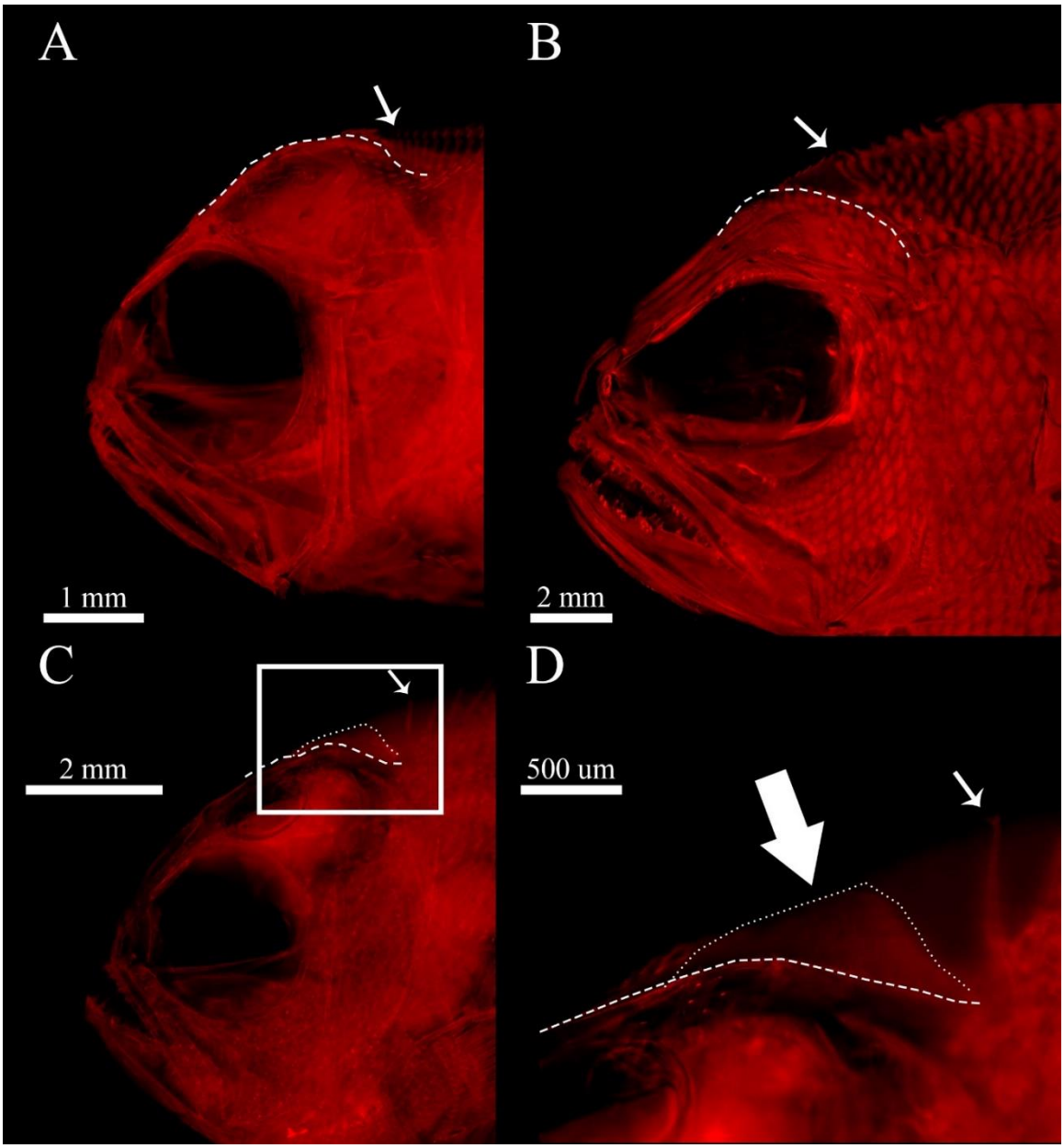

Supplemental Figure 5.3. Cleared and alizarin stained Pterycombus brama larvae **A**) juvenile **B**) and matured Brama dussumieri larvae (**C, D**) under fluorescent light. Dashed lines represent the dorsal profile of the neurocranium, while dotted lines outline the supraoccipital crest. Pterycombus brama larvae and juveniles lack any conspicuous anatomical feature indicating the development of a supraoccipital crest. Although not noticeable in non-cleared and stained specimens, pterygiophores (indicated by the smaller arrows) begin to form above the neurocranium at least as early as larval stages. Brama dussumieri larvae possess a relatively robust supraoccipital crest (**D**, indicated by the large arrow) and pterygiophores appear to be in their expected positions, well posterior to the back of the neurocranium.

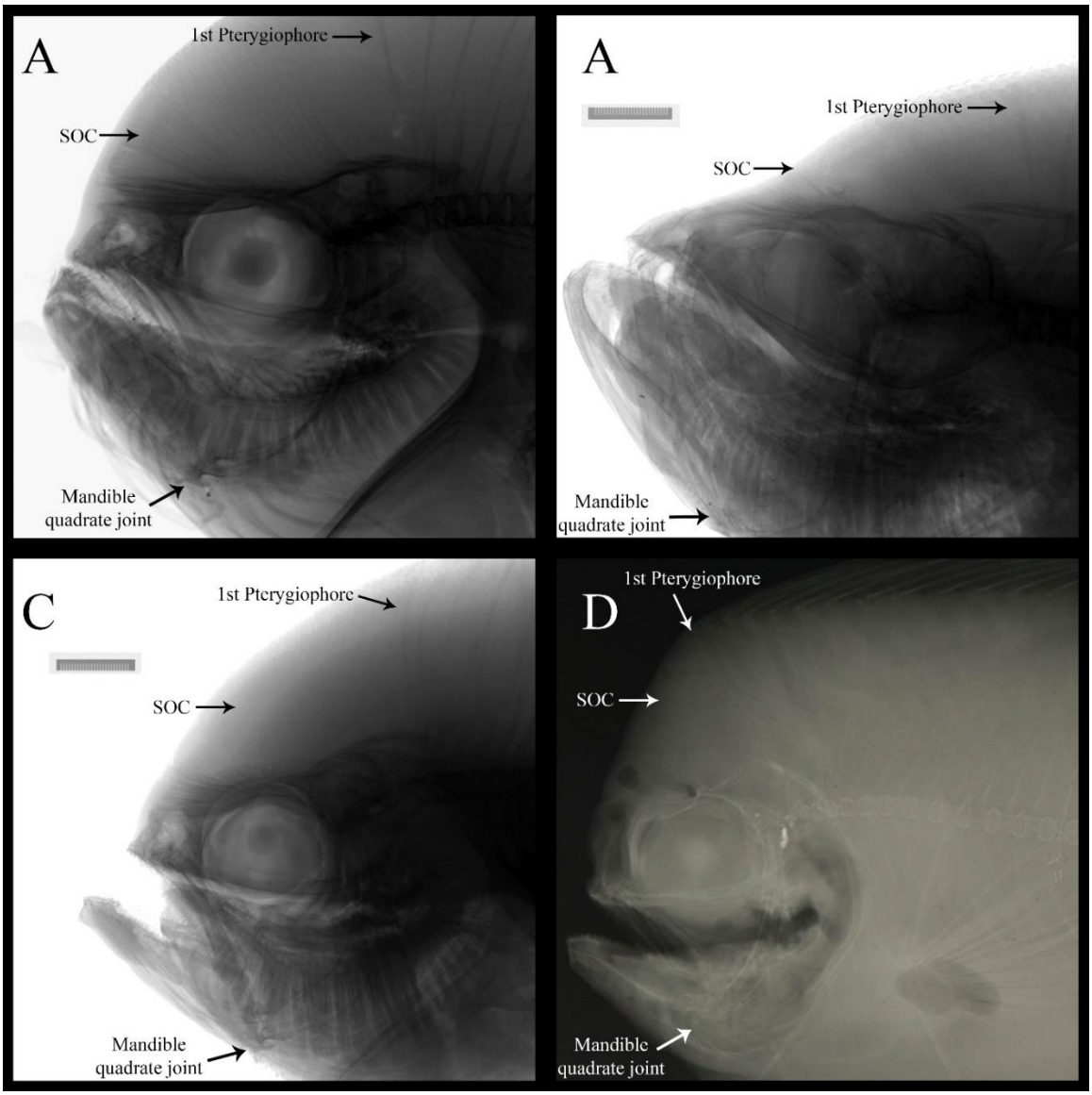

Supplemental Figure 5.4. Craniofacial x-rays of three bramid genera and Caristius. **A)** Brama japonica (MCZ Lot 44142), **B)** Taractes rubescens (MCZ Lot 46326), **C)** Taractichthys steindachneri (MCZ Lot 172796), and **D)** Caristius fasciatus (MCZ Lot 164024). X-ray images courtesy of Harvard Museum of Comparative Zoology. Image panels A-C provided by Meaghan H. Sorce, image panel D taken by Andrew D. Williston. Museum of Comparative Zoology. X-ray photography is ©President and Fellows of Harvard College.

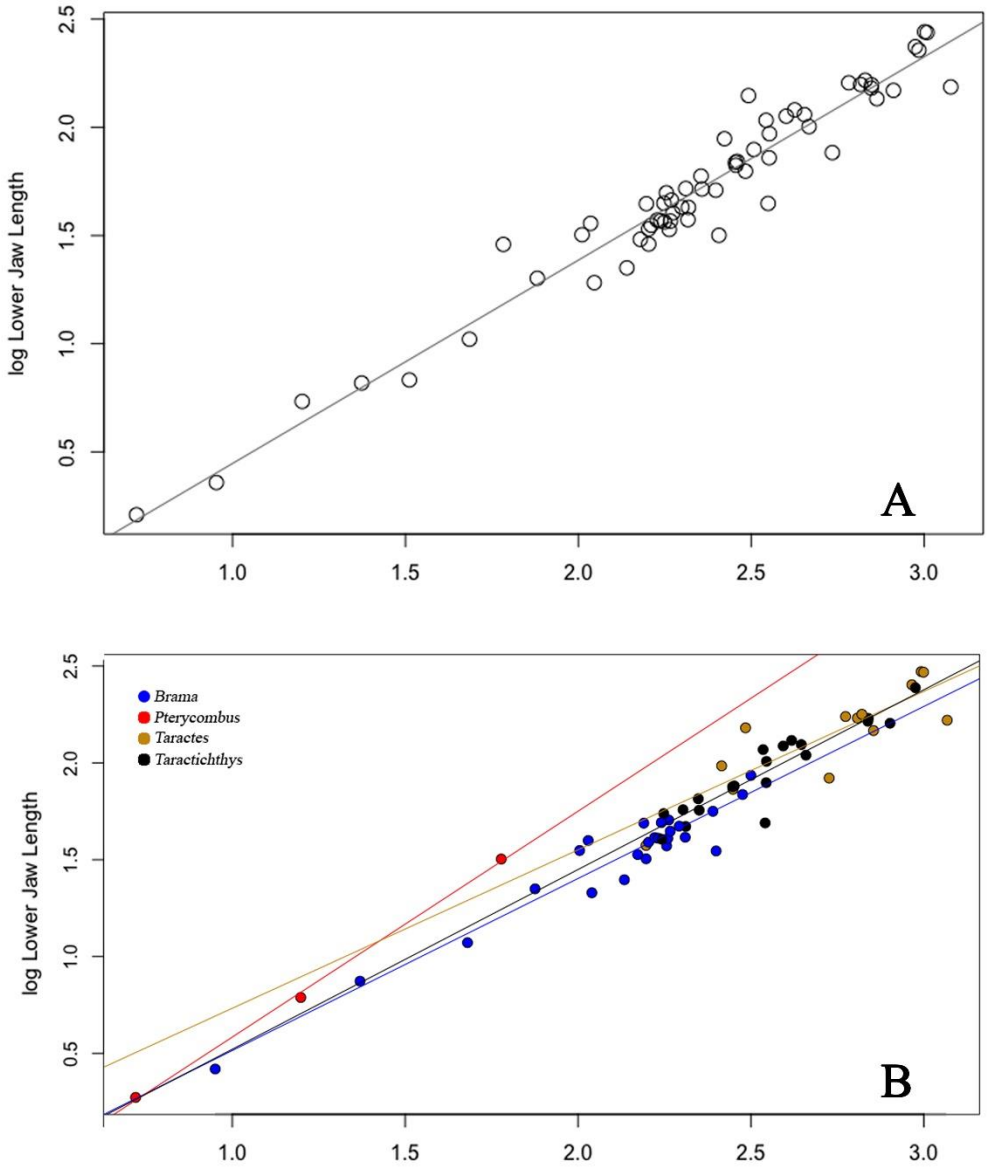

Supplemental Figure 5.5. Linear regression of jaw length x head length across all adult bramid specimes with an n ≥3. **A**) Linear regression of all bramid taxa together. **B**) Linear regression of each bramid genus in comparison to the other three.

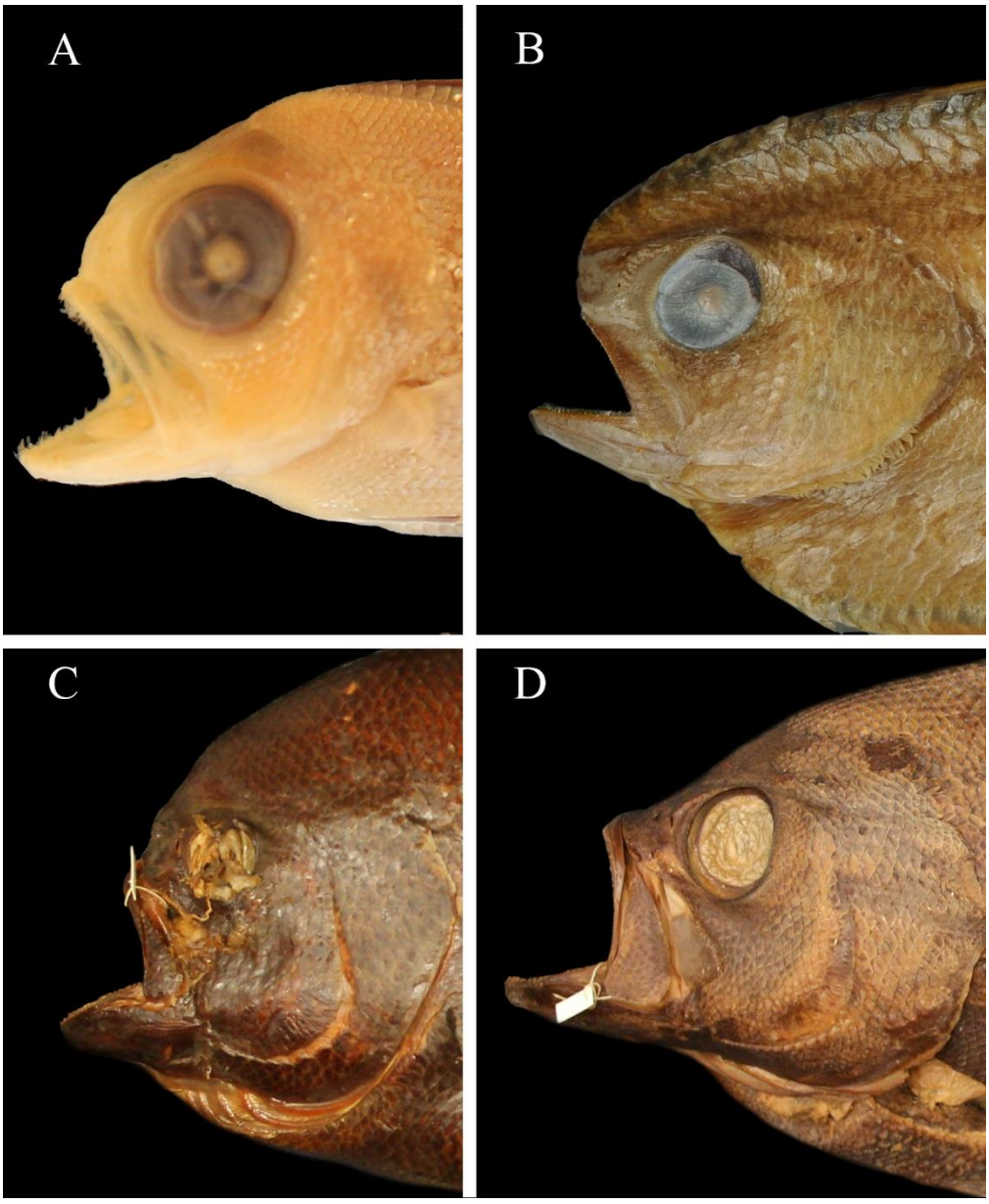

Supplemental Figure 5.6. Images of four fixed bramid specimens with mouths open in a fixed state. **A)** Pterycombus brama (MCZ Lot 76114), **B)** Pteraclis velifera (AUMNH I.21126-002), **C)** Brama japonica (MCZ Lot 46346), and **D)** Taractes rubescens (MCZ Lot 46325). Image panels A,C,D taken by MCG and CSL, image panel B taken by Kerryn Parkinson, Australian Museum.

6. CHAPTER 6

BREAKING CONSTRAINTS: THE DEVELOPMENT AND EVOLUTION OF EXTREME FIN MORPHOLOGY IN THE BRAMIDAE

Michelle Gilbert[1], Catherine S. Lerose[2,3], Andrew J. Conith[2], R. Craig Albertson[2]

1 Organismic and Evolutionary Biology Graduate Program, University of Massachusetts, Amherst, MA 01003

2 Biology Department, Morrill Science Center, University of Massachusetts, 611 North Pleasant Street, Amherst, MA 01003

3 Fisheries, Wildlife, And Conservation Biology Graduate Program, North Carolina State University, Raleigh, North Carolina, 27695

PUBLISHED IN: Evolution and Development

FULL CITATION: Gilbert, M, CS Lerose, AJ Conith, RC Albertson. 2022. Breaking constraints: the development and evolution of extreme fin morphology in the Bramidae. *Evolution and Development.*

Abstract

The developmental process establishes the foundation upon which natural selection may act. In that same sense, it is inundated with numerous constraints that work to limit the directions in which a phenotype may respond to selective pressures. Extreme phenotypes have been used in the past to identify tradeoffs and constraints and may aid in recognizing how alterations to the Baupläne can influence the trajectories of lineages. The Bramidae, a family of Scombriformes consisting of 20 extant species, are unique in that five species greatly deviate from the stout, ovaloid bodies that typify the bramids. The Ptericlinae, or fanfishes, are instead characterized by relatively elongated body plans and extreme modifications to their medial fins. Here, we explore the development of Bramidae morphologies and examine them through a phylogenetic lens to investigate the concepts of developmental and evolutionary constraints. Contrary to our predictions that the fanfishes had been constrained by inherited properties of an ancestral state, we find that the fanfishes exhibit both increased rates of trait evolution and differ substantially from the other bramids in their developmental trajectories. Conversely, the remaining bramid genera differ little, both among one another and in comparison to the sister family Caristiidae. In all, our data suggest that the fanfishes have broken constraints, thereby allowing them to mitigate trade-offs on distinctive aspects of morphology.

Introduction

Development must be flexible enough to create variation upon which natural selection acts, but also rigid enough to limit the phenotype from deviating into a maladaptive space (Darwin, 1859; Wright, 1932; Huxley, 1942; Waddington, 1942, 1956; Maynard Smith et al., 1985). Systems that constrain, maintain, or promote phenotypic variation occur at numerous biological levels, including genetic (Crump et al., 2004; Swartz et al., 2012; Uller et al., 2018), developmental (Cheverud, 1984; Wagner, 1988; Klingenberg, 2005; Green et al., 2017; Uller et al., 2018), behavioral (Holekamp et al., 2013), morphological (Larouche et al., 2018; Evans et al., 2021), physiological (Malcolm and Dunbrack, 1986; Glass, 2003; Briffa and Sneddon, 2007), and evolutionary (Jacob, 1977; Conway Morris, 2003; Pigliucci and Preston, 2004; Schwenk and Wagner, 2004). Constraints, however, regardless of their position in these various biological levels, can be broken (Galis and Metz, 2007; Minelli and Fusco, 2019). A consequence of breaking a constraint may include increased variability, which in turn may allow the population to fluctuate more freely in phenotypic space (McGhee, 2007; Sheftel et al., 2013), providing new variants for selection to act on.

As with most complex biological phenomena, constraints range from rigid and unbending, lest a lethal phenotype is expressed, to flexible, forgiving, and holistically adaptive (Jacob, 1977; Wagner and Misof, 1993; Klingenberg, 2005). Constraints may also be viewed on a different, but not mutually exclusive, spectrum from universal to local. In this view, universal constraints are a result of the laws of physics or the physical, chemical, or functional properties of a material (Jacob, 1977; Maynard Smith et al., 1985). Alternatively, local constraints are limited to some taxonomic level, such as the organization of a Baupläne (Maynard Smith et al., 1985), which result from biases in

development that limit the variants that it can express (Gould, 1980; Cheverud, 1984; Maynard Smith et al., 1985; Emlen, 2000). Thus, evolution requires a delicate balance between the generation of sufficient levels of variation for selection to act upon but limiting it enough so that function is not compromised (Pigliucci and Preston, 2004; Schwenk and Wagner, 2004). The history of evolutionary biology has largely been dominated by seeking out mechanisms that precipitate change. However, despite billions of years of evolution, there remain obvious lacunae in morphological space that can provide invaluable insights into the flip side of the evolutionary coin (Gould and Lewontin, 1979; Gould, 1980; Maynard Smith et al., 1985; Arnold, 1992; Schwenk and Wagner, 2004; Holekamp et al., 2013).

It is increasingly recognized that characterizing constraints inherent in developmental processes can contribute to a better understanding of evolutionary processes (Gould, 1980; Schlichting and Pigliucci, 1998; Pigliucci and Preston, 2004; Schwenk and Wagner, 2004; Holekamp et al., 2013). A notable challenge in doing so, however, is differentiating constraints that are imposed by the developmental process from those that arise due to selection (Gould, 1980; Maynard Smith et al., 1985). This difficulty is further exacerbated due to the paradoxical nature of constraints, as constraints limit the phenotypes that natural selection may act upon, but they are themselves products of natural selection (Schwenk and Wagner, 2004). Nevertheless, routinely used methods for identifying developmental constraints include documenting evolutionary stasis over time, as well as identifying unoccupied regions of theoretical morphospace (Vavilov, 1922; Spurway, 1949; Maynard Smith et al., 1985; Wagner and Schwenk, 2000; Schwenk and Wagner, 2001, 2004). Further, it has been suggested that

by comparing ontogenetic trajectories within a clade, one can garner evidence for developmental constraint, which has been predicted to manifest as parallel trajectories (Gould and Lewontin, 1979; Gould, 1980; Maynard Smith et al., 1985; Schwenk and Wagner, 2004)

The study of constraints can be assisted by examining 'extreme' traits, because they are often the product of breaking one or more constraints and precipitating additional constraints. Such traits may therefore be viewed through the lens of trade-offs. For example, bats (Chiroptera), being the only extant mammals to have evolved powered flight, exhibit substantial constraints in body size (Jones, 1994; Moyers Arévalo et al., 2020). Other trade-offs in bats include those between the energetic demands associated with both echolocation and vision (Thiagavel et al., 2018). Similarly, beetle weaponry (i.e., horns and extreme mandibles) has evolved several times across the Coleoptera, and are generally used for male sparring (Emlen, 2000). The size of beetle mandibles and horns varies greatly, and can force trade-offs in other energetic systems, such as flight (Goyens et al., 2015), which ultimately constrains the weight such weaponry can attain. Beetle weaponry also influences the size at which eyes (Nijhout and Emlen, 1998), or wings (Kawano, 1997), can develop. While observations at adult stages can provide insights into trade-offs (e.g., negative correlations between traits), evaluating ontogenetic pathways can inform hypotheses as to *how* (mechanistically) specific traits are correlated with others (Emlen, 2000). Here, we aim to explore the ontogeny and evolution of an array of ecomorphological traits in a group of open water, marine fishes, in which an extreme morphology has evolved.

Bramidae, while modest in species diversity (n = 20), is a relatively understudied group of fishes that offer unique opportunities to investigate evolutionary constraints, and how the development of extreme morphologies can influence the evolvability of other traits (Gilbert et al., 2021). The "fanfishes" refer to a bramid lineage, the Pteraclinae, that includes two genera (*Pterycombus* and *Pteraclis*), characterized by an extreme exaggeration of the medial fins (Gilbert et al., 2021). Ontogenetic trajectories of select traits have been previously studied in this group (Mead, 1972), but data were unable to be interpreted through a phylogenetic lens, rendering hypotheses about evolutionary relationships and constraints untestable. Here, we expand on this previous work (e.g., Mead, 1972; Gilbert et al., 2021) by comparing anatomical divergence across the Bramidae at early and adult life-history stages in a phylogenetic context. Specifically, we will assess the degree to which the evolution of extreme fin morphologies has limited the evolution of other ecomorphological traits. We will first compare juvenile and adult morphospace with respect to patterns and magnitudes of variability. Similar morphospaces would demonstrate that species-specific bramid morphologies arise early in ontogeny, consistent with limited constraints acting on early developmental stages. Next, we will compare ontogenetic trajectories for specific traits among bramid taxa. Divergent (i.e., non-parallel) trajectories would suggest limited constraints acting on later development. Finally, we will compare rates of evolution across the same functionally and ecologically relevant traits, to assess the degree to which any putative developmental constraints are associated with evolutionary patterns. Collectively, these results will provide insights into how an unusual trait, in this case extreme exaggeration of the medial fins, has influenced the development and evolution of the Bramidae.

Methods

Morphometric Data Acquisition

We collected specimens from the Harvard Museum of Comparative Zoology (MCZ, Cambridge, MA, USA) and Smithsonian National Museum of Natural History (NMNH, Washington DC, USA) with additional larval samples from the MCZ, as well as numerous adult specimens from the National Museum of Nature and Science (NMNS, Taito City, Tokyo, Japan) and the Museum of Natural History (Sydney, Australia) that we could not have otherwise acquired in the United States. In total our sampling covered all seven bramid genera for the adult analyses and six for the juvenile (n = 163, Supplemental Table 1).

Methods for acquiring both geometric morphometric data and linear measures are described in detail in Gilbert et al (2021). In short, the left lateral surfaces of specimens were imaged and then digitized using `STEREOMORPH` (Olsen and Westneat, 2015) in R (R Core Team, 2018). The landmark scheme used was identical to that used in Gilbert et al (2021) to cross reference results and expand on testable hypotheses concerning the evolution of the Bramidae. Raw landmark data were subjected to generalized Procrustes analyses (GPA; Boas, 1905; Sneath, 1967; Goodall, 1991) and then the resulting shape data to several statistical tests. Linear measures were then taken on anatomical units of interest using those same 2-D images through MorphoJ (Klingenberg, 2011)

Geometric Morphometric Analyses

To assess differences in shape trajectories throughout ontogeny, we used geometric morphometric methods designed to assess changes in phenotypes and compare differences among group phenotype trajectories (Collyer and Adams, 2013; Collyer et al., 2015). While we were able to perform this analysis with previously published data, the current and much expanded dataset included the addition of numerous difficult to acquire

specimens (e.g., genus *Pteraclis*), allowing for a much deeper and holistic dive into the nuances of bramid shape trajectories. Differences in trajectories among genera were quantified using the `trajectory.analysis` function (Collyer and Adams, 2013; Collyer et al., 2015) in `GEOMORPH` v3.3.6 (Adams et al., 2015, 2018). This function utilizes ANOVA and a `RRPP` v0.4.1 (Collyer and Adams, 2018) to calculate differences in trajectory path distances. Our final model read as SHAPE ~ GENUS * STAGE, ~ CENTROID SIZE to first account for variation attributed to size and was subjected to a total of 10,000 random permutations. To visualize the degree of morphological change from the juvenile to adult stages in all genera, we plotted the first two axes of a principal component analysis (PCA) of all genera across the two stages of development.

Phylogenetic Comparative Methods

By pruning the tree created by Gilbert et al (2021), we produced two smaller trees, one to include genera available in juvenile dataset and another that would include all seven bramid genera and a representative of the closely related sister taxa from Caristiidae, *Caristius*. These two topologies served as the foundation for subsequent comparative analyses for both linear measures and geometric morphometric data and allowed us to assess trends in both the juvenile and adult datasets independently for when genera were not available for both (e.g., *Xenobrama*). For more details, see Gilbert et al (2021).

To create a phylomorphospace for both the juvenile and adult datasets, we utilized both `GEOMORPH` v3.3.6 (Adams et al., 2014, 2018) and `PHYTOOLS` v0.6-60 (Revell, 2012) to map principal component data derived from morphology to the associated phylogenetic relationships. We then calculated mean PC1 and PC2 scores for whole body shape morphology, independently in both adults and juveniles to determine rates of body

shape evolution in both stages. This was accomplished using the BAMM (Bayesian analysis of macroevolutionary mixtures) software package (Rabosky, 2014; Rabosky et al., 2014). Each analysis utilized four reversible MCMC simulations for $1x10^7$ generations with sampling occurring every 1,000 generations. Prior distributions were estimated via BAMMtools (Rabosky et al., 2014) in R (R Core Team, 2018). This was repeated for both PC1 and PC2 means for the juveniles (βInitPrior = 1506.443 & 2401.617, βShiftPrior = 0.020 & 0.020) and adults (βInitPrior = 419.192 & 2399.823, βShiftPrior = 0.020 & 0.020). BAMMtools (Rabosky et al., 2014) was then used to analyze outputs.

Linear Measures

In total, we regressed against standard length the linear measurements of nine traits that we predicted would be constrained or directly altered by extreme medial fin morphology to calculate the phenotypic trajectories of each trait across among the genera. Using the package emmeans (Lenth, 2020) in R (R Core Team, 2018), we then tested for differences in slopes between genera for each of the nine traits of interest. The R package lattice v0.20-35 (Sarkar, 2017) was then used to map the resulting p-values in a visually representative way to observe instances of significance. Due to our inability to acquire juvenile *Xenobrama* specimens, *Xenobrama* data were excluded from these analyses.

Lastly, we wanted to determine if noticeable differences in evolutionary rates across the nine traits were detectable in the adult dataset. To this end, we utilized the same methods in the previous section to assess evolutionary rates in PC1 and PC2 scores by first calculating mean ratios of each trait against standard length. Using those mean ratios, we used BAMM (Rabosky, 2014; Rabosky et al., 2014) to calculate rates of trait

evolution across the Bramidae, each implementing $1x10^7$ generations and sampling once every 1000 generations. Prior distributions for each of the nine traits were determined via `BAMMtools` (Rabosky et al., 2014). Priors were as follows: anal fin length (βInitPrior = 407.215, βShiftPrior = 0.020), body depth (βInitPrior = 1391.950, βShiftPrior = 0.020), breast length (βInitPrior = 8264.754, βShiftPrior = 0.020), dorsal fin length (βInitPrior = 340.709, βShiftPrior = 0.020), head length (βInitPrior = 2615.804, βShiftPrior = 0.020), lower jaw length (βInitPrior = 9972.032, βShiftPrior = 0.020), nape length(βInitPrior = 1002.481, βShiftPrior = 0.020), orbit diameter (βInitPrior = 53675.542, βShiftPrior = 0.020), pelvic to anal fin length (βInitPrior = 2129.310, βShiftPrior = 0.020). `BAMMtools` (Rabosky et al., 2014) was used to analyze outputs. We then quantified differences in evolutionary rates between the fanfishes and remaining bramids for all nine linear measures. To accomplish this, we calculated the Brownian rate of evolution (σ^2) for all traits under a null model that fixed the rate across the tree and compared this to a model that allowed the fanfishes to exhibit a different rate of trait evolution to the remaining bramids. We statistically assessed differences in log likelihood scores between the single and multi-group models via a chi-squared (X^2) test (O'Meara et al., 2006). To compare rates we used the `brownie.lite` function from the R package `phytools` v0.6-60 (Revell, 2012), and gained a distribution of `output` parameters by running the analysis over a previously generated posterior distribution of 1000 phylogenetic trees (Gilbert et al., 2021) to account for phylogenetic uncertainty. To assign taxa to bramid and fanfish groups we used the Stochastic Mutational Mapping on Phylogenies (SIMMAP) tool (Bollback, 2006) from `phytools` and simulated one map for each of

the 1000 trees. We illustrate the distribution of σ^2 parameters as a violin plot and report the median values given their skewed distributions.

Results

Differences in whole body shape morphology are detectable during early stages of ontogeny and largely mirror adult patterns

We initially sought to assess and compare patterns of shape variation in juvenile and adult bramids. For juveniles, size ($Z = 4.631$, $P = < 0.0001$), genus ($Z = 7.536$, $P = < 0.0001$), and the size:genus interaction ($Z = 4.231$, $P = < 0.0001$) were significant. While size explained a substantial percentage of the variation ($R^2 = 0.162$), it explained much less than the effect of genus ($R^2 = 0.497$). The interaction term explained the least amount of variation ($R^2 = 0.043$). For the adults, a similar pattern was revealed, with size ($Z = 5.183$, $P = < 0.0001$), genus ($Z = 8.964$, $P = < 0.0001$), and the interaction ($Z = 6.263$, $P = < 0.0001$) being significant, but genus ($R^2 = 0.724$) had greater explanatory power than size alone ($R^2 = 0.122$). Like juveniles, the interaction term was the weakest for adults ($R^2 = 0.018$).

Subsequent pairwise comparisons of juvenile shape data across genera revealed that 15/21 comparisons were significantly different (Table 1). All comparisons to the fanfishes, *Pterycombus* and *Pteraclis*, were significantly different (including to one another; $P = 0.005$) and all but one comparison to the sister group, *Caristius*, was significant (comparison with *Brama*; $P = 0.236$). The greatest differences in morphological shape were always between the fanfishes and the other bramids, with the comparison between *Pteraclis* and *Taractes* being the most substantial ($Z = 8.458$). With the adult data, we found a comparable number of significant comparisons, at 13/21 (Table 1). Like the juvenile data, all comparisons to fanfishes were significant, apart from the comparison between *Pterycombus* and *Caristius* ($P = 0.065$), and the strongest

Table 6.1. Results of Procrustes MANOVA across all bramid juveniles (above) and adults (below). MANOVA was conducted with 10,000 permutations of residual values (Randomized Residual Permutation Procedure, RRPP). Effect sizes are above, and p-values are below the diagonal. Bolded p-values and z-scores indicate significant differences in mean shapes between species. For significance testing, $\alpha = 0.05$.

JUVENILES	*Brama*	*Caristius*	*Eumegistus*	*Pteraclis*	*Pterycombus*	*Taractes*	*Taractichthys*
Brama		**2.7059**	-0.4984	**7.2863**	**5.9423**	**1.8385**	0.4412
Caristius	**0.0139**		0.64802	**2.7324**	**2.1407**	**2.7261**	**2.0124**
Eumegistus	0.6400	0.2362		**4.10256**	**2.3850**	0.0659	-0.5665
Pteraclis	**0.0001**	**0.0150**	**0.0002**		**3.4702**	**8.4578**	**7.7505**
Pterycombus	**0.0002**	**0.0382**	**0.0280**	**0.0050**		**7.8091**	**6.3575**
Taractes	0.0585	**0.0130**	0.4057	**0.0001**	**0.0001**		-0.0455
Taractichthys	0.2738	**0.0459**	0.6724	**0.0001**	**0.0001**	0.4413	
ADULTS							
Brama		1.0114	**-0.0109**	**13.2629**	**5.7131**	**3.6393**	**2.4933**
Caristius	0.0716		0.3642	**3.2191**	1.4545	1.0068	0.9614
Eumegistus	0.3321	0.2121		**5.8061**	**2.6351**	0.0534	0.3484
Pteraclis	**0.0001**	**0.0236**	**0.0011**		**3.2501**	**13.7096**	**14.9737**
Pterycombus	**0.0003**	0.0646	**0.0277**	**0.0087**		**5.9612**	**5.9631**
Taractes	**0.0051**	0.0763	0.3182	**0.0001**	**0.0001**		**4.4957**
Taractichthys	**0.0245**	0.0759	0.2080	**0.0001**	**0.0003**	**0.0018**	

morphological differences (based on Z-scores) were found in the comparisons with *Pteraclis*, with the most notable comparisons being against *Taractichthys* (Z = 14.397), *Brama* (Z = 13.263), and *Taractes* (Z = 13.710). Unlike the juvenile data, however, only 1/6 comparisons were significant with *Caristius*, suggesting that bramid shape diverged from that of its sister taxon over ontogeny. However, given that we only have a single specimen for juvenile and adult *Caristius* data, we are limited in what can be confidently said regarding comparisons to the outgroup.

Patterns of morphological variation are similar between juvenile and adult stages

We next wanted to see if patterns of morphological variation held between early and late ontogenetic windows in a phylogenetic context. To this end, we conducted a principal component analysis (PCA) of both juvenile and adult body shapes, which

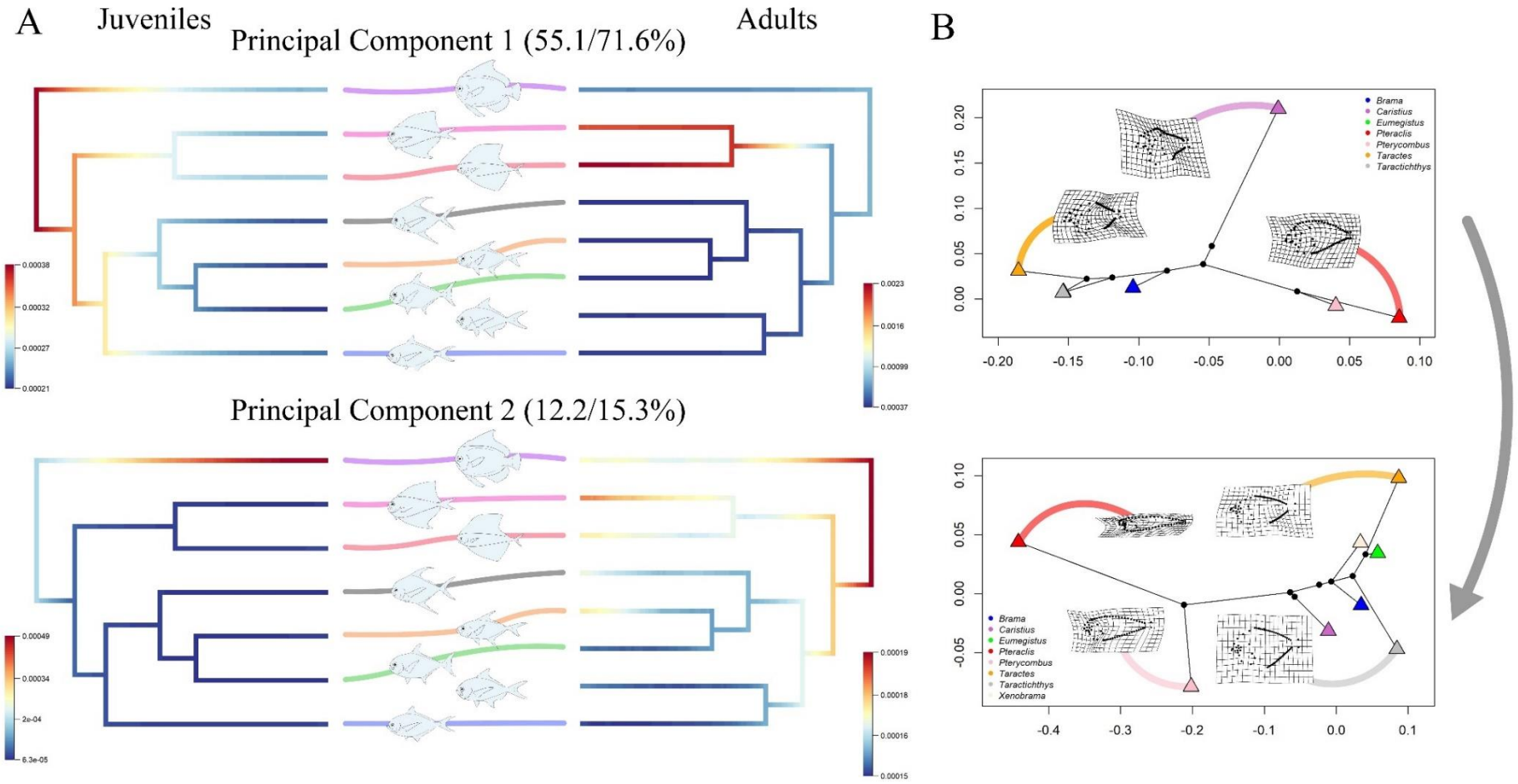

Figure 6.1. (A) Left column portrays the juvenile rates across the phylogeny and are aligned with corresponding adult rates on the phylogeny to the right. Curved, colored lines connect the two sides and colors are representative of the genera throughout the manuscript. Genera read, from top to bottom, *Caristius, Pterycombus, Pteraclis, Taractichthys, Taractes, Eumegistus, Xenobrama* (not present in juvenile analyses), and *Brama*. Warm colors represent faster rates of morphological evolution while cool colors represent slower. **(B)** Phylomorphospace of whole-body shape morphology and the transition of morphospace through ontogeny. Deformation grids are provided for the extremes. Triangles represent overall group means.

revealed that much of the variation, at both stages, was limited to the first two axes (Figure 1A/B). These PC scores were then utilized for two purposes. First, to estimate rates of whole-body shape evolution across the Bramidae, and second, to qualitatively assess distribution of genera in a phylomorphospace.

For PC1, rates of body shape evolution across taxa were similar between stages (Figure 1A), with relatively higher rates of evolution observed in the fanfishes and *Caristius* compared to other lineages; however, the difference in rates between adult fanfishes (notably *Pteraclis*) and the other bramids was an order of magnitude higher in adults than juveniles, which indicates that divergent body shapes in fanfishes are elaborated over ontogeny. For PC2, rates of body shape evolution across taxa were distinct between stages. Among juveniles, rates of evolution were relatively low and similar across bramid species. The one exception to this being *Caristius*, which showed a greatly elevated rate of morphological evolution. In adults, PC2 rates were higher in adult fanfishes, specifically *Pterycombus*, compared to most other bramids, which is similar to what was observed for PC1. Unlike PC1 rates, however, the differencein PC2 between fanfishes and other bramid genera was not as striking.

The distribution of bramid genera across morphospace showed a clear phylogenetic signal for both juveniles and adults (Figure 1B). In both instances, the major axis of variation (i.e., PC1) described difference in medial fin length, and separated fanfishes from the other bramids, with the sister group, *Caristius*, occupying an intermediate position. As juveniles, bramid species exhibited little variation along PC2, and this axis separated bramids from their sister group, *Caristius*, a pattern that is reflected in estimates of evolutionary rates (Figure 1A). As adults, genera became more

disparately distributed throughout morphospace, especially along PC2, which described variation in body depth, with *Taractes* and *Tarachtichthys* showing extreme shapes along PC2.

Table 6.2. Pairwise comparisons of trajectory path distances from `trajectory.analysis`. MANOVA was conducted with 10,000 permutations of residual values (Randomized Residual Permutation Procedure, RRPP). Effect sizes are above, and p-values are below the diagonal. Bolded p-values and z-scores indicate significant differences in mean shapes between species. For significance testing, $\alpha = 0.05$.

	Brama	*Caristius*	*Eumegistus*	*Pteraclis*	*Pterycombus*	*Taractes*	*Taractichthys*
Brama		0.4476	-0.6371	**6.9291**	**1.4562**	-0.6045	0.8271
Caristius	0.2221		0.1629	0.3577	-0.3468	0.3592	-0.1183
Eumegistus	0.7303	0.2983		**1.9509**	-0.8960	-0.7594	-0.6846
Pteraclis	**0.0001**	0.2311	**0.0404**		**4.1031**	**7.2094**	**5.0424**
Pterycombus	**0.0889**	0.5759	0.869	**0.0010**		0.4189	-1.1508
Taractes	0.6734	0.2455	0.8153	**0.0001**	0.2715		0.3712
Taractichthys	0.1614	0.4291	0.7663	**0.0008**	0.9830	0.2631	
Absolute Distances	0.0873	0.1751	0.1101	0.2466	0.1266	0.0971	0.1261

The fanfishes exhibit divergent ontogenetic trajectories in body shape

We next combined the juvenile and adult datasets to compare the phenotypic trajectories of each genus. The results of pairwise comparisons of trajectory path distances revealed that *Pteraclis* had a significantly greater distance (|0.2466|) than any other genera, except the sister group, *Caristius* (|0.1751|; Table 2). Of the bramids, *Pteraclis* exhibited twice the distance as any other genus, with *Pterycombus* and *Taractichthys* exhibiting the second greatest distances (|0.1266| & |0.1261|, respectively). The greatest difference in distance was between *Pteraclis* and *Taractes* (Z = 7.2094), with the comparison between *Pteraclis* and *Brama* being close behind (Z =6.9291). Despite exhibiting the second greatest distance in morphospace, *Caristius'* ontogenetic trajectory was not significantly different from any bramid genus, likely due to a very low sample size.

We next wanted to visualize these genera-specific developmental trends in morphospace. Using the first two PC scores from a PCA, we plotted the juvenile and

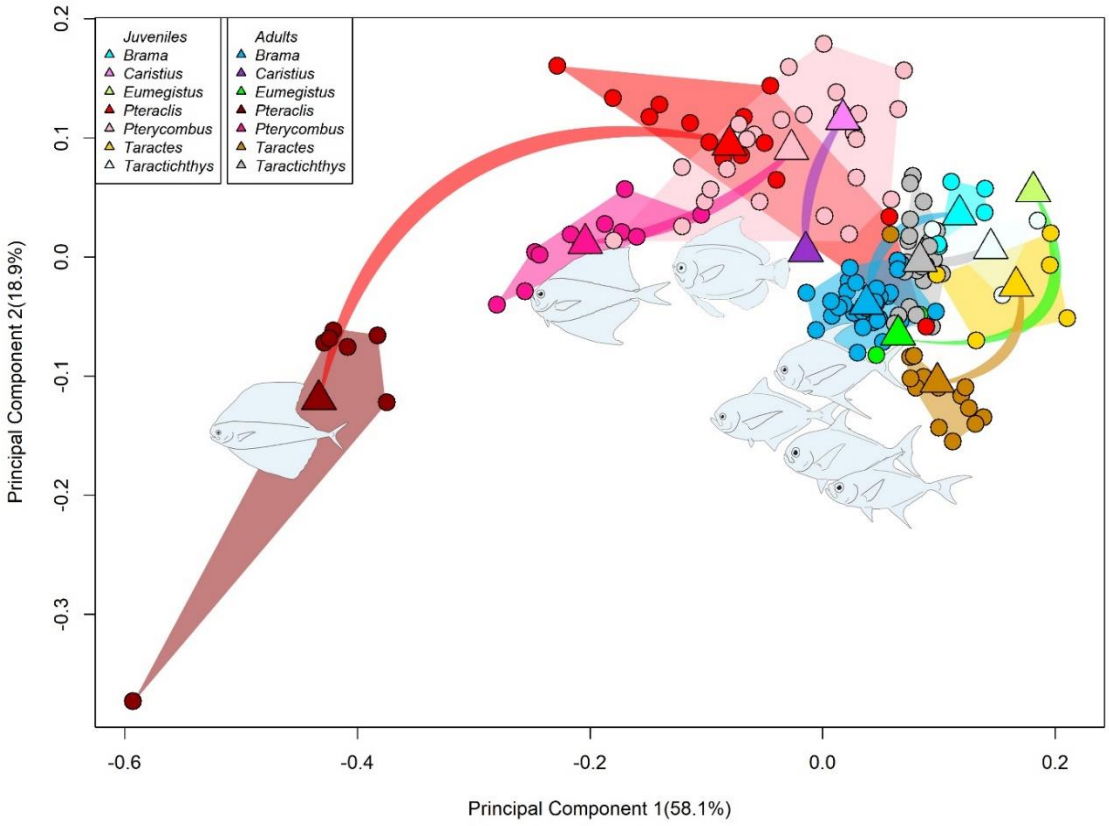

Figure 6.2. Morphospace of the combined juvenile and adult datasets, illustrating phenotypic change in morphospace throughout ontogeny. Triangles represent overall genera means while circles represent individuals with in a genus:stage group. Illustrations of the adult phenotype exist near, but not on, the mean shape for each genus.

adult specimens, along with their general trajectories, in morphospace (Figure 2). Juvenile morphologies, while separate in morphospace, generally occupied the upper right quadrant. In many instances, juvenile morphologies overlapped with one another and with the regions of morphospace occupied by certain adults. While differences in paths can be observed between many genera, path distance in *Pteraclis* was clearly

distinct, moving from the upper right to bottom left of morphospace. The other fanfish genus, *Pterycombus*, exhibited a similar path toward the bottom left of morphospace, albeit to a lesser extent relative to *Pteraclis.* Consistent with previous observations (i.e., Figure 1B), *Caristius* moved from a fanfish region of shape-space at the juvenile stage, towards a generalized bramid phenotype at the adult stage.

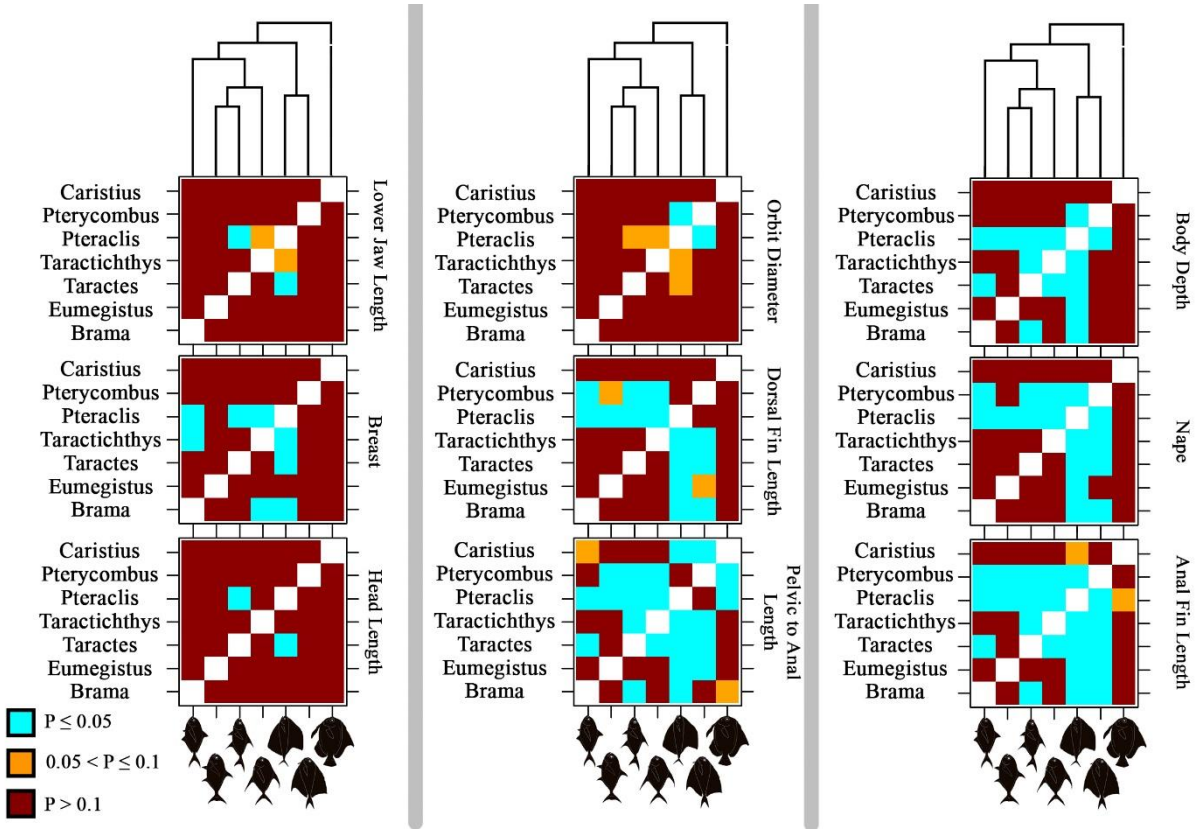

Figure 6.3. Pairwise matrix of p-values illustrating significant differences in slopes between and among genera. Genera are phylogenetically ordered, and a phylogenetic tree demonstrates evolutionary relationships at the top of each column. Typical body shape morphologies are found at the base of each column and are phylogenetically ordered. The white diagonal represents comparisons with self and a p-value of 1. Significant comparisons are cyan, borderline significant comparisons are orange, insignificant comparisons are dark red.

Fanfishes exhibit unique ontogenetic trajectories for specific traits

We next compared specific, ecologically relevant, aspects of morphology. Nine linear measures were regressed against standard length, calculated slopes, and conducted

an ANOVA to test for differences in slopes between genera. We found few significant differences in slopes for cranial traits, including lower jaw length, breast length, orbit diameter, or head length. The significant differences in slopes that occurred within these four traits were generally limited to comparisons that involved the fanfish, *Pteraclis*. The change in these traits appears to be constrained across the Bramidae. Orbit diameter is particularly interesting as the only significant difference was between the two fanfish genera, which exhibited the smallest (*Pteraclis*) and largest (*Pterycombus*) orbits (S1). Thus, while orbit size may be constrained among most bramids, it appears to be more variable in fanfishes.

Analyses of the other five traits (body depth, dorsal fin length, pelvic to anal fin length, nape, and anal fin length) revealed several pairwise differences in the slopes of non-fanfish bramids; however, one or both fanfish genera exhibited statistically distinct trajectories for all these traits. Taken together, these patterns document divergent growth of several traits within the fanfishes compared to other bramid lineages.

Fanfishes exhibit increased rates of trait evolution in medial fin morphology and other traits.

We previously reported that fanfishes experienced rates of whole-body shape (a highly multivariate trait) evolution ~2.9 times faster than their bramid relatives (Gilbert et al., 2021). Given that numerous univariate traits appeared to differ in ontogenetic trajectory across the family (Figure 3), and especially between fanfishes and other

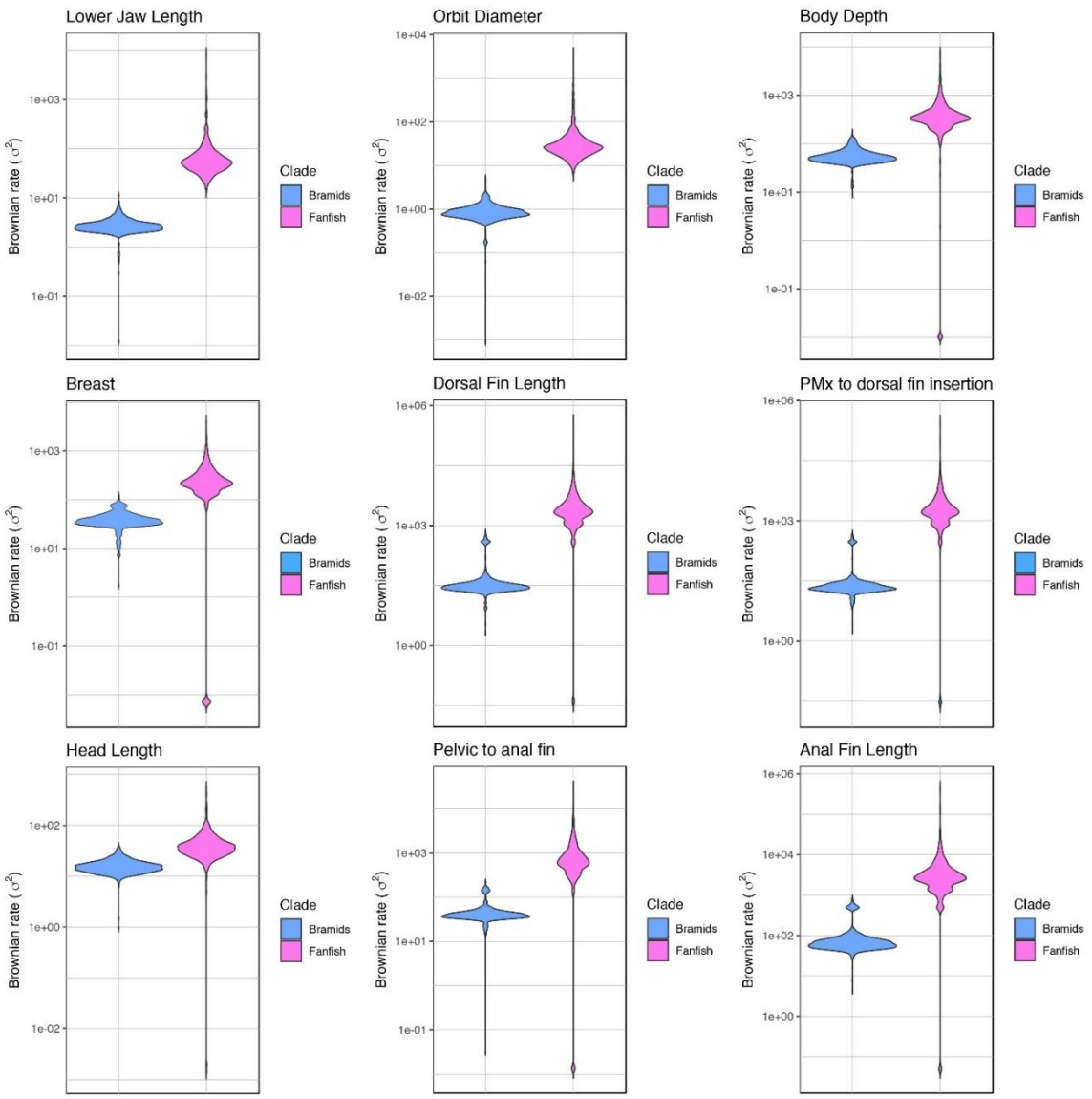

Figure 6.4. Violin plots depicting Brownian rate of morphological evolution of various traits in the Bramidae, comparing the morphologically distinct Ptericlinae to the remaining bramids.

bramids, we wanted to test whether evolutionary rates across those same traits had experienced divergent rates of morphological evolution. Across the nine traits of interest, we found that only four did not differ between the two clades. Using median values for comparison (Figure 4), our analyses showed greater rates of trait evolution in the fanfishes for lower jaw length ($p = 0.009$), orbit diameter ($p = 0.004$), dorsal fin length ($p = 0.002$), nape (premaxilla to dorsal fin insertion; $p = 0.002$), and anal fin length ($p =$

0.009). While no significant differences in breast, pelvic to anal fin distance, body depth, and head length were detected, they were trending in the same direction with fanfishes exhibiting greater rates on average.

Discussion

The evolution of extreme morphologies often involves the breaking of one or more constraints, but at the same time their integration into developmental systems can lead to new constraints. Fanfishes possess exceptionally exaggerated medial fins, as well as many associated putative adaptations to accommodate this structure (Gilbert et al., 2021). In this paper we sought to assess the degree to which the evolution of elaborated medial fins may constrain variability in other morphologies within the bramid lineage.

Did the ancestral state of elaborated dorsal fins constrain the evolution of cranial traits in bramids?

In a previous paper, we showed that exaggerated dorsal fin morphology is likely ancestral in bramids and described changes in the skull of fanfishes that likely arose to support this structure. Specifically, we reported substantial decreases in supraoccipital crest size in the Pteraclinae (Gilbert et al., 2021), a region that had become fully occupied by a deep groove, providing an area for the attachment of associated dorsal fin musculature and architecture. Given that the mechanical space available to any given trait is limited and that the supraoccipital crest is an important craniofacial element required for adequate suction feeding (Carroll et al., 2004), we posited that the evolution of an exaggerated dorsal fin had constrained feeding ecology across the Bramidae by influencing other crucial anatomical elements. Our work here supports this assertion by

showing that most cranial (and some post-cranial) traits exhibit parallel developmental trajectories across the Bramidae. When differences were noted, they were largely between the fanfishes and other members of the Bramidae (Figure 3; S1). However, some notable exceptions were also observed. For instance, *Pteraclis* and *Taractes* are the only two bramids that differed in ontogenetic trajectories for both head length and lower jaw length, with *Pteraclis* possessing the shortest jaws/head length and *Taractes* possessing the longest. In addition, the fanfishes occupied both extremes when concerning eye size, with *Pteraclis* possessing the smallest relative eye size and *Pterycombus* possessing the largest. Differences in eye diameter could be attributed to differences in visual acuity and ecological pressures (Jarvis and Wathes, 2012; Caves et al., 2017, 2018; Beston and Walsh, 2019), and this pattern may hint at undescribed ecological differences between these sister taxa; however, without more formalized tests (Moseley and Jones, 1993; Holladay, 1997; Landgren et al., 2014), any conclusions along these lines would be premature.

Contrary to our predictions, the rate of craniofacial evolution was typically higher in the fanfishes. Lower jaw length and orbit diameter exhibited elevated rates in the fanfish, while head length was comparable across the Bramidae. This could be attributed to the clear differences in body and head morphology between *Pteraclis* and *Pterycombus*. Many ontogenetic trends throughout the Bramidae are similar, with little deviation across the bramid genera. However, the fanfishes have unique ontogenetic trajectories which tend to correlate with their higher rates of evolution. Given that the other genera have overwhelmingly lower rates of evolution across these ontogenetic

trends, it is possible that the fanfishes have broken numerous constraints to further exaggerate their Baupläne, leaving the other bramids constrained.

Breaking Constraints to Extend Medial Fins

Constraints have been shown to be one of the many ways development can influence evolution (Waddington, 1942; Cheverud, 1984; Hendrikse and Parsons, 2007; Hallgrimsson et al., 2009; Conith et al., 2019, 2021). Darwin (1859) noted that increased phenotypic variability during early developmental stages would increase the likelihood of maladaptive outcomes, suggesting that constraints exist to canalize the developmental phenotype during these critical early stages. While this has received increasing attention since the modern incarnation of evo-devo (Raff, 2000), it remains difficult to pinpoint when phenotypic constraints act during development (Cheverud, 1984). Regarding difficult to acquire taxa such as the Bramidae, this question becomes increasingly challenging to answer. While bramid embryos are absent from museum collections, juveniles have been collected across various life stages, providing an opportunity to evaluate differences in morphological traits over ontogeny and reveal stages where variability is more or less constrained.

Here, we report significant shape differences across juvenile bramids, ultimately seeing that morphospace is parsed into three regions, and while shape differences among taxa were relatively small, the pattern was largely similar as that in adults, especially for PC1. At both stages PC1 separates fanfishes from other bramids, with the sister taxon, *Caristius*, occupying an intermediate position. Thus, evolution within the bramid stem lineage may have involved the bending, or breaking, of some constraint, resulting in divergence between the two bramid lineages. We speculate that this involved

conformational changes in several organ systems to accommodate greatly expanded insertions of both medial fins - dorsal and anal.

A general trend among bramids is that medial fins are symmetrically positioned along the dorsal-ventral axis, whether elaborated (as in fanfishes) or not (as in non-fanfishes). Notably, however, medial fin placement is asymmetric in *Caristius*, with the dorsal fin extending anteriorly relative to the anal fin. If this represents the ancestral condition, then the evolution of non-fanfishes involved a loss of dorsal fin elongation, whereas in fanfishes the anal fin was elongated to match the positioning of the dorsal fin. We note that the anterior extension of the dorsal fin in fanfishes is more extreme than that in *Caristius* and extends well into the anterior region of the neurocranium. We have described this unique morphology previously (Gilbert et al., 2021), and suggest that this marks one constraint that needed to be overcome in fanfishes - i.e., the extension of post-cranial skeletal structures onto the cranium.

The anterior position of the anal fin is likely to be under even greater constraint, as it is limited by the positioning of the vent. Extending the anal fin anteriorly requires not only an elaboration of the fin skeleton, but also a reconfiguration of the coelom, digestive, and reproductive organs. That fanfishes were able to circumvent this constraint is significant, and when combined with modifications to the skull to accommodate the extreme anterior extension of the dorsal fin (e.g., up to the naris in *Pteraclis*) speaks to the truly unique Baupläne of this lineage. A timeline of this hypothesis can be seen in Figure 5.

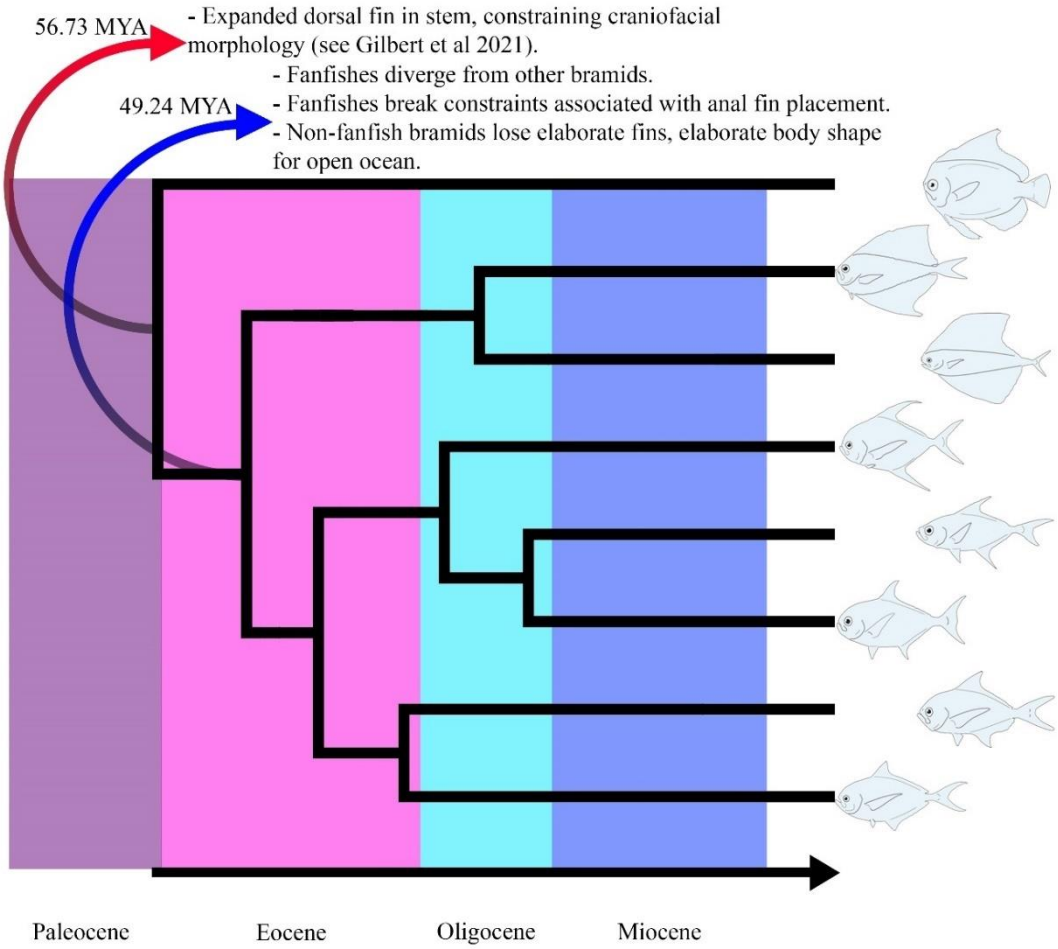

Figure 6.5. End of the Paleocene, 56.73MYA (red arrow): expanded dorsal fins are ancestral in the bramid stem with putative constraints on head/feeding morphology (Gilbert et al 2021). Early Eocene, 49.24MYA (blue arrow); **(1)** non-fanfish bramids lose expanded dorsal fins, instead elaborating body shape for open water speed/ram-feeding, **(2)** fanfishes break constraints associated with anal fin placement and further extend the dorsal fin onto cranium, leading to rapid evolution of fin-insert size, but retain generally low rates of evolution in feeding morphology (e.g., jaw length, orbit size). Thus, all bramids retain largely open-water feeding morphologies (i.e., ram-feeding), possibly due an ancestral constraint. Non-fanfishes exhibit little anatomical diversification; however, fanfishes have broken one or more developmental constraints leading to the evolution of exaggerated medial fins, as well as a series of musculoskeletal changes to accommodate them (e.g., reduced neurocranial mineralization, Gilbert et al., 2021).

The evolution of extreme fin morphology via modular fin development

The evolutionary success of teleosts has been credited to a flexible body plan, possibly facilitated but whole-genome duplication events that have provided the genetic raw material for greater complexity to evolve. Relevant to this study, it has been repeatedly suggested that modular fin architecture can result in a complex array of fin

morphologies, as multiple fin ‘sub-units’ can evolve independently (Mabee et al., 2002; Larouche et al., 2015, 2017, 2018). Medial fins are hypothesized to have evolved before paired fins, roughly 400 million years ago (Coates, 1994), and have since evolved a variety of functions, including locomotion/maneuverability (Breder Jr, 1926; Standen and Lauder, 2005; Loofbourrow, 2006), herding prey (Domenici et al., 2014), and advertising intentions (Allen and Nicoletto, 1997). Modularity can also be observed within medial fins, for example, between hard spines and soft fin-ray elements. The evolvability of medial fins is speculated to be the product of the duplication or deletion, as well as the coupling and decoupling, of various fin modules (Mabee et al., 2002), but many questions remain open. For example, it has been hypothesized that the evolution of taxa possessing multiple dorsal fins, such as a typical scombriform representative (e.g., mackerel, tuna), is due to a duplication of a soft dorsal fin module (Mabee et al., 2002). Alternatively, it has been proposed that the origin of multiple dorsal fins stem from a more elongated fin becoming partitioned and divided (Sandon, 1956; Stewart et al., 2019). Further, it has been proposed, but not tested, that fishes characterized by continuous medial fins and an absence of spines, is due to the secondary loss of regional specification within fins (Wagner, 1996; Mabee et al., 2002).

What is unique about the bramid/caristiid clade is the apparent difference in medial fin placement between these two lineages, with bramids exhibiting symmetric placement of dorsal and anal fins relative to caristiids. This pattern is supported by ontogenetic data presented here (Supplemental Figure 3) that show disproportionately sized medial fins in Caristiidae, but relatively symmetrical fins in the Bramidae. The ancestral condition may be one where dorsal and anal fins are decoupled, which provided

flexibility in the stem lineages to evolve different fin patterns, increasing disparity in the family. Whether the coupling of medial fin growth in bramids is underlain by a coupling of developmental/genetic or ecological mechanisms remains an interesting yet open question.

Conclusions

Evolutionary biology, for decades, has been largely dedicated to seeking out mechanisms of change. While the value of identifying a lack of change has sufficiently increased in recent years, (Gould 1980; Schwenk and Wagner, 2004; Holekamp et al., 2013), our knowledge of these mechanisms is still limited. Over the past 40 years, the field of evolutionary biology has further recognized the value of identifying constraints associated with development and how these mechanisms ultimately shape evolution (Gould, 1980; Cheverud, 1984; Pigliucci and Preston, 2004; Holekamp et al., 2013; Conith et al., 2021). The exploration of extreme traits has shed light on the constraints that may be present in a system and has been done so in various systems (Nijhout and Emlen, 1998; Emlen, 2000; Goyens et al., 2015; Thiagavel et al., 2018; Moyers Arévalo et al., 2020; Gilbert et al., 2021). Here, we build on this by examining how the development, and evolution, of an extreme trait can influence a unique, enigmatic lineage – the Bramidae. To summarize our findings, the developmental paths of the bramid genera are similar, with exception to the fanfishes. Coupled with our results showing elevated rates of evolution in the fanfishes, our data indicate that the Ptericlinae have broken various constraints that have allowed them to substantially differ from their bramid relatives (*Brama, Eugmegistus, Taractes, Tarachtichthys, Xenobrama*). The

challenges that the fanfishes were required to overcome to extend their medial fins are substantial and speak to the unique Baupläne that is the result of these constraints being broken. How these challenges were overcome remains to be seen, but future investigative work into medial fin modularity is promising. Overall, we feel that this system offers opportunities to further explore the topic of constraints and, in the long term, into questions surrounding modularity.

Acknowledgements

The authors are indebted, first and foremost, to Andrew D. Williston and Meaghan H. Sorce from the Harvard Museum of Comparative Zoology in Cambridge, Kerryn Parkinson and Amanda Hay at the Australian Museum in Sydney, and Dr. Masanori Nakae at the National Museum of Nature and Science in Tokyo. Without their efforts, and the continued financial, public, and academic support of museum collections worldwide, this work, and work like it, would be all but impossible. The Albertson Lab is thanked for their support, feedback, intellectual discussion, and discourse. Tom Stewart, Stephen McCormick, Jason Kamilar, and Cristina Cox Fernandes are thanked for their comments and feedback in the first version of the manuscript.

Conflict of interest statement

The authors declare no competing interests.

Literature Cited

Adams, D., Collyer, M.L., and Kaliontzopoulou, A. 2018. Geomorph: Software for geometric morphometric analysis. R package version 3.0.6.

Adams, D.C., Collyer, M.L., and Otarola-Castillo, E. 2014. Geomorph Software for geometric morphometric analysis.

Adams, D.C., Collyer, M.L., and Sherratt, E. 2015. geomorph: Software for geometric morphometric analysis. http://cran.r-project.org/web/ packages/geomorph/i.

Allen, J.M., and Nicoletto, P.F. 1997. Response of *Betta splendens* to computer animations of males with fins of different length. *Copeia* 1997: 195–199.

Arnold, S.J. 1992. Constraints on phenotypic evolution. *Am. Nat.* 140: S85–S107.

Arthur, W. 2004. The effect of development on the direction of evolution: Toward a twenty-first century consensus. *Evol. Dev.* 6: 282–288.

Beston, S.M., and Walsh, M.R. 2019. Natural selection favours a larger eye in response to increased competition in natural populations of a vertebrate. *Funct. Ecol.* 33: 1321–1331.

Boas, F. 1905. The Horizontal plane of the skull and the general problem of the comparison of variable forms. *Science (80).* 21: 862–864.

Bollback, J.P. 2006. SIMMAP: Stochastic character mapping of discrete traits on phylogenies. *BMC Bioinformatics* 7: 1–7.

Breder Jr, C. 1926. The locomotion of fishes. *Zoologica* 4: 159–291.

Briffa, M., and L.U. Sneddon. 2007. Physiological constraints on contest behavior. *Funct. Ecol.* 21(4):627-637.

Carroll, A.M., Wainwright, P.C., Huskey, S.H., Collar, D.C., and Turingan, R.G. 2004. Morphology predicts suction feeding performance in centrarchid fishes. *J. Exp. Biol.* 207: 3873–3881.

Caves, E.M., Brandley, N.C., and Johnsen, S. 2018. Visual Acuity and the Evolution of Signals. *Trends Ecol. Evol.* 33: 358–372.

Caves, E.M., Sutton, T.T., and Johnsen, S. 2017. Visual acuity in ray-finned fishes

correlates with eye size and habitat. *J. Exp. Biol.* 220: 1586–1596.

Charnov, E.L. 1989. Phenotypic evolution under Fisher's fundamental theorem of natural selection. *Heredity (Edinb).* 62: 113–116.

Cheverud, J.M. 1984. Quantitative genetics and developmental constraints on evolution by selection. *J. Theor. Biol.* 110: 155–171.

Coates, M.I. 1994. The origin of vertebrate limbs. *Development* 120: 169–180.

Collyer, M., and Adams, D. 2013. Phenotypic trajectory analysis: comparison of shape change patterns in evolution and ecology. *Hystrix* 24: 75–83.

Collyer, M.L., and Adams, D.C. 2018. RRPP : An r package for fitting linear models to high- - dimensional data using residual randomization. 2018: 1772–1779.

Collyer, M.L., Sekora, D.J., and Adams, D.C. 2015. A method for analysis of phenotypic change for phenotypes described by high-dimensional data. *Heredity (Edinb).* 115: 357–365.

Concannon, M.R., and Albertson, R.C. 2015. The genetic and developmental basis of an exaggerated craniofacial trait in East African cichlids. *J. Exp. Zool. Part B Mol. Dev. Evol.* 324: 662–670.

Conith, A.J., Hope, S.A., Chhouk, B.H., and Albertson, R.C. 2021. Weak genetic signal for phenotypic integration implicates developmental processes as major regulators of trait covariation. *Mol. Ecol.* 464–480.

Conith, M.R., Conith, A.J., and Albertson, R.C. 2019. Evolution of a soft-tissue foraging adaptation in African cichlids: Roles for novelty, convergence, and constraint. *Evolution (N. Y).* 73: 2072–2084.

Conway Morris, S. 2003. Life's Solution (Cambridge: Cambridge University Press).

Crump, J.G., Maves, L., Lawson, N.D., Weinstein, B.M., and Kimmel, C.B. 2004. An essential role for Fgfs in endodermal pouch formation influences later craniofacial skeletal patterning. *Development* 131: 5703–5716.

Darwin, C. 1859. On the origin of species.

Domenici, P., Wilson, A.D.M., Kurvers, R.H.J.M., Marras, S., Herbert-Read, J.E., Steffensen, J.F., Krause, S., Viblanc, P.E., Couillaud, P., and Krause, J. 2014. How sailfish use their bills to capture schooling prey. *Proc. R. Soc. B Biol. Sci.* 281: 1–6.

Emlen, D.J. 2000. Integrating development with evolution: A case study with beetle horns. *Bioscience* 50: 403–418.

Evans, K.M., Larouche, O., Watson, S.J., Farina, S., Habegger, M.L., and Friedman, M. 2021. Integration drives rapid phenotypic evolution in flatfishes. *Proc. Natl. Acad. Sci.* 118: 1–10.

Friedman, M., Feilich, K.L., Beckett, H.T., Alfaro, M.E., Faircloth, B.C., Černý, D., Miya, M., Near, T.J., and Harrington, R.C. 2019. A phylogenomic framework for pelagiarian fishes (Acanthomorpha: Percomorpha) highlights mosaic radiation in the open ocean. *Proc. R. Soc. B Biol. Sci.* 286:.

Galis, F., and Metz, J.A.J. 2007. Evolutionary novelties: The making and breaking of pleiotropic constraints. *Integr. Comp. Biol.* 47: 409–419.

Gilbert, M.C., Conith, A.J., Lerose, C.S., Moyer, J.K., Huskey, S.H., and Albertson, R.C. 2021. Extreme Morphology, Functional Trade-Offs, and Evolutionary Dynamics in a Clade of Open-Ocean Fishes (Perciformes: Bramidae). *Integr. Org. Biol.*

Glass, A. 2003. Nitrogen use efficiency of crop plants: Physiological constraints upon

nitrogen absorption. *Crit. Rev. Pla. Sci.* 22(5): 453-470

Goodall, C. 1991. Procrustes methods in the statistical analysis of shape. *J. R. Stat. Soc.* 53: 285–339.

Gould, S.J. 1980. The evolutionary biology of constraint. *Daedalus* 109: 39–52.

Gould, S.J., and Lewontin, R.C. 1979. The spandrels of San Marco and the Panglossian paradigm: a critique of the adaptationist programme. *Proc. R. Soc. London - Biol. Sci.* 205: 581–598.

Goyens, J., Van Wassenbergh, S., Dirckx, J., and Aerts, P. 2015. Cost of flight and the evolution of stag beetle weaponry. *J. R. Soc. Interface* 12:.

Green, R.M., Fish, J.L., Young, N.M., Smith, F.J., Roberts, B., Dolan, K., Choi, I., Leach, C.L., Gordon, P., Cheverud, J.M., et al. 2017. Developmental nonlinearity drives phenotypic robustness. *Nat. Commun.* 8:.

Hallgrimsson, B., Jamniczky, H., Young, N.M., Rolian, C., Parsons, T.E., Boughner, J.C., and Marcucio, R.S. 2009. Deciphering the palimpsest: Studying the relationship between morphological integration and phenotypic covariation. *Evol. Biol.* 36: 355–376.

Harrington, R.C., Friedman, M., Near, T.J., and Campbell, M.A. 2021. Phylogenomic resolution of the monotypic and enigmatic Amarsipus , the Bagless Glassfish (Teleostei , Amarsipidae). 1–12.

Hendrikse, J.L., and Parsons, T.E. 2007. Evolvability as the proper focus of evolutionary developmental biology. 401: 393–401.

Herrel, A., and Bonneaud, C. 2012. Trade-offs between burst performance and maximal exertion capacity in a wild amphibian, *Xenopus tropicalis*. *J. Exp. Biol.* 215:

3106–3111.

Holekamp, K.E., Swanson, E.M., and Van Meter, P.E. 2013. Developmental constraints on behavioural flexibility. *Philos. Trans. R. Soc. B Biol. Sci.* 368:.

Holladay, J.T. 1997. Proper method for calculating average visual acuity. *J. Refract. Surg.* 13: 388–391.

Huxley, J. 1942. Evolution. The modern synthesis.

Irschick, D.J., Albertson, R.C., Brennan, P., Podos, J., Johnson, N.A., Patek, S., and Dumont, E. 2013. Evo-devo beyond morphology: From genes to resource use. *Trends Ecol. Evol.* 28:.

Jacob, F. 1977. Evolution and Tinkering. *Science (80-.).* 196: 1161–1166.

Jarvis, J.R., and Wathes, C.M. 2012. Mechanistic modeling of vertebrate spatial contrast sensitivity and acuity at low luminance. *Vis. Neurosci.* 29: 169–181.

Jones, G. 1994. Scaling of Wingbeat and Echolocation Pulse Emission Rates in Bats: Why are Aerial Insectivorous Bats so Small? *Funct. Ecol.* 8: 450.

Kawano, K. 1997. Cost of evolving exaggerated mandibles in stag beetles (Coleoptera: Lucanidae). *Entomol. Soc. Am.* 90: 453–461.

Kennedy, M.C. 2010. Functional-structural models optimize the placement of foliage units for multiple whole-canopy functions. *Ecol. Res.* 25: 723–732.

Klingenberg, C.P. 2005. Developmental Constraints, Modules, and Evolvability. In Variation, pp. 219–247.

Klingenberg, C.P. 2011. MorphoJ: an integrated software package for geometric morphometrics. *Mol. Ecol. Resour.* 11: 353–357.

Konuma, J., and Chiba, S. 2007. Trade-offs between force and fit: Extreme morphologies

associated with feeding behavior in carabid beetles. *Am. Nat.* 170: 90–100.

Kuntner, M., and Coddington, J.A. 2020. Sexual size dimorphism: Evolution and perils of extreme phenotypes in spiders. *Annu. Rev. Entomol.* 65: 57–80.

Landgren, E., Fritsches, K., Brill, R., and Warrant, E. 2014. The visual ecology of a deep-sea fish, the escolar Lepidocybium flavobrunneum (Smith, 1843). *Philos. Trans. R. Soc. B Biol. Sci.* 369:.

Larouche, O., Cloutier, R., and Zelditch, M.L. 2015. Head, Body and Fins: Patterns of Morphological Integration and Modularity in Fishes. *Evol. Biol.* 42: 296–311.

Larouche, O., Zelditch, M.L., and Cloutier, R. 2017. Fin modules: An evolutionary perspective on appendage disparity in basal vertebrates. *BMC Biol.* 15:.

Larouche, O., Zelditch, M.L., and Cloutier, R. 2018. Modularity promotes morphological divergence in ray-finned fishes. *Sci. Rep.* 8: 1–6.

Lenth, R. 2020. Emmeans: estimated marginal means, aka. least-squares means.

Leroi, A.M., Kim, S.B., and Rose, M.R. 1994. The evolution of phenotypic life-history trade-offs: An experimental study using *Drosophila melanogaster*. *Am. Nat.* 144: 661–676.

Loofbourrow, H. 2006. Hydrodynamics of balistiform swimming in the picasso triggerfish, *Rhinecanthus aculeatus*. University of British Columbia.

Mabee, P.M., Crotwell, P.L., Bird, N.C., and Burke, A.C. 2002. Evolution of median fin modules in the axial skeleton of fishes. *J. Exp. Zool.* 294: 77–90.

Maynard Smith, J., Burian, R., Kauffman, S., Alberch, P., Campbell, J., Goodwin, B., Lande, R., Raup, D., and Wolpert, L. 1985. Developmental constraints and evolution: A perspective from the mountain lake conference on development and

evolution. *Q. Rev. Biol.* 60: 265–287.

McGhee, G.R. 2007. The Geometry of evolution: Adaptive landscapes and theoretical morphospaces (Cambridge: Cambridge University Press).

Mead, G.W. 1972. Bramidae. (The Carlsberg Foundation's oceanographical expedition round the World 1928-30 and previous Dana-expeditions. Dana-Report.).

Minelli, A., and Fusco, G. 2019. No limits: Breaking constraints in insect miniaturization. *Arthropod Struct. Dev.* 48: 4–11.

Miya, M., Friedman, M., Satoh, T.P., Takeshima, H., Sado, T., Iwasaki, W., Yamanoue, Y., Nakatani, M., Mabuchi, K., Inoue, J.G., et al. 2013. Evolutionary origin of the Scombridae (tunas and mackerels): Members of a Paleogene adaptive radiation with 14 other Pelagic fish families. *PLoS One* 8: e73535.

Moseley, M.J., and Jones, H.S. 1993. Visual acuity: Calculating appropriate averages. *Acta Ophthalmol.* 71: 296–300.

Moyers Arévalo, R.L., Amador, L.I., Almeida, F.C., and Giannini, N.P. 2020. Evolution of Body Mass in Bats: Insights from a Large Supermatrix Phylogeny. *J. Mamm. Evol.* 27: 123–138.

Nijhout, H.F., and Emlen, D.J. 1998. Competition among body parts in the development and evolution of insect morphology. *Proc. Natl. Acad. Sci.* 95: 3685–3689.

O'Meara, B.C., Ané, C., Sanderson, M.J., and Wainwright, P.C. 2006. Testing for Different Rates of Continuous Trait Evolution Using Likelihood. *Evolution (N. Y).* 60: 922.

Olsen, A., and Westneat, M. 2015. StereoMorph: an R package for the collection of 3D landmarks and curves using a stereo camera set-up. *Methods Ecol. Evol.* 6: 351–

356.

Pelegrin, N., Mesquita, D.O., Albinati, P., Caldas, F.L.S., de Queiroga Cavalcanti, L.B., Costa, T.B., Falico, D.A., Galdino, J.Y.A., Tucker, D.B., and Garda, A.A. 2017. Extreme specialization to rocky habitats in Tropidurus lizards from Brazil: Trade-offs between a fitted ecomorph and autoecology in a harsh environment. *Austral Ecol.* 42: 677–689.

Pigliucci, M., and Preston, K. 2004. Phenotypic integration: studying the ecology and evolution of complex phenotypes (Oxford, UK: Oxford University Press).

R Core Team 2018. R: A language and environment for statistical computing. *R A Lang. Environ. Stat. Comput.*

Rabosky, D.L. 2014. Automatic detection of key innovations, rate shifts, and diversity-dependence on phylogenetic trees. *PLoS One* 9.

Rabosky, D.L., Grundler, M., Anderson, C., Title, P., Shi, J.J., Brown, J.W., Huang, H., and Larson, J.G. 2014. BAMMtools: An R package for the analysis of evolutionary dynamics on phylogenetic trees. *Methods Ecol. Evol.* 5: 701–707.

Raff, R.A. 2000. Evo-devo: the evolution of a new discipline. *Nat. Rev. Genet.* 1: 74–79.

Ramsay, M., and R. Dunbrack. 2003. Physiological constraints on life history phenomena: Examples of small bear cubs. *Am. Nat.* 127(6): 735-743

Revell, L.J. 2012. phytools: An R package for phylogenetic comparative biology (and other things). *2Methods Ecol. Evol.* 3: 217–223.

Sandon, H. 1956. An abnormal specimen of Synodontis membranaceus (Teleostei, Siluroidea), with a discussion on the evolutionary history of the adipose fin in fish. *Proceeding Zool. Soc. London* 127: 453–459.

Sarkar, D. 2017. Trellis graphics for R.

Schlichting, C.D., and Pigliucci, M. 1998. Phenotypic evolution: a reaction norm perspective (Sunderland, MA: Sinauer).

Schluter, D. 1996. Adaptive radiation along genetic lines of least resistance. *Evolution (N. Y).* 50: 1766.

Schwenk, K., and Wagner, G.P. 2001. Function and the evolution of phenotypic stability: Connecting pattern to process. *Am. Zool.* 41: 552–563.

Schwenk, K., and Wagner, G.P. 2004. The relativism of constraints on phenotypic evolution. In Phenotypic Integration: Stuyding the Ecology and Evolution of Complex Phenotypes, M. Pigliucci, and K. Preston, eds. (Oxford, UK: Oxford University Press), pp. 390–408.

Sheftel, H., Shoval, O., Mayo, A., and Alon, U. 2013. The geometry of the Pareto front in biological phenotype space. *Ecol. Evol.* 3: 1471–1483.

Shoval, O., Sheftel, H., Shinar, G., Hart, Y., Ramote, O., Mayo, A., Dekel, E., Kavanagh, K., and Alon, U. 2012. Evolutionary trade-offs, pareto optimality, and the geometry of phenotype space. *Science (80-.).* 336: 1157–1161.

Sneath, P.H.A. 1967. Trend-surface analysis of transformation grids. *J. Zool.* 151: 65–122.

Spurway, H. 1949. Remarks on Vavilov's law of homologous variation. *Ric. Sci.* 19: 3–9.

Standen, E.M., and Lauder, G. V. 2005. Dorsal and anal fin function in bluegill sunfish *Lepomis macrochirus*: Three-dimensional kinematics during propulsion and maneuvering. *J. Exp. Biol.* 208: 2753–2763.

Stearns, S.C. 1989. The evolutionary significance of phenotypic plasticity. *Bioscience* 39:

436–445.

Stewart, T.A., Bonilla, M.M., Ho, R.K., and Hale, M.E. 2019. Adipose fin development and its relation to the evolutionary origins of median fins. *Sci. Rep.* 9: 1–12.

Swartz, M.E., Nguyen, V., McCarthy, N.Q., and Eberhart, J.K. 2012. Hh signaling regulates patterning and morphogenesis of the pharyngeal arch-derived skeleton. *Dev. Biol.* 369: 65–75.

Thiagavel, J., Cechetto, C., Santana, S.E., Jakobsen, L., Warrant, E.J., and Ratcliffe, J.M. 2018. Auditory opportunity and visual constraint enabled the evolution of echolocation in bats. *Nat. Commun.* 9:.

Toro, E., Herrel, A., and Irschick, D. 2004. The evolution of jumping performance in Caribbean Anolis lizards: Solutions to biomechanical trade-offs. *Am. Nat.* 164:.

Uller, T., Moczek, A.P., Watson, R.A., and Laland, K.N. 2018. Developmental bias and evolution : a regulatory network perspective. *Genetics* 209: 949–966.

Vavilov, N.I. 1922. The law of homologous series in variation. *J. Genet.* 12: 47–89.

Waddington, C. 1942. Canalization of development and the inheritance of acquired characters. *Nature* 150: 563–565.

Waddington, C. 1956. Genetic assimilation of the bithorax phenotype. *Evolution (N. Y).* 10: 1–13.

Wagner, G.P. 1988. The influence of variation on the rate of multivariate and of developmental phenotypic evolution. *J. Evol. Biol.* 1: 45–66.

Wagner, G.P. 1996. Homologues, natural kinds and the evolution of modularity. *Am. Zool.* 36: 36–43.

Wagner, G.P., and Misof, B.Y. 1993. How can a character be developmentally

constrained despite variation in developmental pathways? *J. Evol. Biol.* 6: 449–455.

Wagner, G.P., and Schwenk, K. 2000. Evolutionary stable configurations: functional integration and the evolution of phenotypic stability. In Evolutionary Biology, pp. 155–217.

Waltzek, T.B., and Wainwright, P.C. 2003. Functional morphology of extreme jaw protrusion in Neotropical cichlids. *J. Morphol.* 257: 96–106.

Wright, S. 1932. The roles of mutation, inbreeding, crossbreeding and selection in evolution. *Sixth Int. Congr. Genet.* 1: 356–366.

Supplemental Data

Supplemental Table 6.1. Museum prefixes and lot number for each specimen used in morphometric analyses. Museum prefixes: MCZ - Museum of Comparative Zoology, Harvard College, AUNMH - Australian Museum of Natural History, NSMT – National Museum of Nature and Science.

ID	Name	Dev	Number
MCZ_148056	*Taractes asper*	Juvenile	1
MCZ_148060	*Taractes rubescens*	Juvenile	1
MCZ_148085	*Pterycombus brama*	Juvenile	1
MCZ_148087	*Pterycombus brama*	Juvenile	1
MCZ_148092	*Pterycombus brama*	Juvenile	1
MCZ_148113	*Pterycombus brama*	Juvenile	1
MCZ_148116	*Pterycombus brama*	Juvenile	3
MCZ_148117	*Pterycombus brama*	Juvenile	5
MCZ_148124	*Pterycombus brama*	Juvenile	1
MCZ_148260	*Pteraclis carolinus*	Juvenile	1
MCZ_148261	*Pteraclis carolinus*	Juvenile	1
MCZ_148262	*Pteraclis carolinus*	Juvenile	1
MCZ_148264	*Pteraclis carolinus*	Juvenile	2
MCZ_148265	*Pteraclis carolinus*	Juvenile	1
MCZ_148266	*Pteraclis carolinus*	Juvenile	1
MCZ_148267	*Pteraclis carolinus*	Juvenile	1
MCZ_148268	*Pteraclis carolinus*	Juvenile	1
MCZ_148269	*Pteraclis carolinus*	Juvenile	1
MCZ_148270	*Pteraclis carolinus*	Juvenile	1
MCZ_148271	*Pteraclis carolinus*	Juvenile	1
MCZ_148381	*Caristius fasciatus*	Juvenile	1
MCZ_150538	*Taractichthys steindachneri*	Juvenile	2
MCZ_161671	*Taractes asper*	Juvenile	1
MCZ_171433	*Pteraclis carolinus*	Juvenile	1
MCZ_40826	*Brama brama*	Juvenile	5
MCZ_41558	*Taractes rubescens*	Juvenile	1
MCZ_55043	*Eumegistus brevorti*	Juvenile	1
MCZ_55044	*Taractichthys longipinnis*	Juvenile	1
MCZ_55045	*Taractichthys longipinnis*	Juvenile	1
MCZ_55338	*Pteraclis carolinus*	Juvenile	1
MCZ_76100	*Pterycombus brama*	Juvenile	1
MCZ_76104	*Pterycombus brama*	Juvenile	5
MCZ_76111	*Pterycombus brama*	Juvenile	4
MCZ_76112	*Pterycombus brama*	Juvenile	1
MCZ_76115	*Pterycombus brama*	Juvenile	1
MCZ_39974	*Taractes rubescens*	Adult	1
MCZ_44137	*Brama japonica*	Adult	1

MCZ_44138	*Brama japonica*	Adult	1
MCZ_44139	*Taractichthys steindachneri*	Adult	1
MCZ_44140	*Taractes rubescens*	Adult	1
MCZ_44141	*Taractichthys steindachneri*	Adult	1
MCZ_44142	*Brama japonica*	Adult	1
MCZ_44143	*Brama japonica*	Adult	1
MCZ_44144	*Brama japonica*	Adult	1
MCZ_44145	*Taractes rubescens*	Adult	1
MCZ_44147	*Taractichthys steindachneri*	Adult	1
MCZ_46322	*Taractes rubescens*	Adult	1
MCZ_46324	*Taractichthys steindachneri*	Adult	1
MCZ_46325	*Taractes rubescens*	Adult	1
MCZ_46326	*Taractes rubescens*	Adult	1
MCZ_46327	*Brama japonica*	Adult	1
MCZ_46328	*Taractes rubescens*	Adult	1
MCZ_46329	*Taractichthys steindachneri*	Adult	1
MCZ_46330	*Taractichthys longipinnis*	Adult	1
MCZ_46331	*Taractichthys longipinnis*	Adult	1
MCZ_46333	*Brama japonica*	Adult	1
MCZ_46334	*Brama japonica*	Adult	1
MCZ_46335	*Brama japonica*	Adult	1
MCZ_46336	*Brama brama*	Adult	1
MCZ_46337	*Brama brama*	Adult	1
MCZ_46339	*Brama japonica*	Adult	1
MCZ_46340	*Brama japonica*	Adult	1
MCZ_46341	*Brama japonica*	Adult	1
MCZ_46342	*Brama japonica*	Adult	1
MCZ_46343	*Brama japonica*	Adult	1
MCZ_46344	*Brama japonica*	Adult	1
MCZ_46345	*Brama japonica*	Adult	1
MCZ_46346	*Taractichthys steindachneri*	Adult	1
MCZ_46347	*Taractes asper*	Adult	1
MCZ_46348	*Taractes asper*	Adult	1
MCZ_46349	*Taractes asper*	Adult	1
MCZ_46350	*Taractichthys steindachneri*	Adult	1
MCZ_46351	*Taractichthys steindachneri*	Adult	1
MCZ_46352	*Taractichthys steindachneri*	Adult	1
MCZ_46353	*Taractichthys steindachneri*	Adult	1
MCZ_46354	*Taractichthys steindachneri*	Adult	1
MCZ_46355	*Taractes rubescens*	Adult	1
MCZ_46356	*Brama japonica*	Adult	1
MCZ_46357	*Brama japonica*	Adult	1
MCZ_46358	*Brama japonica*	Adult	1

MCZ_57530	*Taractichthys steindachneri*	Adult	1
MCZ_57531	*Taractes rubescens*	Adult	1
MCZ_57532	*Taractichthys steindachneri*	Adult	1
MCZ_57533	*Taractichthys steindachneri*	Adult	1
MCZ_57534	*Taractichthys steindachneri*	Adult	1
MCZ_57535	*Taractichthys steindachneri*	Adult	1
MCZ_96428	*Taractichthys longipinnis*	Adult	1
MCZ_172796	*Taractichthys steindachneri*	Adult	1
AUMNH_I_16126_001	*Pteraclis aesticola*	Adult	1
AUMNH_I_21126_002	*Pteraclis velifera*	Adult	1
AUMNH_I_22821_035	*Eumegistus illustris*	Adult	1
AUMNH_I_27500_001	*Xenobrama microlepis*	Adult	1
AUMNH_I_32757_001	*Pteraclis aesticola*	Adult	1
AUMNH_I_33330_001	*Taractichthys steindachneri*	Adult	1
AUMNH_I_34097_001	*Taractichthys steindachneri*	Adult	1
AUMNH_I_34633_001	*Taractichthys steindachneri*	Adult	1
AUMNH_I_34990_001	*Pteraclis velifera*	Adult	1
AUMNH_I_37875_001	*Taractes asper*	Adult	1
AUMNH_I_39920_002	*Taractichthys steindachneri*	Adult	1
AUMNH_I_43350_001	*Pteraclis aesticola*	Adult	1
AUMNH_IB_3555	*Pteraclis aesticola*	Adult	1
Custody of M Gilbert	*Pterycombus petersii*	Adult	1
MCZ_131846	*Taractichthys longipinnis*	Adult	1
MCZ_148057	*Taractes asper*	Adult	1
MCZ_148066_1	*Brama orcini*	Adult	2
MCZ_148276_1	*Pterycombus brama*	Adult	2
MCZ_148277	*Pterycombus brama*	Adult	1
MCZ_148287	*Brama dussumieri*	Adult	2
MCZ_161934	*Pterycombus brama*	Adult	1
MCZ_161935	*Pterycombus brama*	Adult	1
MCZ_163284	*Pterycombus brama*	Adult	1
MCZ_164530	*Brama brama*	Adult	1
MCZ_165872	*Brama brama*	Adult	1
MCZ_174129	*Pterycombus brama*	Adult	1
MCZ_31600	*Brama sp.*	Adult	1
MCZ_46332	*Brama sp.*	Adult	1
MCZ_46338	*Brama sp.*	Adult	1
MCZ_57529	*Brama sp.*	Adult	1
MCZ_59501	*Pterycombus brama*	Adult	1
MCZ_59503	*Pterycombus petersii*	Adult	1
MCZ_98532	*Brama japonica*	Adult	1
NSMT_P_41654	*Xenobrama microlepis*	Adult	1
NSMT_P_41655	*Xenobrama microlepis*	Adult	1

NSMT_P_41694	*Xenobrama microlepis*	Adult	1
NSMT_P_41695	*Xenobrama microlepis*	Adult	1
NSMT_P_41696	*Xenobrama microlepis*	Adult	1
NSMT_P_41697	*Xenobrama microlepis*	Adult	1
NSMT_P_41698	*Xenobrama microlepis*	Adult	1
NSMT_P_41848	*Xenobrama microlepis*	Adult	1
NSMT_P_41927	*Xenobrama microlepis*	Adult	1
NSMT_P_41947	*Xenobrama microlepis*	Adult	1
NSMT_P_41949	*Xenobrama microlepis*	Adult	1
NSMT_P_43079	*Xenobrama microlepis*	Adult	1
NSMT_P_43080	*Xenobrama microlepis*	Adult	1
NSMT_P_44284	*Xenobrama microlepis*	Adult	1
NSMT_P_44297	*Xenobrama microlepis*	Adult	1
NSMT_P_44299	*Xenobrama microlepis*	Adult	1
NSMT_P_64804	*Pteraclis aesticola*	Adult	1
NSMT_P_64809	*Eumegistus illustris*	Adult	1
MCZ_UC_raii	*Brama brama*	Adult	1
MCZ_Uc_sp19-3	*Taractichthys longipinnis*	Adult	1

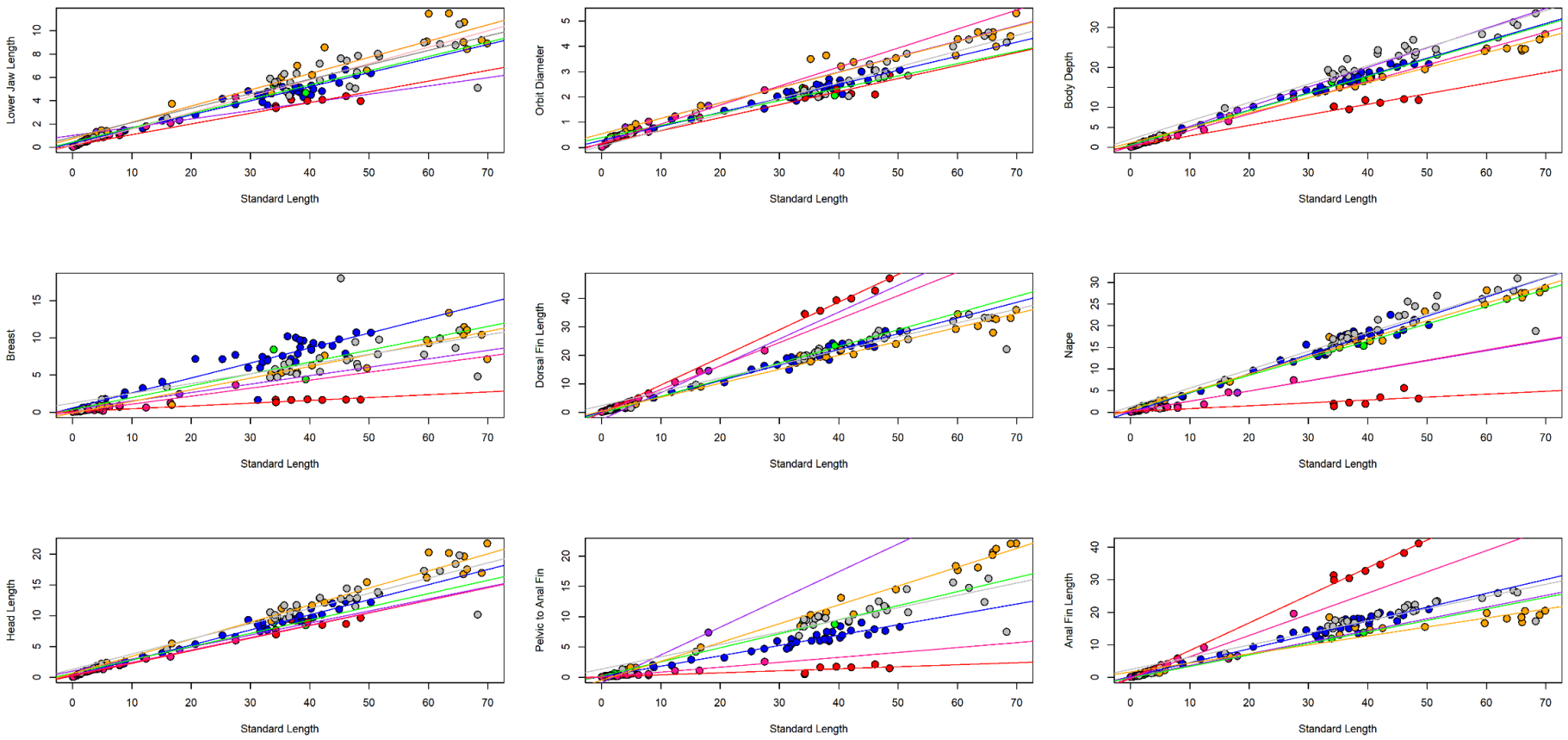

Supplemental Figure 6.1. Linear regressions of each trait against standard length, across genera. Colors are consistent with colors used in the manuscript. Caristius: purple, Pterycombus: pink, Pteraclis: red, Taractichthys: grey, Taractes: orange, Eumegsitus: green, Brama: blue.

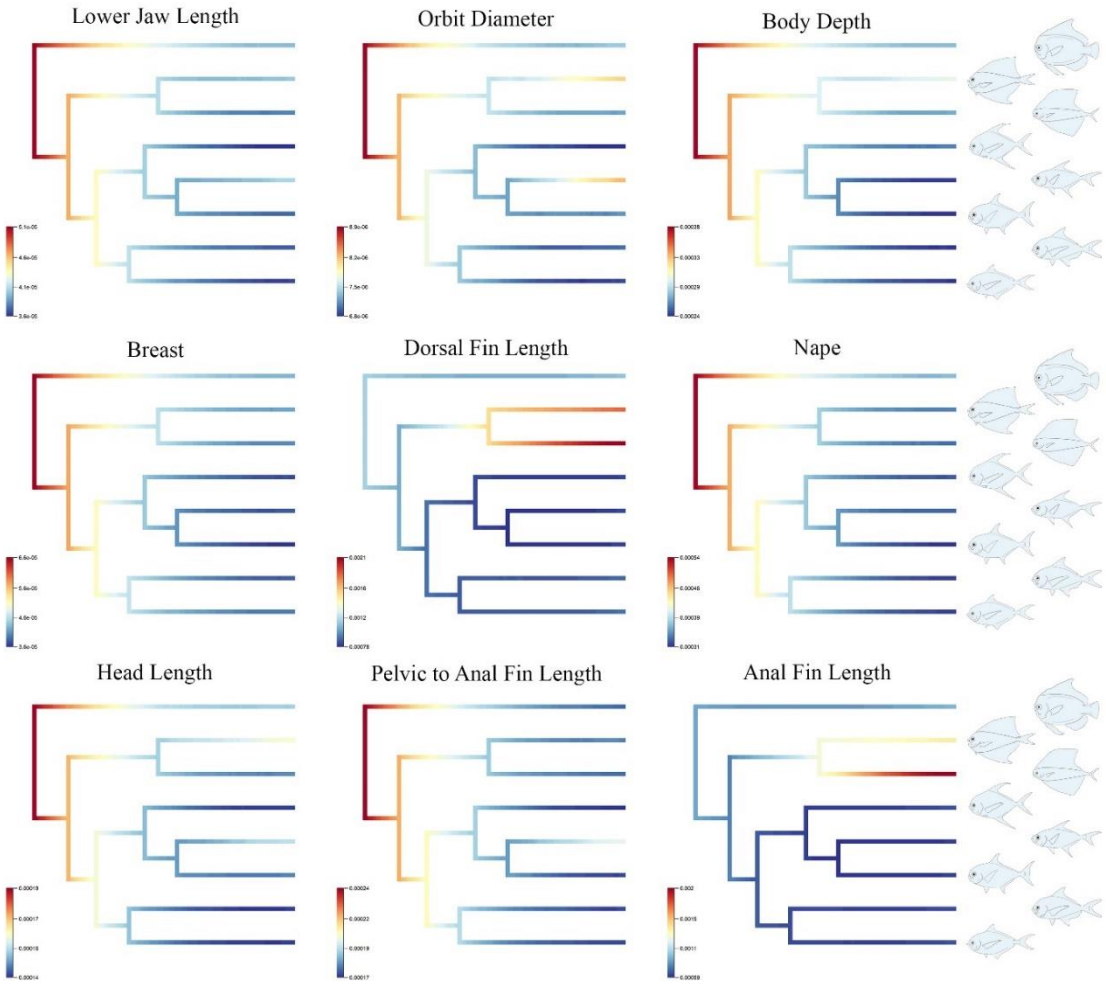

Supplemental Figure 6.2. Evolutionary rates across the Bramidae for various linear measures regressed against standard length. Warm colors indicate faster rates of morphological evolution, cool colors indicate slower rates of morphological evolution.

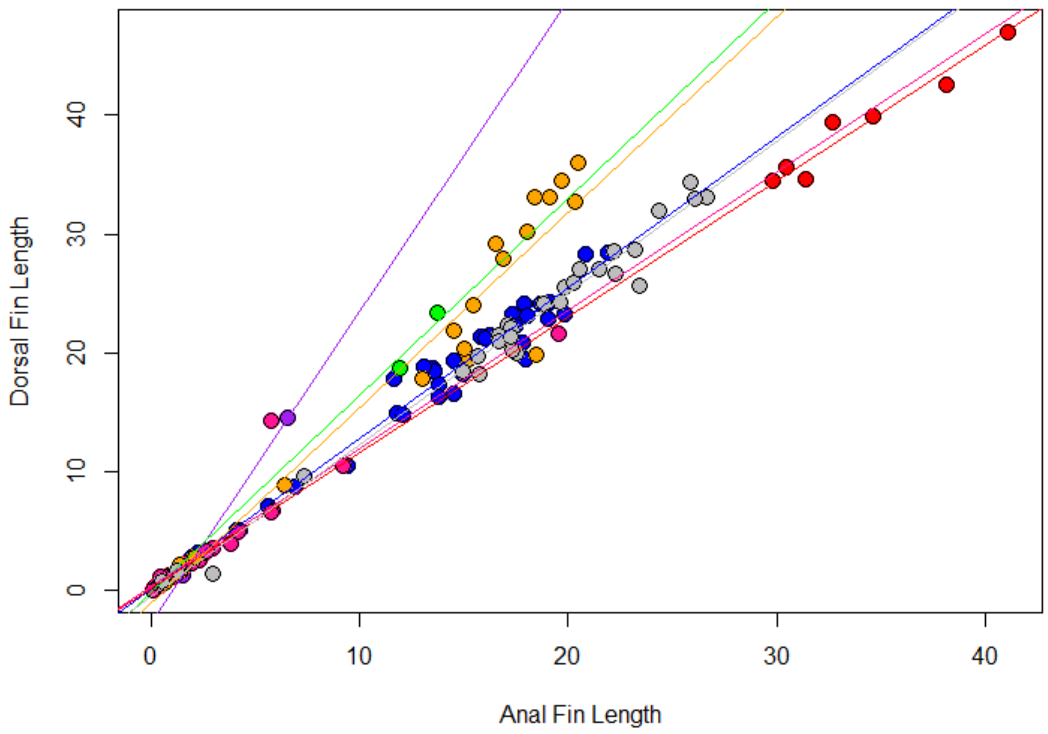

Supplemental Figure 6.3. Dorsal and anal fin lengths regressed *against* one another. Slope intercepts are as follows: *Brama*, 0.175; *Caristius*, -2.603; *Eumegistus*, -0.101; Pteraclis, 0.159; *Pterycombus*, 0.302; *Taractes*, -0.996; *Taractichthyes*, -0.467.

LITERATURE CITED

Abu-Issa R, Smyth G, Smoak I, Yamamura KI, Meyers EN. Fgf8 is required for pharyngeal arch and cardiovascular development in the mouse. Development. 2002;129(19):4613-4625.

Abzhanov A, Protas M, Grant BR, Grant PR, Tabin CJ. Bmp4 and morphological variation of beaks in Darwin's finches. Science. 2004;305(5689):1462-1465. doi:10.1126/science.1098095

Abzhanov A, Kuo WP, Hartmann C, Rosemary Grant B, Grant PR, Tabin CJ. The calmodulin pathway and evolution of elongated beak morphology in Darwin's finches. Published online 2006. doi:10.1038/nature04843

Adams, D. C., Rohlf, F. J., & Slice, D. E. (2004). Geometric morphometrics : Ten years of progress following the ' revolution '. *Italian Journal of Zoology, 71*(January 2015), 5–16. doi:10.1080/11250000409356545

Adams DC. A generalized K statistic for estimating phylogenetic signal from shape and other high-dimensional multivariate data. Syst Biol. 2014;63(5):685-697. doi:10.1093/sysbio/syu030

Adams DC. 2014. Quantifying and comparing phylogenetic evolutionary rates for shape and other high-dimensional phenotypic data. Syst Biol 63:166–77.

Adams DC, Felice RN. 2014. Assessing trait covariation and morphological integration on phylogenies using evolutionary covariance matrices. PLoS One 9.

Adams DC, Collyer ML, Otarola-Castillo E. 2014. R: package, geomorph: Software for geometric morphometric analysishttp//cranr Proj.

Adams, D. C., Collyer, M. L., & Sherratt, E. (2015). geomorph: Software for geometric morphometric analysis. Retrieved from http://cran.r-project.org/web/

packages/geomorph/index.html

Adams, D. C., and M. L. Collyer. 2016. On the comparison of the strength of morphological integration across morphometric datasets. Evolution (N. Y). 70:2623–2631.

Adams, D., Collyer, M. L., & Kaliontzopoulou, A. (2018). Geomorph: Software for geometric morphometric analysis. R package version 3.0.6. Retrieved from https://cran.r-project.org/package=geomorphAdams DC, Collyer ML. Phylogenetic ANOVA: Group-clade aggregation, biological challenges, and a refined permutation procedure. Evolution. 2018;72(6):1204-1215. doi:10.1111/evo.13492

Adams DC, Collyer ML. 2018. Multivariate phylogenetic comparative methods: Evaluations, comparisons, and recommendations. Syst Biol 67:14–31.

Adams, D. C., and M. L. Collyer. 2019. Comparing the strength of modular signal, and evaluating alternative modular hypotheses, using covariance ratio effect sizes with morphometric data. Evolution (N. Y). 73:2352–2367.

Adel Al-Lami H, Barrell WB, Liu KJ. Micrognathia in mouse models of ciliopathies. Biochem Soc Trans. 2016;44(6):1753-1759. doi:10.1042/BST20160241

Adriaens D, Herrel A. 2009. Functional consequences of extreme morphologies in the craniate trophic system. Physiol Biochem Zool 82:1–6.

Adzhubei I, Jordan DM, Sunyaev SR. 2013. Predicting functional effect of human missense mutations using PolyPhen-2. *Curr Protoc Hum Genet.* Chapter 7: Unit7.20.

Aghajanian P, Mohan S. The art of building bone: emerging role of chondrocyte-to-osteoblast transdifferentiation in endochondral ossification. Bone Res. 2018;6:19. doi:10.1038/s41413-018-0021-z

Agostinho, A., Pelicice, F., & Gomes, L. (2008). Dams and the fish fauna of the Neotropical region : impacts and management related to diversity and fisheries. *Brazilian Journal of Biology*, *68*(4), 1119–1132.

Aguirre, W. E., Shervette, V. R., Navarrete, R., Calle, P., & Agorastos, S. (2013). Morphological and Genetic Divergence of Hoplias microlepis (Characiformes: Erythrinidae) in Rivers and Artificial Impoundments of Western Ecuador. *Copeia*, *2013*(2), 312–323. doi:10.1643/CI-12-083

Aigouy B, Farhadifar R, Staple DB, et al. Cell flow reorients the axis of planar polarity in the wing epithelium of *Drosophila*. Cell. 2010;142(5):773-786. doi:10.1016/j.cell.2010.07.042

Akama, A. (2017). Impacts of the hydroelectric power generation over the fish fauna of the Tocantins river, Brazil: Marabá dam, the final blow. *Oecologia Australis*, *21*(3), 222–231. doi:10.4257/oeco.2017.2103.01

Albertson RC, Streelman JT, Kocher TD. 2003. Directional selection has shaped the oral jaws of Lake Malawi cichlid fishes. *Proc Natl Acad Sci USA* 100(9):5252-7.

Albertson RC, Streelman JT, Kocher TD, Yelick PC. 2005. Integration and evolution of the cichlid mandible: the molecular basis of alternate feeding strategies. *Proc Natl Acad Sci USA* 102(45):16287-92.

Albertson, R. C., & Kocher, T. D. (2005). Genetic architecture sets limits on

transgressive segregation in hybrid cichlid fishes. *Evolution*, *59*(3), 686–690.

Albertson RC, Yelick PC. 2007. *Fgf8* haploinsufficiency results in distinct craniofacial defects in adult zebrafish. *Dev Biol*. 306(2):505-15.

Albertson RC, Cresko W, Detrich HW, Postlethwait JH. Evolutionary mutant models for human disease. Trends in Genetics. 2009;25(2):74-81. doi:10.1016/j.tig.2008.11.006

Albertson RC, Pauers MJ. 2019. Morphological disparity in ecologically diverse versus constrained lineages of Lake Malawi rock-dwelling cichlids. *Hydrobiologia* 832:153-174.

Alexander, G. D., & Adams, C. E. (2004). Exposure to a common environment erodes inherited between-population trophic morphology differences in Arctic charr. *Journal of Fish Biology*, *64*, 253–257. doi:10.1111/j.1095-8649.2004.00276.x

Ali AM, McNoon A. 2010. Additions to benthopelagic fish fauna of the Aden Gulf-Arabian Sea (Actinopterygii: Bramidae and Sternoptychidae). J Fish Aquat Sci 5:23–32.

Allan, J. D., & Flecker, A. S. (1993). Biodiversity conservation in running waters. *BioScience*, *43*(1), 32–43. doi:10.2307/1312104

Allen JM, Nicoletto PF. 1997. Response of *Betta splendens* to computer animations of males with fins of different length. Copeia 1997:195–99.

Alman BA. 2015. The role of hedgehog signalling in skeletal health and disease. *Nat Rev Rheumatol*. 11(9):552-60.

Alò, D., & Turner, T. F. (2005). Effects of habitat fragmentation on effective population size in the endangered Rio Grande silvery minnow. *Conservation Biology*, *19*(4),

1138–1148. doi:10.1111/j.1523-1739.2005.00081.x

Antoniades I, Stylianou P, Skourides PA. Making the connection: ciliary adhesion complexes anchor basal bodies to the actin cytoskeleton. Dev Cell. 2014;28(1):70-80. doi:10.1016/j.devcel.2013.12.003

Angermeier, P. L. (1995). Ecological attributes of extinction-prone species: loss of freshwater fishes of Virginia. *Conservation Biology*, *9*(1), 143–158. Retrieved from https://www.jstor.org/stable/pdf/2386396.pdf

Araújo-Lima, C., Agostinho, A., & Fabré, N. (1995). Trophic aspects of fish communities in Brazilian rivers and reservoirs. In *Limnology in Brazil* (pp. 105–136). Rio de Janeiro: Brazilian Academy of Sciences.

Arbour, J. H., & López-Fernández, H. (2013). Ecological variation in South American geophagine cichlids arose during an early burst of adaptive morphological and functional evolution. *Proceedings of the Royal Society B: Biological Sciences*, *280*(1763), 20130849–20130849. doi:10.1098/rspb.2013.0849

Arbour JH, López-Fernández H. 2014. Adaptive landscape and functional diversity of Neotropical cichlids: implications for the ecology and evolution of Cichlinae (Cichlidae; Cichliformes). *J Evol Biol.* 27(11):2431-42.

Arnold SJ. 1983. Morphology, performance and fitness. Integr Comp Biol 23:347–61.

Arnold SJ. Constraints on phenotypic evolution. The American Naturalist. 1992;140:S85-S107.

Arthur, W. 2004. The effect of development on the direction of evolution: Toward a twenty-first century consensus. *Evol. Dev.* 6: 282–288.

Aw WY, Devenport D. Planar cell polarity: global inputs establishing cellular asymmetry. Current Opinion in Cell Biology. 2017;44:110-116. doi:10.1016/j.ceb.2016.08.002

Baciu D, Bannikov AF. 2003. *Paucaichthys neamtensis* gen . et sp . nova-the first discovery of sea breams (Bramidae) in the Oligocene of Romania. Vopr ikhtiologii 43:598–602.

Bahe S, Stierhof YD, Wilkinson CJ, Leiss F, Nigg EA. Rootletin forms centriole-associated filaments and functions in centrosome cohesion. Journal of Cell Biology. 2005;171(1):27-33. doi:10.1083/jcb.200504107

Bailey AP, Bhattacharyya S, Bronner-Fraser M, Streit A. Lens specification is the ground state of all sensory placodes, from which FGF promotes olfactory identity. Dev Cell. 2006;11(4):505-517. doi:10.1016/j.devcel.2006.08.009

Bannikov AF. 2012. The first record of the genus *Isurichthys* (Perciformes, Ariommatidae) in the Lower Oligocene of the Northern Caucasus. Paleontol J 46:171–76.

Bannikov AF, Tyler JC. 1994. A revision of the Eocene fish family Exelliidae (Perciformes). Paleontol J 28:128–40.

Bastos, R. F., Condini, M. V., Varela, A. S., & Garcia, A. M. (2011). Diet and food consumption of the pearl cichlid Geophagus brasiliensis (Teleostei: Cichlidae): Relationships with gender and sexual maturity. *Neotropical Ichthyology*, *9*(4), 825–830. doi:10.1590/S1679-62252011005000049

Batchelor, G. (1967). *An introduction to fluid dynamics*. New York: Cambridge University Press.

Bechert DW, Bruse M, Hage W, Van Der Hoeven JGT, Hoppe G. 1997. Experiments on drag-reducing surfaces and their optimization with an adjustable geometry. J Fluid Mech 338:59–87.

Bellottii C. 1903. Di un nuovo pteraclide giapponese. Atti della Soc Ital di Sci Nat di Milano 42:136–39.

Benfield MC, Caruso JH, Sulak KJ. 2009. In situ video observations of two manefishes (Perciformes: Caristiidae) in the Mesopelagic zone of the northern Gulf of Mexico. Copeia 2009:637–41.

Benson DA, Cavanaugh M, Clark K, Karsch-Mizrachi I, Lipman DJ, Ostell J, Sayers EW. 2013. GenBank. Nucleic Acids Res 41:36–42.

Berbari NF, O'Connor AK, Haycraft CJ, Yoder BK. 2009. The Primary Cilium as a Complex Signaling Center. *Curr Biol.* 19(13):R526-R535.

Bergert BA, Wainwright PC. 1997. Morphology and kinematics of prey capture in the syngnathid fishes *Hippocampus erectus* and *Syngnathus floridae*. Mar Biol 127:563–70.

Bell, M. A., & Travis, M. P. (2005). Hybridization, transgressive segregation, genetic covariation, and adaptive radiation. *Trends in Ecology and Evolution*, *20*(7), 358–361. doi:10.1016/j.tree.2005.03.015

Beston, S.M., and Walsh, M.R. 2019. Natural selection favours a larger eye in response to increased competition in natural populations of a vertebrate. *Funct. Ecol.* 33: 1321–1331.

Blount ZD, Barrick JE, Davidson CJ, Lenski RE. 2012. Genomic analysis of a key innovation in an experimental *Escherichia coli* population. Nature 489:513–18.

Blower MD. Molecular insights into intracellular RNA localization. Int Rev Cell Mol Biol. 2013;302:1-39. doi:10.1016/B978-0-12-407699-0.00001-7

Boas, F. 1905. The Horizontal plane of the skull and the general problem of the comparison of variable forms. *Science (80).* 21: 862–864.

Bollback, J.P. 2006. SIMMAP: Stochastic character mapping of discrete traits on phylogenies. *BMC Bioinformatics* 7: 1–7.

Bonatto Paese CL, Brooks EC, Aarnio-Peterson M, Brugmann SA. Ciliopathic micrognathia is caused by aberrant skeletal differentiation and remodeling. Development (Cambridge, England). 2021;148(4). doi:10.1242/dev.194175

Borovina A, Superina S, Voskas D, Ciruna B. Vangl2 directs the posterior tilting and asymmetric localization of motile primary cilia. Nature Cell Biology. 2010;12(4):407-412. doi:10.1038/ncb2042

Bouckaert R, Heled J, Kühnert D, Vaughan T, Wu CH, Xie D, Suchard MA, Rambaut A, Drummond AJ. 2014. BEAST 2: A software platform for Bayesian evolutionary analysis. PLoS Comput Biol 10:1–6.

Bouckaert RR, Drummond AJ. 2017. bModelTest: Bayesian phylogenetic site model averaging and model comparison. BMC Evol Biol 17:1–11.

Bouton N, Witte F, Van Alphen JJM. 2002. Experimental evidence for adaptive phenotypic plasticity in a rock-dwelling cichlid fish from Lake Victoria. *Biol J Linn Soc.* 77(2):185-192.

Bradshaw AD. 1965. Evolutionary significance of phenotypic plasticity in plants. *Adv Gene.* 13:115-55.

Breder Jr C. 1926. The locomotion of fishes. Zoologica 4:159–291.

Brinsmead, J., & Fox, M. G. (2002). Morphological variation between lake- and stream-dwelling rock bass and pumpkinseed populations. *Journal of Fish Biology, 61*, 1619–1638. doi:10.1006/jfbi.2002.2179

Briffa, M., and L.U. Sneddon. 2007. Physiological constraints on contest behavior. *Funct. Ecol.* 21(4):627-637.

Brodie III ED, Brodie Jr ED. 1999. Costs of exploiting poisonous prey: Evolutionary trade-offs in a predator-prey arms race. Evolution (N Y) 53:626–31.

Brooks, H., G. E. Haines, M. Carly Lin, and S. Laurie Sanderson. 2018. Physical modeling of vortical cross-step flow in the American paddlefish, Polyodon spathula. PLoS One 13:1–25.

Brugmann SA, Goodnough LH, Gregorieff A, et al. Wnt signaling mediates regional specification in the vertebrate face. Development. 2007;134(18):3283-3295. doi:10.1242/dev.005132

Brunt LH, Roddy KA, Rayfield EJ, Hammond CL. Building finite element models to investigate zebrafish jaw biomechanics. Journal of Visualized Experiments. 2016;2016(118). doi:10.3791/54811

Brunt LH, Begg K, Kague E, Cross S, Hammond CL. Wnt signalling controls the response to mechanical loading during zebrafish joint development. Development. 2017;144(15):2798-2809. doi:10.1242/dev.153528

Busch-Nentwich E, Kettleborough R, Dooley CM, Scahill C, Sealy I, White R, Herd C, Mehroke S, Wali N, Carruthers S, et al. 2013. Sanger Institute Zebrafish Mutation Project mutant data submission. ZFIN Direct Data Submission. (http://zfin.org).

Burress, E. D. (2014). Cichlid fishes as models of ecological diversification: patterns,

mechanisms, and consequences. *Hydrobiologia*, *748*(1), 7–27. doi:10.1007/s10750-014-1960-z

Burress, E. D., F. Alda, A. Duarte, M. Loureiro, J. W. Armbruster, and P. Chakrabarty. 2018. Phylogenomics of pike cichlids (Cichlidae: *Crenicichla*): the rapid ecological speciation of an incipient species flock. J. Evol. Biol. 31:14–30.

Burress, E. D., L. Piálek, J. Casciotta, A. Almirón, and O. Říčan. 2022. Rapid parallel morphological and mechanical diversification of South American Pike Cichlids (*Crenicichla*). Syst. Biol. 0:1–14.

Camp AL, Brainerd EL. 2014. Role of axial muscles in powering mouth expansion during suction feeding in largemouth bass (Micropterus salmoides). J Exp Biol 217:1333–45.

Candolin, U. (2009). Population responses to anthropogenic disturbance: Lessons from three-spined sticklebacks Gasterosteus aculeatus in eutrophic habitats. *Journal of Fish Biology*, *75*(8), 2108–2121. doi:10.1111/j.1095-8649.2009.02405.x

Carroll AM, Wainwright PC. 2006. Muscle function and power output during suction feeding in largemouth bass, Micropterus salmoides. Comp Biochem Physiol - A Mol Integr Physiol 143:389–99.

Carroll AM, Wainwright PC, Huskey SH, Collar DC, Turingan RG. 2004. Morphology predicts suction feeding performance in centrarchid fishes. J Exp Biol 207:3873–81.

Carvalho-filho A, Marcovaldi G, Sampaio CLS, Paiva MIG, Duarte LAG. 2009. First report of rare pomfrets (Teleostei: Bramidae) from Brazilian waters, with a key to Western Atlantic species. Zootaxa 2290:1–26.

Casanovas-Vilar I, van Dam J. 2013. Conservatism and adaptability during squirrel radiation: what is mandible shape telling us? *PLoS One* 8(4):e61298.

Casier E. 1966. Faune ichthyologique du London Clay. London Trust Br Museum (Natural Hist London.

Chapman, L. G., Galis, F., & Shinn, J. (2000). Phenotypic plasticity and the possible role of genetic assimilation: Hypoxia-induced trade-offs in the morphological traits of an African cichlid. *Ecology Letters*, *3*(5), 387–393. doi:10.1046/j.1461-0248.2000.00160.x

Caves, E.M., Brandley, N.C., and Johnsen, S. 2018. Visual Acuity and the Evolution of Signals. *Trends Ecol. Evol.* 33: 358–372.

Caves, E.M., Sutton, T.T., and Johnsen, S. 2017. Visual acuity in ray-finned fishes correlates with eye size and habitat. *J. Exp. Biol.* 220: 1586–1596.

Charlesworth B, Lande R, Slatkin M. A Neo-Darwinian commentary on macroevolution. Evolution. 1982;36(3):474-498. doi:10.1111/j.1558-5646.1982.tb05068.x

Charnov EL. 1989. Phenotypic evolution under Fisher's fundamental theorem of natural selection. Heredity (Edinb) 62:113–16.

Chen JW, Galloway JL. The development of zebrafish tendon and ligament progenitors. Development (Cambridge). 2014;141(10):2035-2045. doi:10.1242/dev.104067

Chen JV, Kao LR, Jana SC, et al. Rootletin organizes the ciliary rootlet to achieve neuron sensory function in Drosophila. The Journal of Cell Biology. 2015;211(2):435-453. doi:10.1083/jcb.201502032

Chen F, Ma H, Ma C, Zhang H, Zhao M, Meng Y, Wei H, Ma L. 2016. Sequencing and characterization of mitochondrial DNA genome for *Brama japonica* (Perciformes:

Bramidae) with phylogenetic consideration. Biochem Syst Ecol 68:109–18.

Cheong SS, Akram KM, Matellan C, et al. The planar polarity component vangl2 is a key regulator of mechanosignaling. Frontiers in cell and developmental biology. 2020;8:577201-577201. doi:10.3389/fcell.2020.577201

Cheverud JM. Quantitative genetics and developmental constraints on evolution by selection. Journal of Theoretical Biology. 1984;110(2):155-171. doi:10.1016/S0022-5193(84)80050-8

Cheverud, J. M. 1996. Developmental integration and the evolution of pleiotropy. Am. Zool. 36:44–50.

Cheverud, J. M., E. J. Routman, and D. J. Irschick. 1997. Pleiotropic effects of individual gene loci on mandibular morphology. Evolution (N. Y). 51:2006–2016.

Cichocki, F. (1976). Cladistic history of cichlid fishes and reproductive strategies of the American genera Acarichthys, Biotodoma and Geophagus. *Ph.D. Thesis*. University of Michigan.

Cignoni P, Callieri M, Corsini M, Dellepiane M, Ganovelli F, Ranzuglia G. 2008. MeshLab: An open-source mesh processing tool. 6th Eurographics Ital Chapter Conf 2008 - Proc 129–36.

Chutimanitsakun Y, Nipper RW, Cuesta-Marcos A, Cistue L, Corey A, Filichkina T, Johnson EA, Hayes PM. 2011. Construction and application for QTL analysis of a restriction site associated DNA (RAD) linkage map in barley. *BMC Genomics* 12:4.

Ciruna B, Jenny A, Lee D, Mlodzik M, Schier AF. Planar cell polarity signalling couples cell division and morphogenesis during neurulation. Published online 2006. doi:10.1038/nature04375

Clavel, J., Julliard, R., & Devictor, V. (2011). Worldwide decline of specialist species: toward a global functional homogenization? *Frontiers in Ecology and the Environment*, *9*(4), 222–228. doi:10.1890/080216

Coates, M.I. 1994. The origin of vertebrate limbs. *Development* 120: 169–180.

Collin H, Fumagalli L. Evidence for morphological and adaptive genetic divergence between lake and stream habitats in European minnows (*Phoxinus phoxinus*, Cyprinidae). Molecular Ecology. 2011;20(21):4490-4502. doi:10.1111/j.1365-294X.2011.05284.x

Collinet C, Lecuit T. Programmed and self-organized flow of information during morphogenesis. Nat Rev Mol Cell Biol. 2021;22(4):245-265. doi:10.1038/s41580-020-00318-6

Collyer, M. L., Novak, J. M., & Stockwell, C. A. (2005). Morphological Divergence of Native and Recently Established Populations of White Sands Pupfish (Cyprinodon tularosa). *Copeia*, *2005*(1), 1–11.

Collyer ML, Adams DC. Analysis of two-state multivariate phenotypic change in ecological studies. Ecology. 2007;88(3):683-692. doi:10.1890/06-0727

Collyer M, Adams D. Phenotypic trajectory analysis: Comparison of shape change patterns in evolution and ecology. Hystrix. 2013;40. doi:10.4404/hystrix-24.1-6298

Collyer, M. L., Hall, M. E., Smith, M. D., & Hoagstrom, C. W. (2015). Habitat-

morphotype associations of Pecos pupfish (Cyprinodon pecosensis) in isolated habitat complexes. *Copeia*, *2015*, 181–199. doi:10.1643/OT-14-084

Collyer, M. L., Sekora, D. J., & Adams, D. C. (2015). A method for analysis of phenotypic change for phenotypes described by high-dimensional data. *Heredity*, *115*(4), 357–365. doi:10.1038/hdy.2014.75

Collyer ML, Adams DC. 2018. RRPP : An r package for fitting linear models to high-dimensional data using residual randomization. 2018:1772–79.

Collyer ML, Sekora DJ, Adams DC. 2015. A method for analysis of phenotypic change for phenotypes described by high-dimensional data. *Heredity (Edinb)* 115:357–65.

Concannon, M.R., and Albertson, R.C. 2015. The genetic and developmental basis of an exaggerated craniofacial trait in East African cichlids. *J. Exp. Zool. Part B Mol. Dev. Evol.* 324: 662–670.

Conith, M.R., Conith, A.J., and Albertson, R.C. 2019. Evolution of a soft-tissue foraging adaptation in African cichlids: Roles for novelty, convergence, and constraint. *Evolution (N. Y).* 73: 2072–2084.

Conith, A. J., and R. C. Albertson. 2021. The cichlid oral and pharyngeal jaws are evolutionarily and genetically coupled. Nat. Commun. 12:1–11. Springer US

Conith, A.J., Hope, S.A., Chhouk, B.H., and Albertson, R.C. 2021. Weak genetic signal for phenotypic integration implicates developmental processes as major regulators of trait covariation. *Mol. Ecol.* 464–480.

Conway Morris S. 2003. Life's Solution Cambridge: Cambridge University Press.

Cooper WJ, Westneat MW. 2009. Form and function of damselfish skulls: Rapid and

repeated evolution into a limited number of trophic niches. BMC Evol Biol 9:1–17.

Cooper WJ, Parsons K, McIntyre A, Kern B, McGee-Moore A, Albertson RC. 2010. Bentho-Pelagic Divergence of Cichlid Feeding Architecture Was Prodigious and Consistent during Multiple Adaptive Radiations within African Rift-Lakes. *PLoS One* 5(3):e9551.

Cooper WJ, Wernle J, Mann K, Albertson RC. 2011. Functional and Genetic Integration in the Skulls of Lake Malawi Cichlids. *Evol Biol.* 38(3):316-334.

Cooper WJ, Wirgau RM, Sweet EM, Albertson RC. 2013. Deficiency of zebrafish *fgf20a* results in aberrant skull remodeling that mimics both human cranial disease and evolutionarily important fish skull morphologies. *Evol Dev*. 15(6):426-41.

Cooper KL, Oh S, Sung Y, Dasari RR, Kirschner MW, Tabin CJ. Multiple phases of chondrocyte enlargement underlie differences in skeletal proportions. Nature. 2013;495(7441):375-378. doi:10.1038/nature11940

Corbit KC, Shyer AE, Dowdle WE, Gaulden J, Singla V, Reiter JF. Kif3a constrains β-catenin-dependent Wnt signalling through dual ciliary and non-ciliary mechanisms. Nature Cell Biology. 2008;10(1):70-76. doi:10.1038/ncb1670

Cortés CR, Metzis V, Wicking C. Unmasking the ciliopathies: Craniofacial defects and the primary cilium. Wiley Interdisciplinary Reviews: Developmental Biology. 2015;4(6):637-653. doi:10.1002/wdev.199

Coughlin DJ, Carroll AM. 2006. In vitro estimates of power output by epaxial muscle during feeding in largemouth bass. Comp Biochem Physiol - A Mol Integr Physiol 145:533–39.

Creuzet S, Schuler B, Couly G, Le Douarin NM. Reciprocal relationships between Fgf8 and neural crest cells in facial and forebrain development. Proceedings of the National Academy of Sciences of the United States of America. 2004;101(14):4843-4847. doi:10.1073/pnas.0400869101

Creuzet S, Couly G, Le Douarin NM. Patterning the neural crest derivatives during development of the vertebrate head: Insights from avian studies. Journal of Anatomy. 2005;207(5):447-459. doi:10.1111/j.1469-7580.2005.00485.x

Crump JG, Maves L, Lawson ND, Weinstein BM, Kimmel CB. An essential role for Fgfs in endodermal pouch formation influences later craniofacial skeletal patterning. Development. 2004;131(22):5703-5716. doi:10.1242/dev.01444

Cureton II, J. C., & Broughton, R. E. (2014). Rapid morphological divergence of a stream fish in response to changes in water flow. *Biology Letters*, *10*, 8–11. Retrieved from http://dx.doi.org/10.1098/rsbl.2014.0352

Czaplinski K. Understanding mRNA trafficking: Are we there yet? Seminars in Cell and Developmental Biology. 2014;32:63-70. doi:10.1016/j.semcdb.2014.04.025

Darwin C. On the Origin of Species; 1859.

Dash S, Trainor PA. The development, patterning and evolution of neural crest cell differentiation into cartilage and bone. Bone. 2020;137. doi:10.1016/j.bone.2020.115409

Datovo A, Vari RP. 2013. The Jaw Adductor Muscle Complex in Teleostean Fishes: Evolution, Homologies and Revised Nomenclature (Osteichthyes: Actinopterygii). PLoS One 8.

Dawe HR, Adams M, Wheway G, et al. Nesprin-2 interacts with meckelin and mediates ciliogenesis via remodelling of the actin cytoskeleton. Journal of Cell Science. 2009;122(15):2716-2726. doi:10.1242/jcs.043794

de Mérona, Bernard, Mendes Dos Santos, G., & Goncçalves de Almeida, R. (2001). Short term effects of Tucuruí Dam (Amazonia, Brazil) on the trophic organization of fish communities. *Environmental Biology of Fishes*, *60*(4), 375–392. doi:10.1023/A:1011033025706

Denton JSS, Adams DC. 2015. A new phylogenetic test for comparing multiple high-dimensional evolutionary rates suggests interplay of evolutionary rates and modularity in lanternfishes (Myctophiformes; Myctophidae). Evolution (N Y) 69:2425–40.

Dias, M. S., Cornu, J. F., Oberdorff, T., Lasso, C. A., & Tedesco, P. A. (2013). Natural fragmentation in river networks as a driver of speciation for freshwater fishes. *Ecography*, *36*(6), 683–689. doi:10.1111/j.1600-0587.2012.07724.x

Dietrich K, Fiedler I, Kurzyukova A, et al. Skeletal biology and disease modeling in zebrafish. Journal of Bone and Mineral Research. Published online 2021. doi:10.1002/jbmr.4256

Domenici P, Wilson ADM, Kurvers RHJM, Marras S, Herbert-Read JE, Steffensen JF, Krause S, Viblanc PE, Couillaud P, Krause J. 2014. How sailfish use their bills to capture schooling prey. Proc R Soc B Biol Sci 281:1–6.

Drucker EG, Lauder G V. 2001. Locomotor function of the dorsal fin in teleost fishes: Experimental analysis of wake forces in sunfish. J Exp Biol 204:2943–58.

Drummond AJ, Ho SYW, Phillips MJ, Rambaut A. 2006. Relaxed phylogenetics and

dating with confidence. PLoS Biol 4:699–710.

Du W, Bhojwani A, Hu JK. FACEts of mechanical regulation in the morphogenesis of craniofacial structures. International Journal of Oral Science. 2021;13(1):4-4. doi:10.1038/s41368-020-00110-4

Dugan, P. J., Barlow, C., Agostinho, A. A., Baran, E., Cada, G. F., Chen, D., … Winemiller, K. O. (2010). Fish migration, dams, and loss of ecosystem services in the mekong basin. *Ambio*, *39*(4), 344–348. doi:10.1007/s13280-010-0036-1

Dumont ER, Dávalos LM, Goldberg A, Santana SE, Rex K, Voigt CC. 2012. Morphological innovation, diversification and invasion of a new adaptive zone. *Proc R Soc B.* 279:1797–1805

Dumont ER, Samadevam K, Grosse IR, Warsi OM, Baird B, Dávalos LM. 2014. Selection for mechanical advantage underlies multiple cranial optima in new world leaf-nosed bats. *Evolution* 68(5):1436-1449.

Eames B, DeLaurier A, Ullmann B, et al. FishFace: interactive atlas of zebrafish craniofacial development at cellular resolution. BMC Developmental Biology. 2013;13(1):23-23. doi:10.1186/1471-213X-13-23

Echevarría-Andino ML, Allen BL. The hedgehog co-receptor boc differentially regulates shh signaling during craniofacial development. Development. 147(23) doi:10.1101/2020.02.04.934497.

Ehrenreich IM, Pfennig DW. 2016. Genetic assimilation: a review of its potential proximate causes and evolutionary consequences. *Ann Bot.* 117(5):769-79.

ELETROBRÁS/DNAEE. (1997). *Manual de Inventário Hidrelétrico de Bacias Hidrográficas*. Brasília.

Elliott KH, Brugmann SA. Sending mixed signals: Cilia-dependent signaling during development and disease. Developmental Biology. 2019;447(1):28-41. doi:10.1016/j.ydbio.2018.03.007

Ellison R, Knox R, Jolley D, King C. 1994. A revision of the lithostratigraphical classification of the early Palaeogene strata of the London Basin and East Anglia. Proc Geol Assoc 105:187–97.

Emlen, D.J. 2000. Integrating development with evolution: A case study with beetle horns. *Bioscience* 50: 403–418.

Evans, K.M., Larouche, O., Watson, S.J., Farina, S., Habegger, M.L., and Friedman, M. 2021. Integration drives rapid phenotypic evolution in flatfishes. *Proc. Natl. Acad. Sci.* 118: 1–10.

Farnsworth KD, Niklast KJ. 1995. Theories of optimization, form and function in branching architecture in plants. Funct Ecol 9:355–63.

Favero, J. M. del, Pompeu, P. dos S., & Prado-Valladares, A. C. (2010). Biologia reprodutiva de Heros efasciatus Heckel, 1840 (Pisces, Cichlidae) na Reserva de Desenvolvimento Sustentável Amanã-AM, visando seu manejo sustentável. *Acta Amazônica*, *40*(2), 373–380.

Fearnside, P. M. 2001. Environmental impacts of Brazil's Tucuruı´ Dam: Unlearned lessons for hydroelectric development in Amazonia. Environ. Manage. 27:377–396.

Feilich, K. L. 2016. Correlated evolution of body and fin morphology in the cichlid fishes. Evolution (N. Y). 70:2247–2267.

Felsenthal N, Zelzer E. Mechanical regulation of musculoskeletal system development. Development (Cambridge). 2017;144(23):4271-4283. doi:10.1242/dev.151266

Ferry-Graham LA, Wainwright PC, Bellwood DR. 2001. Prey capture in long-jawed butterflyfishes (Chaetodontidae): The functional basis of novel feieding habits. J Exp Mar Bio Ecol 256:167–84.

Ferry-Graham LA, Wainwright PC, Darrin Hulsey C, Bellwood DR. 2001. Evolution and mechanics of long jaws in butterflyfishes (Family Chaetodontidae). J Morphol 248:120–43.

Fierstine H, Huddleston R, Takeuchi G. 2012. Neogene bony fishes of California: a systematic inventory of all published accounts. Calif Acad Sci.

Fitzjohn RG. 2012. Diversitree: Comparative phylogenetic analyses of diversification in R. Methods Ecol Evol 3:1084–92.

Fisher RA. The possible modification of the response of the wild type to recurrent mutations. Am Nat. 1928;62(679):115-126.

Fitzjohn RG. 2012. Diversitree: Comparative phylogenetic analyses of diversification in R. Methods Ecol Evol 3:1084–92.

Foote, M. 1997. The evolution of morphological diversity. Annu. Rev. Ecol. Syst. 28:129–152.

Franssen, N. R. (2011). Anthropogenic habitat alteration induces rapid morphological divergence in a native stream fish. *Evolutionary Applications*, *4*(6), 791–804. doi:10.1111/j.1752-4571.2011.00200.x

Fridolfsson HN, Ly N, Meyerzon M, Starr DA. UNC-83 coordinates kinesin-1 and dynein activities at the nuclear envelope during nuclear migration. Dev Biol. 2010;338(2):237-250. doi:10.1016/j.ydbio.2009.12.004

Friedman M. 2009. Ecomorphological selectivity among marine teleost fishes during the

end-Cretaceous extinction. Proc Natl Acad Sci U S A 106:5218–23.

Friedman M. 2010. Explosive morphological diversification of spiny-finned teleost fishes in the aftermath of the end-Cretaceous extinction. Proc R Soc B Biol Sci 277:1675–83.

Friedman M, Feilich KL, Beckett HT, Alfaro ME, Faircloth BC, Černý D, Miya M, Near TJ, Harrington RC. 2019. A phylogenomic framework for pelagiarian fishes (Acanthomorpha: Percomorpha) highlights mosaic radiation in the open ocean. Proc R Soc B Biol Sci 286.

Fuchs Y, Steller H. Live to die another way: Modes of programmed cell death and the signals emanating from dying cells. Nature Reviews Molecular Cell Biology. 2015;16(6):329-344. doi:10.1038/nrm3999

Fugi, R, Agostinho, a a, & Hahn, N. S. (2001). Trophic morphology of five benthic-feeding fish species of a tropical floodplain. *Revista Brasleira de Biologia*, *61*(1), 27–33. doi:10.1590/S0034-71082001000100005

Fugi, Rosemara, Luz-Agostinho, K. D. G., & Agostinho, A. A. (2008). Trophic interaction between an introduced (peacock bass) and a native (dogfish) piscivorous fish in a Neotropical impounded river. *Hydrobiologia*, *607*(1), 143–150. doi:10.1007/s10750-008-9384-2

Galea GL, Zein MR, Allen S, Francis-West P. Making and shaping endochondral and intramembranous bones. Dev Dyn. 2021;250(3):414-449. doi:10.1002/dvdy.278

Galis, F., and Metz, J.A.J. 2007. Evolutionary novelties: The making and breaking of pleiotropic constraints. *Integr. Comp. Biol.* 47: 409–419.

Gao B, Yang Y. Planar cell polarity in vertebrate limb morphogenesis. Curr Opin Genet Dev. 2013;23(4):438-444. doi:10.1016/j.gde.2013.05.003

Garcia G, Reiter JF. A primer on the mouse basal body. Cilia. 2016;5(1). doi:10.1186/s13630-016-0038-0

Garduño-Paz, M. V., Couderc, S., & Adams, C. E. (2010). Habitat complexity modulates phenotype expression through developmental plasticity in the threespine stickleback. *Biological Journal of the Linnean Society*, *100*(2), 407–413. doi:10.1111/j.1095-8312.2010.01423.x

Gaston, K. A., & Lauer, T. E. (2015). Morphometric variation in bluegill Lepomis macrochirus and green sunfish Lepomis cyanellus in lentic and lotic systems. *Journal of Fish Biology*, *86*(1). doi:10.1111/jfb.12581

Gebuijs IGE, Raterman ST, Metz JR, et al. Fgf8a mutation affects craniofacial development and skeletal gene expression in zebrafish larvae. Biology Open. 2019;8(9). doi:10.1242/bio.039834

Geister KA, Camper SA. Advances in skeletal dysplasia genetics. Annu Rev Genomics Hum Genet. 2015;16:199-227. doi:10.1146/annurev-genom-090314-045904

Geladi, I., De León, L. F., Torchin, M. E., Hendry, A. P., González, R., & Sharpe, D. M. T. (2019). 100-year time series reveal little morphological change following impoundment and predator invasion in two Neotropical characids. *Evolutionary Applications*, *12*(7), 1385–1401. doi:10.1111/eva.12763

Ghalambor, C. K., McKay, J. K., Carroll, S. P., & Reznick, D. N. (2007). Adaptive versus non-adaptive phenotypic plasticity and the potential for contemporary adaptation in new environments. *Functional Ecology*, *21*(3), 394–407.

doi:10.1111/j.1365-2435.2007.01283.x

Gibb AC, Dickson KA, Lauder G V. 1999. Tail kinematics of the chub mackerel *Scomber japonicus*: Testing the homocercal tail model of fish propulsion. J Exp Biol 202:2433–47.

Gibert JM, 2017. The flexible stem hypothesis: Evidence from genetic data. *Dev Genes Evol.* 227:297–307.

Gilbert, M. C., A. Akama, C. Cox, and R. C. Albertson. 2020. Rapid morphological change in multiple cichlid ecotypes following the damming of a major clearwater river in Brazil. 2754–2771.

Gilbert MC, Tetrault E, Packard M, Navon D, Albertson RC. Ciliary rootlet coiled-coil 2 (crocc2) is associated with evolutionary divergence and plasticity of cichlid jaw shape. Mol Biol Evol. 2021;38(8):3078-3092. doi:10.1093/molbev/msab071

Gilbert, M. C., A. J. Conith, C. S. Lerose, J. K. Moyer, S. H. Huskey, and R. C. Albertson. 2021. Extreme Morphology, Functional Trade-Offs, and Evolutionary Dynamics in a Clade of Open-Ocean Fishes (Perciformes: Bramidae). Integr. Org. Biol. 3:obab003.

Gibson G, Hogness DS. Effect of polymorphism in the Drosophila regulatory gene Ultrabithorax on homeotic stability. Science. 1996;271(5246):200-203. doi:10.1126/science.271.5246.200

Gilliam JC, Chang JT, Sandoval IM, et al. Three-dimensional architecture of the rod sensory cilium and its disruption in retinal neurodegeneration. Cell. 2012;151(5):1029-1041. doi:10.1016/j.cell.2012.10.038

Goetz SC, Ocbina PJR, Anderson KV. 2009. The Primary Cilium as a Hedgehog Signal Transduction Machine. *Primary Cilia* 94:199-122.

Goetz SC, Anderson KV. The primary cilium: A signalling centre during vertebrate development. Nature Reviews Genetics. 2010;11(5):331-344. doi:10.1038/nrg2774

González-lorenzo G, González-jiménez JF, Brito A, González JF. 2013. The family Bramidae (Perciformes) from the Canary Islands (Northeastern Atlantic Ocean), with three new records. Cybium 37:295–303.

Goodall C. 1991. Procrustes methods in the statistical analysis of shape. *J R Stat Soc.* 53:285–339.

Gosline, W. A. (1971). *Functional Morphology and Classification of Teleostean Fishes*. Honolulu: University Press of Hawaii.

Gould, S.J. 1980. The evolutionary biology of constraint. *Daedalus* 109: 39–52.

Gould, S.J., and Lewontin, R.C. 1979. The spandrels of San Marco and the Panglossian paradigm: a critique of the adaptationist programme. *Proc. R. Soc. London - Biol. Sci.* 205: 581–598.

Gould SJ, Woodruff DS. 1990. History as a cause of area effects: an illustration from *Cerion* on Great Inagua, Bahamas. Biol J Linn Soc 40:67–98.

Goyens, J., Van Wassenbergh, S., Dirckx, J., and Aerts, P. 2015. Cost of flight and the evolution of stag beetle weaponry. *J. R. Soc. Interface* 12:.

Gutiérrez E, Fernandez A, Hernández R. 2005. *Brama caribbea* (Pisces: Bramidae), un nuevo registro para las aguas cubanas. Solenodon 5:78–79.

Green RM, Feng W, Phang T, et al. Tfap2a-dependent changes in mouse facial morphology result in clefting that can be ameliorated by a reduction in Fgf8 gene dosage. DMM Disease Models and Mechanisms. 2015;8(1):31-43. doi:10.1242/dmm.017616

Green, R.M., Fish, J.L., Young, N.M., Smith, F.J., Roberts, B., Dolan, K., Choi, I., Leach, C.L., Gordon, P., Cheverud, J.M., et al. 2017. Developmental nonlinearity drives phenotypic robustness. *Nat. Commun.* 8:.

Ghose P, Shaham S. Cell death in animal development. Development (Cambridge). 2020;147(14). doi:10.1242/dev.191882

Griffin JN, Compagnucci C, Hu D, et al. Fgf8 dosage determines midfacial integration and polarity within the nasal and optic capsules. Developmental Biology. 2013;374(1):185-197. doi:10.1016/j.ydbio.2012.11.014

Gunter HM, Schneider RF, Karner I, Sturmbauer C, Meyer A. 2017. Molecular investigation of genetic assimilation during the rapid adaptive radiations of East African cichlid fishes. *Mol Ecol*. 26(23): 6634-6653.

Gunz P, Mitteroecker P. 2013. Semilandmarks: A method for quantifying curves and surfaces. *Hystrix It J Mamm.* 24(1):103–109.

Haas, T. C., Blum, M. J., & Heins, D. C. (2010). Morphological responses of a stream fish to water impoundment. *Biology Letters*, *6*, 803–806. doi:10.1098/rsbl.2010.0401

Hahn, N. S., & Cunha, F. (2005). Feeding and trophic ecomorphology of Satanoperca pappaterra (Pisces, Cichlidae) in the Manso Reservoir, Mato Grosso State, Brazil. *Brazilian Archives of Biology and Technology*, *48*(6), 1007–1012.

doi:10.1590/S1516-89132005000800017

Hall J, Jheon AH, Ealba EL, et al. Evolution of a developmental mechanism: Species-specific regulation of the cell cycle and the timing of events during craniofacial osteogenesis. Developmental Biology. 2014;385(2):380-395. doi:10.1016/j.ydbio.2013.11.011

Hallgrimsson B. Variation: A Central Concept in Biology. Academic Press; 2005.

Hallgrimsson, B., H. Jamniczky, N. M. Young, C. Rolian, T. E. Parsons, J. C. Boughner, and R. S. Marcucio. 2009. Deciphering the palimpsest: Studying the relationship between morphological integration and phenotypic covariation. Evol. Biol. 36:355–376.

Hammond CL, Schulte-Merker S. Two populations of endochondral osteoblasts with differential sensitivity to Hedgehog signalling. Development. 2009;136(23):3991-4000. doi:10.1242/dev.042150

Han S, Park HR, Lee EJ, et al. Dicam promotes proliferation and maturation of chondrocyte through Indian hedgehog signaling in primary cilia. Osteoarthritis and Cartilage. 2018;26(7):945-953. doi:10.1016/j.joca.2018.04.008

Handa A, Voss U, Hammarsjö A, Grigelioniene G, Nishimura G. Skeletal ciliopathies: a pattern recognition approach. Japanese Journal of Radiology. 2020;38(3):193-206. doi:10.1007/s11604-020-00920-w

Harrington, R.C., Friedman, M., Near, T.J., and Campbell, M.A. 2021. Phylogenomic resolution of the monotypic and enigmatic Amarsipus , the Bagless Glassfish (Teleostei , Amarsipidae). 1–12.

Haycraft CJ, Banizs B, Aydin-Son Y, Zhang Q, Michaud EJ, Yoder BK. 2005. Gli2 and Gli3 localize to cilia and require the intraflagellar transport protein polaris for processing and function. *PLoS Genet.* 1(4):e53.

Helfman, G. (2007). Fish Conservation: A guide to understanding and restoring global aquatic biodiversity and fishery resources. Washington, D.C.: Island Press.

Hendrikse JL, Parsons TE, Hallgrimsson B. 2007. Evolvability as the proper focus of evolutionary developmental biology. *Evol Dev*. 9(4):393-401.

Hernandez LP, Bird NC, Staab KL. 2007. Using Zebrafish to Investigate Cypriniform Evolutionary Novelties: Functional Development and Evolutionary Diversification of the Kinethmoid. *J Exp Zool B Mol Dev Evol.* 308:625–41.

Herrel A, Bonneaud C. 2012. Trade-offs between burst performance and maximal exertion capacity in a wild amphibian, *Xenopus tropicalis*. J Exp Biol 215:3106–11.

Herrel A, Podos J, Vanhooydonck B, Hendry AP. 2009. Force-velocity trade-off in Darwin's finch jaw function: A biomechanical basis for ecological speciation? Funct Ecol 23:119–25.

Higgins, K., & Lynch, M. (2001). Metapopulation extinction caused by mutation accumulation. *Proceedings of the National Academy of Science*, *98*(5), 2928–2933.

Hoeinghaus, D. J., Layman, C. A., Arrington, D. A., & Winemiller, K. O. (2003). Movement of Cichla species (Cichlidae) in a Venezuelan floodplain river. *Neotropical Ichthyology*, *1*(2), 121–126. doi:10.1590/s1679-62252003000200006

Hoey DA, Downs ME, Jacobs CR. The mechanics of the primary cilium: An intricate structure with complex function. Journal of Biomechanics. 2012;45(1):17-26. doi:10.1016/j.jbiomech.2011.08.008

Holladay, J.T. 1997. Proper method for calculating average visual acuity. *J. Refract. Surg.* 13: 388–391.

Holzman R, Collar DC, Price SA, Darrin Hulsey C, Thomson RC, Wainwright PC. 2012. Biomechanical trade-offs bias rates of evolution in the feeding apparatus of fishes. Proc R Soc B Biol Sci 279:1287–92.

Hoogland R, Morris D, Tinbergen N. 1956. The spines of sticklebacks (*Gasterosteus* and *Pygosteus*) as means of defence against predators (*Perca* and *Esox*). Behaviour 10:205–36.

Hossain D, Shih SYP, Xiao X, White J, Tsang WY. Cep44 functions in centrosome cohesion by stabilizing rootletin. Journal of cell science. 2020;133(4). doi:10.1242/jcs.239616

Hu D, Marcucio RS. A SHH-responsive signaling center in the forebrain regulates craniofacial morphogenesis via the facial ectoderm. Development. 2009;136(1):107-116. doi:10.1242/dev.026583

Hu D, Young NM, Li X, Xu Y, Hallgrımsson B, Marcucio RS. A dynamic shh expression pattern, regulated by shh and bmp signaling, coordinates fusion of primordia in the amniote face. Development (Cambridge). 2015;142(3):567-574. doi:10.1242/dev.114835

Hu Y-N, Albertson RC. 2017. Baby fish working out: an epigenetic source of adaptive variation in the cichlid jaw. *Proc Biol Sci*. 284(1860):20171018.

Huber C, Cormier-Daire V. Ciliary disorder of the skeleton. American Journal of Medical Genetics, Part C: Seminars in Medical Genetics. 2012;160 C(3):165-174. doi:10.1002/ajmg.c.31336

Hulsey, C. D., Hendrickson, D. A., & García De León, F. J. (2005). Trophic morphology, feeding performance and prey use in the polymorphic fish Herichthys minckleyi. *Evolutionary Ecology Research, 7*, 303–324.

Huxley, J. 1942. Evolution. The modern synthesis.

Huybrechts Y, Mortier G, Boudin E, Van Hul W. WNT signaling and bone: Lessons from skeletal dysplasias and disorders. Front Endocrinol (Lausanne). 2020;11:165. doi:10.3389/fendo.2020.00165

Ibarra BA, Atit R. What do animal models teach us about congenital craniofacial defects? Advances in Experimental Medicine and Biology. 2020;1236:137-155. doi:10.1007/978-981-15-2389-2_6

Irisarri I, Singh P, Koblmüller S, Torres-Dowdall J, Henning F, Franchini P, Fischer C, Lemmon AR, Lemmon EM, Thallinger GG, et al. 2018. Phylogenomics uncovers early hybridization and adaptive loci shaping the radiation of Lake Tanganyika cichlid fishes. *Nat Commun.* 9(1):3159.

Irschick, D.J., Albertson, R.C., Brennan, P., Podos, J., Johnson, N.A., Patek, S., and Dumont, E. 2013. Evo-devo beyond morphology: From genes to resource use. *Trends Ecol. Evol.* 28:.

Jacob F. Evolution and tinkering. Science. 1977;196(4295):1161-1166.

Jagnandan K, Sanford CP. 2013. Kinematics of ribbon-fin locomotion in the bowfin, *Amia calva*. J Exp Zool Part A Ecol Genet Physiol 319:569–83.

Jamniczky HA, Boughner JC, Rolian C, Gonzalez PN, Powell CD, Schmidt EJ, Parsons TE, Bookstein FL, Hallgrimsson B. 2010. Rediscovering Waddington in the post-genomic age. *Bioessays* 32(7):553-558.

Janssen J, Gibbs RH, Pugh PR. 1989. Association of *Caristius sp.* (Pisces : Caristiidae) with a Siphonophore, *Bathyphysa conifera*. Copeia 1989:198–201

Jarvis, J.R., and Wathes, C.M. 2012. Mechanistic modeling of vertebrate spatial contrast sensitivity and acuity at low luminance. *Vis. Neurosci.* 29: 169–181.

Jawad LA, Al-Mamry JM, Al-Busaidi HK. 2014. New record of the keeltail pomfret, *Taractes rubescens* (Jordan & Evermann, 1887) (Perciformes : Bramidae) from the Sea of Oman. Int J Mar Sci 4:227–30.

Jimenez YE, Camp AL, Grindall JD, Brainerd EL. 2018. Axial morphology and 3D neurocranial kinematics in suction-feeding fishes. Biol Open 7.

Jones, G. 1994. Scaling of Wingbeat and Echolocation Pulse Emission Rates in Bats: Why are Aerial Insectivorous Bats so Small? *Funct. Ecol.* 8: 450.

Joukov V, De Nicolo A. The Centrosome and the primary cilium: the yin and yang of a hybrid organelle. Cells. 2019;8(7):701-701. doi:10.3390/cells8070701

Jussila M, Ciruna B. Zebrafish models of non-canonical Wnt/planar cell polarity signalling: fishing for valuable insight into vertebrate polarized cell behavior. Wiley Interdisciplinary Reviews: Developmental Biology. 2017;6(3):e267-e267. doi:10.1002/wdev.267

Kague E, Hughes SM, Lawrence EA, et al. Scleraxis genes are required for normal musculoskeletal development and for rib growth and mineralization in zebrafish. FASEB Journal. 2019;33(8):9116-9130. doi:10.1096/fj.201802654RR

Kawano, K. 1997. Cost of evolving exaggerated mandibles in stag beetles (Coleoptera: Lucanidae). *Entomol. Soc. Am.* 90: 453–461.

Kennedy MC. 2010. Functional-structural models optimize the placement of foliage units for multiple whole-canopy functions. Ecol Res 25:723–32

Kaseda K, McAinsh AD, Cross RA. Dual pathway spindle assembly increases both the speed and the fidelity of mitosis. Biology Open. 2012;1(1):12-18. doi:10.1242/bio.2011012

Kettleborough RNW, Busch-Nentwich EM, Harvey SA, et al. A systematic genome-wide analysis of zebrafish protein-coding gene function. Nature. 2013;496(7446):494-497. doi:10.1038/nature11992

Kirby TJ, Lammerding J. Emerging views of the nucleus as a cellular mechanosensor. Nature Cell Biology. 2018;20(4):373-381. doi:10.1038/s41556-018-0038-y

Klingenberg CP. Developmental Constraints, Modules, and Evolvability. Variation. Published online 2005:219-247.

Klingenberg, C. P. 2008. Morphological Integration and Developmental Modularity. Annu. Rev. Ecol. Evol. Syst. 39:115–132.

Klingenberg CP. 2011. MorphoJ: an integrated software package for geometric morphometrics. Mol Ecol Resour 11:353–57.

Ko D, Kim J, Rhee K, Choi HJ. Identification of a structurally dynamic domain for oligomer formation in rootletin. Journal of Molecular Biology. 2020;432(13):3915-3932. doi:10.1016/j.jmb.2020.04.012

Kocher, T. D. (2004). Adaptive evolution and explosive speciation: the cichlid fish model. *Nature Reviews Genetics*, *5*(4), 288–298. doi:10.1038/nrg1316

Konuma J, Chiba S. 2007. Trade-offs between force and fit: Extreme morphologies associated with feeding behavior in carabid beetles. Am Nat 170:90–100.

Kovalenko, K. E., Dibble, E. D., Agostinho, A. A., Cantanhêde, G., & Fugi, R. (2010). Direct and indirect effects of an introduced piscivore, Cichla kelberi and their modification by aquatic plants. *Hydrobiologia*, *638*, 245–253. doi:10.1007/s10750-009-0049-6

Kristjansson, B. K., Skulason, S., Noakes, D. L. G., & Kristjánsson, B. (2002). Rapid divergence in a recently isolated population of threespine stickleback (Gasterosteus aculeatus L.). *Evolutionary Ecology Research*, *4*, 659–672. Retrieved from http://cat.inist.fr/?aModele=afficheN&cpsidt=14395917%5Cn%3CGo to ISI%3E://WOS:000177011200003

Kullander, S. O., & Ferreira, E. J. G. (2006). A review of the South American cichlid genus Cichla, with descriptions of nine new species (Teleostei: Cichlidae). *Ichthyological Exploration of Freshwaters*, *17*(4), 289–398.

Kuntner, M., and Coddington, J.A. 2020. Sexual size dimorphism: Evolution and perils of extreme phenotypes in spiders. *Annu. Rev. Entomol.* 65: 57–80.

Kuratani, S. 2009. Modularity, comparative embryology and evo-devo: Developmental dissection of evolving body plans. Dev. Biol. 332:61–69. Elsevier Inc.

Lahti, D. C., Johnson, N. A., Ajie, B. C., Otto, S. P., Hendry, A. P., Blumstein, D. T., … Foster, S. A. (2009). Relaxed selection in the wild. *Trends in Ecology and Evolution*, *24*(9), 487–496. doi:10.1016/j.tree.2009.03.010

Lamb H. 1975. Hydrodynamics New York: Dover.

Lande R, Shannon S. The Role of genetic variation in adaptation and population persistence in a changing environment. Evolution. 1996;50(1):434-437.

Langerhans RB, Layman CA, DeWitt TJ. 2005. Male genital size reflects a tradeoff between attracting mates and avoiding predators in two live-bearing fish species. Proc Natl Acad Sci U S A 102:7618–23.

Lande, R., & Shannon, S. (1996). The Role of genetic variation in adaptation and population persistence in a changing environment. *Evolution*, *50*(1), 434–437.

Landgren, E., Fritsches, K., Brill, R., and Warrant, E. 2014. The visual ecology of a deep-sea fish, the escolar Lepidocybium flavobrunneum (Smith, 1843). *Philos. Trans. R. Soc. B Biol. Sci.* 369:.

Langerhans, R. B., Layman, C. A., Langerhans, A. K., & Dewitt, T. J. (2003). Habitat-associated morphological divergence in two Neotropical fish species, 689–698.

Larochelle, C. R., Pickens, F. A. T., Burns, M. D., & Sidlauskas, B. L. (2016). Long-term isopropanol storage does not alter fish morphometrics. *Copeia*, *104*(2), 411–420. doi:10.1643/CG-15-303

Larouche, O., Cloutier, R., and Zelditch, M.L. 2015. Head, Body and Fins: Patterns of Morphological Integration and Modularity in Fishes. *Evol. Biol.* 42: 296–311.

Larouche, O., Zelditch, M.L., and Cloutier, R. 2017. Fin modules: An evolutionary perspective on appendage disparity in basal vertebrates. *BMC Biol.* 15:.

Larouche, O., Zelditch, M.L., and Cloutier, R. 2018. Modularity promotes morphological divergence in ray-finned fishes. *Sci. Rep.* 8: 1–6.

Lau, J. K., T. E. Lauer, and M. L. Weinman. 2006. Impacts of channelization of stream

habitats and associated fish assemblages in east central Indiana. Am. Midl. Nat. 156:319–330

Larsson A. 2014. AliView: A fast and lightweight alignment viewer and editor for large datasets. Bioinformatics 30:3276–78.

Lauder G V., Liem KF. 1981. Prey capture by *Luciocephalus pulcher*: implications for models of jaw protrusion in teleost fishes. Environ Biol Fishes 6:257–68.

Lauder G V. 1981. Intraspecific functional repertoires in the feeding mechanism of the characoid fishes *Lebiasina, Hoplias* and *Chalceus*. Copeia 1981:154–68.

Lawrence EA, Kague E, Aggleton JA, Harniman RL, Roddy KA, Hammond CL. The mechanical impact of col11a2 loss on joints; col11a2 mutant zebrafish show changes to joint development and function, which leads to early-onset osteoarthritis. Philosophical Transactions of the Royal Society B: Biological Sciences. 2018;373(1759). doi:10.1098/rstb.2017.0335

Lau, J. K., Lauer, T. E., & Weinman, M. L. (2006). Impacts of channelization of stream habitats and associated fish assemblages in east central Indiana. *American Midland Naturalist*, *156*(2), 319–330.

Le Pabic P, Ng C, Schilling TF. Fat-dachsous signaling coordinates cartilage differentiation and polarity during craniofacial development. Mullins MC, ed. PLoS Genetics. 2014;10(10):e1004726-e1004726. doi:10.1371/journal.pgen.1004726

Le Pabic P, Cooper WJ, Schilling TF. Developmental basis of phenotypic integration in two Lake Malawi cichlids. EvoDevo. 2016;7(1):3-3. doi:10.1186/s13227-016-0040-z

Lee WJ, Kim JK. 2015. New record of *Brama dussumieri* (Pisces: Bramidae) from Korea, as revealed by morphological and molecular analyses. Fish Aquat Sci 18:311–16.

Lee J, Lee W, Kim J. 2019. First reliable record of the keeltail pomfret *Taractes rubescens* (Bramidae : Perciformes) from Korea. Korean J Fish Aquat Sci 52:283–87.

Lee BT, Barber GP, Benet-Pagès A, et al. The UCSC Genome Browser database: 2022 update. Nucleic Acids Res. 2022;50(D1):D1115-D1122. doi:10.1093/nar/gkab959

Legendre R. 1924. *Brama raii* Bl.: sa présence au large des côtes sud de la Bretagne. Bull la Société Zool Fr 49:218–25.

Lema, S. C., & Nevitt, G. a. (2006). Testing an ecophysiological mechanism of morphological plasticity in pupfish and its relevance to conservation efforts for endangered Devils Hole pupfish. *The Journal of Experimental Biology*, *209*(Pt 18), 3499–509. doi:10.1242/jeb.02417

Lenov Y. 1998. Late Eocene-Early Oligocene geological and biotical events on the territory of the former Soviet Union. Part II. The geological and biotical events, Moscow: GEOS.

Lenth, R. 2020. Emmeans: estimated marginal means, aka. least-squares means.

Leroi AM, Kim SB, Rose MR. 1994. The evolution of phenotypic life-history trade-offs: An experimental study using *Drosophila melanogaster*. Am Nat 144:661–76.

Li X, Young NM, Tropp S, et al. Quantification of shape and cell polarity reveals a novel mechanism underlying malformations resulting from related FGF mutations

during facial morphogenesis. Human Molecular Genetics. 2013;22(25):5160-5172. doi:10.1093/hmg/ddt369

Li M, Liao L, Tian W. Extracellular vesicles derived from apoptotic cells: an essential link between death and regeneration. Frontiers in Cell and Developmental Biology. 2020;8. doi:10.3389/fcell.2020.573511

Liem, K. F., & Osse, J. (1975). Biological versatility, evolution, and food resource exploitation in African cichlid fishes. *American Zoologist*, *15*(2), 427–454.

Liermann, C. R., Nilsson, C., Robertson, J., & Ng, R. Y. (2012). Implications of dam obstruction for global freshwater fish diversity. *BioScience*, *62*(6), 539–548. doi:10.1525/bio.2012.62.6.5

Lindsey, C. C. (1981). Stocks are chameleons: Plasticity in gill rakers of coregonid fishes. *Canadian Journal of Fisheries and Aquatic Sciences*, *38*, 1497–1506.

Ling IT, Rochard L, Liao EC. Distinct requirements of wls, wnt9a, wnt5b and gpc4 in regulating chondrocyte maturation and timing of endochondral ossification. Developmental Biology. 2017;421(2):219-232. doi:10.1016/j.ydbio.2016.11.016

Liu X, Tian S, Li W, Wu F, Dai X. 2016. Complete mitochondrial genome of the *Taractes rubescens* (Perciformes: Bramidae). Mitochondrial DNA 27:2809–10.

Livak KJ, Schmittgen TD. 2001. Analysis of relative gene expression data using real-time quantitative PCR and the 2(-Δ Δ C(T)) Method. *Methods* 25:402–408.

Lobo C, Erzini K. 2001. Age and growth of Ray's bream (*Brama brama*) from the south of Portugal. Fish Res 51:343–47.

Long F. 2011. Building strong bones: molecular regulation of the osteoblast lineage. *Nat Rev Mol Cell Biol.* 13:27–38.

Loofbourrow H. 2006. Hydrodynamics of balistiform swimming in the picasso triggerfish, *Rhinecanthus aculeatus*. University of British Columbia.

López-Fernández, H., Honeycutt, R. L., & Winemiller, K. O. (2005). Molecular phylogeny and evidence for an adaptive radiation of geophagine cichlids from South America (Perciformes: Labroidei). *Molecular Phylogenetics and Evolution*, *34*(1), 227–244. doi:10.1016/j.ympev.2004.09.004

López-Fernández, H., K. O. Winemiller, C. Montaña, and R. L. Honeycutt. 2012. Diet-morphology correlations in the radiation of south American geophagine cichlids (Perciformes: Cichlidae: Cichlinae). PLoS One 7.

López-Fernández, H., J. H. Arbour, K. O. Winemiller, and R. L. Honeycutt. 2013. Testing for ancient adaptive radiations in neotropical cichlid fishes. Evolution (N. Y). 67:1321–1337.

Losos JB, Jackman TR, Larson A, De Queiroz K, Rodríguez-Schettino L. 1998. Contingency and determinism in replicated adaptive radiations of island lizards. Science (80-) 279:2115–18.

Losos, J. B. (2010). Adaptive Radiation, Ecological Opportunity, and Evolutionary Determinism. *The American Naturalist*, *175*(6), 623–639. doi:10.1086/652433

Mabee, P.M., Crotwell, P.L., Bird, N.C., and Burke, A.C. 2002. Evolution of median fin modules in the axial skeleton of fishes. *J. Exp. Zool.* 294: 77–90.

Maingi, J. K., & Marsh, S. E. (2002). Quantifying hydrologic impacts following dam construction along the Tana River, Kenya. *Journal of Arid Environments*, *50*(1), 53–79. doi:10.1006/jare.2000.0860

Male I, Tuba Ozacar A, Fagan RR, et al. Hedgehog signaling regulates neurogenesis in the larval and adult zebrafish hypothalamus. bioRxiv. Published online 2019:740613-740613. doi:10.1101/740613

Malinsky, M., Svardal, H., Tyers, A. M., Miska, E. A., Genner, M. J., Turner, G. F., & Durbin, R. (2018). Whole-genome sequences of Malawi cichlids reveal multiple radiations interconnected by gene flow. *Nature Ecology and Evolution*, *2*(12), 1940–1955. doi:10.1038/s41559-018-0717-x

Mallarino R, Grant PR, Grant BR, Herrel A, Kuo WP, Abzhanov A. Two developmental modules establish 3D beak-shape variation in Darwin's finches. Proceedings of the National Academy of Sciences of the United States of America. 2011;108(10):4057-4062. doi:10.1073/pnas.1011480108

Manabu S. 2010. Jaw biomechanics and the evolution of biting performance in theropod dinosaurs. *Proc R Soc B.* 277:3327–3333.

Man-Ger Sun M, Beier F. Chondrocyte hypertrophy in skeletal development, growth, and disease. doi:10.1002/bdrc.21062

Mansfield JH, Abzhanov A. Hox expression in the american alligator and evolution of archosaurian axial patterning. J Exp Zool (Mol Dev Evol). 2010;314:629-644. doi:10.1002/jez.b.21364

Martín-Guerrero E, Tirado-Cabrera I, Buendía I, Alonso V, Gortázar AR, Ardura JA. Primary cilia mediate parathyroid hormone receptor type 1 osteogenic actions in osteocytes and osteoblasts via Gli activation. J Cell Physiol. 2020;235(10):7356-7369. doi:10.1002/jcp.29636

Mason JM, Schmitz MA, Muller KM, Arndt KM. 2006. Semirational design of Jun-Fos coiled coils with increased affinity: Universal implications for leucine zipper prediction and design. *Proc Natl Acad Sci USA* 103(24):8989-94.

Maynard Smith, J., Burian, R., Kauffman, S., Alberch, P., Campbell, J., Goodwin, B., Lande, R., Raup, D., and Wolpert, L. 1985. Developmental constraints and evolution: A perspective from the mountain lake conference on development and evolution. *Q. Rev. Biol.* 60: 265–287.

Mayr E. 1993. What was the evolutionary synthesis? *Trends Ecol Evol.* 8:31-33.

McCoy, M. W., Bolker, B. M., Osenberg, C. W., Miner, B. G., & Vonesh, J. R. (2006). Size correction: Comparing morphological traits among populations and environments. *Oecologia*, *148*(4), 547–554. doi:10.1007/s00442-006-0403-6

Mcgee, M. D., B. C. Faircloth, S. R. Borstein, J. Zheng, C. D. Hulsey, P. C. Wainwright, M. E. Alfaro, W. Pc, and A. M. E. Replicated. 2016. Replicated divergence in cichlid radiations mirrors a major vertebrate innovation. 1–6.

McGhee, G. R. 2007. The geometry of evolution: Adaptive landscapes and theoretical morphospaces. Cambridge University Press, Cambridge.

McGowan C. 1999. A practical guide to vertebrate mechanics Cambridge, U.K.: Cambridge University Press.

McGurk PD, Swartz ME, Chen JW, Galloway JL, Eberhart JK. In vivo zebrafish morphogenesis shows Cyp26b1 promotes tendon condensation and musculoskeletal patterning in the embryonic jaw. PLoS Genetics. 2017;13(12). doi:10.1371/journal.pgen.1007112.

Mead GW. 1972. Bramidae. The Carlsberg Foundation's oceanographical expedition

round the World 1928-30 and previous Dana-expeditions. Dana-Report.

Merkes C, Turkalo TK, Wilder N, et al. Ewing sarcoma ewsa protein regulates chondrogenesis of meckel's cartilage through modulation of sox9 in zebrafish. Sabaawy HE, ed. PLOS ONE. 2015;10(1):e0116627-e0116627. doi:10.1371/journal.pone.0116627

Mérona, B. (1987). Aspectos ecológicos da ictiofauna no Baixo Tocantins. *Acta Amazônica*, *1*, 109–124.

Milgrom-Hoffman M, Humbert PO. Regulation of cellular and PCP signalling by the Scribble polarity module. Seminars in Cell and Developmental Biology. 2018;81:33-45. doi:10.1016/j.semcdb.2017.11.021

Miller, R. R. (1961). *Man and the Changing fish fauna of the American Southwest*. Alma: Michigan Academy of Science, Arts, and Letters.

Miller MA, Pfeiffer W, Schwartz T. 2010. Creating the CIPRES Science Gateway for inference of large phylogenetic trees. 2010 Gatew Comput Environ Work GCE 2010 1–8.

Mina, M. V. (2001). Morphological diversification of fish as a consequence of the divergence of ontogenetic trajectories. *Ontogenez*, *32*(6), 471–476. doi:10.1023/A:1012842221732

Minelli, A., and Fusco, G. 2019. No limits: Breaking constraints in insect miniaturization. *Arthropod Struct. Dev.* 48: 4–11.

Mitchell B, Stubbs JL, Huisman F, Taborek P, Yu C, Kintner C. The PCP pathway instructs the planar orientation of ciliated cells in the *Xenopus* larval skin. Current Biology. 2009;19(11):924-929. doi:10.1016/j.cub.2009.04.018.

Miya M, Friedman M, Satoh TP, Takeshima H, Sado T, Iwasaki W, Yamanoue Y, Nakatani M, Mabuchi K, Inoue JG, Poulsen JY, Fukunaga T, Sato Y, Nishida M. 2013. Evolutionary origin of the Scombridae (tunas and mackerels): Members of a Paleogene adaptive radiation with 14 other Pelagic fish families. PLoS One 8:e73535.

Mlodzik M. Planar cell polarity: moving from single cells to tissue-scale biology. Development (Cambridge, England). 2020;147(24). doi:10.1242/dev.186346

Moczek AP. 2008. On the origins of novelty in development and evolution. *Bioessays* 30(5):432-47.

Mohan S, Timbers TA, Kennedy J, Blacque OE, Leroux MR. 2013. Striated rootlet and nonfilamentous forms of rootletin maintain ciliary function. *Curr Biol.* 23(20):2016-22.

Montero JA, Lorda-Diez CI, Hurle JM. Confluence of cellular degradation pathways during interdigital tissue remodeling in embryonic tetrapods. Frontiers in Cell and Developmental Biology. 2020;8. doi:10.3389/fcell.2020.593761

Mork L, Crump G. Zebrafish Craniofacial Development. A window into early patterning. Current Topics in Developmental Biology. 2015;115:235-269. doi:10.1016/bs.ctdb.2015.07.001

Moseley, M.J., and Jones, H.S. 1993. Visual acuity: Calculating appropriate averages. *Acta Ophthalmol.* 71: 296–300.

Moteki M, Arai M, Tsuchiya K, Okamoto H. 2001. Composition of piscine prey in the diet of large pelagic fish in the eastern tropical Pacific Ocean. Fish Sci 67:1063–74.

Moyers Arévalo, R.L., Amador, L.I., Almeida, F.C., and Giannini, N.P. 2020. Evolution

of Body Mass in Bats: Insights from a Large Supermatrix Phylogeny. *J. Mamm. Evol.* 27: 123–138.

Murillo-Rincón AP, Kaucka M. Insights into the complexity of craniofacial development from a cellular perspective. Frontiers in cell and developmental biology. 2020;8:620735-620735. doi:10.3389/fcell.2020.620735

Muschick, M., Barluenga, M., Salzburger, W., & Meyer, A. (2011). Adaptive phenotypic plasticity in the Midas cichlid fish pharyngeal jaw and its relevance in adaptive radiation. *BMC Evolutionary Biology*, *11*(1), 116. doi:10.1186/1471-2148-11-116

Muschick, M., A. Indermaur, and W. Salzburger. 2012. Convergent Evolution within an Adaptive Radiation of Cichlid Fishes. Curr. Biol. 22:2362–2368. Elsevier Ltd.

Narita Y, Kuratani S. Evolution of the vertebral formulae in mammals: A perspective on developmental constraints. Journal of Experimental Zoology Part B: Molecular and Developmental Evolution. 2005;304(2):91-106. doi:10.1002/jez.b.21029

Nauen JC, Lauder G V. 2001. Locomotion in scombrid fishes: Visualization of flow around the caudal peduncle and finlets of the chub mackerel *Scomber japonicus*. J Exp Biol 204:2251–63.

Navon D, Male I, Tetrault ER, Aaronson B, Karlstrom RO, Craig Albertson R. Hedgehog signaling is necessary and sufficient to mediate craniofacial plasticity in teleosts. Proceedings of the National Academy of Sciences of the United States of America. 2020;117(32):19321-19327. doi:10.1073/pnas.1921856117

Nei, M., Maruyama, T., & Chakraborty, R. (1975). The Bottleneck effect and genetic variability in populations. *Evolution*, *29*(1), 1–10.

Nei M. 1987. *Molecular Evolutionary Genetics*. Columbia University Press, New York, NY. USA.

Nijhout, H.F., and Emlen, D.J. 1998. Competition among body parts in the development and evolution of insect morphology. *Proc. Natl. Acad. Sci.* 95: 3685–3689.

Nguyen AM, Jacobs CR. 2013. Emerging role of primary cilia as mechanosensors in osteocytes. *Bone* 54(2):196-204.

Niwa, N., A. Akimoto-Kato, T. Niimi, K. Tojo, R. Machida, and S. Hayashi. 2010. Evolutionary origin of the insect wing via integration of two developmental modules. Evol. Dev. 12:168–176.

Novaes, J. L. C., Caramaschi, É. P., & Winemiller, K. O. (2004). Feeding of Cichla monoculus Spix, 1829 (Teleostei: Cichlidae) during and after reservoir formation in the Tocantins River, Central Brazil. *Acta Limnologica Brasiliensia*, *16*(1), 41–49. doi:10.5829/idosi.mejsr.2016.24.04.23231

Oeffner J, Lauder G V. 2012. The hydrodynamic function of shark skin and two biomimetic applications. J Exp Biol 215:785–95.

Ohba S. Hedgehog signaling in skeletal development: Roles of Indian hedgehog and the mode of its action. International Journal of Molecular Sciences. 2020;21(18):1-17. doi:10.3390/ijms21186665

Olsson R. The relationship between ciliary rootlets and other cell structures. Journal of Cell Biology. 1962;15(3) :doi:10.1083/jcb.15.3.596

Olsen A, Westneat M. 2015. StereoMorph: an R package for the collection of 3D landmarks and curves using a stereo camera set-up. *Methods Ecol Evol.* 6:351–56

Olsen A, Haber A. StereoMorph: Stereo Camera Calibration and Reconstruction. Published 2017. https://cran.r-project.org/web/packages/StereoMorph/index.html

O'Meara, B.C., Ané, C., Sanderson, M.J., and Wainwright, P.C. 2006. Testing for Different Rates of Continuous Trait Evolution Using Likelihood. *Evolution (N. Y).* 60: 922.

Orr JW, Tuttle V, Donovan C. 2018. *Pterycombus petersii* (Bramidae: Teleostei): First record for the eastern North Pacific. Northwest Nat 99:236–38.

Pala R, Alomari N, Nauli S. Primary cilium-dependent signaling mechanisms. International Journal of Molecular Sciences. 2017;18(11):2272-2272. doi:10.3390/ijms18112272

Papachroni KK, Karatzas DN, Papavassiliou KA, Basdra EK, Papavassiliou AG 2009. Mechanotransduction in osteoblast regulation and bone disease. *Trends Mol Med.* 15(5):208-216.

Park JH, Kim JK, Moon JH, Kim CB. 2007. Three unrecorded marine fish species from Korean waters. Ocean Sci J 42:231–40.

Parnell NF, Hulsey CD, Streelman JT. 2012. The Genetic Basis of a complex functional system. *Evolution* 66(11):3352-66.

Parsons KJ, Robinson BW. 2006. Replicated evolution of integrated plastic responses during early adaptive divergence. *Evolution* 60(4):801-813.

Parsons KJ, Robinson BW. 2007. Foraging performance of diet-induced morphotypes in pumpkinseed sunfish (Lepomis gibbosus) favours resource polymorphism. *J Evol Biol.* 20(2):673-684.

Parsons KJ, Trent Taylor A, Powder KE, Albertson RC. 2014. Wnt signalling underlies the evolution of new phenotypes and craniofacial variability in Lake Malawi cichlids. *Nat Commun.* 5:3629.

Parsons KJ, Concannon M, Navon D, Wang J, Ea I, Groveas K, Campbell C, Albertson RC. 2016. Foraging environment determines the genetic architecture and evolutionary potential of trophic morphology in cichlid fishes. *Mol Ecol.* 25(24):6012-6023.

Patek SN, Oakley TH. 2003. Comparative tests of evolutionary trade-offs in a palinurid lobster acoustic system. Evolution (N Y) 57:2082–2100.

Pelegrin N, Mesquita DO, Albinati P, Caldas FLS, de Queiroga Cavalcanti LB, Costa TB, Falico DA, Galdino JYA, Tucker DB, Garda AA. 2017. Extreme specialization to rocky habitats in Tropidurus lizards from Brazil: Trade-offs between a fitted ecomorph and autoecology in a harsh environment. Austral Ecol 42:677–89.

Perkin, J. S., & Bonner, T. H. (2011). Long-term changes in flow regime and fish assemblage composition in the Guadelupe and San Marcos rivers of Texas. *River Research and Applications*, *27*, 566–579. doi:10.1002/rra

Pfennig DW, Wund MA, Snell-Rood EC, Cruickshank T, Schlichting CD, Moczek AP. 2010. Phenotypic plasticity's impacts on diversification and speciation. *Trends Ecol Evol.* 25(8):459-467.

Pigliucci, M., and Preston, K. 2004. Phenotypic integration: studying the ecology and evolution of complex phenotypes (Oxford, UK: Oxford University Press).

Pigliucci M. 2005. Evolution of phenotypic plasticity: where are we going now? *Trends Ecol Evol.* 20(9):481-6.

Pigliucci M. 2007. Do we need an extended evolutionary synthesis? *Evolution* 61(12):2743-9.

Pigliucci M. 2008. Is evolvability evolvable? *Nat Rev Genet.* 9(1):75-82.

Pigliucci M. 2009. An extended synthesis for evolutionary biology. *Ann NY Acad Sci.* 1168:218-28.

Platania, S. (1991). Fishes of the Rio Chama and Upper Rio Grande , New Mexico , with preliminary comments on their longitudinal distribution. *The Southwestern Naturalist*, *36*(2), 186–193.

Platania, S. P., & Altenbach, C. S. (1998). Reproductive strategies and egg types of seven Rio Grande Basin cyprinids. *Copeia*, *1998*(3), 559–569.

Porter HT, Motta PJ. 2004. A comparison of strike and prey capture kinematics of three species of piscivorous fishes: Florida gar (*Lepisosteus platyrhincus*), redfin needlefish (*Strongylura notata*), and great barracuda (*Sphyraena barracuda*). Mar Biol 145:989–1000.

Potter C, Zhu W, Razafsky D, et al. Multiple isoforms of nesprin1 are integral components of ciliary rootlets. Current Biology. 2017;27(13):2014-2022.e6. doi:10.1016/j.cub.2017.05.066

Potthoff T. 1984. Clearing and staining techniques. *Ontog Syst Fishes* 1:35–37.

Powder KE, Cousin H, McLinden GP, Albertson RC. 2014. A Nonsynonymous Mutation in the Transcriptional Regulator *lbh* Is Associated with Cichlid Craniofacial Adaptation and Neural Crest Cell Development. *Mol Biol Evol.* 31(12):3113-3124.

Powder KE, Milch K, Asselin G, Albertson RC. Constraint and diversification of developmental trajectories in cichlid facial morphologies. EvoDevo. 2015;6(1):25-25. doi:10.1186/s13227-015-0020-8

Powder, K. E., and R. C. Albertson. 2016. Cichlid fishes as a model to understand normal and clinical craniofacial variation. Dev. Biol. 415:338–346.

Price TD, Qvarnstrom A, Irwin DE. 2003. The role of phenotypic plasticity in driving genetic evolution. *Proc R Soc B* 270(1523):1433-1440.

Přikryl T, Bannikov AF. 2014. A new species of the Oligocene pomfret fish *Paucaichthys* (Perciformes; Bramidae) from Iran. Neues Jahrb für Geol und Paläontologie - Abhandlungen 272:325–30.

Prum, R. O. 2005. Evolution of the morphological innovations of feathers. J. Exp. Zool. Part B Mol. Dev. Evol. 304:570–579.

Pybus OG, Harvey PH. 2000. Testing macro-evolutionary models using incomplete molecular phylogenies. Proc R Soc B Biol Sci 267:2267–72.

Qiu N, Xiao Z, Cao L, Buechel MM, David V, Roan E, Quarles LD. 2012. Disruption of Kif3a in osteoblasts results in defective bone formation and osteopenia. *J Cell Sci.* 125(8):1945-57.

R Core Team. 2018. R: A language and environment for statistical computing. R A Lang Environ Stat Comput.

Rabosky DL. 2006. Likelihood methods for detecting temporal shifts in diversification rates. Evolution (N Y) 60:1152–64.

Rabosky DL. 2014. Automatic detection of key innovations, rate shifts, and diversity-dependence on phylogenetic trees. PLoS One 9.

Rabosky DL, Grundler M, Anderson C, Title P, Shi JJ, Brown JW, Huang H, Larson JG. 2014. BAMMtools: An R package for the analysis of evolutionary dynamics on phylogenetic trees. Methods Ecol Evol 5:701–7.

Rabosky DL, Lovette IJ. 2008. Density-dependent diversification in North American wood warblers. Proc R Soc B Biol Sci 275:2363–71.

Rabosky DL, Santini F, Eastman J, Smith SA, Sidlauskas B, Chang J, Alfaro ME. 2013. Rates of speciation and morphological evolution are correlated across the largest vertebrate radiation. Nat Commun 4:1–8.

Rahangdale S, Kumar R, Roul SK, Kannan K, Suresh Kumar K, Ranjith L, Manoj Kumar PP. 2019. Filling missing links in bramids distribution along the indian coast with first record of big tooth pomfret, *Brama orcini* (Perciformes: Bramidae) from the east coast of India. Indian J Geo-Marine Sci 48:654–61.

Rambaut A, Drummond AJ, Xie D, Baele G, Suchard MA. 2018. Posterior summarization in Bayesian phylogenetics using Tracer 1.7. Syst Biol 67:901–4.

Raff, R.A. 2000. Evo-devo: the evolution of a new discipline. *Nat. Rev. Genet.* 1: 74–79.

Ramsay, M., and R. Dunbrack. 2003. Physiological constraints on life history phenomena: Examples of small bear cubs. *Am. Nat*. 127(6): 735-743

Reid, M., & Atz, J. (1958). Oral incubation in the cichlid fish Geophagus jurupari. *Zoologica*, *43*, 77–88.

Revell LJ. 2012. phytools: An R package for phylogenetic comparative biology (and other things). 2Methods Ecol Evol 3:217–23.

Riley BM, Mansilla MA, Ma J, et al. Impaired FGF signaling contributes to cleft lip and palate. Proceedings of the National Academy of Sciences of the United States of America. 2007;104(11):4512-4517. doi:10.1073/pnas.0607956104

Roberts RB, Hu Y-N, Albertson RC, Kocher TD 2011. Craniofacial divergence and ongoing adaptation via the hedgehog pathway. *Proc Natl Acad Sci USA* 108(32):13194-13199.

Robinson, B. W., & Parsons, K. J. (2002). Changing times, spaces, and faces: tests and implications of adaptive morphological plasticity in the fishes of northern postglacial lakes. *Canadian Journal of Fisheries and Aquatic Sciences*, *59*(11), 1819–1833. doi:10.1139/f02-144

Roff DA, Fairbairn DJ. 2007. The evolution of trade-offs: Where are we? J Evol Biol 20:433–47.

Rohatgi R, Milenkovic L, Scott M. Patched1 regulates hedghog signaling at the primary cilium. Science. 2007;317:372-377.

Rohlf FJ, Slice DE. 1990. Extensions of the Procrustes method for the optimal superimposition of landmarks. *Syst Zool.* 39:40–59.

Rohlf, F. J., & Marcus, L. F. (1993). A revolution in morphometrics. *Trends in Ecology and Evolution*, *8*(4), 129–132. doi:10.1016/0169-5347(93)90024-J

Rohlf, F. J., and M. Corti. 2000. Use of two-block partial least-squares to study covariation in shape. Syst. Biol. 49:740–753.

Rohlf, F. J. (2016). tpsDig, digitize landmarks and outlines, version 2.22. Department of Ecology and Evolution: State University of New York at Stony Brook.

Röpke, C. P., Ferreira, E., & Zuanon, J. (2014). Seasonal changes in the use of feeding

resources by fish in stands of aquatic macrophytes in an Amazonian floodplain, Brazil. *Environmental Biology of Fishes, 97*, 401–414. doi:10.1007/s10641-013-0160-4

Roughgarden, J. (1972). The Evolution of niche width. *The American Naturalist*, *106*(952), 683–718.

Rüber, L., & Adams, D. C. (2001). Evolutionary convergence of body shape and trophic morphology in cichlids from Lake Tanganyika. *Journal of Evolutionary Biology*, *14*, 325–332. doi:10.1046/j.1420-9101.2001.00269.x

Salzburger, W., Baric, S., & Sturmbauer, C. (2002). Speciation via introgressive hybridization in East African cichlids? *Molecular Ecology*, *11*, 619–625. doi:10.1046/j.0962-1083.2001.01438.x

Sandon, H. 1956. An abnormal specimen of Synodontis membranaceus (Teleostei, Siluroidea), with a discussion on the evolutionary history of the adipose fin in fish. *Proceeding Zool. Soc. London* 127: 453–459.

Santos, B. A. I., & Araújo, F. G. (2015). Evidence of morphological differences between Astyanax bimaculatus (Actinopterygii : Characidae) from reaches above and below dams on a tropical river. *Environmental Biology of Fishes*, *98*, 183–191. doi:10.1007/s10641-014-0248-5

Santos, G. dos, Jégu, M., & Mérona, B. de. (1984). Catálogo de peixes comerciais do Baixo Rio Tocantins. *Projeto Tucuruí*, 83.

Santos, G. dos, Mérona, B. de, Juras, A., & Jégu, M. (2004). Peixes do Baixo Rio Tocantins: 20 anos depois da Usina Hidroelétrica Tucuruí, 215.

Santos, G. (1995). Impactos da hidrelétrica Samuel sobre as comunidades de peixes do Rio Jamari (Rondônia, Brasil). *Acta Amazônica*, *25*, 247–280.

Santos, G., & Oliveira Jr, A. (1999). A Pesca no reservatório da hidrelétrica de Balbina (Amazonas, Brasil). *Acta Amazônica*, *29*, 147–163

Sarkar, D. 2017. Trellis graphics for R.

Scheiner SM. 1993. Genetics and evolution of phenotypic plasticity. *Anna Rev Ecol Syst.* 24:35-68.

Schlichting CD, Pigliucci M. *Phenotypic evolution. A reaction norm perspective*. 1998, Suntherland: Sinauer Associates.

Schluter D. Adaptive radiation along genetic lines of least resistance. Evolution. 1996;50(5):1766-1766. doi:10.2307/2410734

Schluter, D. (2000). *The Ecology of Adaptive Radiation*. Oxford University Press.

Schneider RA, Hu D, Helms JA. From head to toe: Conservation of molecular signals regulating limb and craniofacial morphogenesis. Cell and Tissue Research. 1999;296(1):103-109. doi:10.1007/s004410051271

Schneider RF, Meyer A. 2017. How plasticity, genetic assimilation and cryptic genetic variation may contribute to adaptive radiations. *Mol Ecol*. 26(1):330-350.

Schneider RA, Richard Schneider CA. Neural crest and the origin of species-specific pattern. Genesis 2018; 56(6-7): doi:10.1002/dvg.23219

Schock EN, Chang CF, Youngworth IA, Davey MG, Delany ME, Brugmann SA. Utilizing the chicken as an animal model for human craniofacial ciliopathies. Dev Biol. 2016;415(2):326-337. doi:10.1016/j.ydbio.2015.10.024

Schock EN, Brugmann SA. Neural crest cells utilize primary cilia to regulate ventral forebrain morphogenesis via Hedgehog-dependent regulation of oriented cell division. Developmental Biology. 2017;431(2):168-178. doi:10.1016/j.ydbio.2017.09.026

Sharpe, D. M. T., De León, L. F., González, R., & Torchin, M. E. (2017). Tropical fish community does not recover 45 years after predator introduction. *Ecology*, *98*(2), 412–424. doi:10.1002/ecy.1648

Schwenk, K., and Wagner, G.P. 2001. Function and the evolution of phenotypic stability: Connecting pattern to process. *Am. Zool.* 41: 552–563.

Schwenk, K., and Wagner, G.P. 2004. The relativism of constraints on phenotypic evolution. In Phenotypic Integration: Stuyding the Ecology and Evolution of Complex Phenotypes, M. Pigliucci, and K. Preston, eds. (Oxford, UK: Oxford University Press), pp. 390–408.

Sheftel, H., O. Shoval, A. Mayo, and U. Alon. 2013. The geometry of the Pareto front in biological phenotype space. 1471–1483.

Shoval O, Sheftel H, Shinar G, Hart Y, Ramote O, Mayo A, Dekel E, Kavanagh K, Alon U. 2012. Evolutionary trade-offs, pareto optimality, and the geometry of phenotype space. Science (80-) 336:1157–61.

Shwartz Y, Farkas Z, Stern T, Aszódi A, Zelzer E. Muscle contraction controls skeletal morphogenesis through regulation of chondrocyte convergent extension. Developmental Biology. 2012;370(1):154-163. doi:10.1016/j.ydbio.2012.07.026

Sisson BE, Dale RM, Mui SR, Topczewska JM, Topczewski J. A role of glypican4 and wnt5b in chondrocyte stacking underlying craniofacial cartilage morphogenesis. Mechanisms of Development. 2015;138:279-290. doi:10.1016/j.mod.2015.10.001

Smith PF, Konings A, Kornfield I. Hybrid origin of a cichlid population in Lake Malawi: Implications for genetic variation and species diversity. Molecular Ecology. 2003;12(9):2497-2504. doi:10.1046/j.1365-294X.2003.01905.x

Sneath, P.H.A. 1967. Trend-surface analysis of transformation grids. *J. Zool.* 151: 65–122.

Sorokin SP. Reconstructions of centriole formation and ciliogenesis in mammalian lungs. Journal of Cell Science. 1968;3:207-230.

Spurway, H. 1949. Remarks on Vavilov's law of homologous variation. *Ric. Sci.* 19: 3–9.

St-Jacques B, Hammerschmidt M, McMahon AP. Indian hedgehog signaling regulates proliferation and differentiation of chondrocytes and is essential for bone formation. Genes and Development. 1999;13(16):2072-2086. doi:10.1101/gad.13.16.2072

Staab KL, Hernandez LP. 2010. Development of the cypriniform protrusible jaw complex in Danio rerio: constructional insights for evolution. *J Morphol*. 271(7):814-25.

Standen EM, Lauder G V. 2005. Dorsal and anal fin function in bluegill sunfish *Lepomis macrochirus*: Three-dimensional kinematics during propulsion and maneuvering. J Exp Biol 208:2753–63.

Stauffer JRJ, van Snik-Gray E. 2004. Phenotypic plasticity: its role in trophic radiation and explosive speciation in cichlids (Teleostei: Cichlidae). *Animal Biology* 54:137-158.

Stearns SC. 1989. Trade-offs in life-history evolution. Funct Ecol 3:259–68.

Stearns, S.C. 1989. The evolutionary significance of phenotypic plasticity. *Bioscience* 39: 436–445.

Stewart, T.A., Bonilla, M.M., Ho, R.K., and Hale, M.E. 2019. Adipose fin development and its relation to the evolutionary origins of median fins. *Sci. Rep.* 9: 1–12.

Styczynska-Soczka K, Jarman AP. The *Drosophila* homologue of rootletin is required for mechanosensory function and ciliary rootlet formation in chordotonal sensory neurons. Cilia. 2015;4(1):9-9. doi:10.1186/s13630-015-0018-9

Svanbäck R, Wainwright PC, Ferry-Graham LA. 2002. Linking cranial kinematics, buccal pressure, and suction feeding performance in largemouth bass. Physiol Biochem Zool 75:532–43.

Svandova E, Anthwal N, Tucker AS, Matalova E. Diverse fate of an enigmatic structure: 200 years of meckel's cartilage. Front Cell Dev Biol. 2020;8:821. doi:10.3389/fcell.2020.00821

Swartz ME, Nguyen V, McCarthy NQ, Eberhart JK. Hh signaling regulates patterning and morphogenesis of the pharyngeal arch-derived skeleton. Developmental Biology. 2012;369(1):65-75. doi:10.1016/j.ydbio.2012.05.032.

Tachi S, Tachi C, Lindner HR. Influence of ovarian hormones on formation of solitary cilia and behavior of the centrioles in uterine epithelial cells of the rat. Biology of Reproduction. 1974;10(4):391-403. doi:10.1095/biolreprod10.4.391

Tao H, Zhu M, Lau K, et al. Oscillatory cortical forces promote three-dimensional cell intercalations that shape the murine mandibular arch. Nature Communications. 2019;10(1). doi:10.1038/s41467-019-09540-z

Taylor WR, Van Dyke GC. 1985. Revised procedures for staining and clearing small fishes and other vertebrates for bone and cartilage study. *Cybium* 9:107–19.

Tegge S, Hall J, Huskey S. 2020. Spatial and temporal changes in buccal pressure during prey-capture in the trumpetfish (*Aulostomus maculatus*). Zoomorphology 139:85–95.

Temiyasathit S, Jacobs CR. Osteocyte primary cilium and its role in bone mechanotransduction. Ann N Y Acad Sci. 2010;1192:422-428. doi:10.1111/j.1749-6632.2009.05243.x

Temiyasathit S, Tang WJ, Leucht P, Anderson CT, Monica SD, Castillo AB, Helms JA, Stearns T, Jacobs CR. 2012. Mechanosensing by the Primary Cilium: Deletion of Kif3A Reduces Bone Formation Due to Loading. *Plos One* 7(3).

Tendler A, Mayo A, Alon U. 2015. Evolutionary tradeoffs, Pareto optimality and the morphology of ammonite shells. BMC Syst Biol 9:1–12.

Teraoka H, Dong W, Okuhara Y, et al. Impairment of lower jaw growth in developing zebrafish exposed to 2,3,7,8-tetrachlorodibenzo-p-dioxin and reduced hedgehog expression. Aquatic Toxicology. 2006;78(2):103-113. doi:10.1016/j.aquatox.2006.02.009

Thiagavel, J., Cechetto, C., Santana, S.E., Jakobsen, L., Warrant, E.J., and Ratcliffe, J.M. 2018. Auditory opportunity and visual constraint enabled the evolution of echolocation in bats. *Nat. Commun.* 9:.

Thompson, D. (1917). *On growth and form*. Cambridge, U.K.: Cambridge University Press.

Thys T. 1997. Spatial variation in epaxial muscle activity during prey strike in

largemouth bass (Micropterus salmoides). J Exp Biol 200:3021–31.

Tobin JL, Di Franco M, Eichers E, et al. Inhibition of neural crest migration underlies craniofacial dysmorphology and hirschsprung's disease in bardet-biedl syndrome. Proceedings of the National Academy of Sciences of the United States of America. 2008;105(18):6714-6719. doi:10.1073/pnas.0707057105.

Toro E, Herrel A, Irschick D. 2004. The evolution of jumping performance in Caribbean Anolis lizards: Solutions to biomechanical trade-offs. Am Nat 164.

Trautman, M. (1939). The Effects of man-made modifications on the fish fauna in Lost and Gordon Creeks , Ohio , between 1887-1938. *The Ohio Journal of Science*, *39*(5), 275–288.

Truett GE, Heeger P, Mynatt RL, Truett AA, Walker JA, Warman ML. Preparation of PCR-quality mouse genomic DNA with hot sodium hydroxide and tris (HotSHOT). Biotechniques. 2000;29(1):52, 54. doi:10.2144/00291bm09

Turner, G. F. 2007. Adaptive radiation of cichlid fish. Curr. Biol. 17:827–831.

Uller, T., Moczek, A.P., Watson, R.A., and Laland, K.N. 2018. Developmental bias and evolution : a regulatory network perspective. *Genetics* 209: 949–966.

VanderVorst K, Hatakeyama J, Berg A, Lee H, Carraway KL. Cellular and molecular mechanisms underlying planar cell polarity pathway contributions to cancer malignancy. Semin Cell Dev Biol. 2018;81:78-87. doi:10.1016/j.semcdb.2017.09.026

Van Wassenbergh, S., N. Z. Potes, and D. Adriaens. 2015. Hydrodynamic drag constrains head enlargement for mouthbrooding in cichlids. J. R. Soc. Interface 12

Van Wassenbergh S, Day SW, Hernández LP, Higham TE, Skorczewski T. 2015. Suction

power output and the inertial cost of rotating the neurocranium to generate suction in fish. J Theor Biol 372:159–67.

Vaughan TJ, Mullen CA, Verbruggen SW, McNamara LM. Bone cell mechanosensation of fluid flow stimulation: a fluid–structure interaction model characterising the role integrin attachments and primary cilia. Biomechanics and Modeling in Mechanobiology. 2015;14(4):703-718. doi:10.1007/s10237-014-0631-3

Vavilov, N.I. 1922. The law of homologous series in variation. *J. Genet.* 12: 47–89.

Vázquez, D. P., & Simberloff, D. (2002). Ecological specialization and susceptibility to disturbance: conjectures and refutations. *The American Naturalist*, *159*(6), 606–623. doi:10.1086/339991

Via S, Gomulkiewicz R, Dejong G, Scheiner SM, Schlichting CD, Vantienderen PH. 1995. Adaptive Phenotypic Plasticity - Consensus and Controversy. *Trends Ecol Evol.* 10(5):212-217.

Vitousek, P. M., Mooney, H. a, Lubchenco, J., & Melillo, J. M. (1997). Human Domination of Earth' s Ecosystems. *Science*, *277*(5325), 494–499. doi:10.1126/science.277.5325.494

Vlijm R, Li X, Panic M, et al. STED nanoscopy of the centrosome linker reveals a CEP68-organized, periodic rootletin network anchored to a C-Nap1 ring at centrioles. Proceedings of the National Academy of Sciences. 2018;115(10):E2246-E2253. doi:10.1073/pnas.1716840115

Voss AK, Strasser A. The essentials of developmental apoptosis. F1000Research. 2020;9. doi:10.12688/f1000research.21571.1

Waddington CH. 1953. Genetic assimilation of an acquired character. *Evolution* 7:118–126.

Waddington CH. 1959. Canalization of Development and Genetic Assimilation of Acquired Characters. *Nature* 183(4676):1654-1655.

Wagner G. The influence of variation and developmental constraints on the rate of multivariate phenotypic evolution. Journal of Evolutionary Biology. 1988;1(1):45-66. doi:10.1046/j.1420-9101.1988.1010045.x

Wagner, G. P., and B. Y. Misof. 1993. How can a character be developmentally constrained despite variation in developmental pathways? J. Evol. Biol. 6:449–455.

Wagner, G.P. 1996. Homologues, natural kinds and the evolution of modularity. *Am. Zool.* 36: 36–43.

Wagner GP, Altenberg L. 1996. Perspective: Complex adaptations and the evolution of evolvability. *Evolution.* 50(3):967-976.

Wagner, G.P., and Schwenk, K. 2000. Evolutionary stable configurations: functional integration and the evolution of phenotypic stability. In Evolutionary Biology, pp. 155–217.

Wagner, G. P., M. Pavlicev, and J. M. Cheverud. 2007. The road to modularity. Nat. Rev. Genet. 8:921–931.

Wainwright, P. C., Osenberg, C. W., & Mittelbach, G. G. (1991). Trophic Polymorphism in the pumpkinseed sunfish (Lepomis-Gibbosus Linnaeus) - effects of environment on ontogeny. *Functional Ecology, 5*(1), 40–55. doi:10.2307/2389554

Wainwright PC, Huskey SH, Turingan RG, Carroll AM. 2006. Ontogeny of suction feeding capacity in snook, *Centropomus undecimalis*. J Exp Zool 305A:246–52.

Walker M, Kimmel C. A two-color acid-free cartilage and bone stain for zebrafish larvae. Biotechnic & Histochemistry. 2007;82(1):23-28. doi:10.1080/10520290701333558

Waltzek, T. B., & Wainwright, P. C. (2003). Functional morphology of extreme jaw protrusion in Neotropical cichlids. *Journal of Morphology*, *257*, 96–106. doi:10.1002/jmor.10111

Wang X, Mao JJ. Chondrocyte proliferation of the cranial base cartilage upon in vivo mechanical stresses. Journal of Dental Research. 2002;81(10):701-705. doi:10.1177/154405910208101009

Wang J, Wainwright DK, Lindengren RE, Lauder G V., Dong H. 2020. Tuna locomotion: a computational hydrodynamic analysis of finlet function. J R Soc Interface 17:20190590.

Ware SM, Aygun MG, Hildebrandt F. Spectrum of clinical diseases caused by disorders of primary cilia. Proceedings of the American Thoracic Society. 2011;8(5):444-450. doi:10.1513/pats.201103-025SD

Webb, P. W. (1984). Body form, locomotion and foraging in aquatic vertebrates. *American Zoologist*, *24*(1), 107–120. doi:10.1093/icb/24.1.107

Webb PW. 1984. Form and function in fish swimming. Sci Am 251:72–83.

Weihs D. 1993. Stability of aquatic animal locomotion. Contemp Math 141:443–61.

Weller, H. I., C. D. Mcmahan, and M. W. Westneat. 2017. Dirt-sifting devilfish: winnowing in the geophagine cichlid Satanoperca daemon and evolutionary implications. Zoomorphology 136:45–59. Springer Berlin Heidelberg.

Weller, H., H. López-Fernández, C. D. McMahan, and E. L. Brainerd. 2022. Relaxed feeding constraints facilitate the evolution of mouthbrooding in Neotropical cichlids. Am. Nat. 199.

Wen L, Weaver JC, Lauder G V. 2014. Biomimetic shark skin: Design, fabrication and hydrodynamic function. J Exp Biol 217:1656–66.

Werner ME, Hwang P, Huisman F, Taborek P, Yu CC, Mitchell BJ. Actin and microtubules drive differential aspects of planar cell polarity in multiciliated cells. J Cell Biol. 2011;195(1):19-26. doi:10.1083/jcb.201106110

West-Eberhard MJ. 1989. Phenotypic plasticity and the origin of diversity. *Ann. Rev Ecol Evol Syst.* 20:249-278.

West-Eberhard MJ. *Developmental Plasticity and Evolution*. 2003, New York: Oxford University Press.

West-Eberhard MJ. 2005. Developmental plasticity and the origin of species differences. *Proc Natl Acad Sci USA* 102:6543-6549.

Westerfield M. The Zebrafish Book; A Guide for the Laboratory Use of Zebrafish (*Danio Rerio*). 5th ed. University of Oregon Press; 2007.

Westneat MW. 1990. Feeding mechanics of teleost fishes (Labridae; Perciformes) – a test of 4-bar linkage models. J Morphol 205:269–95.

Westneat MW. 2004. Evolution of Levers and Linkages in the Feeding Mechanisms of Fishes. *Int Comp Biol.* 44(5):378–389.

Williams, J. D., Winemiller, K. O., Taphorn, D. C., & Balbas, L. (1998). Ecology and Status of Piscivores in Guri, an Oligotrophic Tropical Reservoir. *North American Journal of Fisheries Management, 18*(2), 274–285. doi:10.1577/1548-

8675(1998)018<0274:EASOPI>2.0.CO;2

Willis, S. C., Nunes, M. S., Montaña, C. G., Farias, I. P., & Lovejoy, N. R. (2007). Systematics, biogeography, and evolution of the Neotropical peacock basses Cichla (Perciformes: Cichlidae). *Molecular Phylogenetics and Evolution*, *44*(2007), 291–307. doi:10.1016/j.ympev.2006.12.014

Wilson, S. K., Burgess, S. C., Cheal, A. J., Emslie, M., Fisher, R., Miller, I., … Sweatman, H. P. A. (2008). Habitat utilization by coral reef fish: implications for specialists vs. generalists in a changing environment. *Journal of Animal Ecology*, *77*, 220–228. doi:10.1111/j.1365-2656.2007.0

Wilson MH, Holzbaur ELF. Nesprins anchor kinesin-1 motors to the nucleus to drive nuclear distribution in muscle cells. Development 2015; 142(1): 218-228. doi:10.1242/dev.114769

Wimberger, P. H. (1991). Plasticity of jaw and skull morphology in the neotropical cichlids Geophagus brasiliensis and Geophagus steindachneri. *Evolution*, *45*(7), 1545–1563. doi:10.2307/2409778

Wimberger, P. H. (1992). Plasticity of fish body shape. The effects of diet, development, family and age in two species of Geophagus (Pisces: Cichlidae). *Biological Journal of the Linnean Society*, *45*, 197–218.

Wimberger, P. H. 1993. Effects of Vitamin C Deficiency on Body Shape and Skull Osteology in *Geophagus brasiliensis*: Implications for Interpretations of Morphological Plasticity Author(s): Peter H. Wimberger Published by: American Society of Ichthyologists and Herpetologis. Copeia 1993:343–351.

Winemiller, K. O., McIntyre, P. B., Castello, L., Fluet-Chouinard, E., Giarrizzo, T., Nam, S., … Sáenz, L. (2016). Balancing hydropower and biodiversity in the Amazon, Congo, and Mekong. *Science, 351*(6269), 128–129. doi:10.1126/science.aac7082

Wong FK, Marín O. Developmental cell death in the cerebral cortex. Annual Review of Cell and Developmental Biology. 2019;35:523-542. doi:10.1146/annurev-cellbio-100818-125204

Woolfson DN. 2005. The design of coiled-coil structures and assemblies. *Adv Protein Chem.* 70:79-112.

Wright S. The roles of mutation, inbreeding, crossbreeding and selection in evolution. Sixth International Congress on Genetics. 1932;1(6):356-366.

Wund MA, Baker JA, Clancy B, Golub JL, Foster SA. 2008. A test of the "Flexible stem" model of evolution: Ancestral plasticity, genetic accommodation, and morphological divergence in the threespine stickleback radiation. *Am Nat.* 172(4):449-462.

Xavier GM, Seppala M, Barrell W, Birjandi AA, Geoghegan F, Cobourne MT. Hedgehog receptor function during craniofacial development. Developmental Biology. 2016;415(2):198-215. doi:10.1016/j.ydbio.2016.02.009

Xiao Z, Zhang S, Mahlios J, Zhou G, Magenheimer BS, Guo D, Dallas SL, Maser R, Calvet JP, Bonewald L, Quarles LD. 2006. Cilia-like structures and polycystin-1 in osteoblasts/osteocytes and associated abnormalities in skeletogenesis and *Runx2* expression. *J Biol Chem.* 281(41):30884-95.

Xu L, Wang X, Li H, Du F. 2018. The complete mitochondrial genome of Perciformes fish (*Brama dussumieri*) from South China Sea. Mitochondrial DNA Part B Resour

3:876–77.

Yang J, Liu X, Yue G, Adamian M, Bulgakov O, Li T. 2002. Rootletin, a novel coiled-coil protein, is a structural component of the ciliary rootlet. *J Cell Biol.* 159(3):431-40.

Yang J, Gao J, Adamian M, Wen XH, Pawlyk B, Zhang L, Sanderson MJ, Zuo J, Makino CL, Li T. 2005. The ciliary rootlet maintains long-term stability of sensory cilia. *Mol Cell Biol.* 25(10):4129-37.

Yang J, Li T. The ciliary rootlet interacts with kinesin light chains and may provide a scaffold for kinesin-1 vesicular cargos. Experimental cell research. 2005;309(2):379-389. doi:10.1016/j.yexcr.2005.05.026

Yang J, Adamian M, Li T. Rootletin interacts with C-Nap1 and may function as a physical linker between the pair of centrioles/basal bodies in cells. Molecular Biology of the Cell. 2006;17(2):1033-1040. doi:10.1091/mbc.E05-10-0943

Yang J, Andre P, Ye L, Yang YZ. The Hedgehog signalling pathway in bone formation. International journal of oral science. 2015;7(2):73-79. doi:10.1038/ijos.2015.14

Yang L, Tsang KY, Tang HC, Chan D, Cheah KSE. Hypertrophic chondrocytes can become osteoblasts and osteocytes in endochondral bone formation. Proceedings of the National Academy of Sciences of the United States of America. 2014;111(33):12097-12102. doi:10.1073/pnas.1302703111

Yatsu A, Nakamura I. 1989. *Xenobrama microlepis*, a new genus and species of bramid fish, from the Subantarctic waters of the South Pacific. Japanese J Ichthyol 36:190–95.

Yoder, J. B., Clancey, E., Des Roches, S., Eastman, J. M., Gentry, L., Godsoe, W., …

Harmon, L. J. (2010). Ecological opportunity and the origin of adaptive radiations. *Journal of Evolutionary Biology*, *23*(8), 1581–1596. doi:10.1111/j.1420-9101.2010.02029.x

Young NM, Chong HJ, Hu D, Hallgrímsson B, Marcucio RS. Quantitative analyses link modulation of sonic hedgehog signaling to continuous variation in facial growth and shape. Development. 2010;137(20):3405-3409. doi:10.1242/dev.052340

Yuan X, Serra RA, Yang S. 2015. Function and regulation of primary cilia and intraflagellar transport proteins in the skeleton. *Ann N Y Acad Sci.* 1335:78-99.

Zaghloul NA, Brugmann SA. The emerging face of primary cilia. Genesis. 2011;49(4):231-246. doi:10.1002/dvg.20728

Zarfl, C., Lumsdon, A. E., Berlekamp, J., Tydecks, L., & Tockner, K. (2014). A global boom in hydropower dam construction. *Aquatic Sciences*, *77*(1), 161–170. doi:10.1007/s00027-014-0377-0

Zelditch, M. L., Swiderski, D., Sheets, H., & Fink, W. (2012). *Geometric Morphometrics for Biologists: A Primer*. Amsterdam: Elsevier/Academic Press.

Zelditch, M. L., and A. Goswami. 2021. What does modularity mean? Evol. Dev. 23:377–403

Zogbaum L, Friend PG, Albertson RC. 2020. Plasticity and genetic basis of cichlid gill arch anatomy reveal novel roles for Hedgehog signaling. *Mol. Ecol.* Dec 5. doi: 10.1111/mec.15766. Online ahead of print.